2-D and 3-D Adipocyte Cell Culture

Promising Tools for Basic Research and Approaches towards Clinical Therapies

Dissertation zur Erlangung des Doktorgrades der Naturwissenschaften

(Dr. rer. nat.)

der Fakultät Chemie und Pharmazie

der Universität Regensburg

vorgelegt von

Anna Katharina Seitz

aus Neumarkt i.d.OPf.

im Juni 2010

Diese Doktorarbeit entstand in der Zeit von März 2006 bis Juni 2010 am Lehrstuhl Pharmazeutische Technologie der Universität Regensburg.

Die Arbeit wurde von Prof. Dr. Achim Göpferich angeleitet.

Promotionsgesuch eingereicht am:	21.06.2010	
Mündliche Prüfung am:	30.07.2010	
Prüfungsausschuss:	Prof. Dr. S. Elz	(Vorsitzender)
	Prof. Dr. A. Göpferich	(Erstgutachter)
	Prof. Dr. T. Blunk	(Zweitgutachter)
	Prof. Dr. E. Tamm	(Drittprüfer)

Meinen Eltern

in Liebe und Dankbarkeit

Table of Contents

2-D and 3-D Adipocyte Cell Culture

Promising Tools for Basic Research and Approaches towards Clinical Therapies

You must have a plan, if you don´t have a plan,
you´ll become part of somebody else´s plan.

(Terence McKenna)

Chapter 1

Introduction

1. Characteristics of adipose tissue

1.1. Structure of adipose tissue

Adipose tissue represents a loose connective tissue mainly consisting of mature lipid-filled adipocytes and, a variety of other cell types such as stromal vascular cells including blood cells, endothelial cells, pericytes, adipose precursor cells, and fibroblasts as well as immune cells [1-3]. The mature adipocytes are closely arranged within the tissue resulting in a hexagonal configuration. Spaces between the cells are filled by a specific fiber network referred to as extracellular matrix (ECM) which is interspersed with capillaries. Not only due to its color, adipose tissue is classified into two subtypes, white adipose tissue (WAT) and brown adipose tissue (BAT), which differ in their abundance and function in humans [4]. BAT is principally found in neonates and only marginally in the adult body and is specialized for heat production by adaptive non-shivering thermogenesis [4-6]. The BAT is extremely well vascularized and the adipocytes are characterized by densely packed mitochondria as well as by the accumulation of triglycerides (TGs) in multiple small lipid droplets [4,7]. However, this work focuses only on WAT as it is the major object of the current adipose research. WAT is the predominant type of fat tissue in adult humans and is widely distributed in multiple depots in the body. The total fat mass is locally classified into subcutaneous (~ 80%) and internal (~ 20%) adipose compartments. The internal fat depots include visceral and nonvisceral fat as well as other small fat depots [4]. White fat acts as the major energy reservoir by storing TGs in periods of energy excess and releasing free fatty acids during energy deprivation. The growth of WAT results from increased adipocyte number (hyperplasia) and, respectively, adipocyte size (hypertrophy) [2]. Due to the accumulation of lipids, adipocytes reach sizes ranging from 20 µm to 200 µm in diameter [4]. The mature unilocular adipocyte contains a large single droplet surrounded by a thin rim of cytoplasm, and a nucleus located peripherally which gives the cell a so called signet-ring form [8]. However, developing adipocytes temporarily contain multiple lipid droplets, before these finally coalesce into a single large droplet. Multilocular appearance is also present at periods of nutrient deprivation due to mobilization of TGs.

1.2. Functions of adipose tissue

Until the 1980s, the most important functions of fat seemed to be heat insulation, mechanical cushion, and of course, a source of energy. Adipose tissue stores energy in times of nutritional excess in the form of TGs and release free fatty acids and glycerol when energy is required

[9,10]. However, during the last two decades, particularly through the identification of leptin in 1994 [11], it became increasingly clear that the fat tissue also has active roles in physiological processes by mediating endocrine, paracrine, and autocrine signals. Aside from the primary function as energy reservoir, the WAT is also described as a highly active metabolic and endocrine organ secreting a large number of protein factors and signals termed as adipokines [5,12,13]. Adipokines and other adipocyte-secreted factors include leptin, adiponectin, resistin, visfatin, apelin, and inflammatory cytokines like tumor necrosis factor alpha (TNF-α), monocyte chemoattractant protein-1 (MCP-1), and plasminogen activator inhibitor protein (PAI) as well as growth factors, enzymes, complement factors, and matrix proteins [4,6]. These factors act as mediators for multiple physiological processes, i.e., energy homeostasis, insulin sensitivity, lipid metabolism, inflammatory and immunological responses, angiogenesis, blood pressure, and reproductive function [14,15]. A large body of evidence indicates that many factors secreted by adipocytes are dysregulated in obesity contributing to hyperglycemia, hyperlipidemia, chronic inflammation, and insulin resistance [9,16-18]. Thus, WAT dysfunction is involved in the pathogenesis of type 2 diabetes and other metabolic diseases, such as atherosclerosis. Particularly leptin, a hormone that is primarily synthesized and secreted by mature adipocytes is elevated in human obesity and in animal models of obesity. Different roles of leptin are suggested including regulation of body fat mass, modulation of insulin action in liver, production of steroids in ovary, and direct effects on adrenocortical steroidogenesis. Another adipokine, the cytokine TNF-α, is upregulated in obesity which contributes to insulin resistance by the inhibition of the insulin receptor signalling through the insulin receptor substrate 1 (IRS-1) [19,20].

The two vascular function-related proteins angiotensinogen and plasminogen activator inhibitor type I (PAI-1) are responsible for mediating vasoregulatory functions of adipose tissue such as blood supply and fatty acid efflux from fat [21]. Angiotensin II, the cleavage product of angiotensinogen, increases lipogenesis in adipocytes and, thus, angiotensin II may play a role in the control of adiposity through regulation of lipid synthesis and storage in adipocytes [22]. Higher levels of PAI-1, a fibrinolytic protein, have been reported in obesity. Therefore, PAI-1 is assumed to be involved in the development of cardiovascular diseases associated with obesity [23,24].

Taken together, multiple studies from literature have clearly shown that adipose tissue can be regarded as endocrine organ which is involved in various physiological processes in addition to its main role in regulation of energy balance.

1.3. Adipocyte differentiation

The adipose lineage arises from a pluripotent stem cell population of mesodermal origin which has the capacity to differentiate into various cell types such as adipocytes, chondrocytes, osteoblasts, and myocytes [9]. These multipotential precursor cells reside in the stromal vascular compartment of adipose tissue and undergo a commitment step, in which cells become restricted to the adipocyte lineage. Figure 1 illustrates an overview of the different stages of adipocyte development [9].

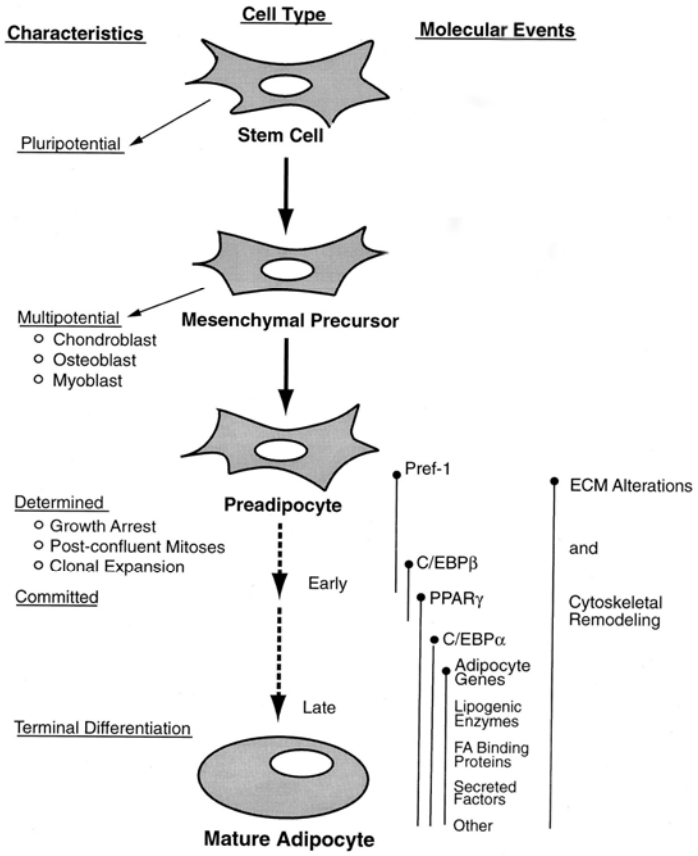

Figure 1: Overview of the adipocyte development (from Gregoire *et al*. [9]).
Abbreviations: C/EBP=CCAAT/enhancer binding protein, PPAR=peroxisome proliferator-activated receptor, pref-1=preadipocyte factor 1, ECM=extracellular matrix.

Adipocyte differentiation is induced on the molecular level by a coordinated transcriptional program resulting in lipid-laden and insulin-responsive adipocytes. The cellular and molecular mechanisms of adipogenesis have been extensively studied using model preadipocytes, notably 3T3-L1, 3T3-F442A, C3H10T1/2 and NIH 3T3 cell lines [25]. Adipogenesis of preadipocytes is stimulated by a combination of adipogenic inducers *in vitro*. Commonly used combinations mainly consist of glucocorticoids, agonists which increase intracellular cyclic adenosine monophosphate (cAMP) levels, insulin which stimulates

insulin-like growth factor-I receptors, and thiazolidinediones known as peroxisome proliferator-activated receptor gamma (PPARγ) ligands [26]. Upon induction of confluent preadipocytes with the cocktail of differentiation inducers, the cells synchronously re-enter the cell cycle and undergo last rounds of cell division, referred to as mitotic clonal expansion before they enter a unique growth-arrested state of the cell cycle which is required for terminal differentiation [27]. It was reported that both clonal expansion and growth arrest are prerequisites for adipogenesis [9,28,29]. Subsequently, a cascade of transcription factors is induced which activate the expression of adipocyte genes and ultimately produce the adipocyte phenotype. An overview of the genetic cascade is shown in Figure 2 [26].

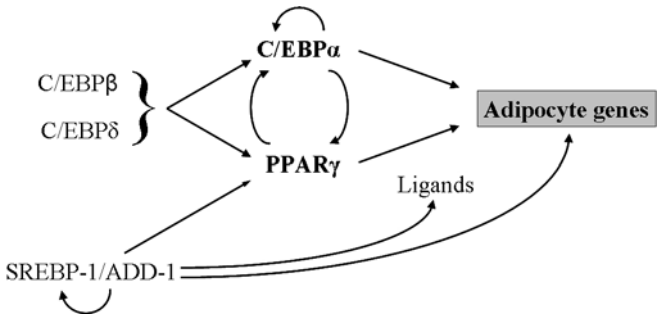

Figure 2: Genetic cascade of adipogenesis leading to the adipogenic phenotype.
Abbreviations: C/EBP=CCAAT/enhancer binding protein, PPAR=peroxisome proliferator-activated receptor, SREBP-1/ADD-1=sterol regulatory element binding protein 1/adipocyte differentiation and determination factor 1. The figure was modified from MacDougald *et al.* [26].

First of all, the early regulators of preadipocyte differentiation C/EBPβ and δ are induced which are responsible for subsequent activation of the master adipogenic transcription factors C/EBPα and PPARγ [26,30]. PPARγ, the central regulator of adipogenesis, is necessary and sufficient for the adipogenic process *in vitro* and *in vivo* [31,32], whereas C/EBPα is required for insulin-dependent glucose uptake in mature adipocytes [30]. Once C/EBPα and PPARγ are expressed, the differentiation state is maintained through autoactivation of their expression [28,33] and, additionally, they positively regulate each other's expression [15,34]. Furthermore, C/EBPα and PPARγ, along with the sterol regulatory element binding protein 1/adipocyte differentiation and determination factor 1 (SREBP-1/ADD-1), coordinately activate the transcription of adipocyte-specific genes including adipocyte fatty acid binding protein and lipid-metabolizing enzymes that produce and maintain the adipocyte phenotype [35]. However, besides C/EBPβ, δ, α and PPARγ, adipogenesis is also regulated by other transcription factors. Some factors such as T cell-specific transcription factor/lymphoid enhancer-binding factor (TCF/LEF), GATA2/3, retinoic acid receptor α or SMAD6/7 are

described as negative regulators of adipogenesis, whereas active cAMP-responsive element binding protein (CREB) induces adipogenesis [26].
Recent studies have identified that many other factors, e.g., cell cycle proteins, clock proteins, interferon-regulatory factors (IRFs) and various proteins in the external environment are involved in the regulation of the adipogenic process [9,36-38].

1.4. Adipocyte metabolism

TGs are an efficient form to accumulate fatty acids as energy reservoirs or as building blocks for membrane lipid synthesis. In adipose tissue, TGs are continuously synthesized and simultaneously mobilized. In times of energy excess, free fatty acids (FFAs) are assimilated into TG-rich lipid droplets resulting in an increase of the fat cell size.
The fatty acids are mainly synthesized in the liver, a process referred to as lipogenesis, whereas only small amounts are synthesized in the adipocytes. After synthesis of the fatty acids in the liver, they are esterified to TGs that are packaged into very low density lipoproteins (VLDL). The TG-rich lipoproteins are secreted into the blood followed by the hydrolysis of TGs by the lipoprotein lipase. The fatty acids are transported via blood circulation to the adipose tissue for storage [39]. Their uptake through the adipocyte plasma membrane is regulated by fatty acid transporters. Within the adipocytes, the fatty acids together with glycerol are immediately reesterified to TGs.
Lipolysis is the chemical decomposition of adipose tissue under fasting conditions or in periods of increased energy demand to provide fuel to other organs and to deliver substrates to the liver for gluconeogenesis and lipoprotein synthesis [40]. Regarding pathophysiology, dysregulations of lipolysis are involved in obesity, insulin resistance in type 2 diabetes and related disorders [41-44]. During lipolysis, the TGs stored in adipocytes are hydrolyzed by different lipases into glycerol and FFAs which are released into the circulation and transported to other tissues (Figure 3). The adipose triglyceride lipase (ATGL) is predominantly responsible for the initial hydrolysis of TGs into diglycerides (DGs). Although hormone-sensitive lipase (HSL) is able to hydrolyze TGs, DGs, and monoglycerides (MGs) *in vitro*, HSL acts preferentially on DGs [45-47,47]. Finally, the hydrolysis of MGs into FFAs and glycerol is catalyzed by the monoglyceride lipase [47]. Subsequently, FFAs leave the adipose tissue bound to albumin or other carrier proteins [48] and are transported via the blood circulation to target tissues such as skeletal as well as cardiac muscle and liver in order to be metabolized. However, some FFAs never leave the adipocyte but are reesterified to new TGs after food intake [49].

Lipolysis in adipocytes is intensively regulated by hormones. In humans, the major hormones are catecholamines, the most abundant lipolytic hormones, and insulin, the most potent antilipolytic hormone [40]. The lipolysis-regulating action of these hormones have been extensively studied with regard to HSL [50,51]. HSL is stimulated by the natural catecholamines adrenaline and noradrenaline which bind to β-adrenergic receptors resulting in the activation of adenylyl cyclase via a stimulatory G-protein (Figure 3). This leads to increased levels of cAMP and subsequent activation of the protein kinase A which induces lipolysis by phosphorylation of several proteins in the lipolytic cascade, primarily HSL and perilipin A. Perilipin is an abundant structural protein covering the surface of adipocyte lipid droplets. In the non-phosphorylated state, perilipin protects the lipid store from hydrolysis by blocking access of the lipases to the droplet [52,53]. Phosphorylation of this protein induces reorganization of the lipid droplet coating which facilitates the translocation of HSL from the cytosol to the surface of the lipid droplet where efficient hydrolysis occurs [45,54]. Subsequently, binding of HSL to adipocyte lipid binding protein favors the export of the released FFAs [54].

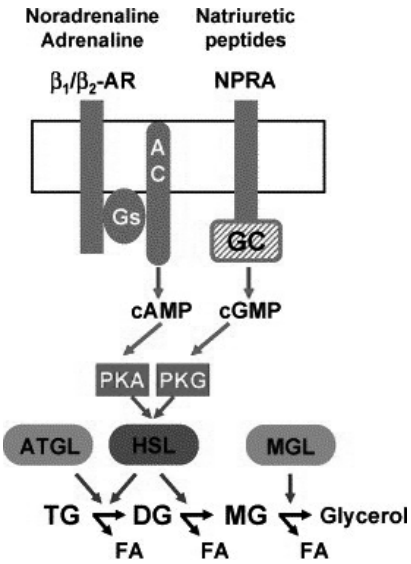

Figure 3: Stimulatory lipolysis pathway in human adipose tissue.
Abbreviations: AC=adenylyl cyclase, AR=adrenoreceptor, ATGL=adipose triglyceride lipase, cAMP=cyclic adenosine monophosphate, cGMP=cyclic guanosine monophosphate, DG=diglyceride, FA=fatty acid, GC=guanylate cyclase, Gs=stimulatory GTP-binding protein, HSL=hormone-sensitive lipase, MG=monoglyceride, MGL=monoglyceride lipase, NPRA=natriuretic peptide receptor A, PKA=protein kinase A, PKG=protein kinase G, TG=triglyceride.
Reprinted with permission from Langin *et al.* [54]. ©2010 Elsevier B.V.

Additionally, catecholamines which bind to α2-adrenoreceptors have been reported to result in antilipolytic effects. The stimulation of the α2-adrenoreceptor leads to decreased cAMP-

levels through the activation of inhibitory G-proteins [55]. Similar antilipolytic effects are caused by insulin inhibiting HSL. Insulin stimulates the phosphodiesterase 3B resulting in reduced cAMP levels and in turn inhibits protein kinase A activity which leads to reduced phosphorylation of HSL [56].

However, the regulation of adipocyte lipolysis is additionally modulated by numerous other lipolytic and antilipolytic factors and (adipo)cytokines such as growth hormones, glucocorticoids, atrial and brain natriuretic peptide, leptin, resistin, adrenomedullin, TNF-α, IL-6, and adiponectin [50,54,57].

Up to now, the molecular mechanisms and pathways that regulate lipolysis in response to these factors are not fully understood. Natriuretic peptides induce a signal transduction pathway which is distinct from catecholamines (Figure 3). They activate their corresponding receptor A which possesses intrinsic guanylyl cyclase activity leading to an increase in cyclic guanosine monophosphate (cGMP) level and an activation of protein kinase G which induces phosphorylation and activation of HSL [58]. Regarding TNF-α, it is supposed that this cytokine stimulates lipolysis by decreasing the perilipin level at the surface of lipid droplets [59]. Furthermore, TNFα induces lipolysis by downregulation of inhibitory G-proteins [60] as well as phosphodiesterase 3B that are responsible for the degradation of cAMP [61,62].

2. The adipocyte extracellular matrix

2.1. The extracellular matrix composition of adipose tissue

Structural integrity and functionality in tissues are determined by a highly organized architecture of the ECM which is generated by residing cells. Thereby, the ECM is not only giving shape and physical support for cells, but it is also a reservoir of growth factors, enzymes, and plasma proteins and it is involved in complex cell-matrix interactions. This microenvironment influences various cell functions such as cell differentiation, proliferation, adhesion, migration, and polarization and hence, it is implicated in biological processes such as development, tissue maintenance, regeneration, and repair, as well as in various pathological processes such as tumor growth and metastasis. The ECM comprises glycosaminoglycans (GAGs), proteoglycans, collagens and further non-collagenous components. Although the ECM constituents are similar in different tissues, their composition and organization vary according to tissue-specific requirements. Furthermore, changes occur within the same tissue depending on developmental stage, viability, and subtype of the cells [63].

The ECM of adipose tissue is a thick matrix network referred to as basement membrane [64]. This network structure represents a close arrangement of collagen fibrils and fibrillar bundles as detected by scanning electron microscopy (SEM) [65]. However, differences are described between the ECM composition of WAT and BAT resulting from the distinct characteristics of monovacuolated and multivacuolated adipocytes. The basement membrane of WAT is mainly composed of collagen IV and laminin, whereas heparan sulfate proteoglycan and fibronectin were less abundant, in contrast to BAT in which all components are present [66].

Previous *in vitro* studies using immunological techniques have identified several ECM molecules being present in adipose culture. Currently, with the emerging usage of microarray and proteomic techniques, novel proteins were discovered that seem to be constituent parts of the adipocyte ECM [67-72]. Mariman *et al*. have summarized various components being a part of the ECM in different adipocyte models [73]. Distinct proteoglycans, a variety of collagens, fibulins, fibronectin, different isoforms of laminin, nidogens and versican, for example, are counted among these matrix components. Different families of ECM molecules in adipocytes are separately discussed in the following sections.

2.1.1. Proteoglycans

GAGs are linear unbranched polymers of repeating disaccharides composed of a hexosamine and an uronic acid. The abundance of carboxyl, hydroxyl, and sulfate groups in these molecules divides them into chondroitin-, dermatin-, keratin-, and heparin-sulfate GAGs and gives them distinct physical properties [63]. One or more GAG chains are covalently linked to core proteins resulting in the formation of proteoglycans [74]. The structure and function of proteoglycans in cartilage have been extensively studied by many researchers [75-77], but much less attention has been given to proteoglycans in adipose tissue.

The major proteoglycans expressed by mature adipocytes are of high molecular weight and contain a large amount of heparan and chondroitin sulfates [78]. Particularly, the chondroitin sulfate proteoglycan versican and hyaluronan were detected in mature 3T3-L1 adipocytes [79,80]. Furthermore, it was reported that the proteoglycans decorin and biglycan were expressed in differentiated 3T3-L1 adipocytes although the level was decreased in comparison to preadipocytes [81]. Decorin was also identified *in vivo* in adipose tissue, primarily adjacent to blood vessels [82]. Additionally, aggrecan was investigated during adipose tissue development in mice. At early differentiation stages, high levels of this chondroitin sulphate/keratin sulphate proteoglycan were observed but during adipocyte maturation, this component was degraded [83]. Another specific proteoglycan which is

distributed in adipose tissue is syndecan-4, a transmembrane heparan sulfate proteoglycan which mediates cell binding [84]. In agreement to this, syndecan-4 and also syndecan-1 expression was shown in 3T3-L1 and 3T3-F442A adipocytes [85,86].

2.1.2. Non-collagenous glycoproteins

During development of adipose cells, the adipocyte ECM converts from a fibronectin-rich stroma to a laminin-rich basal lamina. Laminins together with collagen IV form the main networks of the basement membrane which are connected via nidogen/entactin bridges (Figure 4). These components, i.e., collagen IV, laminin complexes, and nidogen/entactin have been identified in the ECM of murine 3T3-L1 adipocytes by Aratani *et al.* [87]. Alexander *et al.* have also reported nidogen-1/entactin as a prominent component of adipocyte basement membranes [88].

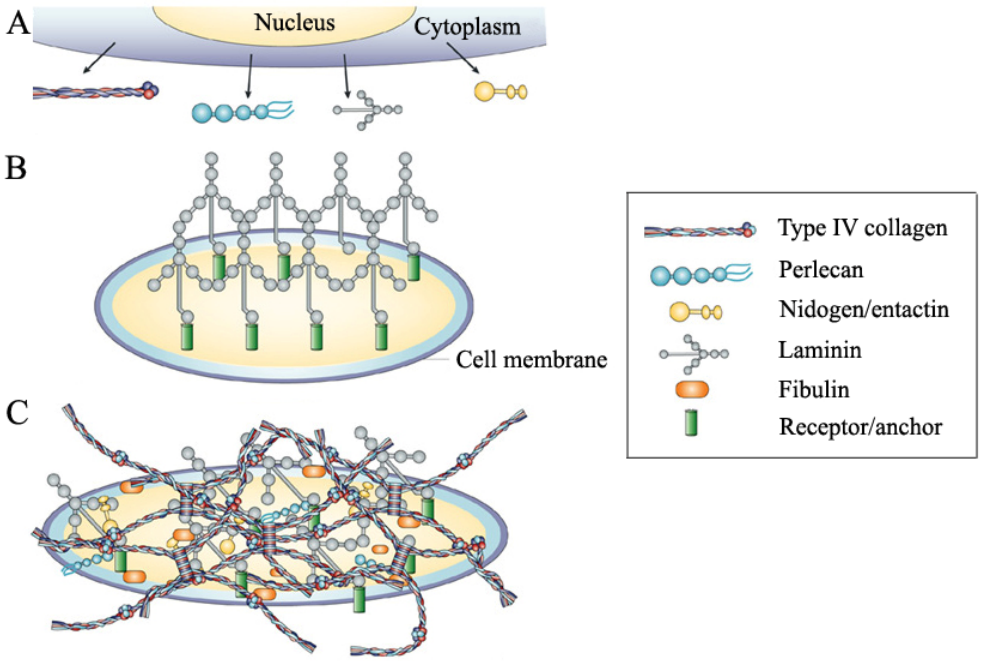

Figure 4: Scaffold formation of the basement membrane. Reprinted with permission from Kalluri *et al.* [89]. ©2010 Nature Publishing Group.
A) Inside the cell, the basement membrane components are assembled into functional units and then secreted into the extracellular space. **B)** Laminins which are anchored to the cells via receptor proteins (integrins, dystroglycans) polymerize and initiate the scaffold formation. **C)** Laminin and collagen type IV networks are connected via nidogen/entactin bridges. The other components interact with this main network resulting in a functional basement membrane.

Another important component of the ECM is fibronectin, a high molecular weight glycoprotein. Previous *in vitro* studies from Pierleoni *et al.* demonstrated that fibronectin is not expressed around mature subcutaneous adipocytes in contrast to laminin [64]. However,

in differentiated bovine intramuscular preadipocytes (BIP), fibronectin and also laminin were detected in the ECM [90].

2.1.3. Collagens

The collagens represent a large and complex family of structurally diverse ECM molecules and are the most abundant proteins in the human body [91]. All collagen molecules are composed of three polypeptide chains referred to as α-chains which are characterized by unique Gly-X-Y motifs. The amino acids hydroxyproline and hydroxylysine are mainly found at the X and Y position [92]. These Gly-X-Y sequences including the hydroxylated forms of proline and lysine are essential for the formation and stability of the triple helix consisting of three identical or different α-chains.

Up to date, 28 different collagens are known which can be classified into several subgroups based on their structure and assemblies [91,93,94]. The different subgroups are presented in Table 1. Collagen XXVIII does not easily fit into any category.

Table 1: Members of the collagen family. The table was modified from Myllyharju *et al.* and Kielty *et al.* [91,94].

A – Fibrillar collagens	
Fibril-forming collagens	Type I, II, III, V, XI, XXIV, XXVII
B – Non-fibrillar collagens	
Basement membrane collagens	Type IV, VII
Short-chain collagens	Type VI, VIII, X
Fibril associated collagens with interrupted triple helices (FACIT)	Type IX, XII, XIV, XVI, XIX, XX, XXI, XXII, XXVI
Transmembrane collagens	Type XIII, XVII, XXIII, XXV
Multiplexin collagens	Type XV, XVIII

The large number of collagen types and their structural diversity implies that they play an important role in numerous different biological functions including adipocyte differentiation [90,92,94,95].

Synthesis of fibril-forming collagens involves many posttranslational modifications that require different modifying enzymes such as hydroxylases, glycosyltransferases, proteinases,

isomerases, and the lysyl oxidase [92,96-99]. At first, the proline and lysine residues are hydroxylated by specific hydroxylases. Notably, collagen-4-prolyl hydroxlase located in the lumen of the endoplasmic reticulum plays a crucial role in collagen synthesis since the 4-hydroxyprolines are essential for the formation of the triple helical molecule [96]. Subsequently, several glycosylation reactions occur at some hydroxylysine and asparagine residues before the three alpha chains assemble to a triple helix which is stabilized by intra- and intermolecular disulfide bonds. Afterwards, the triple helical procollagen molecules are transported from the endoplasmic reticulum through the Golgi stacks into the extracellular space. After cleavage of the C- and N-propeptides from the soluble procollagen molecule, the resulting insoluble collagen molecules self-assemble into fibrils which are covalently cross-linked by oxidation of the amino group in certain lysine and hydroxylysine residues [91,92,94].

Up to date, 20 subunits of 12 different collagen types (type I-VI, XI, XII, XIV, XV, XVIII, and XXIII) have been identified in the adipocyte ECM from rodent cells [73]. A lot of studies showed the presence of the main basement membrane collagen type IV around adipocytes in *in vivo* adipose tissue [64] as well as in *in vitro* adipocyte cultures of different species [87,90]. Additionally to collagen IV, Nakajima *et al.* detected collagen type I, II, III, V, and VI in differentiated BIP preadipocytes, whereas collagen type II was much less abundant [90]. Especially collagen VI which is highly enriched in adipocytes seems to be a specific factor in the adipocyte ECM structure. Collagen VI binds to many cell types and also interacts with other matrix proteins, such as collagen type I, II and IV, fibronectin, hyaluronan, decorin, and biglycan [73,100-104]. Therefore, collagen VI is proposed to be an adaptor molecule which mediates anchoring of the basement membrane to surrounding cells [105].

2.2. Extracellular matrix dynamics during adipogenesis

During adipogenesis, spindle-shaped preadipocytes change their morphology into sphere-shaped adipocytes due to the accumulation of lipids which is accompanied by extensive ECM remodeling, changes in cell-ECM interactions, and cytoskeletal rearrangement. The continuous reorganization of the ECM is primarily regulated by matrix metalloproteinases (MMPs), specific enzymes implicated in the degradation of matrix molecules, and also by tissue inhibitors of MMPs (TIMPs) [106,107]. In human adipose tissue, MMP-2 and -9 are highly expressed and secreted. For the murine 3T3-F442A cell line, a differentiation-dependent secretion of these proteins was demonstrated [108].

The specific structural organization of the ECM components is crucial for the differentiation and maintenance of unilocular adipocytes [65]. However, only few studies focused on the components of the ECM that are associated with the development of the adipocytes and many discrepancies are reported in the literature. One of the first ultrastructural changes is the increase in the levels of laminins, entactin, and GAGs [87,109-111]. Additionally, decreased amounts of cell-associated fibronectin were detected during differentiation of 3T3-L1 and 3T3-F442A resulting in degradation of the fibronectin network [65,87,112,113]. Collagens, the most abundant and best-characterized proteins of the ECM, have also been implicated in the differentiation of adipocytes. Green *et al.* demonstrated that collagens were synthesized at substantial levels in 3T3-L1 preadipocytes [114]. During differentiation of 3T3-L1 preadipocytes into adipocytes, the gene expression of the fibrillar collagens type I and III declined [111], whereas the gene expression of the basement membrane collagen type IV increased [87,111]. However, Dijan *et al.* reported that the levels of collagen type I mRNA were not altered during differentiation of 3T3-F442A adipocytes [115]. Studies from Renes *et al.* confirmed the increased expression of collagen IV during adipogenesis of 3T3-L1 on protein level and additionally, they determined an enhanced collagen V expression [72]. However, concerning collagen I and III, they did not agree with Weiner *et al.* [72,111]. Renes *et al.* suggested a biphasic expression pattern of collagen I, III, and VI during the adipogenic differentiation. Firstly, the expression of collagen I and III decreased, before it increased again at later differentiation stages. A contrary pattern was observed for collagen VI whose expression was initially enhanced and then decreased at later differentiation time points. However, the collagen VI level was finally increased compared to the preadipocyte state [72]. Biphasic expression patterns of various ECM components including collagen VI were also described by other research groups [70]. However, controversial results were presented by Dani *et al.* who described collagen VI as a marker of the preadipose state which is downregulated during adipogenesis [116]. Interestingly, Nakajima *et al.* showed changes in the network structure of this type of collagen. They elucidated that collagen V and VI altered their network structure during the differentiation process from fine and spiny fibrils to a rough and thick network [90]. Kubo *et al.* have also investigated the changes of the collagen network during adipocyte differentiation using stromal vascular cells from mouse adipose tissue [65]. As detected by SEM, collagen networks of type I, III, V, and VI developed and remained well organized through the stages of adipocyte differentiation, whereas the network structure of collagen IV was degraded during adipogenesis [65].

These controversial results from literature reflect the complexity of the adipocyte ECM. In summary, the expression and synthesis of various matrix molecules, particularly collagens, seem to underlay strong changes during adipogenesis that are accompanied by alterations of the structural ECM organization. This specific development and remodeling of the ECM during adipocyte differentiation likely is of crucial significance for adipocyte functions. Thus, disruption of the specifically organized matrix structure, e.g., through inhibition of the collagen synthesis by ethyl-3,4-dihydroxybenzoate (EDHB), results in loss of adipocyte development [90,95].

2.3. Novel culture systems for the investigation of the extracellular matrix

Three-dimensional (3-D) culture systems which create a microenvironment including cell-cell and cell-ECM interactions provide new possibilities to study the complex mechanisms of adipose development and function. Tissue-inherent factors have been recently found to exert influence on cell adhesion, proliferation, differentiation, signal transduction, and other biological responses in various tissues [117] [118]. Many studies showed notable differences in cell morphology, function, and behavior between 2-D and 3-D cell culture systems [118-126] and have demonstrated that cells behave more *in vivo*-like when cultured in 3-D environments [127] [128]. The most currently used adipogenic 3-D constructs, mainly for tissue engineering approaches, consist of polymeric or natural cell carriers in which cells are distributed. However, these 3-D model systems exhibit several drawbacks for the use in basic research. Particularly, the cellular inhomogeneity within the construct due to their size and the resulting insufficient nutrient and oxygen supply constitutes a severe impairment. Furthermore, most of the 3-D constructs contain exogenous materials as scaffolds which may affect the behavior and functions of the cells. Moreover, the cell carrier in which the cells are initially situated separately, prevents the formation of a coherent cellular context, at least at early stages of the culture, resulting in limited cell-cell and cell-matrix interactions [123,129-132]. For other cell types, a novel 3-D model system based on the generation of cellular aggregates was developed which is suggested to form a more homogeneous tissue-like construct [133,134]. These multicellular spheroids are generated according to the liquid overlay technique by seeding adherent cells onto non-adherent surfaces. As a consequence, cells are forced to aggregate to multicellular spheroids. Thus, from the beginning of the culture, the cells are closely connected and secrete their own ECM resulting in a coherent tissue-like context. Recently, an adipogenic spheroid model with 3T3-L1 cells was developed by our group [135]. Additionally, Wang *et al.* have introduced a similar adipogenic spheroid

model with multipotent mesenchymal stem cells. However, their spheroid culture technique was based on photolithography and micropatterning techniques [136].

3. Adipocyte culture in reconstructive and plastic surgery

3.1. Injection Lipolysis

The subcutaneous injection of phosphatidylcholine into adipose tissue is an increasingly popular therapy for aesthetic approaches to reduce the volume of smaller fat depositions such as accumulations on the waist and hip, lower eyelid fat herniation, and lipomas [137-140]. This fat dissolution therapy is often referred to as injection lipolysis and is instructed in Germany by the "Network Lipolysis" [137]. Notably, injection lipolysis is restricted to small fat accumulations and is not a slimming treatment for obese humans. Soy-derived PC which is available as Lipostabil® (Natterman & Cie GmbH, Köln, Germany) is often used for the treatment of localized fat accumulation by this procedure [138,139,141-144]. Originally, Lipostabil® was approved as an intravenous therapy to treat hyperlipidemia, peripheral vascular disease, cardiac ischemia, and liver disease [145-150]. However, to date, the subcutaneous injection of Lipostabil® is not licensed and, therefore, injection lipolysis is used as an "off-label" practice which means the use of Lipostabil® aside from its initial field of application.

The Lipostabil® formula is mainly composed of PC and sodium deoxycholate (DC) which is responsible for the aqueous solubility of PC by forming mixed micelles [142,151,152]. Benzyl alcohol is supplemented as a preservative into the formula. In injection lipolysis therapy, many physicians combine the Lipostabil® preparation with various additives, e.g., vasodilators, aminophylline, vitamins or lidocaine in order to increase the fat reducing effect and, respectively, to minimize side effect [153].

The mechanisms by which Lipostabil® causes localized fat reduction are unknown so far. Both PC and DC are proposed to be the actively fat-dissolving component in the Lipostabil® formula. PC has a large influence on the regulation of lipid homeostasis. It has effects on lowering TG and cholesterol levels, increases high density lipoproteins in the cholesterol metabolism, and dissolves atherosclerotic plaques [137,154]. Bobkova *et al.* have demonstrated that PC also influences the receptor properties of cell membranes accompanied by increased insulin sensitivity and lipolysis [149]. In injection lipolysis, it is supposed that one mechanism of action of PC is related to compromising the adipocyte membrane resulting in the secretion of triglyceride-rich lipoproteins [137,140]. Furthermore, PC is proposed to

have a lipolytic action by stimulating the activity of lipases. The resulting monoglycerides are emulsified by PC and further transported to the liver and metabolized by beta-oxidation [137,142,155]. However, Rotunda *et al.* have taken the view that DC is responsible for the fat-dissolving effect by its detergent action [140]. As other detergents, bile salts including DC act as potent solubilizers of lipid bilayers [151,156-158]. Recently, it has been demonstrated that DC caused nonspecific cell membrane lysis in cultured cells *in vitro* [140]. Rotunda *et al.* have also shown that the injection of DC into human lipomas induced focal necrosis, acute inflammation, and hemorrhage as detected histologically [159]. Moreover, in tissue biopsies, the architectural organization of fat and muscle tissue was strongly affected by DC in contrast to epidermis and dermis on which DC had less profound effects [140]. A cytolytic effect of Lipostabil® on various cell types, i.e., preadipocytes, vascular smooth muscle cells, skeletal myotubes, and renal epithelial cells was additionally demonstrated in other studies [160,161]. Histological evaluation of lipomas exhibited that the necrosis of fat cells after treatment with Lipostabil® was accompanied by an inflammatory reaction similar to panniculitis [162]. The local inflammation was characterized by the infiltration of granulocytes, lymphocytes as well as macrophages and an increased expression of pro-inflammatory cytokines such as TNF-α, interferon-γ (INF-γ), and several interleukins (e.g. interleukin 6, 8 and 10) [163].

Nevertheless, to date, the subcutaneous injection of Lipostabil® has not been associated with serious adverse effects. The observed complications were relatively rare, mild, and temporary [164]. The most frequently observed side effects after injection included transient burning, edema and erythema at the injection site, swelling, persistent pain beyond two weeks, late itching, hyperpigmentation, hives, bacterial infections, and skin contour deformities [141,143,153]. Lipid, liver and renal profiles did not change after treatment with PC [142]. No patients were reported to die or need hospitalization. It has been shown that the fat deposits did not return for approximately four years, but if necessary, the application may be repeated [141].

However, due to lack of scientific studies, the safety and efficacy of injection lipolysis has still remained ambiguous to many patients and physicians. Thus, in order to further establish injection lipolysis as a serious option in plastic surgery, investigations into the mechanisms of action are indispensable.

3.2. Adipose tissue engineering

3.2.1. Clinical need for adipose tissue augmentation

Largely defected adipose tissue caused by congenital abnormalities, tumor resections or traumas such as large burns or chronically open wounds does not regenerate spontaneously and requires tissue reconstruction. Increasingly, transplantable and, ideally, biologically functional adipose tissue substitutes appear promising to restore a variety of soft tissue defects in reconstructive and plastic surgery. Cosmetic and aesthetic surgeons are also interested in natural adipose tissue grafts in order to compensate disfigurement. Thereby, the generated substitutes should be equivalent to native adipose tissue concerning its cellular and extracellular composition and organization as well as its biological functions to guarantee integration of the engineered construct into the host tissue including rapid and sufficient vascularization.

3.2.2. Strategies for adipose tissue augmentation

Currently, different strategies are used to augment soft tissue defects in clinical practice. One strategy to treat smaller deformities is the single-cell injection of mature adipocytes which, however, is an out-dated method for tissue augmentation without promising outcome. The exposure of the fragile adipocytes to the mechanical forces of liposuction results in about 90% traumatized adipocytes leading to cyst formation and localized necrosis after injection [165,166].

Another strategy, especially for reconstruction of larger tissue defects, e.g. after breast tumor resection, includes the implantation of autologous fat tissue. Even if this implant seems to be ideal in terms of biocompatibility and immune response, graft resorption due to insufficient neovascularization limits its application [167].

A third strategy for adipose tissue augmentation is the induction of *de novo* adipogenesis *in vivo*. Without the application of exogenous cells, adipose tissue-inducing substances or/and materials are administered which supports the development of adipose tissue *in vivo*. This acellular approach avoids the time- and cost-intensive *in vitro* cell culture and, additionally, the problem of immunological compatibility of the cells [167].

Tissue engineering represents a new promising alternative to augment adipose tissue. For engineering 3-D adipose tissue constructs, cells are isolated from the donor tissue and, subsequently, propagated *in vitro* until a sufficient number is available (Figure 5). Afterwards, the scaffold is seeded with the propagated cells which can be differentiated *in vitro*, before the

cell-containing construct is re-implanted into the host. The several components of tissue engineering strategies, i.e., cells, cell carriers and tissue-inducing substances are discussed in detail in the following sections.

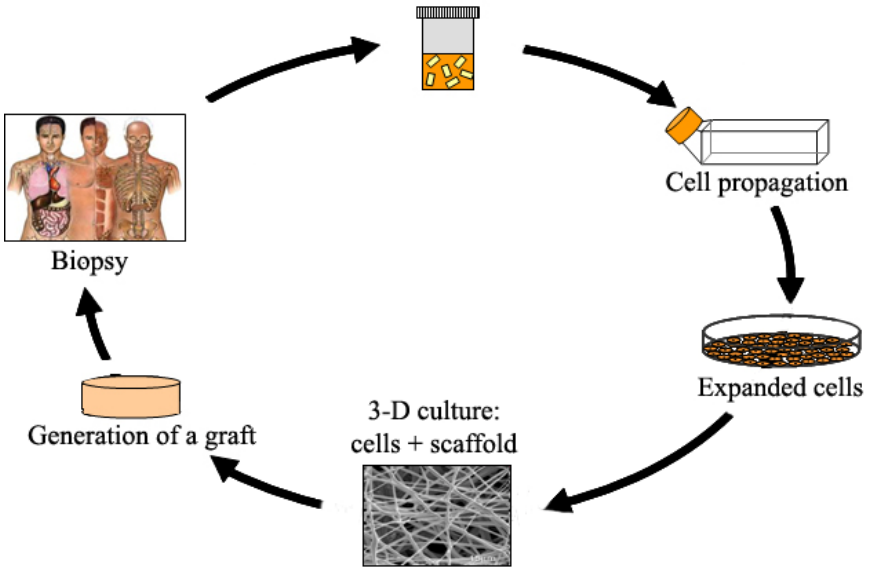

Figure 5: Strategy of cell-based tissue engineering approaches. Cells are isolated from the donor, expanded in monolayer culture *in vitro* and then seeded onto or into cell carriers. The cell-containing construct can be directly re-implanted or after previous *in vitro* cultivation.

3.2.3. Components needed for adipose tissue engineering

3.2.3.1 Cell sources

The use of suitable cells is crucial for successful transplantation of adipose tissue engineered substitutes. The cells have to be autologous or nonimmunogenic, and also have to be available in sufficient quantities. The abundance of some cells, e.g. bone marrow derived mesenchymal stem cells (BMSCs) is very low after isolation and, therefore, requires an *in vitro* expansion to obtain sufficient cell quantities for clinical therapies [168]. However, the propagation of cells is sometimes accompanied by the decline of their proliferation and differentiation potential, which, therefore, has to be monitored [169,170]. Furthermore, the harvest of cells should occur with minimally invasive procedures that are standardized as well as the processing procedures.

Mature adipocytes

The characteristics of mature adipocytes make them an inapplicable source for regenerative medicine. Due to their high lipid content, these cells are very fragile resulting in a vast majority of traumatized adipocytes during isolation and processing procedures [165]. Even if

these cells can principally be cultured *in vitro*, culturing is difficult to perform because of the buoyancy of the lipid-filled cells [171,172] and the incapability to proliferate due to their terminal differentiation state [165].

Preadipocyte cell lines

Murine preadipocyte cell lines such as the 3T3-L1 and 3T3-F442A preadipocytes are widely used in basic research and also for characterization of adipose tissue engineering principles [123,129,130,166,173]. These preadipocyte cell lines have the advantage that they are well characterized, easily to expand and uniform in their differentiation potential. However, for clinical therapies, cell lines are not beneficial due to their aneuploid status and xenogeneic origin [167].

Embryonic stem cells

The tremendous proliferation and differentiation potential suggest the embryonic stem cells to be a highly promising cell source for repair of soft tissue defects [174,175]. However, up to date, only a limited number of studies are performed for adipose tissue engineering [131,176], primarily due to ethical concerns and legal constraints which limit the application and availability of human embryonic stem cells. Nevertheless, embryonic stem cell lines from other species, such as mouse models are available and are used for basic research.

Adipose-derived stem cells

Adipose tissue is an abundant and easily obtained tissue and was previously identified as an alternative cell source of autologous stem cells for engineering tissues. The stromal vascular fraction of adipose tissue can be easily harvested in a large quantity by enzymatic digestion of lipoaspirates or liposections and, subsequently, cultured, expanded and differentiated *in vitro* [177]. This cell fraction represents a heterogeneous cell pool containing, among others, noncommitted multipotent stem cells that have the capacity to differentiate into several mesenchymal lineages including adipocytes [178,179]. A lot of different designations, such as adipose-derived stem cells, adipose-derived stromal cells, stromal vascular fraction, preadipocytes etc. are used in literature for this isolated cell population. In accordance to the International Fat Applied Technology Society (IFATS) [180], this cell pool is denominated adipose-derived stem cells (ADSCs) in this work. ADSCs can be expanded *in vitro* over several passages without senescing or loosing their adipogenic differentiation potential [177,181]. Previous studies have reported that yield, growth, and differentiation characteristics are influenced by the handling of the cells including isolation and harvest but also by the age, sex, and health status of the donor as well as by the donor site (epididymal, mammary, subcutaneous, omentum, etc.) [182-185].

Bone marrow-derived stem cells

Mesenchymal stem cells can also be isolated from bone marrow aspirates derived from the iliac crest or bone marrow biopsies [186] and were accordingly designated bone marrow-derived stem cells (BMSCs). Similar to ADSCs, BMSCs have a high self-renewal potential and are able to differentiate into adipocytes, chondrocytes, osteoblasts, neurons, and myoblasts *in vitro* and *in vivo* [168,187]. Unfortunately, in contrast to ADSCs, the use of BMSCs is limited because of their invasive isolation procedure and the low yield of stem cells being present in bone marrow [168,188,189]. Therefore, significant *in vitro* propagation of BMSCs is necessary resulting in the decrease of their proliferation and multilineage differentiation capacity [168-170,190,191].

The properties of ADSCs and BMSCs are highly similar regarding to morphology, differentiation capacity, expression of main marker genes, gene expression, and cytokine profiles [192-194]. However, based on gene expression studies, BMSCs have been reported to show a higher capacity to differentiate into osteoblasts and chondrocytes compared to ADSCs whose differentiation ability towards adipocytes appears to be slightly better [195].

In conclusion, although both ADSCs and BMSCs are appropriate cell sources for adipose tissue engineering approaches, ADSCs currently appear to be the most promising cell source for clinical therapies due to their easy harvesting conditions, high abundance, and adipogenic differentiation capacity [167,196,197].

3.2.3.2 Cell carriers

Cells can be seeded onto or into an artificial structure referred to as scaffold which mainly gives mechanical support for the formation of a 3-D tissue engineered construct that is subsequently implanted into the host tissue. For successful repair of soft tissue defects, the scaffold materials have to meet different requirements such as biocompatibility and biodegradability. Furthermore, the material has to provide a structure and chemistry allowing cell attachment, distribution as well as differentiation and supporting the maintenance of the biological functions of the cells. For this, the structure of the scaffold must be highly porous and interconnective and additionally facilitates capillary ingrowth, nutrient, and oxygen supply [167]. Especially for adipose tissue constructs, large pore sizes within the scaffolds are required to enable enlargement of the adipocytes during their maturation [198]. During recent years, novel cell carrier principles have been developed. Aside from the implantable porous scaffolds, injectable sytems such as hydrogels or microspheres in which the cells are encapsulated or to which they are attached, have been used.

Implantable porous scaffolds

In many previous studies of different adipose tissue engineering approaches, the used scaffold materials consisted of synthetic polymers, such as polylactic acid (PLA), polyglycolic acid (PGA), and poly(lactic-co-glycolic) acid (PLGA) [123,199,200]. However, possible limitations may be caused by their acidic degradation products affecting cell functions and the lack of chemically reactive groups which makes the polymers easily accessible for surface modifications. Recent studies have reported that modifications of these scaffolds such as electrospun nanofibrous PLA scaffolds or PLGA hollow fiber scaffolds encapsulated within hydrogel capsules promote the adipogenic development of the engineered substitutes *in vitro* and *in vivo* [201,202].

Other synthetic scaffolds that were used for characterization of adipose tissue engineering approaches are composed of polyethylene terephthalate or electrospun polycaprolactone [130,131]. However, the seeding and culturing of these two cell carriers with adipogenic precursor cells did not result in the formation of a coherent adipose tissue.

Scaffolds do not have to be made of synthetic origin, they also can be composed of natural materials, e.g. silk. Mauney *et al.* have recently investigated the adipogenic development of human ADSCs and BMSCs integrated in silk fibroin-derived scaffolds *in vitro* [203]. Even if further *in vivo* studies have shown that the development of adipose tissue was marginal four weeks after implantation, the silk scaffolds proved to be resistant to degradation and thus, guaranteed a longer-term integrity compared to collagen or PLA scaffolds.

For creating a cellular environment more resembling the one within adipose tissue, porous scaffolds composed of ECM compounds are used which are additionally characterized by low toxicity. Besides the application of collagen and hyaluronic acid esters sponges for adipose reconstruction [198,204,205], it is also possible to use autologous ECM materials derived from diverse tissues, e.g., adipose tissue ECM or placental ECM, resulting in minimized immunological response [206-208].

Injectable hydrogels and microspheres

Hydrogels represent an alternative type of cell carrier as they are less invasive resulting in a reduced risk of infections and scarring. Hydrogels can be applied as injectables which is advantageous for filling irregularly shaped defect sites and as implants if gelling occurs in advance *in vitro*. In both cases, the cells are encapsulated within the gel during formation.

Similar to porous scaffolds, hydrogels can be composed of synthetic materials such as polyethylene glycol (PEG), PEG-diacrylate and Pluronic F-127 [176,209-211] or natural materials like alginate [212]. Additionally, hydrogels consisting of various ECM components

such as collagen, hyaluronan or fibrin have been successfully used in adipose tissue engineering [213-218]. Among these, fibrin glue is already approved by the Food and Drug Administration (FDA) for a variety of clinical applications. A specialized ECM hydrogel represents Matrigel, an ECM extract derived from Engelbreth-Holm-Swarm mouse sarcoma. This gel contains the main components of basement membranes, i.e., proteoglycans, laminin, collagen type IV as well as nidogen/entactin, and additionally various growth factors such as platelet-derived growth factor (PDGF), transforming growth factor β (TGF-β), and basic fibroblast growth factor (bFGF). It was reported that this hydrogel has a promoting effect on adipogenesis and angiogenesis *in vivo* [219,220]. Unfortunately, Matrigel is a mouse tumor product and therefore, its clinical use is limited. A promising alternative to Matrigel that is comparably rich in ECM components is the recently developed Myogel and an adipose protein-derived as well as dermis-derived gel [221-223]. However, their utility for clinical applications has not been extensively studied, yet.

Another injectable application strategy is the use of microspheres to which adipogenic precursor cells are attached. Different kinds of microspheres such as PLGA microspheres [224-227], alginate beads [228], porous collagenous microbeads [229], human ECM powders derived from adipose tissue [230] or particulate small intestinal submoca microparticles [231] were investigated with regard to their utility for adipose tissue engineering.

3.2.3.3 Adipose tissue-inducing substances

Adipose tissue-inducing substances include a variety of growth factors as well as biological and pharmaceutical agents promoting adipogenesis *in vitro* and *in vivo*.

As mentioned above, the generation of adipose tissue substitutes often requires the *in vitro* expansion of adipogenic precursor cells. Several growth factors such as insulin-like growth factors (IGF-1, IGF-2), acidic FGF, bFGF, epidermal growth factor (EGF), and PDGF were identified to stimulate the proliferation of ADSCs and BMSCs. However, some of these growth factors are also able to influence the adipogenesis of precursor cells. Basic FGF was reported to be a positive stimulator for the adipogenic conversion of BMSCs [200] and ADSCs [232] whereas the effect of this growth factor is controversially discussed in literature. Gregoire *et al.* have reported that bFGF acts as an adipogenic inhibitor in preadipocyte cell lines and ADSCs [9]. Basic FGF or other inducing substances such as IGF-1 or insulin have been repeatedly applied in combination with distinct biomaterials, such as Matrigel or microspheres to induce *de novo* adipogenesis *in vivo* [220,233-238]. With regard to adipose tissue development, the combination of the substances was more effective than

when applied alone. So far, it is unclear whether bFGF modulates adipogenesis by directly affecting the adipocytes or whether it modulates adipogenesis indirectly through its angiogenic effect.

In conclusion, during the recent years, many promising approaches have emerged in adipose tissue engineering to reconstruct fat substitutes for reconstructive and plastic surgery as well as for basic science. Various types of cell carriers and cell sources enabling adipose tissue development have been characterized. Several studies have shown that a long-term survival of distinct engineered construct was successful over a period of six months and beyond. However, the size of generated constructs still rarely exceeds one milliliter. Thus, further improvements are required regarding long-term maintenance and optimal vascularization to finally generate a standardized, coherent, and functional adipose tissue graft of considerable size which can be successfully used for clinical applications.

References

1. Ailhaud G, Grimaldi P, Negrel R. Cellular and molecular aspects of adipose tissue development. *Annu.Rev.Nutr.* 1992; **12:** 207-233.
2. Niemela S M, Miettinen S, Konttinen Y, Waris T, Kellomaki M, Ashammakhi N A, Ylikomi T. Fat tissue: views on reconstruction and exploitation. *J.Craniofac.Surg.* 2007; **18:** 325-335.
3. Frayn K N, Karpe F, Fielding B A, Macdonald I A, Coppack S W. Integrative physiology of human adipose tissue. *Int.J.Obes.Relat Metab Disord.* 2003; **27:** 875-888.
4. Fruhbeck G. Overview of adipose tissue and its role in obesity and metabolic disorders. *Methods Mol.Biol.* 2008; **456:** 1-22.
5. Trayhurn P. Adipocyte biology. *Obes.Rev.* 2007; **8 Suppl 1:** 41-44.
6. Wozniak S E, Gee L L, Wachtel M S, Frezza E E. Adipose tissue: the new endocrine organ? A review article. *Dig.Dis.Sci.* 2009; **54:** 1847-1856.
7. Rosen E D, Spiegelman B M. Molecular regulation of adipogenesis. *Annu.Rev.Cell Dev.Biol.* 2000; **16:** 145-171.
8. Napolitano L. The differentiation of white adipose cells. An electron microscope study. *J.Cell Biol.* 1963; **18:** 663-679.
9. Gregoire F M, Smas C M, Sul H S. Understanding adipocyte differentiation. *Physiol Rev.* 1998; **78:** 783-809.
10. Diamond F B, Jr., Eichler D C. Leptin and the adipocyte endocrine system. *Crit Rev.Clin.Lab Sci.* 2002; **39:** 499-525.
11. Zhang Y, Proenca R, Maffei M, Barone M, Leopold L, Friedman J M. Positional cloning of the mouse obese gene and its human homologue. *Nature* 1994; **372:** 425-432.
12. Kershaw E E, Flier J S. Adipose tissue as an endocrine organ. *J.Clin.Endocrinol.Metab* 2004; **89:** 2548-2556.
13. Ahima R S, Flier J S. Adipose tissue as an endocrine organ. *Trends Endocrinol.Metab* 2000; **11:** 327-332.
14. Lefterova M I, Lazar M A. New developments in adipogenesis. *Trends Endocrinol.Metab* 2009; **20:** 107-114.
15. Otto T C, Lane M D. Adipose development: from stem cell to adipocyte. *Crit Rev.Biochem.Mol.Biol.* 2005; **40:** 229-242.
16. Saltiel A R. You are what you secrete. *Nat.Med.* 2001; **7:** 887-888.
17. Flier J S. Diabetes. The missing link with obesity? *Nature* 2001; **409:** 292-293.
18. Trayhurn P. Endocrine and signalling role of adipose tissue: new perspectives on fat. *Acta Physiol Scand.* 2005; **184:** 285-293.
19. Hotamisligil G S, Peraldi P, Budavari A, Ellis R, White M F, Spiegelman B M. IRS-1-mediated inhibition of insulin receptor tyrosine kinase activity in TNF-alpha- and obesity-induced insulin resistance. *Science* 1996; **271:** 665-668.
20. Kern P A, Saghizadeh M, Ong J M, Bosch R J, Deem R, Simsolo R B. The expression of tumor necrosis factor in human adipose tissue. Regulation by obesity, weight loss, and relationship to lipoprotein lipase. *J.Clin.Invest* 1995; **95:** 2111-2119.
21. Frederich R C, Jr., Kahn B B, Peach M J, Flier J S. Tissue-specific nutritional regulation of angiotensinogen in adipose tissue. *Hypertension* 1992; **19:** 339-344.

22. Jones B H, Standridge M K, Moustaid N. Angiotensin II increases lipogenesis in 3T3-L1 and human adipose cells. *Endocrinology* 1997; **138:** 1512-1519.

23. Alessi M C, Peiretti F, Morange P, Henry M, Nalbone G, Juhan-Vague I. Production of plasminogen activator inhibitor 1 by human adipose tissue: possible link between visceral fat accumulation and vascular disease. *Diabetes* 1997; **46:** 860-867.

24. Lundgren C H, Brown S L, Nordt T K, Sobel B E, Fujii S. Elaboration of type-1 plasminogen activator inhibitor from adipocytes. A potential pathogenetic link between obesity and cardiovascular disease. *Circulation* 1996; **93:** 106-110.

25. Cornelius P, MacDougald O A, Lane M D. Regulation of adipocyte development. *Annu.Rev.Nutr.* 1994; **14:** 99-129.

26. MacDougald O A, Mandrup S. Adipogenesis: forces that tip the scales. *Trends Endocrinol.Metab* 2002; **13:** 5-11.

27. Tang Q Q, Otto T C, Lane M D. Mitotic clonal expansion: a synchronous process required for adipogenesis. *Proc.Natl.Acad.Sci.U.S.A* 2003; **100:** 44-49.

28. Tang Q Q, Zhang J W, Daniel L M. Sequential gene promoter interactions by C/EBPbeta, C/EBPalpha, and PPARgamma during adipogenesis. *Biochem.Biophys.Res.Commun.* 2004; **318:** 213-218.

29. Reichert M, Eick D. Analysis of cell cycle arrest in adipocyte differentiation. *Oncogene* 1999; **18:** 459-466.

30. Wu Z, Puigserver P, Spiegelman B M. Transcriptional activation of adipogenesis. *Curr.Opin.Cell Biol.* 1999; **11:** 689-694.

31. Tontonoz P, Spiegelman B M. Fat and beyond: the diverse biology of PPARgamma. *Annu.Rev.Biochem.* 2008; **77:** 289-312.

32. Rosen E D, Sarraf P, Troy A E, Bradwin G, Moore K, Milstone D S, Spiegelman B M, Mortensen R M. PPAR gamma is required for the differentiation of adipose tissue in vivo and in vitro. *Mol.Cell* 1999; **4:** 611-617.

33. Christy R J, Kaestner K H, Geiman D E, Lane M D. CCAAT/enhancer binding protein gene promoter: binding of nuclear factors during differentiation of 3T3-L1 preadipocytes. *Proc.Natl.Acad.Sci.U.S.A* 1991; **88:** 2593-2597.

34. Schwarz E J, Reginato M J, Shao D, Krakow S L, Lazar M A. Retinoic acid blocks adipogenesis by inhibiting C/EBPbeta-mediated transcription. *Mol.Cell Biol.* 1997; **17:** 1552-1561.

35. Kim J B, Spiegelman B M. ADD1/SREBP1 promotes adipocyte differentiation and gene expression linked to fatty acid metabolism. *Genes Dev.* 1996; **10:** 1096-1107.

36. Farmer S R. Transcriptional control of adipocyte formation. *Cell Metab* 2006; **4:** 263-273.

37. Rosen E D, MacDougald O A. Adipocyte differentiation from the inside out. *Nat.Rev.Mol.Cell Biol.* 2006; **7:** 885-896.

38. Shimba S, Ishii N, Ohta Y, Ohno T, Watabe Y, Hayashi M, Wada T, Aoyagi T, Tezuka M. Brain and muscle Arnt-like protein-1 (BMAL1), a component of the molecular clock, regulates adipogenesis. *Proc.Natl.Acad.Sci.U.S.A* 2005; **102:** 12071-12076.

39. Large V, Peroni O, Letexier D, Ray H, Beylot M. Metabolism of lipids in human white adipocyte. *Diabetes Metab* 2004; **30:** 294-309.

40. Large V, Arner P. Regulation of lipolysis in humans. Pathophysiological modulation in obesity, diabetes, and hyperlipidaemia. *Diabetes Metab* 1998; **24:** 409-418.

41. Arner P. Insulin resistance in type 2 diabetes: role of fatty acids. *Diabetes Metab Res.Rev.* 2002; **18 Suppl 2:** S5-S9.

42. Blaak E E. Fatty acid metabolism in obesity and type 2 diabetes mellitus. *Proc.Nutr.Soc.* 2003; **62:** 753-760.

43. Boden G, Shulman G I. Free fatty acids in obesity and type 2 diabetes: defining their role in the development of insulin resistance and beta-cell dysfunction. *Eur.J.Clin.Invest* 2002; **32 Suppl 3:** 14-23.

44. Bergman R N, Van Citters G W, Mittelman S D, Dea M K, Hamilton-Wessler M, Kim S P, Ellmerer M. Central role of the adipocyte in the metabolic syndrome. *J.Investig.Med.* 2001; **49:** 119-126.

45. Zechner R, Strauss J G, Haemmerle G, Lass A, Zimmermann R. Lipolysis: pathway under construction. *Curr.Opin.Lipidol.* 2005; **16:** 333-340.

46. Zimmermann R, Strauss J G, Haemmerle G, Schoiswohl G, Birner-Gruenberger R, Riederer M, Lass A, Neuberger G, Eisenhaber F, Hermetter A, Zechner R. Fat mobilization in adipose tissue is promoted by adipose triglyceride lipase. *Science* 2004; **306:** 1383-1386.

47. Fredrikson G, Tornqvist H, Belfrage P. Hormone-sensitive lipase and monoacylglycerol lipase are both required for complete degradation of adipocyte triacylglycerol. *Biochim.Biophys.Acta* 1986; **876:** 288-293.

48. Potter B J, Sorrentino D, Berk P D. Mechanisms of cellular uptake of free fatty acids. *Annu.Rev.Nutr.* 1989; **9:** 253-270.

49. Frayn K N, Humphreys S M, Coppack S W. Fuel selection in white adipose tissue. *Proc.Nutr.Soc.* 1995; **54:** 177-189.

50. Holm C, Osterlund T, Laurell H, Contreras J A. Molecular mechanisms regulating hormone-sensitive lipase and lipolysis. *Annu.Rev.Nutr.* 2000; **20:** 365-393.

51. Londos C, Brasaemle D L, Schultz C J, Adler-Wailes D C, Levin D M, Kimmel A R, Rondinone C M. On the control of lipolysis in adipocytes. *Ann.N.Y.Acad.Sci.* 1999; **892:** 155-168.

52. Tansey J T, Sztalryd C, Hlavin E M, Kimmel A R, Londos C. The central role of perilipin a in lipid metabolism and adipocyte lipolysis. *IUBMB.Life* 2004; **56:** 379-385.

53. Zhang H H, Souza S C, Muliro K V, Kraemer F B, Obin M S, Greenberg A S. Lipase-selective functional domains of perilipin A differentially regulate constitutive and protein kinase A-stimulated lipolysis. *J.Biol.Chem.* 2003; **278:** 51535-51542.

54. Langin D. Adipose tissue lipolysis as a metabolic pathway to define pharmacological strategies against obesity and the metabolic syndrome. *Pharmacol.Res.* 2006; **53:** 482-491.

55. Taleb S, Cancello R, Clement K, Lacasa D. Cathepsin s promotes human preadipocyte differentiation: possible involvement of fibronectin degradation. *Endocrinology* 2006; **147:** 4950-4959.

56. Shakur Y, Holst L S, Landstrom T R, Movsesian M, Degerman E, Manganiello V. Regulation and function of the cyclic nucleotide phosphodiesterase (PDE3) gene family. *Prog.Nucleic Acid Res.Mol.Biol.* 2001; **66:** 241-277.

57. Ruan H, Lodish H F. Insulin resistance in adipose tissue: direct and indirect effects of tumor necrosis factor-alpha. *Cytokine Growth Factor Rev.* 2003; **14:** 447-455.

58. Sengenes C, Bouloumie A, Hauner H, Berlan M, Busse R, Lafontan M, Galitzky J.

Involvement of a cGMP-dependent pathway in the natriuretic peptide-mediated hormone-sensitive lipase phosphorylation in human adipocytes. *J.Biol.Chem.* 2003; **278:** 48617-48626.

59. Souza S C, de Vargas L M, Yamamoto M T, Lien P, Franciosa M D, Moss L G, Greenberg A S. Overexpression of perilipin A and B blocks the ability of tumor necrosis factor alpha to increase lipolysis in 3T3-L1 adipocytes. *J.Biol.Chem.* 1998; **273:** 24665-24669.
60. Gasic S, Tian B, Green A. Tumor necrosis factor alpha stimulates lipolysis in adipocytes by decreasing Gi protein concentrations. *J.Biol.Chem.* 1999; **274:** 6770-6775.
61. Rahn L T, Mei J, Karlsson M, Manganiello V, Degerman E. Down-regulation of cyclic-nucleotide phosphodiesterase 3B in 3T3-L1 adipocytes induced by tumour necrosis factor alpha and cAMP. *Biochem.J.* 2000; **346 Pt 2:** 337-343.
62. Mei J, Holst L S, Landstrom T R, Holm C, Brindley D, Manganiello V, Degerman E. C(2)-ceramide influences the expression and insulin-mediated regulation of cyclic nucleotide phosphodiesterase 3B and lipolysis in 3T3-L1 adipocytes. *Diabetes* 2002; **51:** 631-637.
63. Rozario T, Desimone D W. The extracellular matrix in development and morphogenesis: A dynamic view. *Dev.Biol.* 2009.
64. Pierleoni C, Verdenelli F, Castellucci M, Cinti S. Fibronectins and basal lamina molecules expression in human subcutaneous white adipose tissue. *Eur.J.Histochem.* 1998; **42:** 183-188.
65. Kubo Y, Kaidzu S, Nakajima I, Takenouchi K, Nakamura F. Organization of extracellular matrix components during differentiation of adipocytes in long-term culture. *In Vitro Cellular & Developmental Biology-Animal* 2000; **36:** 38-44.
66. Haraida S, Nerlich A G, Wiest I, Schleicher E, Lohrs U. Distribution of basement membrane components in normal adipose tissue and in benign and malignant tumors of lipomatous origin. *Mod.Pathol.* 1996; **9:** 137-144.
67. Burton G R, Guan Y, Nagarajan R, McGehee R E, Jr. Microarray analysis of gene expression during early adipocyte differentiation. *Gene* 2002; **293:** 21-31.
68. Soukas A, Socci N D, Saatkamp B D, Novelli S, Friedman J M. Distinct transcriptional profiles of adipogenesis in vivo and in vitro. *J.Biol.Chem.* 2001; **276:** 34167-34174.
69. Alvarez-Llamas G, Szalowska E, de Vries M P, Weening D, Landman K, Hoek A, Wolffenbuttel B H, Roelofsen H, Vonk R J. Characterization of the human visceral adipose tissue secretome. *Mol.Cell Proteomics.* 2007; **6:** 589-600.
70. Molina H, Yang Y, Ruch T, Kim J W, Mortensen P, Otto T, Nalli A, Tang Q Q, Lane M D, Chaerkady R, Pandey A. Temporal profiling of the adipocyte proteome during differentiation using a five-plex SILAC based strategy. *J.Proteome.Res.* 2009; **8:** 48-58.
71. Welsh G I, Griffiths M R, Webster K J, Page M J, Tavare J M. Proteome analysis of adipogenesis. *Proteomics.* 2004; **4:** 1042-1051.
72. Renes J, Bouwman F, Noben J P, Evelo C, Robben J, Mariman E. Protein profiling of 3T3-L1 adipocyte differentiation and (tumor necrosis factor alpha-mediated) starvation. *Cell Mol.Life Sci.* 2005; **62:** 492-503.
73. Mariman E C, Wang P. Adipocyte extracellular matrix composition, dynamics and role in obesity. *Cell Mol.Life Sci.* 2010.

74. Hardingham T E, Fosang A J. Proteoglycans: many forms and many functions. *The FASEB Journal* 1992; **6:** 861-870.

75. Knudson C B, Knudson W. Cartilage proteoglycans. *Semin.Cell Dev.Biol.* 2001; **12:** 69-78.

76. Roughley P J. The structure and function of cartilage proteoglycans. *Eur.Cell Mater.* 2006; **12:** 92-101.

77. Watanabe H, Yamada Y, Kimata K. Roles of aggrecan, a large chondroitin sulfate proteoglycan, in cartilage structure and function. *J.Biochem.* 1998; **124:** 687-693.

78. Wilsie L C, Chanchani S, Navaratna D, Orlando R A. Cell surface heparan sulfate proteoglycans contribute to intracellular lipid accumulation in adipocytes. *Lipids Health Dis.* 2005; **4:** 2.

79. Calvo J C, Rodbard D, Katki A, Chernick S, Yanagishita M. Differentiation of 3T3-L1 preadipocytes with 3-isobutyl-1-methylxanthine and dexamethasone stimulates cell-associated and soluble chondroitin 4-sulfate proteoglycans. *J.Biol.Chem.* 1991; **266:** 11237-11244.

80. Zizola C F, Julianelli V, Bertolesi G, Yanagishita M, Calvo J C. Role of versican and hyaluronan in the differentiation of 3T3-L1 cells into preadipocytes and mature adipocytes. *Matrix Biol.* 2007; **26:** 419-430.

81. Ajuwon K M, Cruz M, Buhman K. Changes in ECM proteins, decorin and biglycan, during adipogenesis in 3T3-L1 cells and in adipose tissue of mice on a high fat diet. *The FASEB Journal* 2009; **23:** 1022.

82. Bolton K, Segal D, McMillan J, Jowett J, Heilbronn L, Abberton K, Zimmet P, Chisholm D, Collier G, Walder K. Decorin is a secreted protein associated with obesity and type 2 diabetes. *Int.J.Obes.(Lond)* 2008; **32:** 1113-1121.

83. Voros G, Sandy J D, Collen D, Lijnen H R. Expression of aggrecan(ases) during murine preadipocyte differentiation and adipose tissue development. *Biochim.Biophys.Acta* 2006; **1760:** 1837-1844.

84. Rioux V, Landry R Y, Bensadoun A. Sandwich immunoassay for the measurement of murine syndecan-4. *J.Lipid Res.* 2002; **43:** 167-173.

85. Reizes O, Goldberger O, Smith A C, Xu Z, Bernfield M, Bickel P E. Insulin promotes shedding of syndecan ectodomains from 3T3-L1 adipocytes: a proposed mechanism for stabilization of extracellular lipoprotein lipase. *Biochemistry* 2006; **45:** 5703-5711.

86. Landry R, Rioux V, Bensadoun A. Characterization of syndecan-4 expression in 3T3-F442A mouse adipocytes: link between syndecan-4 induction and cell proliferation. *Cell Growth Differ.* 2001; **12:** 497-504.

87. Aratani Y, Kitagawa Y. Enhanced synthesis and secretion of type IV collagen and entactin during adipose conversion of 3T3-L1 cells and production of unorthodox laminin complex. *J.Biol.Chem.* 1988; **263:** 16163-16169.

88. Alexander C M, Selvarajan S, Mudgett J, Werb Z. Stromelysin-1 regulates adipogenesis during mammary gland involution. *J.Cell Biol.* 2001; **152:** 693-703.

89. Kalluri R. Basement membranes: structure, assembly and role in tumour angiogenesis. *Nat.Rev.Cancer* 2003; **3:** 422-433.

90. Nakajima I, Muroya S, Tanabe R, Chikuni K. Extracellular matrix development during differentiation into adipocytes with a unique increase in type V and VI collagen. *Biol.Cell* 2002; **94:** 197-203.

91. Myllyharju J, Kivirikko K I. Collagens, modifying enzymes and their mutations in

humans, flies and worms. *Trends Genet.* 2004; **20:** 33-43.

92. Prockop D J, Kivirikko K I. Collagens: molecular biology, diseases, and potentials for therapy. *Annu.Rev.Biochem.* 1995; **64:** 403-434.
93. Gordon M K, Hahn R A. Collagens. *Cell Tissue Res.* 2010; **339:** 247-257.
94. Kielty C M, Grant M E. The collagen family:structure, assembly, and organization in the extracellular matrix. In: *Connective Tissue and Its Heritable Disorders. Molecular, Genetic, and Medical Aspects.* 2nd edn edition (eds. Royce P. M., Steinmann B.). Wiley-Liss: 2002; 159-221.
95. Ibrahimi A, Bonino F, Bardon S, Ailhaud G, Dani C. Essential role of collagens for terminal differentiation of preadipocytes. *Biochem.Biophys.Res.Commun.* 1992; **187:** 1314-1322.
96. Kivirikko K I, Pihlajaniemi T. Collagen hydroxylases and the protein disulfide isomerase subunit of prolyl 4-hydroxylases. *Adv.Enzymol.Relat Areas Mol.Biol.* 1998; **72:** 325-398.
97. Myllyharju J, Kivirikko K I. Collagens and collagen-related diseases. *Ann.Med.* 2001; **33:** 7-21.
98. Prockop D J, Sieron A L, Li S W. Procollagen N-proteinase and procollagen C-proteinase. Two unusual metalloproteinases that are essential for procollagen processing probably have important roles in development and cell signaling. *Matrix Biol.* 1998; **16:** 399-408.
99. Kagan H M, Li W. Lysyl oxidase: properties, specificity, and biological roles inside and outside of the cell. *J.Cell Biochem.* 2003; **88:** 660-672.
100. Wayner E A, Carter W G. Identification of multiple cell adhesion receptors for collagen and fibronectin in human fibrosarcoma cells possessing unique alpha and common beta subunits. *J.Cell Biol.* 1987; **105:** 1873-1884.
101. Bidanset D J, Guidry C, Rosenberg L C, Choi H U, Timpl R, Hook M. Binding of the proteoglycan decorin to collagen type VI. *J.Biol.Chem.* 1992; **267:** 5250-5256.
102. McDevitt C A, Marcelino J, Tucker L. Interaction of intact type VI collagen with hyaluronan. *FEBS Lett.* 1991; **294:** 167-170.
103. Chu M L, Pan T C, Conway D, Kuo H J, Glanville R W, Timpl R, Mann K, Deutzmann R. Sequence analysis of alpha 1(VI) and alpha 2(VI) chains of human type VI collagen reveals internal triplication of globular domains similar to the A domains of von Willebrand factor and two alpha 2(VI) chain variants that differ in the carboxy terminus. *EMBO J.* 1989; **8:** 1939-1946.
104. Svensson L, Oldberg A, Heinegard D. Collagen binding proteins. *Osteoarthritis.Cartilage.* 2001; **9 Suppl A:** S23-S28.
105. Bonaldo P, Russo V, Bucciotti F, Doliana R, Colombatti A. Structural and functional features of the alpha 3 chain indicate a bridging role for chicken collagen VI in connective tissues. *Biochemistry* 1990; **29:** 1245-1254.
106. Christiaens V, Scroyen I, Lijnen H R. Role of proteolysis in development of murine adipose tissue. *Thromb.Haemost.* 2008; **99:** 290-294.
107. Chavey C, Mari B, Monthouel M N, Bonnafous S, Anglard P, Van Obberghen E, Tartare-Deckert S. Matrix metalloproteinases are differentially expressed in adipose tissue during obesity and modulate adipocyte differentiation. *J.Biol.Chem.* 2003; **278:** 11888-11896.
108. Bouloumie A, Sengenes C, Portolan G, Galitzky J, Lafontan M. Adipocyte produces

matrix metalloproteinases 2 and 9: involvement in adipose differentiation. *Diabetes* 2001; **50:** 2080-2086.

109. Kuri-Harcuch W, Arguello C, Marsch-Moreno M. Extracellular matrix production by mouse 3T3-F442A cells during adipose differentiation in culture. *Differentiation* 1984; **28:** 173-178.

110. Ono M, Aratani Y, Kitagawa I, Kitagawa Y. Ascorbic-Acid Phosphate Stimulates Type-Iv Collagen-Synthesis and Accelerates Adipose Conversion of 3T3-L1 Cells. *Experimental Cell Research* 1990; **187:** 309-314.

111. Weiner F R, Shah A, Smith P J, Rubin C S, Zern M A. Regulation of collagen gene expression in 3T3-L1 cells. Effects of adipocyte differentiation and tumor necrosis factor alpha. *Biochemistry* 1989; **28:** 4094-4099.

112. Rodriguez Fernandez J L, Ben Ze'ev A. Regulation of fibronectin, integrin and cytoskeleton expression in differentiating adipocytes: inhibition by extracellular matrix and polylysine. *Differentiation* 1989; **42:** 65-74.

113. Antras J, Hilliou F, Redziniak G, Pairault J. Decreased biosynthesis of actin and cellular fibronectin during adipose conversion of 3T3-F442A cells. Reorganization of the cytoarchitecture and extracellular matrix fibronectin. *Biol.Cell* 1989; **66:** 247-254.

114. Green H, Meuth M. An established pre-adipose cell line and its differentiation in culture. *Cell* 1974; **3:** 127-133.

115. Djian P, Phillips M, Green H. The activation of specific gene transcription in the adipose conversion of 3T3 cells. *J.Cell Physiol* 1985; **124:** 554-556.

116. Dani C, Doglio A, Amri E Z, Bardon S, Fort P, Bertrand B, Grimaldi P, Ailhaud G. Cloning and regulation of a mRNA specifically expressed in the preadipose state. *J.Biol.Chem.* 1989; **264:** 10119-10125.

117. Green J A, Yamada K M. Three-dimensional microenvironments modulate fibroblast signaling responses. *Adv.Drug Deliv.Rev.* 2007; **59:** 1293-1298.

118. Mazzoleni G, Di Lorenzo D, Steimberg N. Modelling tissues in 3D: the next future of pharmaco-toxicology and food research? *Genes Nutr.* 2009; **4:** 13-22.

119. Bissell M J, Radisky D C, Rizki A, Weaver V M, Petersen O W. The organizing principle: microenvironmental influences in the normal and malignant breast. *Differentiation* 2002; **70:** 537-546.

120. Cukierman E, Pankov R, Stevens D R, Yamada K M. Taking cell-matrix adhesions to the third dimension. *Science* 2001; **294:** 1708-1712.

121. Yamada K M, Cukierman E. Modeling tissue morphogenesis and cancer in 3D. *Cell* 2007; **130:** 601-610.

122. Pedersen J A, Swartz M A. Mechanobiology in the third dimension. *Ann.Biomed.Eng* 2005; **33:** 1469-1490.

123. Fischbach C, Spruss T, Weiser B, Neubauer M, Becker C, Hacker M, Goepferich A, Blunk T. Generation of mature fat pads in vitro and in vivo utilizing 3-D long-term culture of 3T3-L1 preadipocytes. *Experimental Cell Research* 2004; **300:** 54-64.

124. Hishikawa K, Miura S, Marumo T, Yoshioka H, Mori Y, Takato T, Fujita T. Gene expression profile of human mesenchymal stem cells during osteogenesis in three-dimensional thermoreversible gelation polymer. *Biochem.Biophys.Res.Commun.* 2004; **317:** 1103-1107.

125. Huang W, Carlsen B, Wulur I, Rudkin G, Ishida K, Wu B, Yamaguchi D T, Miller T A. BMP-2 exerts differential effects on differentiation of rabbit bone marrow stromal

cells grown in two-dimensional and three-dimensional systems and is required for in vitro bone formation in a PLGA scaffold. *Exp.Cell Res.* 2004; **299:** 325-334.

126. McBeath R, Pirone D M, Nelson C M, Bhadriraju K, Chen C S. Cell shape, cytoskeletal tension, and RhoA regulate stem cell lineage commitment. *Dev.Cell* 2004; **6:** 483-495.

127. Shaw K R, Wrobel C N, Brugge J S. Use of three-dimensional basement membrane cultures to model oncogene-induced changes in mammary epithelial morphogenesis. *J.Mammary.Gland.Biol.Neoplasia.* 2004; **9:** 297-310.

128. Lee G Y, Kenny P A, Lee E H, Bissell M J. Three-dimensional culture models of normal and malignant breast epithelial cells. *Nat.Methods* 2007; **4:** 359-365.

129. Fischbach C, Seufert J, Staiger H, Hacker M, Neubauer M, Goepferich A, Blunk T. Three-dimensional in vitro model of adipogenesis: Comparison of culture conditions. *Tissue Engineering* 2004; **10:** 215-229.

130. Kang X, Xie Y, Kniss D A. Adipose tissue model using three-dimensional cultivation of preadipocytes seeded onto fibrous polymer scaffolds. *Tissue Eng* 2005; **11:** 458-468.

131. Kang X, Xie Y, Powell H M, James L L, Belury M A, Lannutti J J, Kniss D A. Adipogenesis of murine embryonic stem cells in a three-dimensional culture system using electrospun polymer scaffolds. *Biomaterials* 2007; **28:** 450-458.

132. Daya S, Loughlin A J, Macqueen H A. Culture and differentiation of preadipocytes in two-dimensional and three-dimensional in vitro systems. *Differentiation* 2007; **75:** 360-370.

133. Kunz-Schughart L A, Freyer J P, Hofstaedter F, Ebner R. The use of 3-D cultures for high-throughput screening: the multicellular spheroid model. *J.Biomol.Screen.* 2004; **9:** 273-285.

134. Santini M T, Rainaldi G. Three-dimensional spheroid model in tumor biology. *Pathobiology* 1999; **67:** 148-157.

135. Weiser, B. Adipose Tissue Engineering - Precultivation Strategies towards Clinical Applications & A Novel 3-D Model of Adipogenesis for Basic Research. *Ph.D. thesis* 2008. University of Regensburg, Regensburg, Germany.

136. Wang W, Itaka K, Ohba S, Nishiyama N, Chung U I, Yamasaki Y, Kataoka K. 3D spheroid culture system on micropatterned substrates for improved differentiation efficiency of multipotent mesenchymal stem cells. *Biomaterials* 2009; **30:** 2705-2715.

137. Hasengschwandtner F. Phosphatidylcholine treatment to induce lipolysis. *J.Cosmet.Dermatol.* 2005; **4:** 308-313.

138. Duncan D I, Hasengschwandtner F. Lipodissolve for subcutaneous fat reduction and skin retraction. *Aesthet.Surg.J.* 2005; **25:** 530-543.

139. Rittes P G. The use of phosphatidylcholine for correction of lower lid bulging due to prominent fat pads. *Dermatol.Surg.* 2001; **27:** 391-392.

140. Rotunda A M, Suzuki H, Moy R L, Kolodney M S. Detergent effects of sodium deoxycholate are a major feature of an injectable phosphatidylcholine formulation used for localized fat dissolution. *Dermatol.Surg.* 2004; **30:** 1001-1008.

141. Rittes P G. The use of phosphatidylcholine for correction of localized fat deposits. *Aesthetic Plast.Surg.* 2003; **27:** 315-318.

142. Hexsel D, Serra M, Mazzuco R, Dal'forno T, Zechmeister D. Phosphatidylcholine in the treatment of localized fat. *J.Drugs Dermatol.* 2003; **2:** 511-518.

143. Ablon G, Rotunda A M. Treatment of lower eyelid fat pads using phosphatidylcholine: clinical trial and review. *Dermatol.Surg.* 2004; **30:** 422-427.

144. Rose P T, Morgan M. Histological changes associated with mesotherapy for fat dissolution. *J.Cosmet.Laser Ther.* 2005; **7:** 17-19.

145. Khashimov K, Okur F, Orekhov A N, Kurdanov K, Tertov V. Effect of lipostabil on cholesterol levels in atherosclerotic plaques of the human aorta and the aggregative capacity of thrombocytes (in vitro study). *Biull.Vsesoiuznogo.Kardiol.Nauchn. Tsentra.AMN.SSSR* 1988; **11:** 95-98.

146. Ma X, Zhao J, Lieber C S. Polyenylphosphatidylcholine attenuates non-alcoholic hepatic fibrosis and accelerates its regression. *J.Hepatol.* 1996; **24:** 604-613.

147. Lieber C S. Alcoholic liver injury: pathogenesis and therapy in 2001. *Pathol.Biol.(Paris)* 2001; **49:** 738-752.

148. Pogozheva A V, Bobkova S N, Samsonov M A, Vasil'ev A V. [Comparative evaluation of hypolipidemic effects of omega-3 polyunsaturated acids and lipostabil]. *Vopr.Pitan.* 1996; 31-33.

149. Bobkova V I, Lokshina L I, Korsunskii V N, Tananova G V. [Metabolic effect of lipostabil-forte]. *Kardiologiia.* 1989; **29:** 57-60.

150. Kirsten R, Heintz B, Nelson K, Hesse K, Schneider E, Oremek G, Nemeth N. Polyenylphosphatidylcholine improves the lipoprotein profile in diabetic patients. *Int.J.Clin.Pharmacol.Ther.* 1994; **32:** 53-56.

151. Jones M N. Surfactants in membrane solubilisation. *Int.J.Pharm.* 1999; **177:** 137-159.

152. le Maire M, Champeil P, Moller J V. Interaction of membrane proteins and lipids with solubilizing detergents. *Biochim.Biophys.Acta* 2000; **1508:** 86-111.

153. Hasengschwandtner F, Furtmueller F, Spanbauer M, Silye R, Linz W J. Detailed documentation of one lipolysis treatment: blood values, histology, and ultrasound findings. *Aesthet.Surg.J.* 2007; **27:** 204-211.

154. Brook J G, Linn S, Aviram M. Dietary soya lecithin decreases plasma triglyceride levels and inhibits collagen- and ADP-induced platelet aggregation. *Biochem.Med.Metab Biol.* 1986; **35:** 31-39.

155. Young V L. Lipostabil: the effect of phosphatidylcholine on subcutaneous fat. *Aesthet.Surg.J.* 2003; **23:** 413-417.

156. Lichtenberg D, Zilberman Y, Greenzaid P, Zamir S. Structural and kinetic studies on the solubilization of lecithin by sodium deoxycholate. *Biochemistry* 1979; **18:** 3517-3525.

157. Banerjee P, Joo J B, Buse J T, Dawson G. Differential solubilization of lipids along with membrane proteins by different classes of detergents. *Chem.Phys.Lipids* 1995; **77:** 65-78.

158. Almgren M. Mixed micelles and other structures in the solubilization of bilayer lipid membranes by surfactants. *Biochim.Biophys.Acta* 2000; **1508:** 146-163.

159. Rotunda A M, Kolodney M S. Mesotherapy and phosphatidylcholine injections: historical clarification and review. *Dermatol.Surg.* 2006; **32:** 465-480.

160. Janke J, Engeli S, Gorzelniak K, Luft F C, Jordan J. Compounds used for 'injection lipolysis' destroy adipocytes and other cells found in adipose tissue. *Obes.Facts.* 2009; **2:** 36-39.

161. Schuller-Petrovic S, Wolkart G, Hofler G, Neuhold N, Freisinger F, Brunner F. Tissue-toxic effects of phosphatidylcholine/deoxycholate after subcutaneous injection

for fat dissolution in rats and a human volunteer. *Dermatol.Surg.* 2008; **34:** 529-542.

162. Bechara F G, Sand M, Hoffmann K, Sand D, Altmeyer P, Stucker M. Fat tissue after lipolysis of lipomas: a histopathological and immunohistochemical study. *J.Cutan.Pathol.* 2007; **34:** 552-557.

163. Bechara F G, Skrygan M, Kreuter A, Altmeyer P, Gambichler T. Cytokine mRNA levels in human fat tissue after injection lipolysis with phosphatidylcholine and deoxycholate. *Arch.Dermatol.Res.* 2008; **300:** 455-459.

164. Bechara F G, Sand M, Sand D, Rotterdam S, Stucker M, Altmeyer P, Hoffmann K. Lipolysis of lipomas in patients with familial multiple lipomatosis: an ultrasonography-controlled trial. *J.Cutan.Med.Surg.* 2006; **10:** 155-159.

165. Patrick C W, Jr. Tissue engineering strategies for adipose tissue repair. *Anat.Rec.* 2001; **263:** 361-366.

166. Beahm E K, Walton R L, Patrick C W, Jr. Progress in adipose tissue construct development. *Clin.Plast.Surg.* 2003; **30:** 547-58.

167. Weiser B, Neubauer M, Goepferich A, Blunk T. Tissue Engineering, Fat. In: *Encyclopedia of Biomaterials and Biomedical Engineering* 1 edition 2005.

168. Bruder S P, Jaiswal N, Haynesworth S E. Growth kinetics, self-renewal, and the osteogenic potential of purified human mesenchymal stem cells during extensive subcultivation and following cryopreservation. *J.Cell Biochem.* 1997; **64:** 278-294.

169. Fehrer C, Lepperdinger G. Mesenchymal stem cell aging. *Exp.Gerontol.* 2005; **40:** 926-930.

170. Banfi A, Muraglia A, Dozin B, Mastrogiacomo M, Cancedda R, Quarto R. Proliferation kinetics and differentiation potential of ex vivo expanded human bone marrow stromal cells: Implications for their use in cell therapy. *Exp.Hematol.* 2000; **28:** 707-715.

171. Sugihara H, Yonemitsu N, Miyabara S, Toda S. Proliferation of unilocular fat cells in the primary culture. *J.Lipid Res.* 1987; **28:** 1038-1045.

172. Tholpady S S, Aojanepong C, Llull R, Jeong J H, Mason A C, Futrell J W, Ogle R C, Katz A J. The cellular plasticity of human adipocytes. *Ann.Plast.Surg.* 2005; **54:** 651-656.

173. Frye C A, Patrick C W. Three-dimensional adipose tissue model using low shear bioreactors. *In Vitro Cell Dev.Biol.Anim* 2006; **42:** 109-114.

174. Dani C, Smith A G, Dessolin S, Leroy P, Staccini L, Villageois P, Darimont C, Ailhaud G. Differentiation of embryonic stem cells into adipocytes in vitro. *J.Cell Sci.* 1997; **110 (Pt 11):** 1279-1285.

175. Dani C. Embryonic stem cell-derived adipogenesis. *Cells Tissues.Organs* 1999; **165:** 173-180.

176. Hillel A T, Varghese S, Petsche J, Shamblott M J, Elisseeff J H. Embryonic germ cells are capable of adipogenic differentiation in vitro and in vivo. *Tissue Eng Part A* 2009; **15:** 479-486.

177. Zuk P A, Zhu M, Mizuno H, Huang J, Futrell J W, Katz A J, Benhaim P, Lorenz H P, Hedrick M H. Multilineage cells from human adipose tissue: Implications for cell-based therapies. *Tissue Engineering* 2001; **7:** 211-228.

178. Zuk P A, Zhu M, Ashjian P, De Ugarte D A, Huang J I, Mizuno H, Alfonso Z C, Fraser J K, Benhaim P, Hedrick M H. Human adipose tissue is a source of multipotent stem cells. *Molecular Biology of the Cell* 2002; **13:** 4279-4295.

179. Romanov Y A, Darevskaya A N, Merzlikina N V, Buravkova L B. Mesenchymal stem cells from human bone marrow and adipose tissue: isolation, characterization, and differentiation potentialities. *Bull.Exp.Biol.Med.* 2005; **140:** 138-143.

180. Gimble J M, Katz A J, Bunnell B A. Adipose-derived stem cells for regenerative medicine. *Circ.Res.* 2007; **100:** 1249-1260.

181. Rodriguez A M, Elabd C, Amri E Z, Ailhaud G, Dani C. The human adipose tissue is a source of multipotent stem cells. *Biochimie* 2005; **87:** 125-128.

182. Kirkland J L, Hollenberg C H, Gillon W S. Age, anatomic site, and the replication and differentiation of adipocyte precursors. *Am.J.Physiol* 1990; **258:** C206-C210.

183. Bunnell B A, Flaat M, Gagliardi C, Patel B, Ripoll C. Adipose-derived stem cells: isolation, expansion and differentiation. *Methods* 2008; **45:** 115-120.

184. Oedayrajsingh-Varma M J, van Ham S M, Knippenberg M, Helder M N, Klein-Nulend J, Schouten T E, Ritt M J, van Milligen F J. Adipose tissue-derived mesenchymal stem cell yield and growth characteristics are affected by the tissue-harvesting procedure. *Cytotherapy* 2006; **8:** 166-177.

185. Schipper B M, Marra K G, Zhang W, Donnenberg A D, Rubin J P. Regional anatomic and age effects on cell function of human adipose-derived stem cells. *Annals of Plastic Surgery* 2008; **60:** 538-544.

186. Baksh D, Song L, Tuan R S. Adult mesenchymal stem cells: characterization, differentiation, and application in cell and gene therapy. *J.Cell Mol.Med.* 2004; **8:** 301-316.

187. Gregory C A, Prockop D J, Spees J L. Non-hematopoietic bone marrow stem cells: molecular control of expansion and differentiation. *Exp.Cell Res.* 2005; **306:** 330-335.

188. Auquier P, Macquart-Moulin G, Moatti J P, Blache J L, Novakovitch G, Blaise D, Faucher C, Viens P, Maraninchi D. Comparison of anxiety, pain and discomfort in two procedures of hematopoietic stem cell collection: leukacytapheresis and bone marrow harvest. *Bone Marrow Transplant.* 1995; **16:** 541-547.

189. Fraser J K, Wulur I, Alfonso Z, Hedrick M H. Fat tissue: an underappreciated source of stem cells for biotechnology. *Trends Biotechnol.* 2006; **24:** 150-154.

190. Sethe S, Scutt A, Stolzing A. Aging of mesenchymal stem cells. *Ageing Res.Rev.* 2006; **5:** 91-116.

191. Bianchi G, Banfi A, Mastrogiacomo M, Notaro R, Luzzatto L, Cancedda R, Quarto R. Ex vivo enrichment of mesenchymal cell progenitors by fibroblast growth factor 2. *Exp.Cell Res.* 2003; **287:** 98-105.

192. Lee R H, Kim B, Choi I, Kim H, Choi H S, Suh K, Bae Y C, Jung J S. Characterization and expression analysis of mesenchymal stem cells from human bone marrow and adipose tissue. *Cell Physiol Biochem.* 2004; **14:** 311-324.

193. De Ugarte D A, Alfonso Z, Zuk P A, Elbarbary A, Zhu M, Ashjian P, Benhaim P, Hedrick M H, Fraser J K. Differential expression of stem cell mobilization-associated molecules on multi-lineage cells from adipose tissue and bone marrow. *Immunol.Lett.* 2003; **89:** 267-270.

194. Kilroy G E, Foster S J, Wu X, Ruiz J, Sherwood S, Heifetz A, Ludlow J W, Stricker D M, Potiny S, Green P, Halvorsen Y D, Cheatham B, Storms R W, Gimble J M. Cytokine profile of human adipose-derived stem cells: expression of angiogenic, hematopoietic, and pro-inflammatory factors. *J.Cell Physiol* 2007; **212:** 702-709.

195. Liu T M, Martina M, Hutmacher D W, Hui J H, Lee E H, Lim B. Identification of common pathways mediating differentiation of bone marrow- and adipose tissue-derived human mesenchymal stem cells into three mesenchymal lineages. *Stem Cells* 2007; **25:** 750-760.

196. Sterodimas A, de Faria J, Nicaretta B, Pitanguy I. Tissue engineering with adipose-derived stem cells (ADSCs): current and future applications. *J.Plast.Reconstr.Aesthet.Surg.* 2009.

197. Hong L, Peptan I A, Colpan A, Daw J L. Adipose tissue engineering by human adipose-derived stromal cells. *Cells Tissues.Organs* 2006; **183:** 133-140.

198. von Heimburg D, Kuberka M, Rendchen R, Hemmrich K, Rau G, Pallua N. Preadipocyte-loaded collagen scaffolds with enlarged pore size for improved soft tissue engineering. *Int.J.Artif.Organs* 2003; **26:** 1064-1076.

199. Patrick C W, Jr., Zheng B, Johnston C, Reece G P. Long-term implantation of preadipocyte-seeded PLGA scaffolds. *Tissue Eng* 2002; **8:** 283-293.

200. Neubauer M, Hacker M, Bauer-Kreisel P, Weiser B, Fischbach C, Schulz M B, Goepferich A, Blunk T. Adipose tissue engineering based on mesenchymal stem cells and basic fibroblast growth factor in vitro. *Tissue Eng* 2005; **11:** 1840-1851.

201. Shanti R M, Janjanin S, Li W J, Nesti L J, Mueller M B, Tzeng M B, Tuan R S. In vitro adipose tissue engineering using an electrospun nanofibrous scaffold. *Ann.Plast.Surg.* 2008; **61:** 566-571.

202. Morgan S M, Ainsworth B J, Kanczler J M, Babister J C, Chaudhuri J B, Oreffo R O. Formation of a human-derived fat tissue layer in P(DL)LGA hollow fibre scaffolds for adipocyte tissue engineering. *Biomaterials* 2009; **30:** 1910-1917.

203. Mauney J R, Nguyen T, Gillen K, Kirker-Head C, Gimble J M, Kaplan D L. Engineering adipose-like tissue in vitro and in vivo utilizing human bone marrow and adipose-derived mesenchymal stem cells with silk fibroin 3D scaffolds. *Biomaterials* 2007; **28:** 5280-5290.

204. Hemmrich K, von Heimburg D, Rendchen R, Di Bartolo C, Milella E, Pallua N. Implantation of preadipocyte-loaded hyaluronic acid-based scaffolds into nude mice to evaluate potential for soft tissue engineering. *Biomaterials* 2005; **26:** 7025-7037.

205. Stillaert F B, Di Bartolo C, Hunt J A, Rhodes N P, Tognana E, Monstrey S, Blondeel P N. Human clinical experience with adipose precursor cells seeded on hyaluronic acid-based spongy scaffolds. *Biomaterials* 2008; **29:** 3953-3959.

206. Choi J S, Yang H J, Kim B S, Kim J D, Lee S H, Lee E K, Park K, Cho Y W, Lee H Y. Fabrication of Porous Extracellular Matrix (ECM) Scaffolds from Human Adipose Tissue. *Tissue Eng Part C Methods* 2009.

207. Flynn L, Woodhouse K A. Adipose tissue engineering with cells in engineered matrices. *Organogenesis.* 2008; **4:** 228-235.

208. Flynn L, Prestwich G D, Semple J L, Woodhouse K A. Adipose tissue engineering in vivo with adipose-derived stem cells on naturally derived scaffolds. *J.Biomed.Mater.Res.A* 2009; **89:** 929-941.

209. Alhadlaq A, Tang M, Mao J J. Engineered adipose tissue from human mesenchymal stem cells maintains predefined shape and dimension: implications in soft tissue augmentation and reconstruction. *Tissue Eng* 2005; **11:** 556-566.

210. Stosich M S, Mao J J. Adipose tissue engineering from human adult stem cells: clinical implications in plastic and reconstructive surgery. *Plast.Reconstr.Surg.* 2007; **119:** 71-83.

211. Vashi A V, Keramidaris E, Abberton K M, Morrison W A, Wilson J L, O'Connor A J, Cooper-White J J, Thompson E W. Adipose differentiation of bone marrow-derived mesenchymal stem cells using Pluronic F-127 hydrogel in vitro. *Biomaterials* 2008; **29:** 573-579.

212. Jing W, Lin Y, Wu L, Li X, Nie X, Liu L, Tang W, Zheng X, Tian W. Ectopic adipogenesis of preconditioned adipose-derived stromal cells in an alginate system. *Cell Tissue Res.* 2007; **330:** 567-572.

213. Gentleman E, Nauman E A, Livesay G A, Dee K C. Collagen composite biomaterials resist contraction while allowing development of adipocytic soft tissue in vitro. *Tissue Eng* 2006; **12:** 1639-1649.

214. Hemmrich K, Van de S K, Rhodes N P, Hunt J A, Di Bartolo C, Pallua N, Blondeel P, von Heimburg D. Autologous in vivo adipose tissue engineering in hyaluronan-based gels--a pilot study. *J.Surg.Res.* 2008; **144:** 82-88.

215. Cho S W, Kim S S, Rhie J W, Cho H M, Choi C Y, Kim B S. Engineering of volume-stable adipose tissues. *Biomaterials* 2005; **26:** 3577-3585.

216. Schoeller T, Lille S, Wechselberger G, Otto A, Mowlavi A, Piza-Katzer H. Histomorphologic and volumetric analysis of implanted autologous preadipocyte cultures suspended in fibrin glue: a potential new source for tissue augmentation. *Aesthetic Plast.Surg.* 2001; **25:** 57-63.

217. Wechselberger G, Russell R C, Neumeister M W, Schoeller T, Piza-Katzer H, Rainer C. Successful transplantation of three tissue-engineered cell types using capsule induction technique and fibrin glue as a delivery vehicle. *Plast.Reconstr.Surg.* 2002; **110:** 123-129.

218. Torio-Padron N, Baerlecken N, Momeni A, Stark G B, Borges J. Engineering of adipose tissue by injection of human preadipocytes in fibrin. *Aesthetic Plast.Surg.* 2007; **31:** 285-293.

219. Kawaguchi N, Toriyama K, Nicodemou-Lena E, Inou K, Torii S, Kitagawa Y. Reconstituted basement membrane potentiates in vivo adipogenesis of 3T3-F442A cells. *Cytotechnology* 1999; **31:** 215-220.

220. Kimura Y, Ozeki M, Inamoto T, Tabata Y. Time course of de novo adipogenesis in matrigel by gelatin microspheres incorporating basic fibroblast growth factor. *Tissue Eng* 2002; **8:** 603-613.

221. Abberton K M, Bortolotto S K, Woods A A, Findlay M, Morrison W A, Thompson E W, Messina A. Myogel, a novel, basement membrane-rich, extracellular matrix derived from skeletal muscle, is highly adipogenic in vivo and in vitro. *Cells Tissues.Organs* 2008; **188:** 347-358.

222. Uriel S, Huang J J, Moya M L, Francis M E, Wang R, Chang S Y, Cheng M H, Brey E M. The role of adipose protein derived hydrogels in adipogenesis. *Biomaterials* 2008; **29:** 3712-3719.

223. Cheng M H, Uriel S, Moya M L, Francis-Sedlak M, Wang R, Huang J J, Chang S Y, Brey E M. Dermis-derived hydrogels support adipogenesis in vivo. *J.Biomed.Mater.Res.A* 2010; **92:** 852-858.

224. Kang S W, Seo S W, Choi C Y, Kim B S. Porous poly(lactic-co-glycolic acid) microsphere as cell culture substrate and cell transplantation vehicle for adipose tissue engineering. *Tissue Eng Part C Methods* 2008; **14:** 25-34.

225. Choi Y S, Park S N, Suh H. Adipose tissue engineering using mesenchymal stem cells attached to injectable PLGA spheres. *Biomaterials* 2005; **26:** 5855-5863.

226. Choi Y S, Park S N, Suh H. The effect of PLGA sphere diameter on rabbit mesenchymal stem cells in adipose tissue engineering. *J.Mater.Sci.Mater.Med.* 2008; **19:** 2165-2171.

227. Chung H J, Park T G. Injectable cellular aggregates prepared from biodegradable porous microspheres for adipose tissue engineering. *Tissue Eng Part A* 2009; **15:** 1391-1400.

228. Halberstadt C, Austin C, Rowley J, Culberson C, Loebsack A, Wyatt S, Coleman S, Blacksten L, Burg K, Mooney D, Holder W, Jr. A hydrogel material for plastic and reconstructive applications injected into the subcutaneous space of a sheep. *Tissue Eng* 2002; **8:** 309-319.

229. Rubin J P, Bennett J M, Doctor J S, Tebbets B M, Marra K G. Collagenous microbeads as a scaffold for tissue engineering with adipose-derived stem cells. *Plast.Reconstr.Surg.* 2007; **120:** 414-424.

230. Choi J S, Yang H J, Kim B S, Kim J D, Kim J Y, Yoo B, Park K, Lee H Y, Cho Y W. Human extracellular matrix (ECM) powders for injectable cell delivery and adipose tissue engineering. *J.Control Release* 2009; **139:** 2-7.

231. Marra K G, Defail A J, Clavijo-Alvarez J A, Badylak S F, Taieb A, Schipper B, Bennett J, Rubin J P. FGF-2 enhances vascularization for adipose tissue engineering. *Plast.Reconstr.Surg.* 2008; **121:** 1153-1164.

232. Kakudo N, Shimotsuma A, Kusumoto K. Fibroblast growth factor-2 stimulates adipogenic differentiation of human adipose-derived stem cells. *Biochem.Biophys.Res. Commun.* 2007; **359:** 239-244.

233. Kimura Y, Ozeki M, Inamoto T, Tabata Y. Adipose tissue engineering based on human preadipocytes combined with gelatin microspheres containing basic fibroblast growth factor. *Biomaterials* 2003; **24:** 2513-2521.

234. Kawaguchi N, Toriyama K, Nicodemou-Lena E, Inou K, Torii S, Kitagawa Y. De novo adipogenesis in mice at the site of injection of basement membrane and basic fibroblast growth factor. *Proc.Natl.Acad.Sci.U.S.A* 1998; **95:** 1062-1066.

235. Tabata Y, Miyao M, Inamoto T, Ishii T, Hirano Y, Yamaoki Y, Ikada Y. De novo formation of adipose tissue by controlled release of basic fibroblast growth factor. *Tissue Eng* 2000; **6:** 279-289.

236. Yuksel E, Weinfeld A B, Cleek R, Wamsley S, Jensen J, Boutros S, Waugh J M, Shenaq S M, Spira M. Increased free fat-graft survival with the long-term, local delivery of insulin, insulin-like growth factor-I, and basic fibroblast growth factor by PLGA/PEG microspheres. *Plast.Reconstr.Surg.* 2000; **105:** 1712-1720.

237. Masuda T, Furue M, Matsuda T. Photocured, styrenated gelatin-based microspheres for de novo adipogenesis through corelease of basic fibroblast growth factor, insulin, and insulin-like growth factor I. *Tissue Eng* 2004; **10:** 523-535.

238. Walton R L, Beahm E K, Wu L. De novo adipose formation in a vascularized engineered construct. *Microsurgery* 2004; **24:** 378-384.

Chapter 2

Goals of the Thesis

1. Two-dimensional (2-D) adipocyte culture

To develop therapeutic strategies, for the treatment of fat-related diseases or for reconstructive and aesthetic surgery, it is of prime importance to understand adipocyte biology and function. Hereby, for many questions, 2-D culture of differentiating preadipocytes still is an adequate model system to study adipocyte biology *in vitro*.

1.1. Investigation of therapeutic substances used for injection lipolysis

In the first part of this thesis, 2-D adipocyte culture was used for *in vitro* studies of therapeutic substances applied in injection lipolysis. Injection lipolysis is a therapeutical strategy to reduce localized fat accumulation in humans. By this treatment, soy-derived PC which is available as Lipostabil® is injected subcutaneously into fat deposits [1,2]. However, the mechanisms by which Lipostabil® induces fat dissolution are controversially discussed and a lipolytic activity of this substance has not yet been investigated. Therefore, the aim of this study was to investigate the action of Lipostabil® and its single components phosphatidylcholine and sodium deoxycholate on adipocytes concerning toxic and lipolytic effects. For a first approach, we used a well established cell line, the murine 3T3-L1 cells (**Chapter 4**). As an additional human cell source, adipose-derived stem cells (ADSCs) were utilized. ADSCs can be differentiated into various lineages including adipocytes [3]. However, many factors such as harvesting and culture conditions have been described to influence the adipocyte culture. Therefore, we tested different isolation procedures and induction media stimulating the adipogenic differentiation to optimize the adipogenic differentiation rate (**Chapter 3**). The established adipocyte model system was further used for the *in vitro* studies of Lipostabil® (**Chapter 4**).

2. Three-dimensional (3-D) adipocyte culture

To study tissue-inherent factors such as cell-cell and cell-matrix interactions, the 2-D culture system is limited and cannot fully capture the relevant complexity of *in vivo* adipose tissue. In contrast, a 3-D tissue-like model system likely is more appropriate attempting to mimic the *in vivo* tissue environment as closely as possible. Furthermore, for tissue reconstruction, the use of 3-D substitutes is inevitable.

2.1. Investigation of collagens in adipogenesis *in vitro*

During the last decades, it was shown that the adipocyte function is strongly influenced by the surroundings of the cells [4,5]. Various studies have described the regulation of several extracellular matrix (ECM) components during adipogenic differentiation [6-10]. Nevertheless, the composition of the ECM in adipose tissue as well as its role in adipogenesis has not been fully understood. To study the influence of various ECM components on adipogenic differentiation *in vitro*, we have previously developed a 3-D adipocyte culture system based on the formation of spheroids [11]. In contrast to scaffold- or gel-based 3-D constructs, this 3-D model system provides a coherent adipose tissue-like context including direct cell-cell and cell-matrix interactions and represents an adequate model for studying the importance of the ECM for adipocyte development. Thereby, the role of collagens in adipogenesis is of major interest since these ECM components are the most abundant molecules in the matrix. However, the role of collagens in adipogenesis has not been investigated in a 3-D tissue-like context so far. As the well organized matrix structure of 3-D adipose tissue seems to modulate adipocyte differentiation, we hypothesized that the inhibition of the collagen synthesis by a prolyl hydroxylase inhibitor has more profound effects in 3-D spheroids compared to 2-D culture. Therefore, we examined the influence of collagens on the adipogenesis of 3T3-L1 cells as well as ADSCs cultured in 3-D spheroids and 2-D culture by using ethyl-3,4-dihydroxybenzoate (EDHB) as an inhibitor of collagen synthesis (**Chapter 5**).

In general, it is known that the expression of collagens, particularly fibrillar collagens, is regulated during adipose conversion [5,8,10]. However, the organization of the collagen network through interactions of the molecules during adipogenesis is not well characterized. The so-called fibril-associated collagens with interrupted triple helices (FACIT) are important for the structure of the ECM network. Members of the FACIT family are localized on the surface of major collagen fibrils and act as molecular bridges that arrange the structural integrity of the ECM. Therefore, we supposed that FACITs may be involved in adipocyte differentiation. So far, FACITs have not been investigated during adipocyte development. One member of the FACIT sub-family is collagen XVI which is mainly expressed in skin and cartilage in humans [12,13]. As collagen XVI mediates anchoring processes and remodelling of the ECM [14,15], we hypothesized that this FACIT collagen is also involved in adipose conversion. Therefore, we investigated the expression of collagen XVI during the *in vitro* adipogenesis of 3T3-L1 preadipocytes and ADSCs in 2-D and 3-D culture (**Chapter 6**).

2.2. Novel hydrogels for adipose tissue engineering

Besides the benefit of 3-D culture systems in basic research, 3-D adipose substitutes are required for clinical applications to augment soft tissue defects, e.g., after traumatic injuries or tumor resections. However, reviewing currently used adipose engineering strategies, it becomes evident that cell carriers that are more adipose-specific are desirable. Hydrogels represent a promising 3-D scaffold for adipose tissue engineering due to effective cell encapsulation and unrestricted diffusion of nutrients and metabolites. Recently, a novel biodegradable poly(ethylene glycol) (PEG)-based hydrogel has been developed by our group [16]. The gel-forming polymers were functionalized with a synthetic tetrapeptide which enables proteolytic degradation of the hydrogel by cell secreted proteases. Furthermore, the hydrogel provides an elastic microenvironment which mimics the properties of native ECM. Another promising approach of this gel system is the possibility to functionalize the hydrogel with adhesion molecules, hormones or growth factors to promote the formation of a coherent adipose tissue. The aim of this study was to investigate the suitability of this novel biointeractive PEG-based hydrogel for adipose tissue engineering. To this end, the hydrogels were seeded and cultured with 3T3-L1 preadipocytes to study the influence of substrate stiffness, adhesiveness, and degradability on cell proliferation and adipogenic differentiation *in vitro* (**Chapter 7**).

References

1. Hasengschwandtner F. Phosphatidylcholine treatment to induce lipolysis. *J.Cosmet.Dermatol.* 2005; **4:** 308-313.
2. Rittes P G. The use of phosphatidylcholine for correction of lower lid bulging due to prominent fat pads. *Dermatol.Surg.* 2001; **27:** 391-392.
3. Zuk P A, Zhu M, Mizuno H, Huang J, Futrell J W, Katz A J, Benhaim P, Lorenz H P, Hedrick M H. Multilineage cells from human adipose tissue: Implications for cell-based therapies. *Tissue Engineering* 2001; **7:** 211-228.
4. Ibrahimi A, Bonino F, Bardon S, Ailhaud G, Dani C. Essential role of collagens for terminal differentiation of preadipocytes. *Biochem.Biophys.Res.Commun.* 1992; **187:** 1314-1322.
5. Nakajima I, Muroya S, Tanabe R, Chikuni K. Extracellular matrix development during differentiation into adipocytes with a unique increase in type V and VI collagen. *Biol.Cell* 2002; **94:** 197-203.
6. Mariman E C, Wang P. Adipocyte extracellular matrix composition, dynamics and role in obesity. *Cell Mol.Life Sci.* 2010.
7. Kuri-Harcuch W, Arguello C, Marsch-Moreno M. Extracellular matrix production by mouse 3T3-F442A cells during adipose differentiation in culture. *Differentiation* 1984; **28:** 173-178.
8. Aratani Y, Kitagawa Y. Enhanced synthesis and secretion of type IV collagen and entactin during adipose conversion of 3T3-L1 cells and production of unorthodox laminin complex. *J.Biol.Chem.* 1988; **263:** 16163-16169.
9. Ono M, Aratani Y, Kitagawa I, Kitagawa Y. Ascorbic-Acid Phosphate Stimulates Type-Iv Collagen-Synthesis and Accelerates Adipose Conversion of 3T3-L1 Cells. *Experimental Cell Research* 1990; **187:** 309-314.
10. Weiner F R, Shah A, Smith P J, Rubin C S, Zern M A. Regulation of collagen gene expression in 3T3-L1 cells. Effects of adipocyte differentiation and tumor necrosis factor alpha. *Biochemistry* 1989; **28:** 4094-4099.
11. Weiser, B. Adipose Tissue Engineering - Precultivation Strategies towards Clinical Applications & A Novel 3-D Model of Adipogenesis for Basic Research. *Ph.D. thesis* 2008. University of Regensburg, Regensburg, Germany.
12. Grassel S, Unsold C, Schacke H, Bruckner-Tuderman L, Bruckner P. Collagen XVI is expressed by human dermal fibroblasts and keratinocytes and is associated with the microfibrillar apparatus in the upper papillary dermis. *Matrix Biol.* 1999; **18:** 309-317.
13. Kassner A, Hansen U, Miosge N, Reinhardt D P, Aigner T, Bruckner-Tuderman L, Bruckner P, Grassel S. Discrete integration of collagen XVI into tissue-specific collagen fibrils or beaded microfibrils. *Matrix Biol.* 2003; **22:** 131-143.
14. Senner V, Ratzinger S, Mertsch S, Grassel S, Paulus W. Collagen XVI expression is upregulated in glioblastomas and promotes tumor cell adhesion. *FEBS Lett.* 2008; **582:** 3293-3300.
15. Eble J A, Kassner A, Niland S, Morgelin M, Grifka J, Grassel S. Collagen XVI harbors an integrin alpha1 beta1 recognition site in its C-terminal domains. *J.Biol.Chem.* 2006; **281:** 25745-25756.
16. Brandl F, Hammer N, Blunk T, Tessmar J, Goepferich A. Biodegradable hydrogels for time-controlled release of tethered peptides or proteins. *Biomacromolecules.* 2010; **11:** 496-504.

Chapter 3

Human Adipose-derived Stem Cells as an *in vitro* Model for Human Adipogenesis

Evaluation of Culture Conditions

1. Abstract

Adipose-derived stem cells (ADSCs) have an equal potential to differentiate into several cell lineages including adipocytes which makes them to a promising cell source for basic research and clinical applications. The aim of this study was to evaluate a two-dimensional (2-D) *in vitro* adipocyte culture system with human ADSCs by optimization of the isolation procedure as well as culture conditions by addition of various factors such as human plasma, basic fibroblast growth factor (bFGF) and ascorbic acid (AA). ADSCs were isolated from subcutaneous adipose tissue, propagated and, subsequently, hormonally induced to undergo adipogenesis. It was shown that modification of the isolation procedure by introduction of two additional filtration steps led to an increased adipogenic differentiation rate within ADSCs, whereas an additional erythrocyte lysis step did not influence the adipogenesis. Similarly, supplementation of human plasma into the culture medium did not enhance the adipogenic differentiation after hormonal induction. However, the addition of bFGF into the medium exerted increased adipogenic conversion of ADSCs, in contrast to AA that strongly inhibited the adipogenic differentiation capacity of ADSCs. We have established an *in vitro* adipocyte culture system with human ADSCs which can be used as model system for the study of the effect of substances used for injection lipolysis as described in chapter 4 (Page 71).

2. Introduction

Adipose tissue was identified as an alternative cell source of autologous stem cells which are found in the stromal vascular fraction (SVF) of subcutaneous adipose tissue and which are referred to as adipose-derived stem cells (ADSCs) in this work. Recently, interest has rapidly grown in ADSCs for use in adipocyte culture *in vitro* and in tissue repair *in vivo*. ADSCs have been classified as mesenchymal stem cells (MSCs) with differentiation abilities and surface marker proteins comparable to those of bone marrow-derived stem cells (BMSCs) [1-4]. However, in contrast to BMSCs, ADSCs are more advantageous by virtue of the unique accessibility from adipose tissue in a less-invasive manner, the easy harvest in a large quantity from abdominoplasties or lipoaspirates by enzymatic digestion, the extensive expansion capacity *in vitro* and the capability to differentiate into multiple cell lineages upon induction cues [5-8]. ADSCs represent a heterogeneous cell population containing fibroblasts, smooth muscle cells, pericytes, endothelial cells, monocytes/macrophages, lymphocytes, mature adipocytes, and also progenitor cells of adipocytes [9-11]. Depending on the inducing stimuli and specific growth factors, these cells are able to undergo osteogenesis, adipogenesis, chondrogenesis, neurogenesis, and myogenesis [1,4]. For a successful *in vitro* adipocyte culture, extensive expansion and adipogenic differentiation of ADSCs is necessary to obtain a sufficient rate of differentiated adipocytes for following research. Thus, it is of great interest to achieve a significant fraction of cells differentiating into adipocytes within the heterogeneous cell population.

A wide variety of exogenous supplements, including serum from different species, low molecular weight drugs and growth factors, has been found to influence proliferation and adipogenesis of ADSCs [12-16]. Previously, it has been shown that long proliferation periods in fetal calf serum (FCS)-supplemented medium markedly reduce the capability for adipogenic differentiation which is most likely caused by serum factors in the FCS [17,18]. Therefore, FCS is mostly missing in the adipogenic differentiation medium of ADSCs. However, some studies have revealed that in contrast to FCS, horse, rabbit, murine, and human serum or human plasma enhances the proliferation and the adipogenesis of MSCs *in vitro* [18-23]. In some cases, the serum or plasma replaced the adipogenic induction cocktail [20,21], whereas in other studies, the serum is supplemented to the induction medium [18,23]. The commonly used adipogenic induction medium contains agents such as insulin, glucocorticoids, 3-isobutyl-methylxanthine (IBMX), and ligands of peroxisome proliferator-activated receptor γ (PPARγ) such as troglitazone. In addition, growth factors like epidermal growth factor (EGF) or bFGF have been shown to modulate the adipogenic induction process

of MSCs and preadipocytes [12,24]. Basic FGF has been identified to act as a mitogen and chemoattractant that enhances angiogenesis, migration and adipogenic differentiation of both ADSCs and BMSCs [12,25-29].

In addition to growth hormones, antioxidants such as AA are also known to stimulate the *in vitro* proliferation and differentiation of several mesenchymal cell types [30-34]. A few basic studies reported that AA also enhances adipogenesis of 3T3-L1 and BMSCs [35-38]. These stimulatory effects likely resulted, at least in part, from the essential role of AA in collagen synthesis [36,37]. AA is an essential cofactor for the enzyme prolyl hydroxylase which is responsible for post-translational modification of collagen molecules [39].

Nevertheless, there is an extensive inconsistency among laboratories concerning the isolation procedure, the culture media, and the addition of supplementary factors for the successful expansion and adipogenic differentiation of ADSCs.

The aim of this chapter was to evaluate the isolation and culture procedures for ADSCs finally leading to a new *in vitro* model for the study of the effect of substances used for injection lipolysis as described in chapter 4 (Page 71). Initially, we advanced the isolation of ADSCs from human adipose tissue to optimize the rate of differentiating adipocytes by varying different steps of the isolation procedure such as filtration or lysis of erythrocytes. Secondly, we searched for improved culture conditions by addition of supplementary factors such as human plasma, bFGF or AA to reach effective adipogenic differentiation of ADSCs.

3. Materials and Methods

Materials

ADSCs were isolated from human abdominoplasties or lipoaspirates obtained from cosmetic surgery. Dulbecco's Modified Eagle's Medium (DMEM) and Dulbecco's Modified Eagle's Medium Ham'sF12 (DMEM Ham'sF12) were purchased from Biochrom (Berlin, Germany). Fetal bovine serum (FBS, Lot. No. 40A0044K), phosphate buffered saline (PBS), 0.25% trypsin-EDTA solution, and penicillin-streptomycin solution were from Invitrogen (Karlsruhe, Germany). Collagenase NB4 and IBMX were bought from Serva Electrophoresis (Heidelberg, Germany). Papainase was from Worthington (Lakewood, NJ, USA). Bovine insulin was kindly provided by Sanofi-Aventis (Frankfurt a. M., Germany). Cortisol, transferrin, biotin, pantothenate, troglitazone, triiodothyronine, glucose, bovine serum albumin, cysteine, bovine DNA, 2-mercaptoethanol, Tris base, dihydroxyacetone phosphate (DHAP), dimethylsulfoxide (DMSO), AA, Nile Red, and oil red O were obtained from

Sigma-Aldrich (Taufkirchen, Germany). Hoechst 33258 dye was obtained from Polysciences (Warrington, PA, USA). Nicotinamide adenine dinucleotide (NADH) was from Roche (Mannheim, Germany). Thesit was obtained from Gepepharm GmbH (Siegburg, Germany). Basic FGF was obtained from R&D Systems (Minneapolis, MN, USA). If not stated otherwise, all other chemicals were from Merck KGaA (Darmstadt, Germany). Deionized water was obtained using a Milli-Q water purification system from Millipore (Schwalbach, Germany). All cell culture plastics were purchased from Corning (Bodenheim, Germany).

Methods

3.1. Isolation of ADSCs from human adipose tissue

ADSCs were isolated from human subcutaneous adipose tissue obtained during abdominoplastic surgery or liposuctions from healthy women or men aged 17-69 years as described by Schling *et al.* [40,41]. Briefly, after removal of connective tissue and blood vessels, adipose tissue was subjected to enzymatic digestion using a 0.1% collagenase solution at 37°C for 4 hours on an orbital shaker at 150 rpm (Heidolph, Schwabach, Germany) in order to obtain a single-cell suspension. Lipoaspirates were directly transferred to the collagenase solution containing 1 mg/ml collagenase NB4, 15 mg/ml bovine serum albumin, 100 mM 2-[-4-(2-hydroxyethyl)1-piperazinyl]-ethan-sulfonic acid (HEPES), pH 7.4, 120 mM NaCl, 50 mM KCl, 1mM $CaCl_2$, and 5 mM glucose. The suspension was filtrated twice through a 100 µm nylon filter (BD Biosciences, San Jose, CA, USA) and centrifuged at 700 g for 7 minutes. The resulting pellet, termed the SVF, was resuspended in basal medium consisting of DMEM/DMEM Ham'sF12-Medium (1:1), 10% FBS, penicillin (100 U/ml), streptomycin (100 µg/ml), 1 µM insulin, 2 µg/ml transferrin, 1 µM biotin, and 17 µM pantothenate [41]. Cells were seeded in T75 culture flasks and cultured in a humidified atmosphere at 37°C and 5% CO_2 or were cryopreserved in liquid nitrogen. Cryopreservation medium consisted of basal medium supplemented with 10% DMSO. In the case of following cultivation, cells were allowed to adhere to the substratum for one day. The flasks were rinsed twice with PBS in order to remove erythrocytes and other non-adherent cells. In the following experiments, cells were expanded (proliferation phase) with basal media up to passage 3. Cyropreserved cells were similarly expanded up to passage 3 after thawing.

3.2. 2-D cell culture of ADSCs

For conventional 2-D monolayer cultures, cells were seeded in basal medium (DMEM/DMEM Ham'sF12-Medium (1:1), 10% FBS, penicillin (100 U/ml), streptomycin (100 µg/ml), 1 µM insulin, 2 µg/ml transferrin, 1 µM biotin, and 17 µM pantothenate) into tissue-culture polystyrene well plates (Corning, Bodenheim, Germany) at a density of 30,000 cells/cm^2 if not stated otherwise. At confluence, cells were induced to undergo adipogenesis by supplementing basal media (without FBS) with 100 nM cortisol, 500 µM IBMX, 1 nM triiodothyronine and 500 nM troglitazone [41] named as induction medium. The time point of induction was referred to as day 0 throughout all experiments. At day 2, the medium was exchanged with differentiation medium (basal medium without FBS, 100 nM cortisol, 1 nM triiodothyronine and 500 nM troglitazone). During the entire culture period, medium was exchanged every two days and cells were incubated in a humidified atmosphere at 37°C and 5% CO_2.

3.3. Oil red O staining

In order to visualize accumulated cytoplasmic triglyceride droplets, oil red O staining was performed at day 12 after hormonal induction of adipogenesis. For this purpose, cells were washed once with PBS, fixed in 10% PBS-buffered formalin overnight and then stained with oil red O (3 mg/ml solution in 60% isopropanol) for 4 hours [42,43]. Excess dye was removed by washing three times with PBS. Microscopical bright field pictures were acquired at 20x and 4x magnification using an inverted microscope (Leica DM IRB, Leica Microsystems, Wetzlar, Germany) equipped with a CCD camera (DS-5M, Nikon, Düsseldorf, Germany) and the software Eclipse Net (Laboratory Imaging, Praha, Czech Republic).

3.4. Quantitative analysis of intracellular triglyceride (TG) accumulation

For analysis of the intracellular TG content, 2-D monolayers were washed twice with PBS and harvested in 0.5% aqueous thesit solution. After sonication with a digital sonifier (Branson Ultrasonic Corporation, Danburg, CT, USA), the spectroscopic quantification of TG was performed using the enzymatic serum triglyceride determination kit from Sigma-Aldrich (Taufkirchen, Germany) according to the manufacturer's instructions. Measurements were done in three biological replicates; one replicate was derived from one well. The amount of TG per well was calculated and normalized to the DNA content of the samples as determined by the DNA assay.

3.5. Determination of the glycerol-3-phosphate dehydrogenase (GPDH) activity

GPDH activity was measured according to a protocol adapted from Pairault and Green [44]. Briefly, after washing with PBS, cells were harvested in lysis buffer (50 mM Tris, 1 mM EDTA, 1 mM 2-mercaptoethanol, pH 7.5), sonicated with a digital sonifier (Branson Ultrasonic Corporation, Danburg, CT, USA) and centrifuged (16,000 g, 5 minutes). GPDH activity was measured by adding an aliquot of the lysate supernatant to the substrate buffer (0.1 M triethanolamine, 2.5 mM EDTA, 0.5 mM 2-mercaptoethanol, 0.12 mM NADH, 2 mM DHAP) and monitoring the consumption of NADH photometrically at 340 nm for 4.2 minutes. Measurements were done in three biological replicates; one replicate was derived from one well. GPDH activities were normalized to the DNA content of the samples as determined by the DNA assay.

3.6. Determination of the DNA content with DNA assay

After washing with PBS, cells were harvested in lysis buffer (50 mM Tris, 1 mM EDTA, 1 mM 2-mercaptoethanol, pH 7.5) and sonicated with a digital sonifier (Branson Ultrasonic Corporation, Danburg, CT, USA). Aliquots of the cell lysates were digested with papainase (3.2 U/ml in 0.1 M Na_2HPO_4 buffer, pH 6.5 containing 1 mM Na_2EDTA and 2.5 mM cysteine) for 16 hours at 60°C, and the DNA content was determined using the intercalating Hoechst 33258 dye (0.1 µg/ml in 0.1 M NaCl containing 1 mM Na_2EDTA, 10 mM Tris, pH 7.4) [45]. Fluorescence intensities were determined at 365 nm excitation wavelength and 458 nm emission wavelength on a LS 55 Fluorescence Spectrometer (PerkinElmer, Wiesbaden, Germany) and correlated to DNA contents using standard dilutions of double-stranded DNA (from calf thymus).

3.7. Flow Cytometry

This method was carried out using a protocol adapted from Gimble *et al.* [46]. ADSCs were carefully harvested by treatment with 0.25% trypsin/EDTA and centrifuged at 200 g at 4°C for 5 minutes. After washing the pellet with PBS, cells were centrifuged as described above and resuspended in PBS containing the lipophilic fluorescent dye Nile Red. Cells were incubated for 30 minutes on ice. Samples were analyzed with a FACSCalibur flow cytometer (Becton Dickinson, Heidelberg, Germany). Nile Red fluorescence was measured on the FL2 emission channel through a 585±21 nm band pass filter, following excitation with an argon ion laser source at 488 nm. For each sample, a selection marker M1 was set in histograms and

the amount of adipocytes was assessed by determining the percentage of cells within the M1 region. The M1 region was adjusted according to unstained differentiated ADSCs taking into account the autofluorescence of each sample.

3.8. Statistics

All quantitative results are presented as mean value ± standard deviation. Significances were determined using GraphPadPrism v.5 (GraphPad Software, La Jolla, CA, USA). Differences between groups were analyzed for significance using unpaired Student's t-test. A value of $p<0.05$ was regarded as statistically significant.

4. Results

4.1. Evaluation of the isolation procedure of ADSCs from adipose tissue

The initial methods to isolate cells from rat adipose tissue were pioneered by Rodbell *et al.* in the 1960s [47,48]. They minced rat fat pads, washed extensively to remove contaminating hematopoietic stem cells, incubated the tissue fragments with collagenase, and centrifuged the digest, thereby separating the floating population of mature adipocytes from the pelleted SVF. In our studies, this procedure has been modified according to the method published by Schling *et al.*, which included additional filtration steps after digestion [40]. The additional filtration steps were performed in order to purify the SVF of the digested tissue from residual connective tissue and other matrix components as well as large mature adipocytes. In a first experiment, we compared the two different procedures with regard to the ability of ADSCs to differentiate into adipocytes. Isolation 1 was performed according to the method of Rodbell as described above, whereas isolation 2 was modified by introducing two filtration steps through a filter of 100 µm pore size. The first filtration was performed after digestion of the tissue with collagenase. Subsequently, the floated mature adipocytes were aspirated carefully followed by another filtration step and centrifugation afterwards. The pelletized cell fraction was seeded into culture flasks and after one day, non-adhered cells and cell debris were removed by washing with PBS. After expansion in basal medium, the adhered ADSCs were induced by a hormonal cocktail consisting of 100 nM cortisol, 500 µM IBMX, 1 nM triiodothyronine, and 500 nM troglitazone to undergo adipogenic differentiation. At day 12 after induction, adipogenic potential of ADSCs was determined by staining of the lipid droplets within adipocytes with oil red O (Figure 1). The additional filtration steps in isolation 2 resulted in increased removal of connective tissue remnants and other matrix

components as well as large cells such as mature adipocytes. After seeding of the SVF of isolation 2 into flasks, less erythrocytes and other non-adhered cells were existing in the culture medium compared to the fraction of isolation 1. After adipogenic induction, ADSCs isolated according to procedure 2 clearly differentiated into adipocytes and even at higher rates than the ADSCs of isolation 1 did.

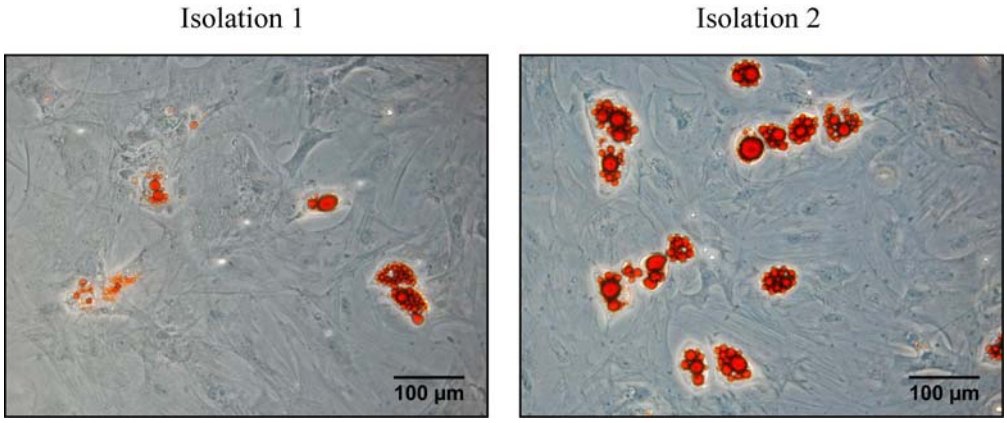

Figure 1: Oil red O staining of adipocytes at day 12 after induction within the heterogeneous population of ADSCs which were isolated according to different procedures. *Isolation 1*: After digestion of adipose tissue with collagenase, the cell suspension was centrifuged without prior filtration steps. *Isolation 2*: After digestion of adipose tissue with collagenase, the cell suspension was filtrated twice through a filter with 100 µm pore size followed by the centrifugation step. Bar=100 µm.

In a second experiment, a final lysis of erythrocytes after the centrifugation was introduced in the isolation procedure 2 referred to as isolation 3. This was supposed to further purify the heterogeneous cell population. Erythrocytes were removed by resuspending the pelletized SVF in erythrocyte lysis buffer (0.16 M NH_4Cl) for 10 minutes at room temperature. Subsequently, the cell suspension was centrifuged again and the obtained cell pellet was seeded into flasks. After expansion, the ADSCs were seeded at a density of 20,000 cells per cm^2 into well plates and at confluence, the cells were hormonally induced to undergo adipogenesis. The adipogenic differentiation capacity of ADSCs was determined at day 12 after induction by oil red O staining. The lysis of erythrocytes did not influence the purity and the growth of ADSCs (Figure 2). The differentiation capacity was not altered by the additional lysis step in isolation procedure 3. Apparently, washing of the cells with PBS one day after attachment, as performed in the first experiment, did remove erythrocytes in a similar manner than lysis did, as performed in the second experiment.

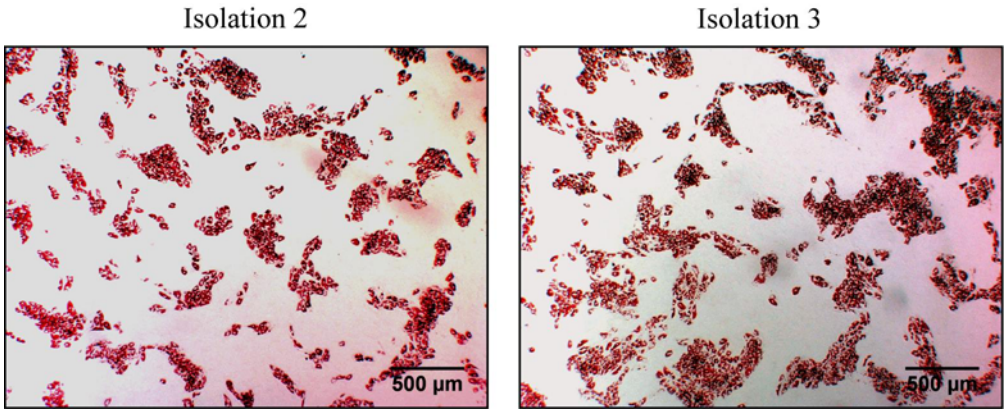

Figure 2: Oil red O staining of adipocytes at day 12 after induction within the heterogeneous population of ADSCs which were isolated according to different procedures. *Isolation 2*: After digestion of adipose tissue with collagenase, the cell suspension was filtrated twice through a filter with 100 µm pore size followed by the centrifugation step. *Isolation 3*: After digestion of adipose tissue with collagenase, the cell suspension was filtrated twice through a filter with 100 µm pore size followed by the centrifugation step. Subsequently, the pelletized cell fraction was treated with erythrocyte lysis buffer for 10 minutes at room temperature. Bar=500 µm.

4.2. Adipogenic differentiation capacity is dependent on donors

We isolated ADSCs from adipose tissue of eleven different donors. Hereby, we detected differences of the adipogenic differentiation capacity of ADSCs dependent on the distinct donors. In this study, exemplarily for two extreme examples, we illustrated the differential adipogenic potential of ADSCs obtained from human adipose tissue of two different donors. To determine the rate of differentiated adipocytes in the heterogeneous cell population, samples were analyzed by flow cytometry using the lipophilic dye Nile Red at day 12 after adipogenic induction. Cell size and granularity were assessed using forward- and side-scatter settings. Samples were corrected for nonspecific fluorescence and autofluorescence. The number of positive events for Nile Red stained cells was expressed as percentage of the total cell number of ADSCs. Consistent with microscopic brightfield pictures (Figure 3 A), the fraction of ADSCs from donor 1 (64.91 ± 11.60%) contained distinctly more adipocytes than the one from donor 2 (11.13 ± 3.94%) (Figure 3 B). Non-induced ADSCs served as control for undifferentiated cells. No lipid droplets were observed in undifferentiated cells and, accordingly, no adipocytes were detected by flow cytometry.

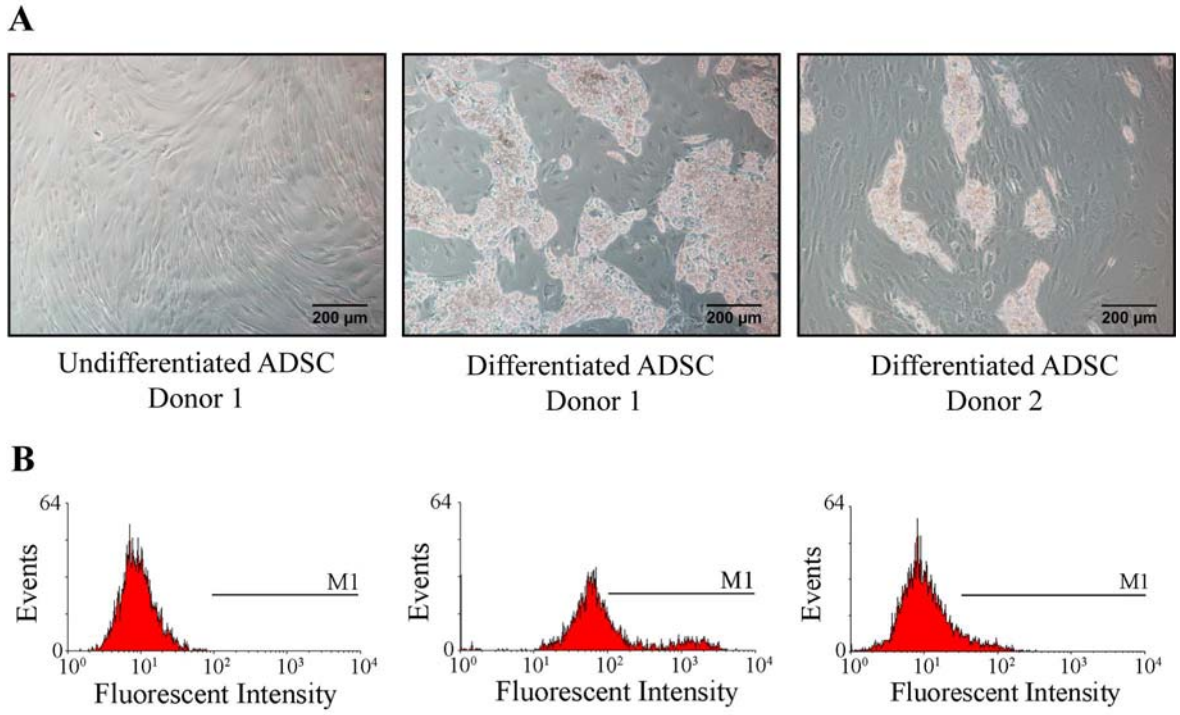

Group	FACS (% cells in M1)
Undifferentiated ADSC (Donor 1)	0.55 ± 0.24
Differentiated ADSC (Donor 1)	64.91 ± 11.60
Differentiated ADSC (Donor 2)	11.13 ± 3.94

Figure 3: Adipogenic differentiation capacity of ADSCs isolated from adipose tissues of two different donors. **A)** Microscopic brightfield images of undifferentiated and differentiated ADSCs at day 12 after induction are shown. Bar=200 µm. **B)** Flow cytometry data from undifferentiated and differentiated ADSCs at day 12 after induction are presented. To determine the number of adipocytes within ADSC population the samples were incubated with the lipophilic dye Nile red. The table represents the number of differentiated cells expressed as a percentage of total cells in culture. Data represent means ± standard deviation of three biological replicates. The group designated as "undifferentiated" were cultivated without induction by the hormonal cocktail.

4.3. Effect of human plasma on adipogenesis of ADSCs

Previous studies have shown that a medium supplemented with murine or human plasma promoted the propagation of BMSCs and preserved the differentiation capacity of the cells [21,22]. Thus, we assumed that the addition of human plasma into both the growth and the induction medium may promote the adipogenic differentiation potential of ADSCs.

Human plasma was obtained by pooling blood collected from healthy volunteers using EDTA as anticoagulant. Blood was then centrifuged and the supernatant was stored frozen until use. First, ADSCs were cultured in basal media supplemented with 5% human plasma in which the concentration was adapted to conditions from literature [21] and afterwards, ADSCs were

hormonally induced to undergo adipogenesis in the presence of human plasma. At day 12 after induction, adipogenic conversion was detected by oil red O staining and the percentage of cells undergoing adipogenesis was calculated by microscopic inspection (Figure 4 A). The number of adipocytes in a field staining positive with oil red O for lipid droplets were determined as a percentage relative to the total number of the cells in the field (Figure 4 B). Oil red O staining revealed that the addition of human plasma did not increase the number of adipocytes. The calculated adipocyte fraction did not vary in cultures differentiated in the presence or absence of human plasma (Figure 4 B).

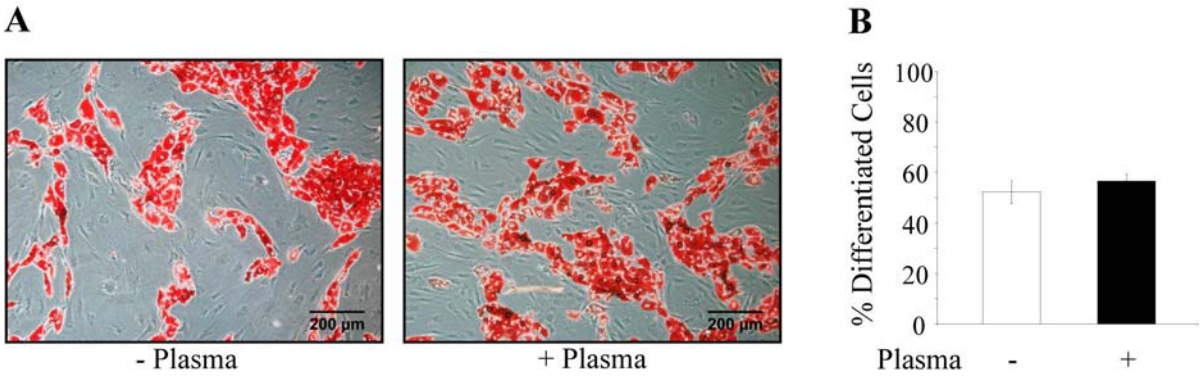

Figure 4: Adipogenic differentiation capacity of ADSCs cultured with or without human plasma. **A)** Oil red O staining of adipocytes within the heterogeneous population of ADSCs at day 12 after adipogenic induction. Bar=200 µm. **B)** Quantification of adipocytes at day 12 after adipogenic induction by microscopic inspection. The number of cells in a field staining positive with oil red O for lipid droplets were determined as a percentage relative to the total number of the cells in the field. The number of adipocytes from three images, each of a different biological replicate, was evaluated.

4.4. Effect of bFGF-supplemented media on adipogenesis of ADSCs

The use of bFGF as a potent mitogen for human MSCs, while maintaining their differentiation potential, has previously been reported in various culture systems [49-52]. With regard to adipogenesis, Neubauer *et al.* have previously shown that bFGF enhances the adipogenic differentiation of BMSCs in 2-D and 3-D cell culture [29,53]. Therefore, we supposed an enhancing effect of bFGF on the adipocyte differentiation of ADSCs as well. ADSCs were seeded at a density of 30,000 cells/cm^2 in basal medium supplemented with 3 ng/ml bFGF and cells grew to confluence within two days. At this time, cell densities were comparable between the groups with or without addition of bFGF as observed by microscopy (data not shown). Subsequently, adipogenic differentiation was induced with induction medium supplemented with 3 ng/ml bFGF. The adipogenic potential after induction of ADSCs was clearly enhanced in the presence of bFGF compared to control. At day 12 after

induction, the number of oil red O stained cells was strongly increased by addition of bFGF (Figure 5 A). This observation was verified by measurement of the intracellular TG content (Figure 5 B) as well as the GPDH activity (Figure 5 C).

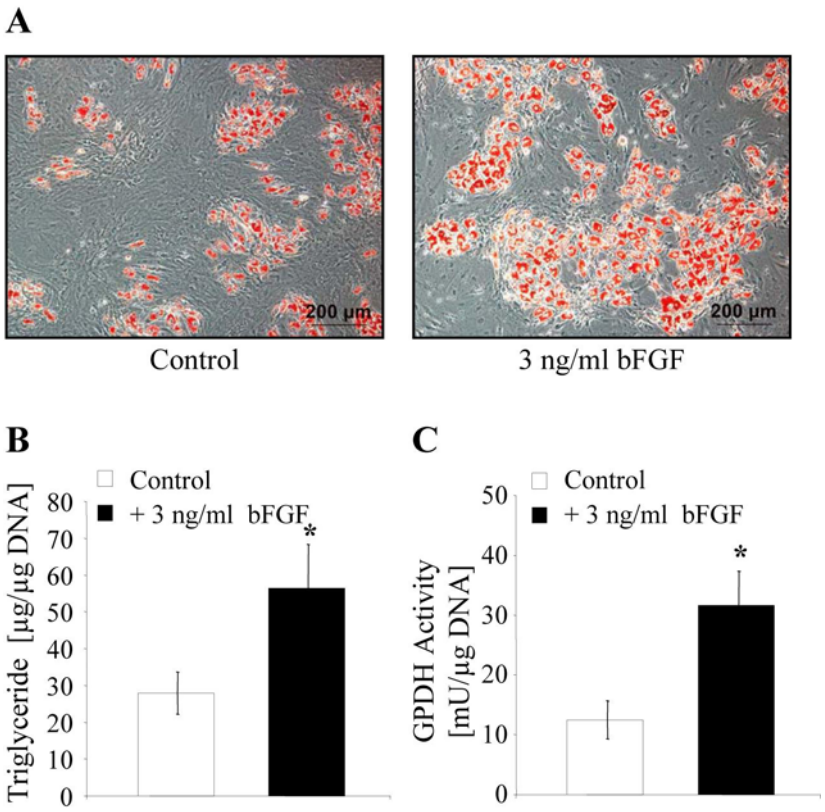

Figure 5: Effect of bFGF on the TG accumulation of ADSCs. ADSCs were expanded and, subsequently, induced to undergo adipogenesis in the absence or presence of 3 ng/ml bFGF. TG accumulation was determined at day 12 after induction. **A)** Oil red O staining of intracellular lipid droplets. Bar=200 µm. **B)** Quantification of intracellular TG content (n=3). TG contents were normalized to DNA contents. **C)** Measurement of specific GPDH activity (n=3). Enzyme activity was normalized to DNA contents. * indicates statistically significant differences to the control group ($p<0.05$).

4.5. Effect of AA-supplemented media on adipogenesis of ADSCs

A promoting effect of AA on adipogenesis of BMSCs was previously reported by Weiser *et al.* [37]. Accordingly, we tested the influence of AA on the adipogenic conversion of ADSCs. For this purpose, expansion, induction and differentiation of ADSCs were performed in the presence of 50 µg/ml AA. Afterwards, adipogenic differentiation of ADSCs was monitored at day 12 after induction (Figure 6). Oil red O staining revealed that AA supplementation remarkably decreased the number of differentiated ADSCs when compared to the respective group propagated without AA (Figure 6 A), whereas the proliferation of ADSCs was increased in presence of AA (Figure 6 A, right). The reduced adipogenic potential of ADSCs

in the presence of AA was confirmed by quantification of the intracellular TG (Figure 6 B) and by measurement of the GPDH activity (Figure 6 C).

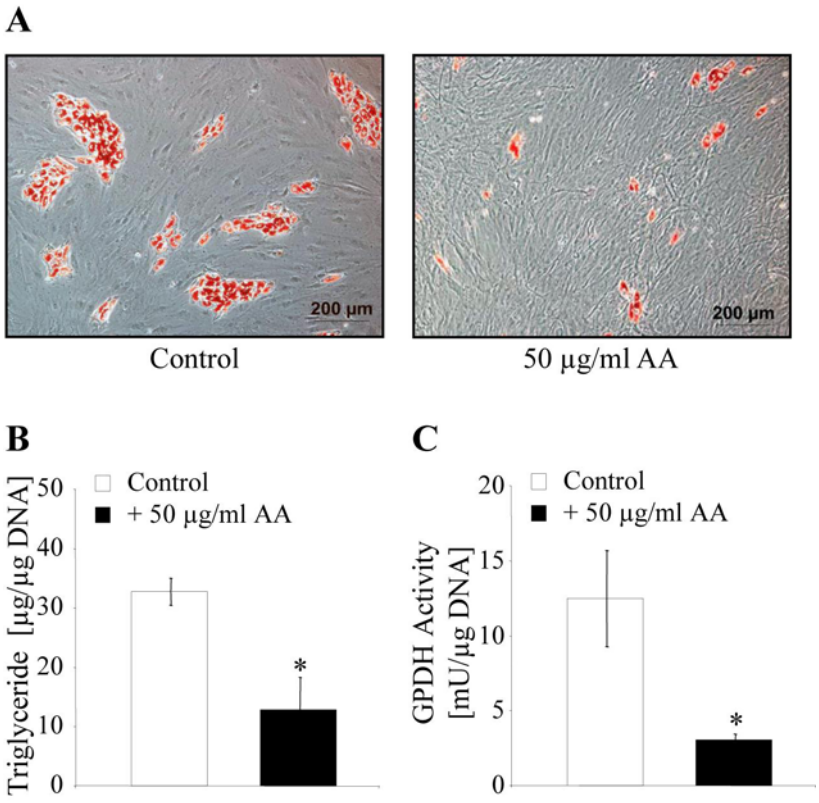

Figure 6: Effect of AA on the TG accumulation of ADSCs. ADSCs were expanded and, subsequently, induced to undergo adipogenesis in the absence or presence of 50 µg/ml AA. TG accumulation was determined at day 12 after induction. **A)** Oil red O staining of intracellular lipid droplets. Bar=200 µm. **B)** Quantification of intracellular TG content (n=3). TG contents were normalized to DNA contents. **C)** Measurement of specific GPDH activity (n=3). Enzyme activity was normalized to DNA contents. * indicates statistically significant differences to the control group ($p<0.05$).

5. Discussion

ADSCs are an attractive *in vitro* model system to study adipocyte biology or adipose-related diseases such as obesity or type 2 diabetes. The major advantages of ADSCs are their easy harvest in a large quantity as well as their expansion and differentiation capacity *in vitro*. However, to date, studies using ADSCs in different models have yielded varying results. Variability may reflect differences between individual donors as well as differences in isolation, culturing, and expansion methods.

In this study we tested different conditions for ADSC isolation and *in vitro* expansion as well as adipogenic differentiation, some of them already being used in experimental protocols.

Evaluation of the isolation procedure

The standard protocol for isolation of ADSCs from adipose tissue introduced by Rodbell *et al.* and broadly applied by most scientists is performed by enzymatic digestion and subsequent centrifugation [47,48]. We modified this standard isolation procedure according to Rodbell *et al.* as well as Schling *et al.* [54] to improve the yield of isolated ADSCs and their adipogenic differentiation potential. Firstly, we introduced two filtration steps after the digestion and tested the effect on adipogenic differentiation of ADSCs. The additional filtrations enhanced the purity of the cell suspension. Debris of digested connective tissue and other ECM components as well as mature adipocytes were removed. Thus, the percentage of adipogenic progenitors within the heterogeneous cell population was enriched and, accordingly, the differentiation efficiency as well. Some protocols reported in literature have implemented the lysis of erythrocytes after the centrifugation [55,56] which is another possibility to advance the purity of ADSCs. In our studies, the erythrocyte lysis did not affect the adipogenic capacity of the cells. Washing of the cells one day after seeding apparently also removed non-adherent cells including erythrocytes, and therefore, it had the same effect than erythrocyte lysis. Besides the modifications in isolation procedure that we have performed, the recovery of ADSCs can be improved further by manipulating the centrifugation speed [57]. Nevertheless, even if we observed an influence of the isolation procedure on adipogenic differentiation, Mizuno *et al.* have described that the immunophenotype of ADSCs was relatively constant regardless of differences in isolation and culture procedures [8].

In conclusion, we modified the standard isolation procedure from Rodbell *et al.* by introduction of two additional filtration steps which was proven to be beneficial for ADSC adipocyte culture. In contrast, the lysis of erythrocytes was not effective and, therefore, not implemented in the protocol.

Differences in adipogenic potential of ADSCs from multiple donors

We have observed that ADSCs isolated from eleven individual human donors showed varying adipogenic differentiation capacity in response to adipogenic stimulation *in vitro*. Microscopic inspection as well as flow cytometry examining lipid accumulation revealed that the fraction of cells within the heterogeneous cell population which was able to differentiate into adipocytes under adipogenic conditions differed extensively between the tested donors. The variability found in ADSC cultures is commonly known. Bunnell *et al.* have previously reported that the percentage of preadipocytes obtained from the SVF after digestion is patient-dependent and, therefore, the differentiation efficiency as well [58]. Various factors such as age, gender or disease state of the donor are discussed to be responsible for the heterogeneous

behavior of ADSCs *in vitro* [9,59-61]. Additionally, different genetic constitution of the donors may play a role for the patient-to-patient variability [62]. Furthermore, different characteristics of ADSCs isolated from different regions of the body have been reported [59,63-66]. For example, human subcutaneous adipose tissue contained more ADSCs compared to omental adipose tissue, and the ADSCs from subcutaneous tissue had a higher adipogenic differentiation capacity [65].

In independent studies, we investigated whether the method to obtain adipose tissue has an influence on the differentiation potential of ADSCs. We compared ADSCs obtained from abdominoplasties and lipoaspirates of the same donor regarding their adipogenic differentiation capacity. The different procedures did not influence the yield as well as the adipogenic potential of isolated ADSCs (data not shown). Differences in ADSC culture depending on the fat harvesting technique used are controversially discussed in literature. Some studies reported that lipoaspiration yielded more isolated ADSCs with better proliferation and adipogenic differentiation rate [67-69], whereas, in contrast, Yoshimura *et al.* reported that disruption of cells was caused in ultrasound-assisted liposuction and the number of isolated ADSC as well as their proliferative capacity was reduced [70]. In turn, other researchers reported that the type of surgical procedure did not affect the total number of viable cells that can be obtained from the SVF [71-73].

Addition of human plasma

It was supposed that human plasma contains multiple components with the potential to promote adipogenic differentiation of ADSCs. However, we have observed that the supplementation of human plasma into the medium during the entire culture period did not enhance the adipogenic potential of ADSCs. In other studies, a positive effect of human plasma on adipogenesis of various cells was reported. Lin *et al.* have shown that a medium supplemented with 10% human plasma promoted the propagation of BMSCs and preserved the adipogenic differentiation capacity of the cells [22]. Furthermore, it was reported that differentiation capacity depended on the concentration of plasma and adult serum as well as the species the plasma was derived from [21,74]. However, comparisons with data from literature are difficult due to different cell species, human plasma, and cultivation conditions.

Addition of bFGF

Under our culture conditions, bFGF did not affect proliferation of ADSCs, whereas adipogenic conversion was significantly increased in the presence of bFGF. The absent effect of bFGF on the proliferation of ADSCs was somehow unexpected since in literature an increasing proliferation was described [75,76]. Different culture conditions including varying

bFGF concentrations could be the reason for this inconsistency. With regard to adipogenesis, a promoting effect of bFGF has previously been reported in BMSCs [29]. Simultaneously to our experiments, Kakudo *et al.* also investigated the effect of bFGF on the adipogenic differentiation of ADSCs and they also observed an enhanced adipogenesis [75]. Additionally, recent studies from Lee *et al.* revealed that ADSCs which were expanded *in vitro* with bFGF and dexamethasone exhibited a higher tendency to differentiate into both osteoblasts and adipocytes [77].

The underlying mechanisms by which bFGF influences proliferation and differentiation of MSCs are poorly characterized. Different hypotheses for this are discussed in literature. It has been reported that bFGF modulates the cell morphology via alterations of the cytoskeletal and ECM organization [78,79] and it is known that matrix remodeling is important for adipocyte conversion during which adipocytes change their morphology from a spread to a spherical shape [80]. Another discussed theory includes bFGF as mitogen for a distinct subset of MSCs [52,79]. Basic FGF is assumed to stimulate the proliferation of a subpopulation of ADSCs within the heterogeneous cell pool which preferentially differentiates into adipocytes. This hypothesis has to be further investigated by culturing single cell clones of ADSCs. Finally, bFGF could influence the adipogenesis of ADSCs on the molecular level. In 3T3-L1, bFGF directly increased the expression of adipogenic key transcription factors like PPARγ and CCAAT/enhancer-binding protein α (C/EBPα) via the MEK/ERK signaling pathways [75,81].

In conclusion, the addition of bFGF was found to be suitable for ADSC culture, most notably due to its enhancing effect on adipogenic differentiation.

Addition of AA

We have demonstrated that AA increased the proliferation of ADSCs, whereas the adipogenic differentiation potential was decreased. However, our findings are inconsistent with data from literature in which AA stimulated both the proliferation and the adipogenic differentiation of various cell types such as 3T3-L1, BMSCs or ADSCs [35,37,38,67]. However, different cell systems as well as culture conditions make the comparison of our results with literature difficult.

We assumed that AA promoted the proliferation of a subpopulation within the heterogeneous cell population that was not capable of undergoing adipogenesis, similar to the hypothesis for bFGF as discussed above. Consequently, the percentage of adipogenic progenitors would be reduced resulting in a decreased adipogenic differentiation rate. The effect of AA is often linked to collagen synthesis and secretion [36,67,82]. AA is an important cofactor for the

activity of prolyl hydroxylase which is responsible for the hydroxylation of proline and lysine residues [39,83]. These hydroxylations are essential for the assembly of collagens into triple helices and subsequent secretion. Although the importance of matrix remodeling including alterations in collagen structures in adipogenesis was previously reported [80,84], we suppose that increased collagen synthesis may be obstructive for the expansion of lipid droplets. During maturation, adipocytes storing TGs within lipid droplets demand flexible surroundings for their development and expansion. Khan *et al.* have reported if the rigidity of the ECM surrounding adipocytes increased, the adipocytes were constricted to further expand due to massive pressure on the plasma membrane [85]. Thus, the correct assembly of the ECM during differentiation is important for adipocyte conversion. Finally, it cannot be excluded that other actions or mechanisms triggered by AA are responsible for the decreased adipogenic differentiation.

In conclusion, we determined an isolation procedure as well as culture conditions for the adipogenic differentiation of ADSCs *in vitro*. Concerning the isolation procedure, we introduced two additional filtration steps resulting in a more purified SVF. Subsequently, the adipogenic culture of the ADSCs was advanced by addition of bFGF into the conventionally used growth, induction, and differentiation media. The developed *in vitro* adipocyte model system with human ADSCs was used for the study of the effect of substances used for injection lipolysis in the following chapter.

References

1. Romanov Y A, Darevskaya A N, Merzlikina N V, Buravkova L B. Mesenchymal stem cells from human bone marrow and adipose tissue: isolation, characterization, and differentiation potentialities. *Bull.Exp.Biol.Med.* 2005; **140:** 138-143.
2. Gronthos S, Franklin D M, Leddy H A, Robey P G, Storms R W, Gimble J M. Surface protein characterization of human adipose tissue-derived stromal cells. *J.Cell Physiol* 2001; **189:** 54-63.
3. Lee R H, Kim B, Choi I, Kim H, Choi H S, Suh K, Bae Y C, Jung J S. Characterization and expression analysis of mesenchymal stem cells from human bone marrow and adipose tissue. *Cell Physiol Biochem.* 2004; **14:** 311-324.
4. Zuk P A, Zhu M, Ashjian P, De Ugarte D A, Huang J I, Mizuno H, Alfonso Z C, Fraser J K, Benhaim P, Hedrick M H. Human adipose tissue is a source of multipotent stem cells. *Molecular Biology of the Cell* 2002; **13:** 4279-4295.
5. Patrick C W, Jr., Chauvin P B, Hobley J, Reece G P. Preadipocyte seeded PLGA scaffolds for adipose tissue engineering. *Tissue Eng* 1999; **5:** 139-151.
6. von Heimburg D, Zachariah S, Low A, Pallua N. Influence of different biodegradable carriers on the in vivo behavior of human adipose precursor cells. *Plast.Reconstr.Surg.* 2001; **108:** 411-420.
7. von Heimburg D, Kuberka M, Rendchen R, Hemmrich K, Rau G, Pallua N. Preadipocyte-loaded collagen scaffolds with enlarged pore size for improved soft tissue engineering. *Int.J.Artif.Organs* 2003; **26:** 1064-1076.
8. Mizuno H. Adipose-derived stem cells for tissue repair and regeneration: ten years of research and a literature review. *J.Nippon Med.Sch* 2009; **76:** 56-66.
9. Niemela S M, Miettinen S, Konttinen Y, Waris T, Kellomaki M, Ashammakhi N A, Ylikomi T. Fat tissue: views on reconstruction and exploitation. *J.Craniofac.Surg.* 2007; **18:** 325-335.
10. Schaffler A, Buchler C. Concise review: adipose tissue-derived stromal cells--basic and clinical implications for novel cell-based therapies. *Stem Cells* 2007; **25:** 818-827.
11. Caspar-Bauguil S, Cousin B, Galinier A, Segafredo C, Nibbelink M, Andre M, Casteilla L, Penicaud L. Adipose tissues as an ancestral immune organ: site-specific change in obesity. *FEBS Lett.* 2005; **579:** 3487-3492.
12. Hauner H, Rohrig K, Petruschke T. Effects of epidermal growth factor (EGF), platelet-derived growth factor (PDGF) and fibroblast growth factor (FGF) on human adipocyte development and function. *Eur.J.Clin.Invest* 1995; **25:** 90-96.
13. Iwashima S, Ozaki T, Maruyama S, Saka Y, Kobori M, Omae K, Yamaguchi H, Niimi T, Toriyama K, Kamei Y, Torii S, Murohara T, Yuzawa Y, Kitagawa Y, Matsuo S. Novel culture system of mesenchymal stromal cells from human subcutaneous adipose tissue. *Stem Cells Dev.* 2009; **18:** 533-543.
14. Skurk T, Ecklebe S, Hauner H. A novel technique to propagate primary human preadipocytes without loss of differentiation capacity. *Obesity (Silver.Spring)* 2007; **15:** 2925-2931.
15. Hebert T L, Wu X, Yu G, Goh B C, Halvorsen Y D, Wang Z, Moro C, Gimble J M. Culture effects of epidermal growth factor (EGF) and basic fibroblast growth factor (bFGF) on cryopreserved human adipose-derived stromal/stem cell proliferation and adipogenesis. *J.Tissue Eng Regen.Med.* 2009; **3:** 553-561.

16. Hemmrich K, von Heimburg D, Rendchen R, Di Bartolo C, Milella E, Pallua N. Implantation of preadipocyte-loaded hyaluronic acid-based scaffolds into nude mice to evaluate potential for soft tissue engineering. *Biomaterials* 2005; **26:** 7025-7037.

17. Hauner H, Entenmann G, Wabitsch M, Gaillard D, Ailhaud G, Negrel R, Pfeiffer E F. Promoting effect of glucocorticoids on the differentiation of human adipocyte precursor cells cultured in a chemically defined medium. *J.Clin.Invest* 1989; **84:** 1663-1670.

18. Hemmrich K, von Heimburg D, Cierpka K, Haydarlioglu S, Pallua N. Optimization of the differentiation of human preadipocytes in vitro. *Differentiation* 2005; **73:** 28-35.

19. Justesen J, Stenderup K, Eriksen E F, Kassem M. Maintenance of osteoblastic and adipocytic differentiation potential with age and osteoporosis in human marrow stromal cell cultures. *Calcif.Tissue Int.* 2002; **71:** 36-44.

20. Diascro D D, Jr., Vogel R L, Johnson T E, Witherup K M, Pitzenberger S M, Rutledge S J, Prescott D J, Rodan G A, Schmidt A. High fatty acid content in rabbit serum is responsible for the differentiation of osteoblasts into adipocyte-like cells. *J.Bone Miner.Res.* 1998; **13:** 96-106.

21. Gerard C, Blouin K, Tchernof A, Doillon C J. Adipogenesis in nonadherent and adherent bone marrow stem cells grown in fibrin gel and in the presence of adult plasma. *Cells Tissues.Organs* 2008; **187:** 186-198.

22. Lin H T, Tarng Y W, Chen Y C, Kao C L, Hsu C J, Shyr Y M, Ku H H, Chiou S H. Using human plasma supplemented medium to cultivate human bone marrow-derived mesenchymal stem cell and evaluation of its multiple-lineage potential. *Transplant.Proc.* 2005; **37:** 4504-4505.

23. Janderova L, McNeil M, Murrell A N, Mynatt R L, Smith S R. Human mesenchymal stem cells as an in vitro model for human adipogenesis. *Obes.Res.* 2003; **11:** 65-74.

24. Zaragosi L E, Ailhaud G, Dani C. Autocrine fibroblast growth factor 2 signaling is critical for self-renewal of human multipotent adipose-derived stem cells. *Stem Cells* 2006; **24:** 2412-2419.

25. Powers C J, McLeskey S W, Wellstein A. Fibroblast growth factors, their receptors and signaling. *Endocr.Relat Cancer* 2000; **7:** 165-197.

26. Locklin R M, Oreffo R O, Triffitt J T. Effects of TGFbeta and bFGF on the differentiation of human bone marrow stromal fibroblasts. *Cell Biol.Int.* 1999; **23:** 185-194.

27. Vashi A V, Abberton K M, Thomas G P, Morrison W A, O'Connor A J, Cooper-White J J, Thompson E W. Adipose tissue engineering based on the controlled release of fibroblast growth factor-2 in a collagen matrix. *Tissue Eng* 2006; **12:** 3035-3043.

28. Schmidt A, Ladage D, Schinkothe T, Klausmann U, Ulrichs C, Klinz F J, Brixius K, Arnhold S, Desai B, Mehlhorn U, Schwinger R H, Staib P, Addicks K, Bloch W. Basic fibroblast growth factor controls migration in human mesenchymal stem cells. *Stem Cells* 2006; **24:** 1750-1758.

29. Neubauer M, Fischbach C, Bauer-Kreisel P, Lieb E, Hacker M, Tessmar J, Schulz M B, Goepferich A, Blunk T. Basic fibroblast growth factor enhances PPARgamma ligand-induced adipogenesis of mesenchymal stem cells. *FEBS Lett.* 2004; **577:** 277-283.

30. Alcain F J, Buron M I. Ascorbate on cell growth and differentiation. *J.Bioenerg.Biomembr.* 1994; **26:** 393-398.

31. Sato H, Takahashi M, Ise H, Yamada A, Hirose S, Tagawa Y, Morimoto H, Izawa A, Ikeda U. Collagen synthesis is required for ascorbic acid-enhanced differentiation of mouse embryonic stem cells into cardiomyocytes. *Biochem.Biophys.Res.Commun.* 2006; **342:** 107-112.

32. Farquharson C, Berry J L, Mawer E B, Seawright E, Whitehead C C. Ascorbic acid-induced chondrocyte terminal differentiation: the role of the extracellular matrix and 1,25-dihydroxyvitamin D. *Eur.J.Cell Biol.* 1998; **76:** 110-118.

33. Otsuka E, Yamaguchi A, Hirose S, Hagiwara H. Characterization of osteoblastic differentiation of stromal cell line ST2 that is induced by ascorbic acid. *Am.J.Physiol* 1999; **277:** C132-C138.

34. Wang Y, Singh A, Xu P, Pindrus M A, Blasioli D J, Kaplan D L. Expansion and osteogenic differentiation of bone marrow-derived mesenchymal stem cells on a vitamin C functionalized polymer. *Biomaterials* 2006; **27:** 3265-3273.

35. Kawada T, Aoki N, Kamei Y, Maeshige K, Nishiu S, Sugimoto E. Comparative investigation of vitamins and their analogues on terminal differentiation, from preadipocytes to adipocytes, of 3T3-L1 cells. *Comp Biochem.Physiol A Comp Physiol* 1990; **96:** 323-326.

36. Ono M, Aratani Y, Kitagawa I, Kitagawa Y. Ascorbic-Acid Phosphate Stimulates Type-IV Collagen-Synthesis and Accelerates Adipose Conversion of 3T3-L1 Cells. *Experimental Cell Research* 1990; **187:** 309-314.

37. Weiser B, Sommer F, Neubauer M, Seitz A, Tessmar J, Goepferich A, Blunk T. Ascorbic acid enhances adipogenesis of bone marrow-derived mesenchymal stromal cells. *Cells Tissues.Organs* 2009; **189:** 373-381.

38. Choi K M, Seo Y K, Yoon H H, Song K Y, Kwon S Y, Lee H S, Park J K. Effect of ascorbic acid on bone marrow-derived mesenchymal stem cell proliferation and differentiation. *J.Biosci.Bioeng.* 2008; **105:** 586-594.

39. Kivirikko K I, Myllyla R, Pihlajaniemi T. Protein hydroxylation: prolyl 4-hydroxylase, an enzyme with four cosubstrates and a multifunctional subunit. *The FASEB Journal* 1989; **3:** 1609-1617.

40. Schling P, Mallow H, Trindl A, Loffler G. Evidence for a local renin angiotensin system in primary cultured human preadipocytes. *International Journal of Obesity* 1999; **23:** 336-341.

41. Schling P, Schafer T. Human adipose tissue cells keep tight control on the angiotensin II levels in their vicinity. *Journal of Biological Chemistry* 2002; **277:** 48066-48075.

42. Ramirez-Zacarias J L, Castro-Munozledo F, Kuri-Harcuch W. Quantitation of adipose conversion and triglycerides by staining intracytoplasmic lipids with Oil red O. *Histochemistry* 1992; **97:** 493-497.

43. Fischbach C, Spruss T, Weiser B, Neubauer M, Becker C, Hacker M, Goepferich A, Blunk T. Generation of mature fat pads in vitro and in vivo utilizing 3-D long-term culture of 3T3-L1 preadipocytes. *Experimental Cell Research* 2004; **300:** 54-64.

44. Pairault J, Green H. A study of the adipose conversion of suspended 3T3 cells by using glycerophosphate dehydrogenase as differentiation marker. *Proc. Natl. Acad . Sci.U.S.A* 1979; **76:** 5138-5142.

45. Kim Y J, Sah R L, Doong J Y, Grodzinsky A J. Fluorometric assay of DNA in cartilage explants using Hoechst 33258. *Anal.Biochem.* 1988; **174:** 168-176.

46. Gimble J M, Morgan C, Kelly K, Wu X, Dandapani V, Wang C S, Rosen V. Bone morphogenetic proteins inhibit adipocyte differentiation by bone marrow stromal cells. *J.Cell Biochem.* 1995; **58:** 393-402.

47. Rodbell M. The metabolism of isolated fat cells. IV. Regulation of release of protein by lipolytic hormones and insulin. *J.Biol.Chem.* 1966; **241:** 3909-3917.

48. Rodbell M, Jones A B. Metabolism of isolated fat cells. 3. The similar inhibitory action of phospholipase C (Clostridium perfringens alpha toxin) and of insulin on lipolysis stimulated by lipolytic hormones and theophylline. *J.Biol.Chem.* 1966; **241:** 140-142.

49. van den B C, Mosca J D, Winkles J, Kerrigan L, Burgess W H, Marshak D R. Human mesenchymal stem cells respond to fibroblast growth factors. *Hum.Cell* 1997; **10:** 45-50.

50. Tsutsumi S, Shimazu A, Miyazaki K, Pan H, Koike C, Yoshida E, Takagishi K, Kato Y. Retention of multilineage differentiation potential of mesenchymal cells during proliferation in response to FGF. *Biochem.Biophys.Res.Commun.* 2001; **288:** 413-419.

51. Solchaga L A, Penick K, Porter J D, Goldberg V M, Caplan A I, Welter J F. FGF-2 enhances the mitotic and chondrogenic potentials of human adult bone marrow-derived mesenchymal stem cells. *J.Cell Physiol* 2005; **203:** 398-409.

52. Bianchi G, Banfi A, Mastrogiacomo M, Notaro R, Luzzatto L, Cancedda R, Quarto R. Ex vivo enrichment of mesenchymal cell progenitors by fibroblast growth factor 2. *Exp.Cell Res.* 2003; **287:** 98-105.

53. Neubauer M, Hacker M, Bauer-Kreisel P, Weiser B, Fischbach C, Schulz M B, Goepferich A, Blunk T. Adipose tissue engineering based on mesenchymal stem cells and basic fibroblast growth factor in vitro. *Tissue Eng* 2005; **11:** 1840-1851.

54. Schling P, Loffler G. Effects of angiotensin II on adipose conversion and expression of genes of the renin-angiotensin system in human preadipocytes. *Hormone and Metabolic Research* 2001; **33:** 189-195.

55. Zuk P A, Zhu M, Mizuno H, Huang J, Futrell J W, Katz A J, Benhaim P, Lorenz H P, Hedrick M H. Multilineage cells from human adipose tissue: Implications for cell-based therapies. *Tissue Engineering* 2001; **7:** 211-228.

56. Wall M E, Bernacki S H, Loboa E G. Effects of serial passaging on the adipogenic and osteogenic differentiation potential of adipose-derived human mesenchymal stem cells. *Tissue Eng* 2007; **13:** 1291-1298.

57. Kurita M, Matsumoto D, Shigeura T, Sato K, Gonda K, Harii K, Yoshimura K. Influences of centrifugation on cells and tissues in liposuction aspirates: optimized centrifugation for lipotransfer and cell isolation. *Plast.Reconstr.Surg.* 2008; **121:** 1033-1041.

58. Bunnell B A, Flaat M, Gagliardi C, Patel B, Ripoll C. Adipose-derived stem cells: isolation, expansion and differentiation. *Methods* 2008; **45:** 115-120.

59. Schipper B M, Marra K G, Zhang W, Donnenberg A D, Rubin J P. Regional anatomic and age effects on cell function of human adipose-derived stem cells. *Annals of Plastic Surgery* 2008; **60:** 538-544.

60. Deslex S, Negrel R, Vannier C, Etienne J, Ailhaud G. Differentiation of human adipocyte precursors in a chemically defined serum-free medium. *Int.J.Obes.* 1987; **11:** 19-27.

61. Kirkland J L, Hollenberg C H, Gillon W S. Age, anatomic site, and the replication and differentiation of adipocyte precursors. *Am.J.Physiol* 1990; **258:** C206-C210.

62. Sen A, Lea-Currie Y R, Sujkowska D, Franklin D M, Wilkison W O, Halvorsen Y D C, Gimble J M. Adipogenic potential of human adipose derived stromal cells from multiple donors is heterogeneous. *Journal of Cellular Biochemistry* 2001; **81:** 312-319.

63. Phinney D G, Kopen G, Righter W, Webster S, Tremain N, Prockop D J. Donor variation in the growth properties and osteogenic potential of human marrow stromal cells. *J.Cell Biochem.* 1999; **75:** 424-436.

64. Fraser J K, Wulur I, Alfonso Z, Zhu M, Wheeler E S. Differences in stem and progenitor cell yield in different subcutaneous adipose tissue depots. *Cytotherapy* 2007; **9:** 459-467.

65. Toyoda M, Matsubara Y, Lin K, Sugimachi K, Furue M. Characterization and comparison of adipose tissue-derived cells from human subcutaneous and omental adipose tissues. *Cell Biochemistry and Function* 2009; **27:** 440-447.

66. Jurgens W J F M, Oedayrajsingh-Varma M J, Helder M N, ZandiehDoulabi B, Scbouten T E, Kuik D J, Ritt M J P F, van Milligen F J. Effect of tissue-harvesting site on yield of stem cells derived from adipose tissue: implications for cell-based therapies. *Cell and Tissue Research* 2008; **332:** 415-426.

67. Vermette M, Trottier V, Menard V, Saint-Pierre L, Roy A, Fradette J. Production of a new tissue-engineered adipose substitute from human adipose-derived stromal cells. *Biomaterials* 2007; **28:** 2850-2860.

68. von Heimburg D, Hemmrich K, Haydarlioglu S, Staiger H, Pallua N. Comparison of viable cell yield from excised versus aspirated adipose tissue. *Cells Tissues.Organs* 2004; **178:** 87-92.

69. Oedayrajsingh-Varma M J, van Ham S M, Knippenberg M, Helder M N, Klein-Nulend J, Schouten T E, Ritt M J, van Milligen F J. Adipose tissue-derived mesenchymal stem cell yield and growth characteristics are affected by the tissue-harvesting procedure. *Cytotherapy* 2006; **8:** 166-177.

70. Yoshimura K, Shigeura T, Matsumoto D, Sato T, Takaki Y, Aiba-Kojima E, Sato K, Inoue K, Nagase T, Koshima I, Gonda K. Characterization of freshly isolated and cultured cells derived from the fatty and fluid portions of liposuction aspirates. *J.Cell Physiol* 2006; **208:** 64-76.

71. Moore J H, Jr., Kolaczynski J W, Morales L M, Considine R V, Pietrzkowski Z, Noto P F, Caro J F. Viability of fat obtained by syringe suction lipectomy: effects of local anesthesia with lidocaine. *Aesthetic Plast.Surg.* 1995; **19:** 335-339.

72. Lalikos J F, Li Y Q, Roth T P, Doyle J W, Matory W E, Lawrence W T. Biochemical assessment of cellular damage after adipocyte harvest. *J.Surg.Res.* 1997; **70:** 95-100.

73. Smith P, Adams W P, Jr., Lipschitz A H, Chau B, Sorokin E, Rohrich R J, Brown S A. Autologous human fat grafting: effect of harvesting and preparation techniques on adipocyte graft survival. *Plast.Reconstr.Surg.* 2006; **117:** 1836-1844.

74. Stute N, Holtz K, Bubenheim M, Lange C, Blake F, Zander A R. Autologous serum for isolation and expansion of human mesenchymal stem cells for clinical use. *Exp.Hematol.* 2004; **32:** 1212-1225.

75. Kakudo N, Shimotsuma A, Kusumoto K. Fibroblast growth factor-2 stimulates adipogenic differentiation of human adipose-derived stem cells. *Biochem.Biophys.Res.Commun.* 2007; **359:** 239-244.

76. Chiou M, Xu Y, Longaker M T. Mitogenic and chondrogenic effects of fibroblast growth factor-2 in adipose-derived mesenchymal cells. *Biochem.Biophys.Res.Commun.* 2006; **343:** 644-652.

77. Lee S Y, Lim J, Khang G, Son Y, Choung P H, Kang S S, Chun S Y, Shin H I, Kim S Y, Park E K. Enhanced ex vivo expansion of human adipose tissue-derived mesenchymal stromal cells by fibroblast growth factor-2 and dexamethasone. *Tissue Eng Part A* 2009; **15:** 2491-2499.

78. McBeath R, Pirone D M, Nelson C M, Bhadriraju K, Chen C S. Cell shape, cytoskeletal tension, and RhoA regulate stem cell lineage commitment. *Dev.Cell* 2004; **6:** 483-495.

79. Martin I, Muraglia A, Campanile G, Cancedda R, Quarto R. Fibroblast growth factor-2 supports ex vivo expansion and maintenance of osteogenic precursors from human bone marrow. *Endocrinology* 1997; **138:** 4456-4462.

80. Kubo Y, Kaidzu S, Nakajima I, Takenouchi K, Nakamura F. Organization of extracellular matrix components during differentiation of adipocytes in long-term culture. *In Vitro Cellular & Developmental Biology-Animal* 2000; **36:** 38-44.

81. Ailhaud G. Cell surface receptors, nuclear receptors and ligands that regulate adipose tissue development. *Clin.Chim.Acta* 1999; **286:** 181-190.

82. Murad S, Grove D, Lindberg K A, Reynolds G, Sivarajah A, Pinnell S R. Regulation of collagen synthesis by ascorbic acid. *Proc.Natl.Acad.Sci.U.S.A* 1981; **78:** 2879-2882.

83. Jacob R A. Three eras of vitamin C discovery. *Subcell.Biochem.* 1996; **25:** 1-16.

84. Ibrahimi A, Bonino F, Bardon S, Ailhaud G, Dani C. Essential role of collagens for terminal differentiation of preadipocytes. *Biochem.Biophys.Res.Commun.* 1992; **187:** 1314-1322.

85. Khan T, Muise E S, Iyengar P, Wang Z V, Chandalia M, Abate N, Zhang B B, Bonaldo P, Chua S, Scherer P E. Metabolic dysregulation and adipose tissue fibrosis: role of collagen VI. *Mol.Cell Biol.* 2009; **29:** 1575-1591.

Chapter 4

In vitro Studies of the Lipolytic Effect of Therapeutic Substances Used for Injection Lipolysis

Research Project in Cooperation with NETWORK-Lipolysis

1. Abstract

In the last years, the interest in non-invasive aesthetic procedures to reduce localized subcutaneous fat deposits has globally increased. Injections with Lipostabil®, a phosphatidylcholine (PC) and sodium deoxycholate (DC) containing agent have been developed to a practicable application for reduction of the volume of small, localized fat deposits and lipomas. The underlying mechanisms are mostly unknown to date. It is controversially discussed which ingredient of the Lipostabil® formula is the active one. Whereas cytolytic actions caused by DC have been already reported, the induction of lipolytic activity by PC, DC or Lipostabil® has not been investigated so far. Therefore, we studied the cellular effects caused by the single components DC and PC as well as by Lipostabil® itself on adipocytes by using *in vitro* cell model systems. *In vitro* dose-response relationships of these three substances were determined for adipocytes derived from 3T3-L1 and human adipose-derived stem cells (ADSCs). Additionally, effective doses of buflomedil and pentoxifyllin, both vasodilators which were supplemented to the injection compound of Lipostabil®, were investigated on 3T3-L1 cells. Changes in cell membrane integrity were evaluated microscopically. In addition, cell viability was determined with dimethyl thiazolyl diphenyl tetrazolium (MTT) assay and lipolytic activity was analyzed by measurement of the glycerol amount as a biochemical lipolysis substrate. Cell membrane lysis resulting in a significant loss of cell viability was seen in differentiated adipocytes treated with different concentrations of isolated DC. In comparison to DC, Lipostabil caused similar effects. In contrast, adipocytes only treated with PC did not show any cytotoxic effects. Furthermore, no membrane and cell damaging effects were caused by the vasodilators. Neither DC, nor PC, nor Lipostabil® led to an induction of lipolytic activity. Further experiments revealed that high concentrations of PC were able to protect cells against the cytotoxic effects caused by DC.
In conclusion, our results suggest that Lipostabil® which is used for injection lipolysis does not induce the lipolytic pathway. On the contrary, the reduction of adipose tissue volume is attributed to disruption of the cell membrane integrity caused by the detergent action of DC.

2. Introduction

Injection lipolysis, also named fat dissolution, describes a procedure in aesthetic medicine for reduction of localized fat accumulations by subcutaneous injection of substances that induce destruction of adipocytes [1-3]. Soy-derived PC which is available as Lipostabil® (Natterman & Cie GmbH, Köln, Germany) is frequently used to treat fat deposits by this procedure [2-7]. However, to date, the subcutaneous injection of Lipostabil® is not licensed, in contrast to oral and intravenous administration of Lipostabil® which is permitted in several countries as therapies for hyperlipidemia, peripheral vascular disease, cardiac ischemia, and liver disease [8-13].

The Lipostabil® formula mainly consists of PC and DC [5]. The bile salt DC is used to dissolve PC by forming mixed micelles [14,15]. For decades, the combination of intravenous medications with bile salts is commonly used to improve the aqueous solubility [16-19]. Many of the physicians supplement the Lipostabil® formula with various additives such as aminophylline, vasodilators, multivitamins, collagenase, hyualuronidase, and lidocaine to increase the efficacy of the formula [20]. The commonly used mixture which is instructed by the "Network-Lipolysis" for injection lipolysis consists of Lipostabil® (50 mg/ml PC) supplemented with 0.9% sodium chloride as diluent (50%), 5% buflomedil as vasodilator, and 1% vitamin B complexes.

The mechanism of Lipostabil® causing localized fat reduction is unknown so far. Several authors described PC as the active component of the subcutaneous injection of Lipostabil®, presumably due to its known lipid-lowering effect in serum following oral and parenteral administration [3,5,21]. Stimulation of lipase activity, emulsification and transport of triglycerides, and detergent effects were suggested as underlying mechanisms of action of PC [1,5,21]. However, some authors proposed that DC was responsible for the reduction of fat deposits by its detergent action [22]. Like other physiologic bile salts, DC possesses detergent properties with polar lipids [23,24]. This detergent action was recently shown to cause nonspecific lysis of cell membranes [22,25]. Injection of DC also reduces sizes of human lipomas which is accompanied by focal necrosis, acute inflammation, and hemorrhage as detected histologically [26]. Other recent studies showed that injection of Lipostabil® affected adipose tissue by disruption of fat cells following an inflammatory reaction similar to panniculitis [2,27]. Investigations of the expression of different pro-inflammatory cytokines after injection of Lipostabil® into lipomas showed changes of the cytokine profile including increased expression of tumor-necrosis factor-α (TNF-α), interferon-γ (INF-γ), and several interleukins (e.g. interleukin 6, 8, and 10) [28].

Nevertheless, complications following injection of Lipostabil® were relatively rare, mild, and temporary [29]. The most frequently observed side effects were transient burning, edema and erythema at the injection site, swelling immediately after injection, persistent pain beyond two weeks, late itching, hyperpigmentation, hives, bacterial infections, and skin contour deformities. Lipid, liver, and renal profiles were not altered after treatment with PC [5]. No patients were reported to die or need hospitalization. Nevertheless, due to lack of scientific studies, the safety and efficacy of this injection lipolysis remain ambiguous to most patients and physicians. The use of Lipostabil® or PC compounds for injection lipolysis is still an "off-label" use which means an application aside from its initial description. For a widely approved use of injection lipolysis, scientific data concerning the mechanism of action and safety are necessary.

Therefore, the aim of our study was to investigate cellular effects of Lipostabil® and the particular components DC and PC on differentiated adipocytes *in vitro*. Different doses and exposure times of Lipostabil®, PC, and DC were analyzed. Furthermore, the concentration-dependent effects of the vasodilators buflomedil and pentoxifyllin were investigated. The murine 3T3-L1 preadipocyte cell line, a widely utilized model system for characterization of adipocyte biology [30-32], was initially used in this study. In addition, further studies were done with adipogenically induced ADSCs as a model system for human cells [33-37]. Finally, we investigated whether the different substances stimulate simple cell death or a lipolytic pathway within the adipocytes by using enzymatic assays and propidium iodide staining.

3. Materials and Methods

Materials

Murine 3T3-L1 preadipocytes were obtained from ATCC (Manassas, VA, USA). ADSCs were isolated from human abdomen lipoaspirate obtained from cosmetic surgery as described in detail in chapter 3 (Page 47). Dulbecco's Modified Eagle's Medium (DMEM) and Dulbecco's Modified Eagle's Medium Ham'sF12 (DMEM Ham'sF12) were purchased from Biochrom (Berlin, Germany). Fetal bovine serum (FBS, Lot. No. 40A0044K), phosphate buffered saline (PBS), 0.25% trypsin-EDTA solution, and penicillin-streptomycin solution were from Invitrogen (Karlsruhe, Germany). Collagenase NB4 and 3-isobutyl-methylxanthine (IBMX) were bought from Serva Electrophoresis (Heidelberg, Germany). Papainase was from Worthington (Lakewood, NJ, USA). Bovine insulin was kindly provided by Sanofi-Aventis (Frankfurt a. M., Germany). Minimum Essential Medium alpha modification (α-MEM),

cortisol, dexamethasone, corticosterone, indomethacin, transferrin, biotin, pantothenic acid, glucose, fatty acid-free bovine serum albumin, cysteine, bovine DNA, 2-mercaptoethanol, dimethylsulfoxide (DMSO), isoproterenol, MTT, DC, propidium iodide, and oil red O were obtained from Sigma-Aldrich (Taufkirchen, Germany). Hoechst 33258 dye was obtained from Polysciences (Warrington, PA, USA). Basic FGF was from R&D Systems (Minneapolis, MN, USA). Pure PC was acquired from Lipoid GmbH (Ludwigshafen, Germany). If not stated otherwise, all other chemicals were from Merck KGaA (Darmstadt, Germany). Deionized water was obtained using a Milli-Q water purification system from Millipore (Schwalbach, Germany). All cell culture plastics were purchased from Corning (Bodenheim, Germany). Lipostabil® was obtained from Nattermann Pharma (Köln, Germany). The exact composition is given in Table 1.

Table 1: Composition of Lipostabil®

Ingredients of injectable Lipostabil® (1 ml)	
Soy-derived phospholipids (93% phosphatidylcholine)	50 mg
Sodium deoxycholate	25.3 mg
Benzyl alcohol	9 mg
Sodium chloride	3.6 mg
Sodium hydroxide	2.53 mg
DL-α-tocopherol	0.15 mg
Ethanol	3 mg
Sterile water	907.8 mg

3.1. Cell culture

3.1.1. Expansion and differentiation of 3T3-L1

3T3-L1 is a mouse embryonic fibroblast cell line. These cells are derived from the original line 3T3-Swiss albino and are used as an *in vitro* model of adipocytes [32]. 3T3-L1 preadipocytes were expanded in DMEM supplemented with 10% FBS, penicillin (100 U/ml), and streptomycin (100 µg/ml) [30,31]. Preadipocytes were seeded in basal medium (α-MEM, 10% FBS, penicillin (100 U/ml), and streptomycin (100 µg/ml)) into tissue-culture polystyrene well plates at a density of 40,000 cells/cm^2. This high seeding density guaranteed that two-dimensional (2-D) cultures grew to confluence within two days after seeding.

Hormonal induction was initiated two days after seeding by replacing the basal medium with induction medium (basal medium with 1 µM insulin, 0.1 µM corticosterone, 0.5 mM IBMX, and 60 µM indomethacin [30,31]. The time point of induction was referred to as day 0 throughout all experiments. At day 2, the medium was exchanged with differentiation medium (basal medium, 1 µM insulin). Subsequently, cells were fed by changing the differentiation medium every other day up to day 8. Cells were incubated in a humidified atmosphere at 37°C and 5% CO_2 during the complete culture period.

3.1.2. Isolation, expansion, and differentiation of ADSCs

ADSCs were isolated from human subcutaneous adipose tissue obtained during abdominal plastic surgery from healthy women or men aged 17 - 69 years as previously described in chapter 3 (Page 47). Briefly, adipose tissue was extensively washed in PBS. After removal of connective tissue and blood vessels, minced adipose tissue was subjected to enzymatic digestion using a 0.1% collagenase solution at 37°C for 4 hours on an orbital shaker (150 rpm) in order to obtain a single-cell suspension. Lipoaspirates were directly transferred to the collagenase solution containing 1 mg/ml collagenase NB4, 15 mg/ml bovine serum albumin, 100 mM 2-[-4-(2-hydroxyethyl)1-piperazinyl]-ethan-sulfonic acid (HEPES), pH 7.4, 120 mM NaCl, 50 mM KCl, 1 mM $CaCl_2$, and 5 mM glucose. The suspension was filtrated twice through a 100 µm nylon filter (BD Biosciences, San Jose, CA, USA) and centrifuged at 700 g for 7 minutes. The resulting pellet, termed the stromal vascular fraction (SVF), was resuspended in basal medium consisting of DMEM/DMEM Ham'sF12-Medium (1:1), 10% FBS, penicillin (100 U/ml), streptomycin (100 µg/ml), 1 µM insulin, 2 µg/ml transferrin, 1 µM biotin, 17 µM pantothenate, and 3 ng/ml bFGF [38]. Cells were seeded in T75 culture flasks and cultured in a humidified atmosphere at 37°C and 5% CO_2 or were cryopreserved in liquid nitrogen. Cryopreservation medium consisted of basal medium supplemented with 10% DMSO. In the case of following cultivation, cells were allowed to adhere to the substratum for one day. The flasks were rinsed twice with PBS in order to remove erythrocytes and other non-adherent cells. Cells were expanded (proliferation phase) in basal medium up to passage 3. Cyropreserved cells were similarly expanded up to passage 3 after thawing.

For experiments, cells were seeded in basal medium into tissue-culture polystyrene well plates (Corning, Bodenheim, Germany) at a density of 30,000 cells/cm^2. At confluence, cells were induced to undergo adipogenesis by supplementing basal media (without FBS) with 100 nM cortisol, 500 µM IBMX, 1 nM triiodothyronine, 500 nM troglitazone, and 3 ng/ml bFGF named as induction medium [38]. The time point of induction was referred to as day 0

throughout all experiments. At day 2, the medium was exchanged with differentiation medium (basal medium without FBS, 100 nM cortisol, 1 nM triiodothyronine, 500 nM troglitazone, and 3 ng/ml bFGF). During the entire culture period, medium was exchanged every two days and cells were incubated in a humidified atmosphere at 37°C and 5% CO_2.

3.2. Microscopical analysis of treated cells

Differentiated adipocytes were incubated with varying concentrations of Lipostabil®, PC, DC, buflomedil, and pentoxifyllin. Afterwards, microscopical bright field pictures of treated cells were acquired at 20x magnification using a CCD camera (DS-5M, Nikon, Düsseldorf, Germany) attached to an inverted microscope (Leica DM IRB, Leica Microsystems, Wetzlar, Germany) or at 63x magnification using a Zeiss Axiovert 200 M microscope equipped with a Zeiss AxioCam HRc camera and the software LSM Image Browser (Carl Zeiss MicroImaging GmbH, Jena, Germany).

3.3. Measurement of lipolysis

The hydrolysis of triglycerides into glycerol and free fatty acids is defined as lipolysis. This reaction is mainly catalyzed by the hormone-sensitive lipase and the adipose-triglyceride-lipase. The lipolytic activity of cells can be determined based on the measurement of the developed glycerol during lipolysis which is secreted by cells into the medium. Subsequently, glycerol is metabolized to glycerol-1-phosphate and following dihydroxyacetone phosphate caused by enzymatic reactions. Thereby, hydrogen peroxides are produced which can be quantified through a peroxidase-coupled reaction. The produced quinoneimine dye shows an absorbance maximum at 540 nm. The increase in absorbance at 540 nm is directly proportional to the free glycerol concentration of the sample. The lipolytic activities of the investigated substances are compared with the basal lipolytic activity of the cells cultured in differentiation medium and with lipolysis stimulated via the β-adrenergic receptor. Isoproterenol is a known agonist of the β-adrenergic receptor and is commonly used experimentally to induce lipolysis [31].

At day 8 after initiation of adipogenesis, the cells were washed with serum-free medium and then maintained in the same medium for 2 hours to avoid interference with serum factors. Subsequently, medium was replaced by PBS supplemented with 3% fatty acid-free bovine serum albumin (BSA) and the experimental substances with varying concentrations and 10 µM isoproterenol, respectively. After incubation for 4 hours, the conditioned buffer was

centrifuged (13,200 rpm, 5 minutes, 4°C) and then frozen at -20°C until the enzyme coupled enzymatic serum triglyceride determination kit from Sigma-Aldrich (Taufkirchen, Germany) was conducted according to the manufacturer's instructions. Briefly, the samples were mixed with GPO-Trinder A, an enzyme that produces quinoneimine dye from glycerol in several steps. The quinoneimine dye was photometrically measured at 540 nm and the absorbance was directly proportional to the glycerol content. The amount of glycerol per well was calculated and normalized to the cell number per sample as determined by the DNA assay.

3.4. Determination of cell viability with MTT assay

Adipogenically differentiated 3T3-L1 were treated at day 8 with indicated concentrations of the reagents for 4 hours at 37°C before determination of cell viability using the MTT assay. In this assay, yellow tetrazolium salts are metabolized by intact mitochondria and produce a color change to blue when bioreduced to formazan derivatives. The treated cells were incubated in differentiation medium containing 0.5 mg/ml MTT for 4 hours at 37°C. Subsequently, the supernatant was removed and the produced formazan derivatives were dissolved by 10% SDS/0.01 M HCl. Cell viability was analyzed photometrically (570-590 nm). The intensity of the blue color correlates with the metabolic activity of living cells. Cells treated with 1% Triton X-100 were used to determine maximally reduced cell viability.

3.5. Determination of the DNA content with DNA assay

After washing with PBS, 3T3-L1 were harvested in lysis buffer (50 mM Tris, 1 mM EDTA, 1 mM 2-mercaptoethanol, pH 7.5) and sonicated with a digital sonifier (Branson Ultrasonic Corporation, Danburg, CT, USA). Aliquots of the cell lysates were digested with papainase (3.2 U/ml in 0.1 M Na_2HPO_4 buffer, pH 6.5 containing 1 mM Na_2EDTA and 2.5 mM cysteine) for 16 hours at 60°C, and the DNA content was determined using the intercalating Hoechst 33258 dye (0.1 µg/ml in 0.1 M NaCl containing 1 mM Na_2EDTA, 10 mM Tris, pH 7.4) [39]. Fluorescence intensities were determined at 365 nm excitation wavelength and 458 nm emission wavelength on a LS 55 Fluorescence Spectrometer (PerkinElmer, Wiesbaden, Germany) and correlated to DNA contents using standard dilutions of double-stranded DNA (from calf thymus).

3.6. Determination of membrane integrity with propidium iodide staining

Propidium iodide (PI) intercalates into double-stranded nucleic acids. Under normal condition, PI is excluded by viable cells but it is ingested by dying or dead cells [40,41]. In our experiments, staining was used to evaluate the cell membrane integrity of the exposed cells. Cells were treated with varying concentrations of Lipostabil®, PC or DC for 4 hours at 37°C, 5% CO_2. Subsequently, cells were stained with 5 µg/ml PI added to medium for 5 minutes. Then, medium was replaced by fresh medium without PI and experimental agents. Cells treated with 1% Triton X-100 served as a positive control. PI has an absorption maximum at 535 nm and a fluorescence emission maximum at 617 nm and can be excited with an argon-ion laser. Microscopical fluorescence pictures were acquired at 63x magnification using a Zeiss Axiovert 200 M microscope equipped with a Zeiss AxioCam HRc camera and the software LSM Image Browser (Carl Zeiss MicroImaging GmbH, Jena, Germany).

3.7. Statistics

All quantitative results are presented as mean values ± standard deviation. Statistical analyses were determined using GraphPadPrism v.5 (GraphPad Software, La Jolla, CA, USA). Differences between multiple groups were analyzed for significance using one-way analysis of variances (ANOVA) with subsequent multiple comparisons according to Tukey's post hoc test. A value of $p<0.05$ was regarded as statistically significant.

4. Results

4.1. Cytotoxic effects of the different substances on 3T3-L1

First, we evaluated the concentrations at which the substances PC, DC, and the combined formula of Lipostabil® affected adipocytes *in vitro* by use of the murine 3T3-L1 preadipocyte cell line.

4.1.1. Effect of doses and exposure times of DC on 3T3-L1

3T3-L1 were hormonally induced to undergo adipogenesis. At day 8 after induction, the adipocytes were incubated with varying concentrations of DC to identify the effective range of the substance *in vitro*. In the first experiment, concentrations of 0.001 mg/ml to 10 mg/ml were used. For comparison, the Lipostabil® formulation which is applied for injection

lipolysis contains 12.65 mg/ml DC. We observed that the lowest concentration of 0.001 mg/ml did not affect cells, whereas concentrations higher than 0.5 mg/ml were toxic resulting in completely dead cell population (data not shown). Therefore, in the following experiment, the concentration range was limited from 0.01 mg/ml to 0.1 mg/ml DC. Differentiated 3T3-L1 were incubated with the indicated concentrations of DC for 4 hours and subsequently analyzed under the microscope (Figure 1 A).

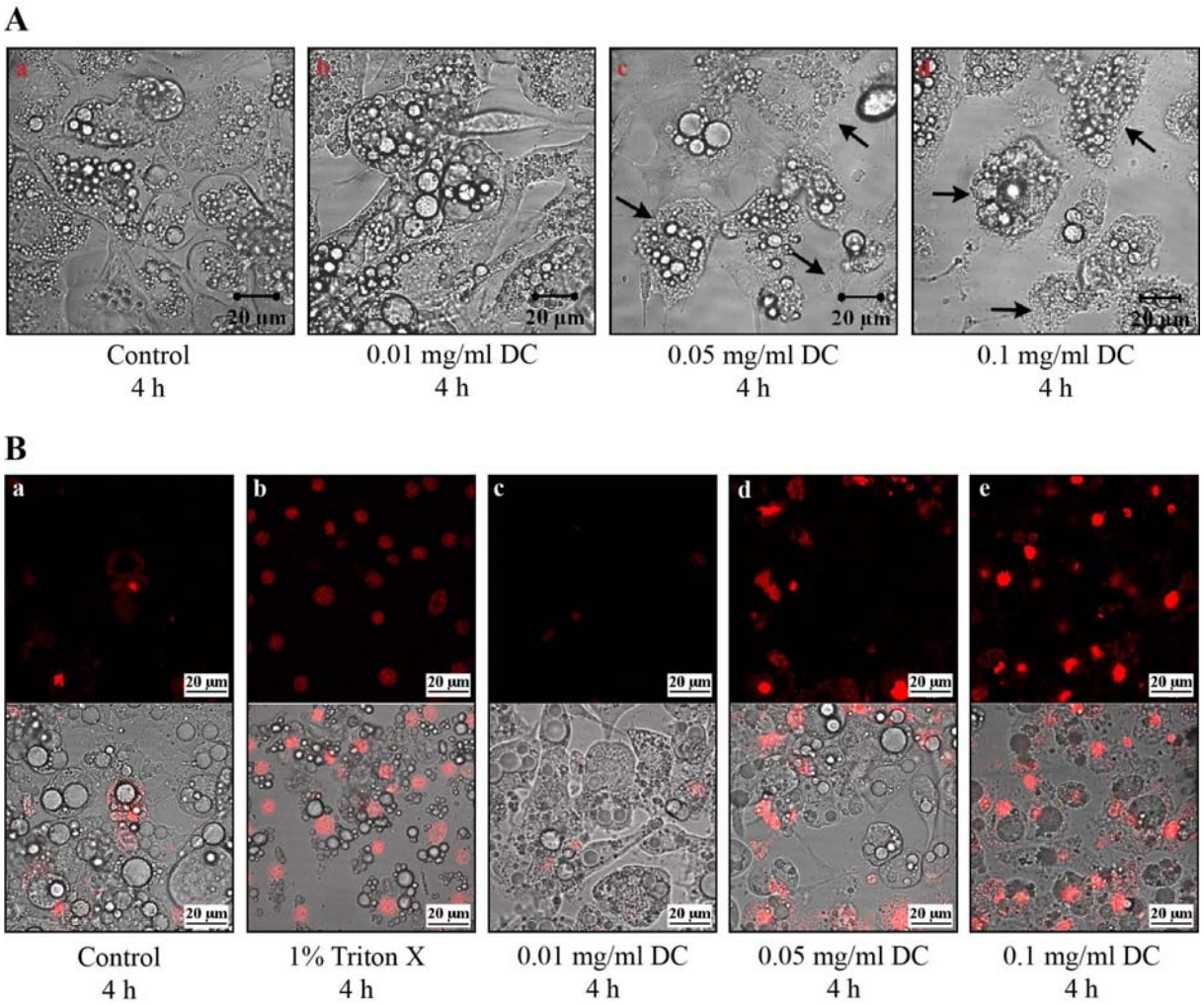

Figure 1: Incubation of 3T3-L1 with varying concentrations of DC. 3T3-L1 were induced by a hormonal cocktail to undergo adipogenic differentiation. **A)** At day 8 after induction, the differentiated adipocytes were treated with 0.01 mg/ml (b), 0.05 mg/ml (c) or 0.1 mg/ml (d) DC for 4 hours. Untreated differentiated adipocytes served as control (a). Black arrows designate cells with disrupted cell membranes. **B)** PI staining of differentiated 3T3-L1 after treatment with DC. At day 8 after induction, the differentiated adipocytes were treated with 0.01 mg/ml (c), 0.05 mg/ml (d) or 0.1 mg/ml (e) DC. Untreated differentiated adipocytes served as negative control (a), whereas adipocytes treated with 1% Triton X-100 were used as positive control (b). After 4 hours, cells were stained with 5 µg/ml PI and, subsequently, inspected under the confocal laser scanning microscope. In the upper row (a-e), PI-stained cells are presented in red on the fluorescence images. The lower row (a'-e') shows an overlap of the fluorescence images with the corresponding phase-contrast images. Bar=20 µm.

The low concentration of 0.01 mg/ml DC did not have effects on 3T3-L1 adipocytes. The cells were vital with intact cell membranes similar to non-treated control cells (Figure 1 A, a and b). An increasing concentration of 0.05 mg/ml DC caused changes in cell morphology indicated by disrupted cell structures and membranes (Figure 1 A, c). This effect was stronger with higher concentration (Figure 1 A, d).

In the following, the previous observations were verified by PI staining (Figure 1 B). PI is a DNA-intercalating agent which is not able to penetrate cells with intact cell membranes. Therefore, this dye is used for staining of necrotic cells with interrupted membranes after treatment with DC. Differentiated 3T3-L1 adipocytes were treated with the same concentrations of DC as described above. After an incubation period of 4 hours, cells were stained with 5 µg/ml PI for 5 minutes and analyzed under the confocal laser scanning microscope (Figure 1 B). PI exposure was kept short otherwise cells would be affected by PI over time. PI-stained cells showed a red fluorescence. Triton X-100 was used as positive control due to its detergent action which causes cell membrane lysis. As shown in Figure 1**Figure 1** B, b, Triton X-100 led to disruption of the cell membranes resulting in penetration of PI into the cells and following red staining of the nucleus. In presence of DC, PI-stained cells were also obvious and the number of stained cells was augmented with increasing concentrations. Consistent with previous results, the dose of 0.01 mg/ml DC did not influence cell integrity (Figure 1 B, c), only few cells were stained by PI which was also the case in the control group (Figure 1 B, a). Enhancement of the concentration to 0.05 mg/ml DC elicited a clear increase of PI-stained adipocytes (Figure 1 B, d). As expected, the number of PI-stained adipocytes indicating necrotic cells further increased with higher DC concentrations (Figure 1 B, e). This experiment verified the effective concentrations of DC. The concentration of 0.05 mg/ml DC was identified as the lowest effective one as shown by brightfield images (Figure 1 A) and fluorescence images (Figure 1 B).

In addition, exposure time of DC was investigated. For this purpose, differentiated 3T3-L1 were incubated with various concentrations of DC and cell behavior was observed at different times over a period of 24 hours (Figure 2). For the determined period, no time-dependent effect of DC was detected. 3T3-L1 incubated with DC for two hours behaved comparable to cells which were exposed to DC for a longer time. The lysis of cell membranes which was observed before (Figure 1) was confirmed in this experiment. Disruption of cells started at the concentration of 0.05 mg/ml and the toxic effect was enhanced with increasing concentrations. These results approved that an incubation period of 4 hours as already used in the previous experiments (Figure 1) was sufficient for identification of toxicity of the

substances. Therefore, we maintained the incubation time of 4 hours in the subsequent experiments.

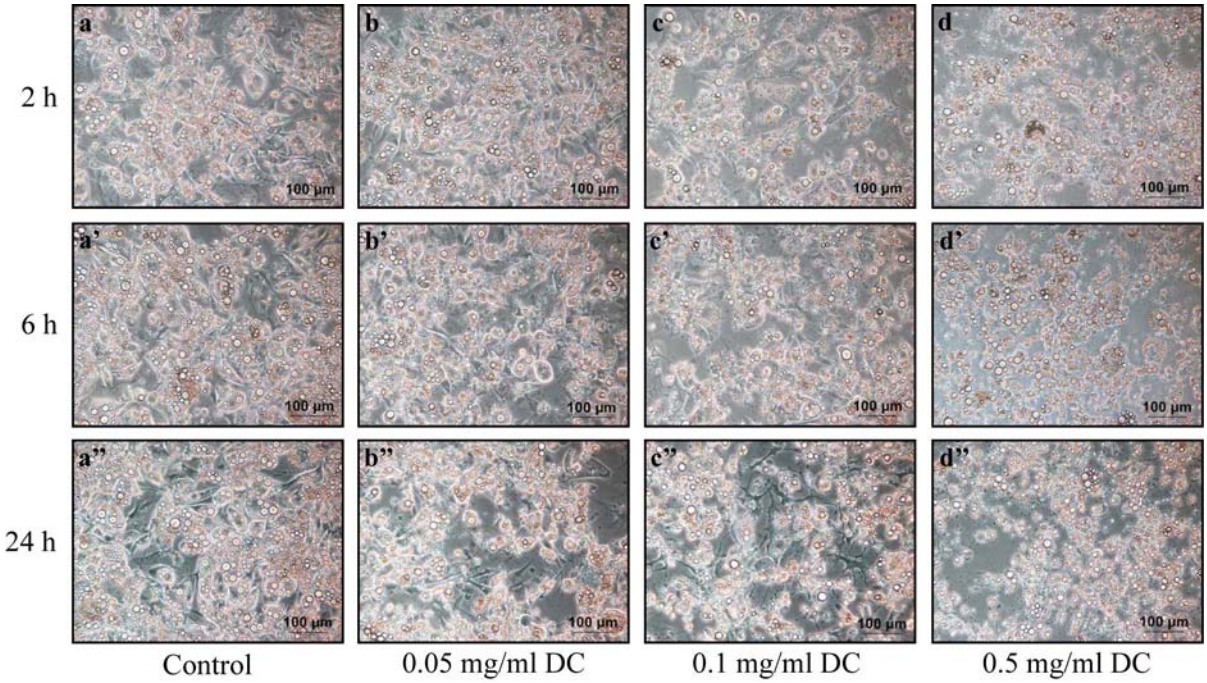

Figure 2: Incubation of 3T3-L1 with varying concentrations of DC over a period of 24 hours. 3T3-L1 were induced by a hormonal cocktail to undergo adipogenic differentiation. At day 8 after induction, the differentiated adipocytes were treated with 0.05 mg/ml (b), 0.1 mg/ml (c) or 0.5 mg/ml (d) DC. The effect of DC on adipocytes was analyzed after 2 hours (a, b, c, d), after 6 hours (a', b', c', d'), and after 24 hours (a'', b'', c'', d''). Untreated differentiated adipocytes served as control (a). Bar=100 µm.

In the following experiment, the viability of cells after treatment with DC was determined by the MTT assay (Figure 3). The MTT assay represents an alternative quantitative method to the previously performed PI staining. In this assay, it was identified which concentration of DC affected the metabolism of 3T3-L1 adipocytes.

The absorption of the control was normalized to 100% which represented a vital and metabolic active cell population. The cytotoxic detergent Triton X-100 caused a decrease of the viability of adipocytes to 40% which was used as positive control. Low DC concentrations up to 0.025 mg/ml did not significantly influence the cell viability. Only at higher concentration of 0.5 mg/ml DC, the number of viable cells was reduced to about 40% comparable to the positive control. The determined toxic concentrations were higher than the doses identified by microscopic inspection. In contrast to microscopic analysis in which we determined membrane-damaged cells, the MTT assay detected metabolic active cells. The disruption of cell membranes is an early event of cell damage finally resulting in the failure of

cell metabolism. Therefore, even if the cell membrane was affected, the cells were able to metabolize. Accordingly, this explains the decrease of the cell viability at higher DC concentrations measured by the MTT assay. The assay was performed exemplarily with 3T3-L1 treated with DC. The following investigation of the other substances like PC and Lipostabil® were done without the additional measurement using MTT assay.

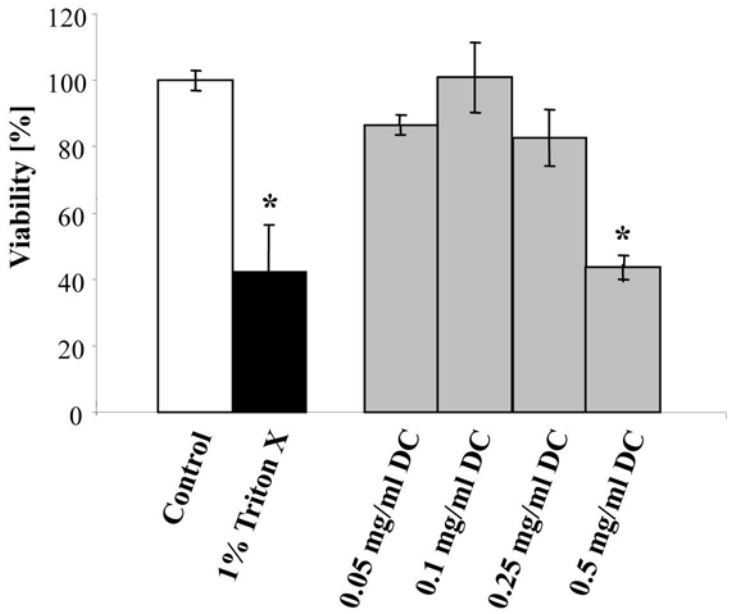

Figure 3: MTT assay of differentiated 3T3-L1 after treatment with DC. 3T3-L1 were induced by a hormonal cocktail to undergo adipogenic differentiation. At day 8 after induction, the differentiated adipocytes were treated with 0.05 mg/ml, 0.1 mg/ml, 0.25 mg/ml or 0.5 mg/ml DC. Untreated differentiated adipocytes served as negative control, whereas adipocytes treated with 1% Triton X-100 were used as positive control. After incubation for 4 hours, the MTT assay was performed (n=3). Two independent cell culture experiments were done; representative data from one experiment are shown. * indicates statistically significant differences to the control group ($p<0.05$).

4.1.2. Effect of varying concentrations of PC on 3T3-L1

Analog DC, 3T3-L1 adipocytes were treated with increasing concentrations of PC for 4 hours and, subsequently, analyzed microscopically (Figure 4 A). The effect of PC was further verified by PI staining of the adipocytes after treatment (Figure 4 B).

Neither low, nor high concentrations of PC affected the 3T3-L1 adipocytes. The morphology of treated cells did not differ from the non-treated control cells. Accordingly, the treated adipocytes were not stained with PI (Figure 4 B). This revealed that PC did not have toxic effects *in vitro*. Even the highest PC dose of 15 mg/ml did not induce cytotoxicity (Figure 4 B, e) in contrast to DC which caused distinct lysis of the cell membranes.

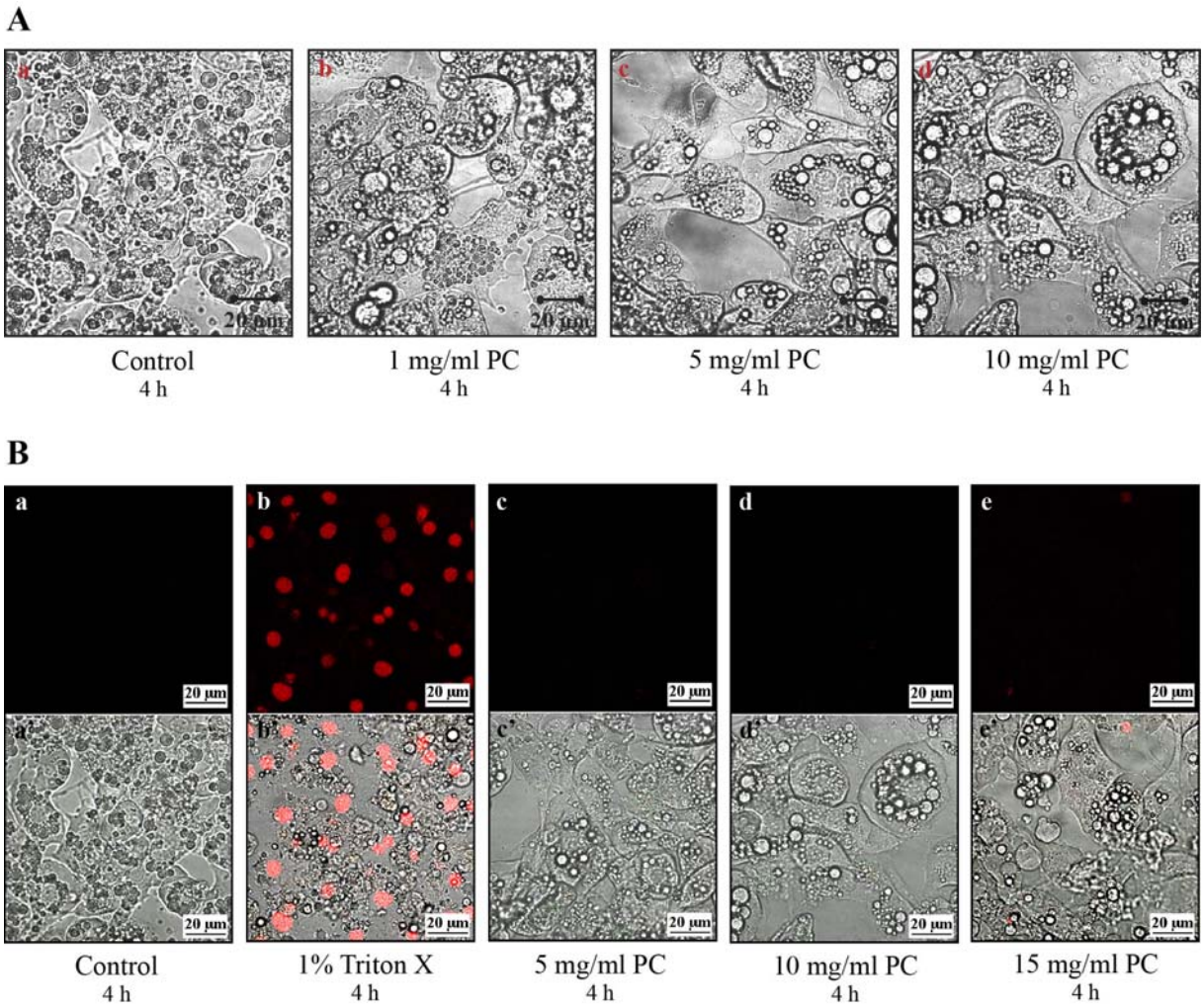

Figure 4: Incubation of 3T3-L1 with varying concentrations of PC. 3T3-L1 were induced by a hormonal cocktail to undergo adipogenic differentiation. **A)** At day 8 after induction, the differentiated adipocytes were treated with 1 mg/ml (b), 5 mg/ml (c) or 10 mg/ml (d) PC for 4 hours. Untreated differentiated adipocytes served as control (a). **B)** PI staining of differentiated 3T3-L1 after treatment with PC. At day 8 after induction, the differentiated adipocytes were treated with 5 mg/ml (c), 10 mg/ml (d) or 15 mg/ml (e) PC. Untreated differentiated adipocytes served as negative control (a), whereas adipocytes treated with 1% Triton X-100 were used as positive control (b). After 4 hours, cells were stained with 5 µg/ml PI and, subsequently, inspected under the confocal laser scanning microscope. In the upper row (a-e), PI-stained cells are presented in red on the fluorescence images. The lower row (a'-e') shows an overlap of the fluorescence images with the corresponding phase-contrast images. Bar=20 µm.

4.1.3. Effect of varying concentrations of Lipostabil® on 3T3-L1

After investigation of the effective concentration range of DC and PC which are the main components of Lipostabil®, further studies were performed with Lipostabil® itself. Firstly, effective *in vitro* doses had to be identified for this substance according to DC and PC. It was assumed that Lipostabil® has similar effects on cells compared to the single components. Based on the previously determined effective DC concentrations (Figure 1), we used doses of Lipostabil® corresponding to DC concentrations between 0.005 mg/ml and 0.5 mg/ml,

resulting in PC concentrations between 0.01 mg/ml and 1 mg/ml. The used PC concentration did not have effects when applied as single substance (Figure 4).

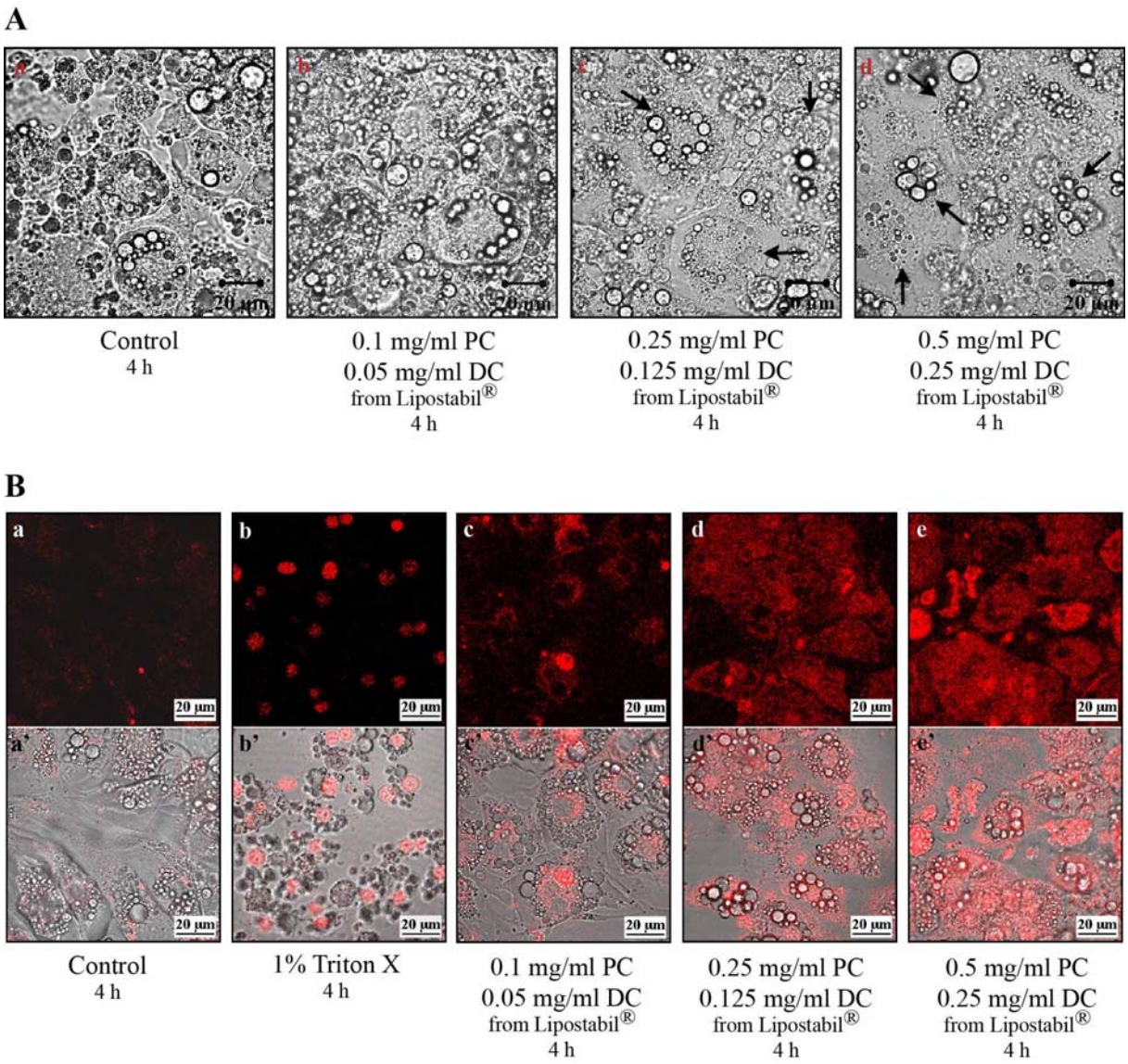

Figure 5: Incubation of 3T3-L1 with varying concentrations of PC and DC from Lipostabil®. 3T3-L1 were induced by a hormonal cocktail to undergo adipogenic differentiation. **A)** At day 8 after induction, the differentiated adipocytes were treated with 0.1 mg/ml (b), 0.25 mg/ml (c) or 0.5 mg/ml (d) PC in combination with 0.05 mg/ml (b), 0.125 mg/ml (c) or 0.25 mg/ml (d) DC for 4 hours. Untreated differentiated adipocytes served as control (a). Black arrows designate cells with disrupted cell membranes. **B)** PI staining of differentiated 3T3-L1 after treatment with Lipostabil®. At day 8 after induction, the differentiated adipocytes were treated with 0.1 mg/ml (c), 0.25 mg/ml (d) or 0.5 mg/ml (e) PC in combination with 0.05 mg/ml (c), 0.125 mg/ml (d) or 0.25 mg/ml (e) DC. Untreated differentiated adipocytes served as negative control (a), whereas adipocytes treated with 1% Triton X-100 were used as positive control (b). After 4 hours, cells were stained with 5 µg/ml PI and, subsequently, inspected under the confocal laser scanning microscope. In the upper row (a-e), PI-stained cells are presented in red on the fluorescence images. The lower row (a'-e') shows an overlap of the fluorescence images with the corresponding phase-contrast images. Bar=20 µm.

The lowest concentration of PC and DC did not have effects on cell morphology (Figure 5 A, b), whereas the PI staining showed slight cytotoxic effects (Figure 5 B, c). Increasing concentrations of DC and PC enhanced the effect and caused cell damages (Figure 5 A and B). Lipostabil® with concentrations of 0.5 mg/ml PC and 0.25 mg/ml DC provoked tremendous cell destruction resulting in cell death (Figure 5 B, e). The effective concentration range of Lipostabil® was comparable to the concentrations which were used for studies with DC as single component (Figure 1). 0.05 mg/ml DC was identified as initial concentration which caused membrane damages. PC as single substance did not cause such effects (Figure 4). These results suggested that DC is the active substance in the Lipostabil® compound being responsible for cell disruption (Figure 1 and 5).
Later, the role of PC in the compound was further investigated with regard to protective effects (see 4.3).

4.1.4. Effect of buflomedil and pentoxifyllin on 3T3-L1

In injection lipolysis therapy, Lipostabil® has been used with various additives such as vasodilators which are assumed to increase the efficacy of the formula [20]. Buflomedil and pentoxifyllin which are commercially available as Loftyl® and Trental® are used as vasodilators in the compound for injection lipolysis. In the following experiments, the effect of both substances on adipocytes was tested *in vitro*. Differentiated 3T3-L1 adipocytes were incubated with different concentrations of buflomedil and pentoxifyllin, respectively. Following 24 hours incubation time, cells were inspected microscopically (Figure 6).
Adipocytes which were incubated with low concentrations of buflomedil were similar to non-treated cells (Figure 6 A, a-c). The cells were vital with intact cell membranes. Increasing concentrations of 2 – 15 mg/ml resulted in cytotoxic effects including membrane damages (Figure 6 A, d-f). Similar observations were made in presence of pentoxifyllin (Figure 6 B). This vasodilator had also a toxic effect on adipocytes starting at a concentration of 2 mg/ml (Figure 6 B, d-f).

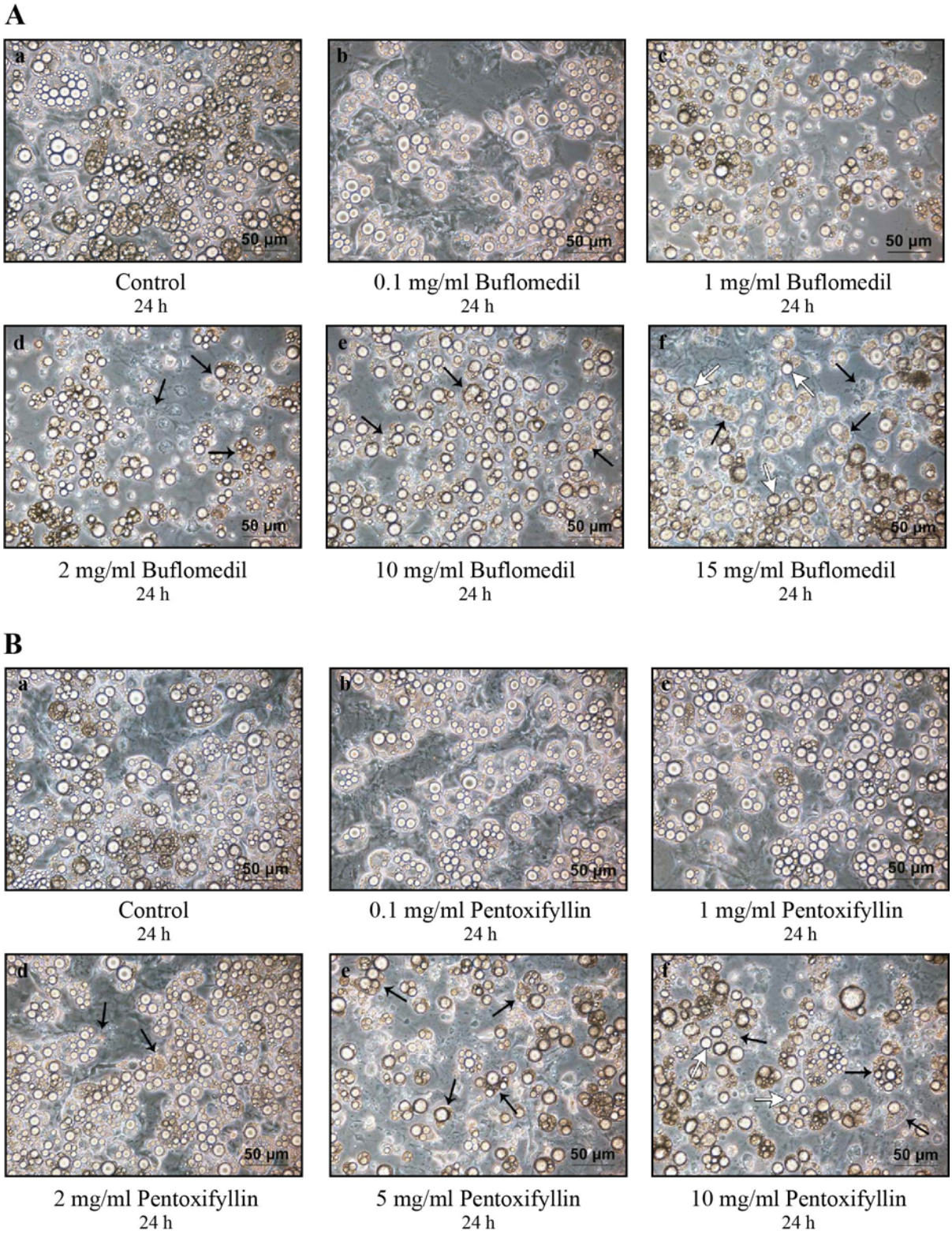

Figure 6: Incubation of 3T3-L1 with varying concentrations of buflomedil and pentoxifyllin. 3T3-L1 were induced by a hormonal cocktail to undergo adipogenic differentiation. **A)** At day 8 after induction, the differentiated adipocytes were treated with 0.1 mg/ml (b), 1 mg/ml (c), 2 mg/ml (d), 10 mg/ml (e) or 15 mg/ml (f) buflomedil for 24 hours. **B)** At day 8 after induction, the differentiated adipocytes were treated with 0.1 mg/ml (b), 1 mg/ml (c), 2 mg/ml (d), 5 mg/ml (e) or 10 mg/ml (f) pentoxifyllin for 24 hours. Untreated differentiated adipocytes served as control (A and B, a). Subsequently, cells were analyzed under the light microscope. Black arrows designate cells with disrupted cell membranes and cell fragments, respectively, whereas white arrows show isolated lipid droplets. Bar=50 µm.

After investigating the effective *in vitro* concentration range of the different substances of the compound for injection lipolysis, the identified *in vitro* concentrations were compared with the concentrations applied for injection lipolysis *in vivo*.

The toxic concentration of DC as single substance or in Lipostabil® *in vitro* is decreased about two orders of magnitude compared to the concentration applied for injection lipolysis. In contrast, PC does not affect adipocytes *in vitro,* even not at concentrations comparable to the *in vivo* applied concentration of 50 mg/ml. Thus, it is assumed that this agent does not cause cell damages *in vivo*, whereas the DC concentration used for injection lipolysis likely acts as detergent on the *in vivo* tissue resulting in cell lysis. Regarding buflomedil and pentoxifyllin, the concentrations employed for injection lipolysis therapy are far below the effective doses which were identified *in vitro*. *In vivo*, 0.25 mg/ml buflomedil and 0.5 mg/ml pentoxifyllin are applied, whereas *in vitro* clearly higher doses have to be used to cause cytotoxic effects. Therefore, it is supposed that the concentrations of the vasodilators in the compound for injection lipolysis are not toxic *in vivo*.

4.2. Lipolytic effect of DC, PC, and Lipostabil® on 3T3-L1

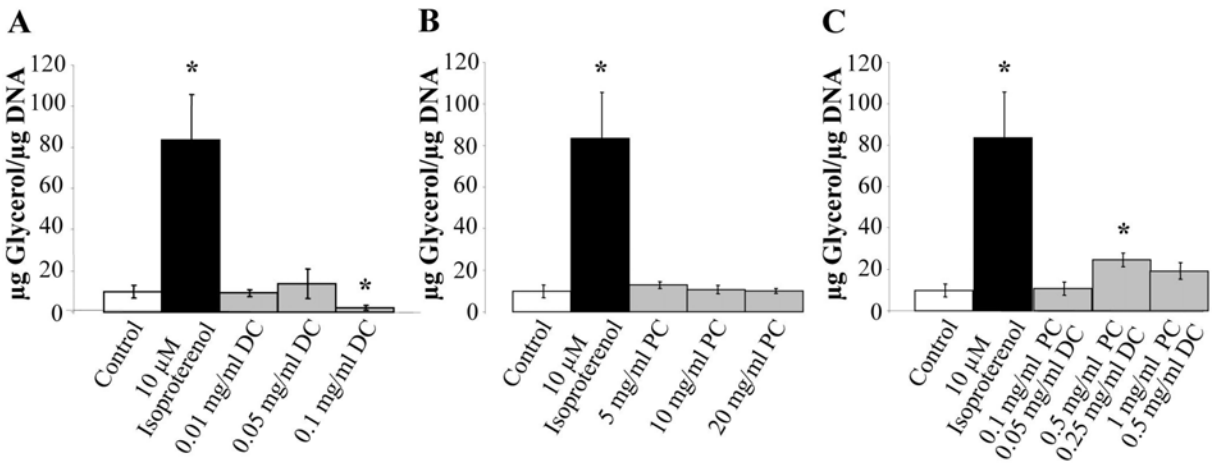

Figure 7: Lipolysis assay with 3T3-L1. 3T3-L1 were induced by a hormonal cocktail to undergo adipogenic differentiation. At day 8 after induction, the differentiated adipocytes were incubated with varying concentrations of the substances. **A)** Cells were treated with 0.01 mg/ml, 0.05 mg/ml or 0.1 mg/ml DC added to 3% BSA/PBS. **B)** Cells were treated with 5 mg/ml, 10 mg/ml or 20 mg/ml PC added to 3% BSA/PBS. **C)** Cells were treated with 0.1 mg/ml, 0.5 mg/ml or 1 mg/ml PC in combination with 0.05 mg/ml, 0.25 mg/ml or 0.5 mg/ml DC added to 3% BSA/PBS. Untreated differentiated adipocytes served as control for basal lipolytic activity, whereas adipocytes treated with 10 µM isoproterenol were used as positive control for stimulated lipolysis. After incubation for 4 hours, the lipolysis assay was performed (n=3). * indicates statistically significant differences to the untreated control group ($p<0.05$).

At day 8 after adipogenic induction, the lipolytic cell response of differentiated 3T3-L1 adipocytes was assessed by measuring the amount of glycerol release into the incubation buffer under control conditions and after treatment with Lipostabil®, PC, and DC (Figure 7).
The stimulation of lipolysis using the receptor agonist isoproterenol resulted in an eight-fold increase of the lipolytic activity compared to the basal level. The exposure of the cells to DC or PC as single substances did not stimulate lipolysis (Figure 7 A and B). The measured glycerol content was similar to the amount released by the non-treated cells. The decreasing lipolytic activity detected at a concentration of 0.1 mg/ml DC is possibly due to the extreme cytotoxic effect caused by DC as detected microscopically in previous experiments (see 4.1.1). Unlike the single substances, incubation of the cells with higher concentrations of Lipostabil® caused a slight increase of the lipolytic activity compared to the basal lipolysis (Figure 7 C).

4.3. Protective effect of PC against the toxicity caused by DC

During previous studies, we observed protective properties of PC against the toxic effect of high ethanol concentrations. Subsequently, we hypothesized that PC is also able to protectively counteract the toxic effect of DC. Protective effects of PC were already discussed in literature. Tsuboi *et al.* reported that lecithins protected from damages of the bile duct by antagonizing the cytotoxic effects of bile salts [42].
To investigate our hypothesis, differentiated 3T3-L1 adipocytes were treated with two different concentrations of DC in combination with increasing PC concentrations. Concerning DC, concentrations of 0.1 mg/ml and 0.5 mg/ml were chosen due to their high cytotoxicity as analyzed previously (see 4.1.1). These samples were supplemented with 5 mg/ml, 10 mg/ml or 15 mg/ml PC. After 4 hours, the treated cells were stained with 5 µg/ml PI followed by analysis under the confocal laser scanning microscope (Figure 8).
Both 0.1 mg/ml and 0.5 mg/ml DC damaged the cell membranes resulting in permeation of PI into the cell nucleus and intercalation with DNA (Figure 8, A and B, a). With increasing PC concentrations the membrane destabilizing effect of DC was reduced which was recognized by decreased number of PI-stained adipocytes with increasing doses of PC (Figure 8, A and B, b-d).

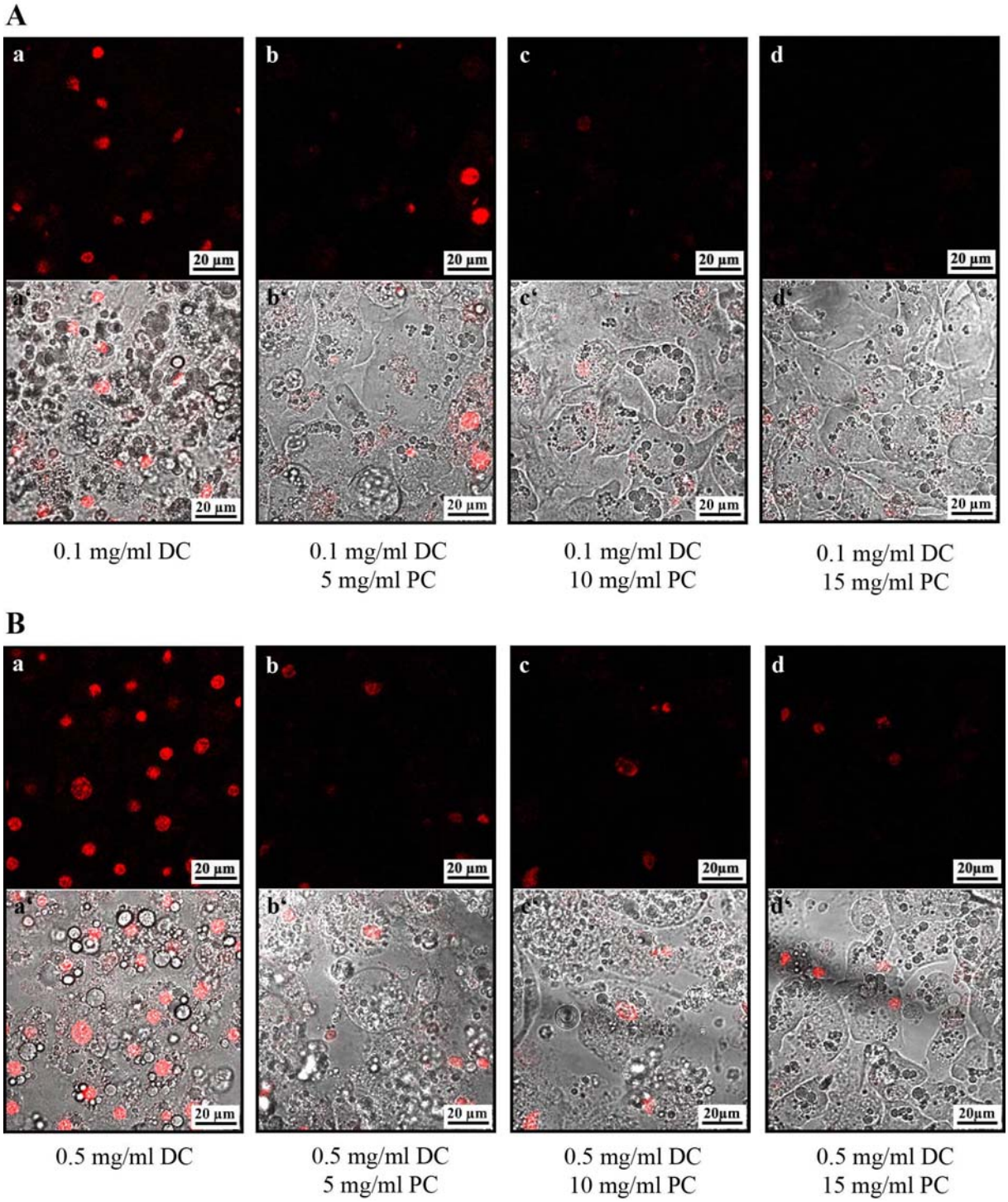

Figure 8: PI staining of differentiated 3T3-L1 after treatment with DC combined with PC. 3T3-L1 were induced by a hormonal cocktail to undergo adipogenic differentiation. At day 8 after induction, the differentiated adipocytes were treated with 0.1 mg/ml (A) or 0.5 mg/ml (B) DC in combination with 5 mg/ml (b), 10 mg/ml (c) or 15 mg/ml (d) PC. After incubation for 4 hours, cells were stained with 5 µg/ml PI and, subsequently, inspected under the confocal laser scanning microscope. In the upper row (a-d), PI-stained cells are presented in red on the fluorescence images. The lower row (a'-d') shows an overlap of the fluorescence images with the corresponding phase-contrast images. Bar=20 µm.

4.4. Cytotoxic effects of the different substances on human ADSCs

As an approach to human conditions, the following studies were performed with human ADSCs as model system. ADSCs were isolated from human subcutaneous adipose tissue as described previously (see 3.1.2).

4.4.1. Effect of varying concentrations of DC on human ADSCs

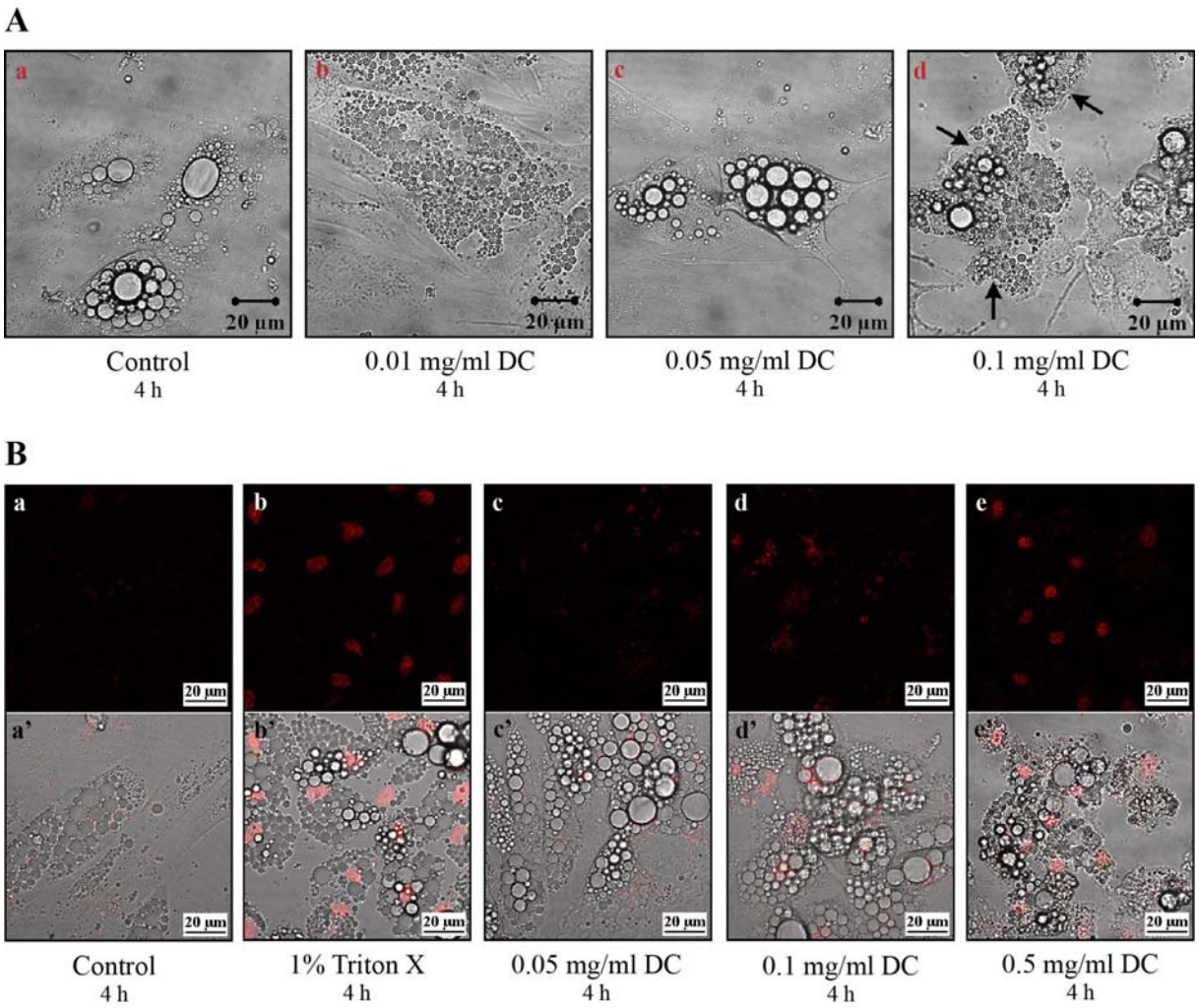

Figure 9: Incubation of ADSCs with varying concentrations of DC. ADSCs were induced by a hormonal cocktail to undergo adipogenic differentiation. **A)** At day 14 after induction, cells were treated with 0.01 mg/ml (b), 0.05 mg/ml (c) or 0.1 mg/ml (d) DC for 4 hours. Untreated ADSCs cultured in differentiation medium served as control (a). Black arrows designate cells with disrupted cell membranes. **B)** PI staining of differentiated ADSCs after treatment with DC. At day 14 after induction, the differentiated adipocytes were treated with 0.05 mg/ml (c), 0.1 mg/ml (d) or 0.5 mg/ml (e) DC. Untreated ADSCs cultured in differentiation medium served as negative control (a), whereas adipocytes treated with 1% Triton X-100 were used as positive control (b). After 4 hours, cells were stained with 5 µg/ml PI and, subsequently, inspected under the confocal laser scanning microscope. In the upper row (a-e), PI-stained cells are presented in red on the fluorescence images. The lower row (a'-e') shows an overlap of the fluorescence images with the corresponding phase-contrast images. Bar=20 µm.

To investigate the effect of DC on ADSCs, the cells were hormonally induced to undergo adipogenesis. At day 14 after induction, the differentiated ADSCs were treated with various concentrations of DC. The concentration range was similar to the one which was identified to be effective on 3T3-L1 cells. After an incubation time of 4 hours, the ADSCs were analyzed under the confocal microscope (Figure 9 A). The membrane-lysing action of DC was verified by PI staining of the cells in additional experiments (Figure 9 B).

The low DC concentration of 0.01 mg/ml did not affect cell morphology and viability (Figure 9 A, b). No differences compared to the control group were visible. The ADSCs were vital with an intact cell membrane structure. An increase of the concentration to 0.05 mg/ml DC resulted in slight damages of the membranes as shown by few PI-stained cells (Figure 9 B, c). The cell lysis progressed with higher concentrations of DC (Figure 9 A and B, d). Serious cell damages were observed after treatment with 0.5 mg/ml DC. The degree of the damage was comparable to the positive control (Figure 9 B, b and e). The effect of DC on ADSCs was not different to that on 3T3-L1 and moreover, identical dose-response relationships were characterized. 0.05 mg/ml DC was determined as the lowest concentration that affected cells and 0.5 mg/ml DC was a highly cytotoxic concentration.

4.4.2. Effect of varying concentrations of PC on human ADSCs

In the following studies, the effect of PC on ADSCs was investigated. ADSCs were induced to differentiate into the adipogenic lineage. After differentiation of 14 days, the cells were treated with varying concentrations of PC for 4 hours. Microscopic inspection including PI staining was performed afterwards (Figure 10).

As observed for 3T3-L1, PC did not have any cytotoxic effects on the human cell system. Even at the highest PC concentration of 15 mg/ml, the cells were vital and did not show any morphological changes (Figure 10 A, d). Cells which were treated with 1% Triton X-100 were extensively stained red by DNA-intercalating PI (Figure 10 B, b), whereas PC treated as well as non-treated cells showed no PI-stained cells (Figure 10 B, a, c, d, e).

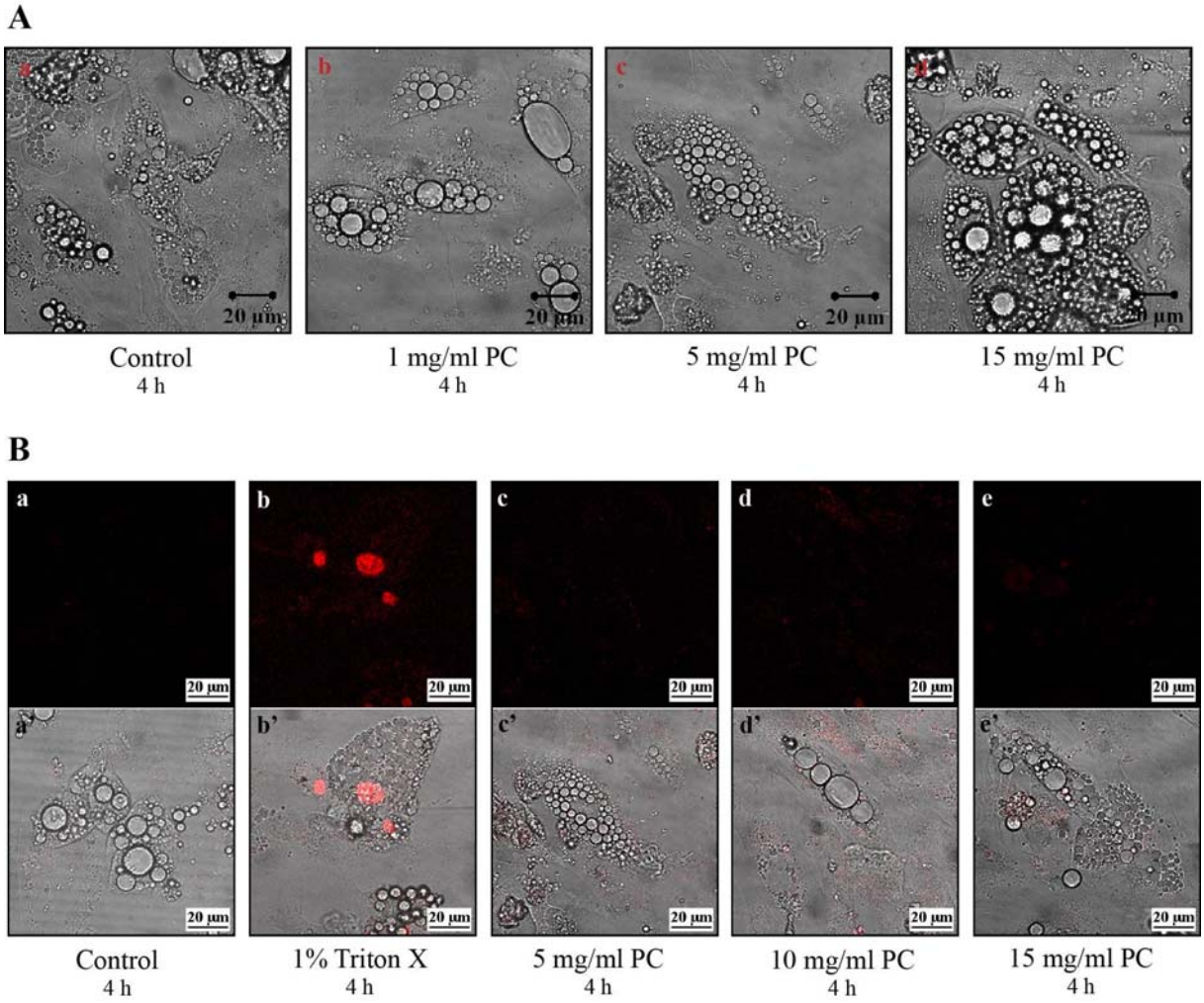

Figure 10: Incubation of ADSCs with varying concentrations of PC. ADSCs were induced by a hormonal cocktail to undergo adipogenic differentiation. **A)** At day 14 after induction, cells were treated with 1 mg/ml (b), 5 mg/ml (c) or 15 mg/ml (d) PC for 4 hours. Untreated ADSCs cultured in differentiation medium served as control (a). **B)** PI staining of differentiated ADSCs after treatment with PC. At day 14 after induction, the differentiated adipocytes were treated with 5 mg/ml (c), 10 mg/ml (d) or 15 mg/ml (e) PC. Untreated ADSCs cultured in differentiation medium served as negative control (a), whereas adipocytes treated with 1% Triton-X 100 were used as positive control (b). After 4 hours, cells were stained with 5 µg/ml PI and, subsequently, inspected under the confocal laser scanning microscope. In the upper row (a-e), PI-stained cells are presented in red on the fluorescence images. The lower row (a'-e') shows an overlap of the fluorescence images with the corresponding phase-contrast images. Bar=20 µm.

4.4.3. Effect of varying concentrations of Lipostabil® on human ADSCs

ADSCs were hormonally induced to undergo adipogenesis and after 14 days, the cells were treated with Lipostabil®. Resulting concentrations of DC between 0.025 mg/ml and 0.5 mg/ml have been shown to be effective when applied as single substance, whereas concentrations of PC between 0.05 mg/ml and 1 mg/ml did not cause any effect. Treated cells were analyzed microscopically after 4 hours incubation with Lipostabil® (Figure 11 A). Using PI staining, the cytotoxic effect of Lipostabil® was verified (Figure 11 B).

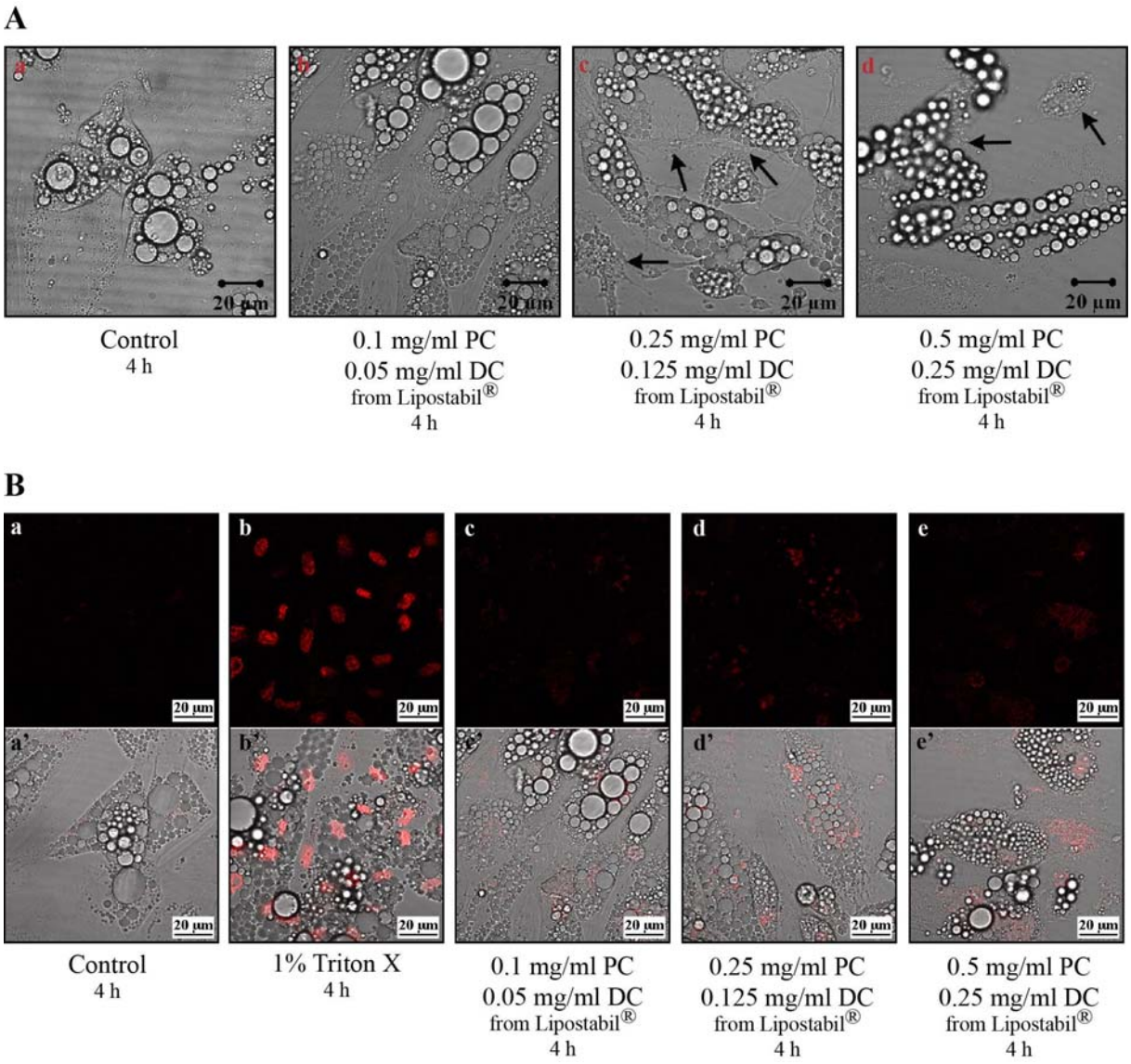

Figure 11: Incubation of ADSCs with varying concentrations of PC and DC from Lipostabil®. ADSCs were induced by a hormonal cocktail to undergo adipogenic differentiation. **A)** At day 14 after induction, cells were treated with 0.1 mg/ml (b), 0.25 mg/ml (c) or 0.5 mg/ml (d) PC in combination with 0.05 mg/ml (b), 0.125 mg/ml (c) or 0.25 mg/ml (d) DC for 4 hours. Untreated ADSCs cultured in differentiation medium served as control (a). Black arrows designate cells with disrupted cell membranes. **B)** PI staining of differentiated ADSCs after treatment with PC and DC from Lipostabil®. At day 14 after induction, the differentiated adipocytes were treated with 0.1 mg/ml (c), 0.25 mg/ml (d) or 0.5 mg/ml (e) PC in combination with 0.05 mg/ml (c), 0.125 mg/ml (d) or 0.25 mg/ml (e) DC. Untreated ADSCs cultured in differentiation medium served as negative control (a), whereas adipocytes treated with 1% Triton X-100 were used as positive control (b). After 4 hours, cells were stained with 5 µg/ml PI and, subsequently, inspected under the confocal laser scanning microscope. In the upper row (a-e), PI-stained cells are presented in red on the fluorescence images. The lower row (a'-e') shows an overlap of the fluorescence images with the corresponding phase-contrast images. Bar=20 µm.

As shown in Figure 11 A and B, concentrations of 0.1 mg/ml PC combined with 0.05 mg/ml DC did not affect the cell membrane in contrast to the following increased concentration of 0.25 mg/ml PC and 0.125 mg/ml DC. The toxicity was more enhanced with increasing

concentrations of the substances (Figure 11 A, d and B, e). The effective concentration range correlated to the concentrations which were identified to be toxic to 3T3-L1. However, human ADSCs seem to be more resistant to the substances than 3T3-L1. Exemplarily, comparison of the two cell types after treatment with 0.5 mg/ml PC in combination with 0.25 mg/ml DC revealed that 3T3-L1 were affected more seriously (Figure 5 and 11).

5. Discussion

Injection of Lipostabil® referred to as injection lipolysis has been reported to reduce localized fat accumulation [21]. Lipostabil® is mainly composed of PC and DC, of which the latter is used for phospholipid solubilization in water. PC has been used for several indications including prevention of fat embolism and fibrosis in damaged liver as well as reduction of hyperlipidemia by decreasing serum triglycerides [5,12,21,43]. Furthermore, subcutaneously injected PC was used for reduction of adipose tissue volume [1,4-6,26,44,45]. The underlying mechanisms of fat reduction after injection of Lipostabil® have not been identified so far. It is controversially discussed which component of Lipostabil® is the crucial agent. Some investigators hypothesized that PC is responsible for the reduction of adipose tissue. They hypothesized that PC bursts the cell membranes of adipocytes due to its bipolar character resulting in the induction of lipase activity. The released lipases produce a local breakdown of fat that is then metabolized via beta-oxidation in the liver [1,46]. In contrast to this hypothesis, other investigators reported that PC is not the active substance in Lipostabil® for subcutaneous lipolysis [7,22,45,47]. Rotunda *et al.* showed that DC alone produced similar effects as Lipostabil® in keratinocyte cell culture *in vitro* [22]. They hypothesized that the cell destruction is previously caused by the detergent action of DC on cell membranes [22,45] followed by fast emulsification of the released fatty acids by means of the PC [5]. Rotunda *et al.* have also reported that after injection of isolated DC into lipomas necrosis was visible resulting in reduction of adipose tissue size [47]. Thus, they suggested DC as the major active component which caused cell lysis of various cell types due to its detergent effects [22,47].

The results of our study correlates with the data published by Rotunda *et al.* [22]. We have shown by light microscopic analyses, PI staining and MTT assay that DC and Lipostabil® have cell damaging effects based on destabilization of the cell membranes. All biological cell membranes are composed of the same bilipid structure [48] and are, therefore, subject to solubilization by detergents [16,49]. The detergent is distributed between lipid bilayers which are subsequently destabilized and disintegrated resulting in the formation of mixed micelles [16,23,49]. Treatment of the adipocytes with DC and Lipostabil® resulted in a loss in cell

viability beginning at concentrations of 0.05 mg/ml DC (Figure 1, 5, 9 and 11, page 80, 85, 91 and 94). Concerning PC, no cytotoxic effect was detected (Figure 4 and 10, page 84 and 93). The cell membranes and consequently cell viability were not affected by this agent. In our studies, we did not investigate the specific mechanism of cell death. It is unclear whether apoptotic or necrotic mechanisms are responsible for loss of cell viability. Nevertheless, the cell death resulted from the detergent effect of DC.

In vitro dose-response relationships were identified for all substances. The efficient *in vitro* concentrations that we identified in our experiments were compared with the *in vivo* concentrations which were used for injection lipolysis. DC as single substance and as component in the Lipostabil® formula showed disrupting effects on cell membranes at concentrations which were decreased compared to the concentration applied *in vivo*. In contrast to this, PC did not cause any effects *in vitro* even not at concentrations comparable to the PC concentration present in Lipostabil®. Therefore, it is supposed that the applied dose of Lipostabil® used *in vivo* cause cytotoxic effects resulting from DC. Moreover, it is assumed that the cytotoxic property of Lipostabil® also affect various other cell types *in vivo*. Studies from Janke *et al.* have shown that Lipostabil® has cytolytic effects on several cell types such as adipocytes, preadipocytes, vascular smooth muscle cells, skeletal myotubes, and renal epithelial cells *in vitro* [25]. Furthermore, dose-response relationships were characterized for the vasodilators buflomedil and pentoxifyllin (Figure 6, page 87). The damaging concentrations of these two substances identified *in vitro* were much higher than the concentrations applied *in vivo*. Therefore, it is assumed that these agents do not play a role in injection lipolysis regarding cell damages.

We did not investigate the effect of benzyl alcohol which is the antimicrobial in the Lipostabil® formula. Although this substance has been discussed to affect the fluidity of cell membranes [50,51], it is not a detergent and therefore, its limited quantity in the compound is supposed to have negligible lytic effects on cell membranes.

Another objective of our study was to investigate whether the substances stimulates lipolysis in adipocytes as previously postulated [1]. We induced lipolysis by the β-agonist isoproterenol resulting in a significant increase of the glycerol release. In contrast, neither DC nor PC were able to stimulate lipolytic activity significantly (Figure 7, page 88). These results suggest that PC does not induce endogenous lipases and activate a lipolytic pathway as hypothesized by others [1,21]. Therefore, they can not be classified as lipolytic active agents. However, Lipostabil® caused a slight increase of the lipolytic activity. This increase was statistically significant at a concentration of 0.5 mg/ml PC and 0.25 mg/ml DC, whereas the

highest concentration of Lipostabil® did not show a significant difference to the control group. It has to be further investigated whether the increased lipolytic activity induced at higher concentrations of Lipostabil® is really present.

In further *in vitro* experiments, a protective property of PC against DC was demonstrated (Figure 8, page 90). At higher concentrations, PC decreased the toxic effect caused by DC. As the protective properties of PC were just observed at high concentrations, PC presumably does not take protective effects in the Lipostabil® compound used for injection lipolysis therapy. However, the protective effect of PC against DC has to be further investigated in *in vivo* experiments. In contrast to our observation, Rotunda *et al.* have observed synergistic effects of PC and DC in the Lipostabil® formula on the cell lysis of human keratinocytes *in vitro* [22].

In summary, the effect of Lipostabil® used in subcutaneous injection for fat reduction is attributed to the detergent action of DC causing nonspecific lysis of cell membranes. Our findings suggest that DC is the major active component for cell lysis. In contrast, PC is assumed to play a minor role during injection lipolysis. A recent study also suggested that PC has no effect on the reduction of fat tissue volume [52]. Furthermore, the substances did not cause lipolysis neither as single substances nor in combination like in Lipostabil®. Therefore, the fat reduction after injection lipolysis is supposed to be due to the cytolytic effect caused by DC and not to lipolytic actions induced by the substances. Thereby, the disrupting effect is not restricted to adipocytes. Physicians have to be well trained and cautious when injecting Lipostabil®. Further investigation has to be made to study the effect under *in vivo* conditions to ensure the safety and efficacy of injection lipolysis.

References

1. Hasengschwandtner F. Phosphatidylcholine treatment to induce lipolysis. *J.Cosmet.Dermatol.* 2005; **4:** 308-313.
2. Duncan D I, Hasengschwandtner F. Lipodissolve for subcutaneous fat reduction and skin retraction. *Aesthet.Surg.J.* 2005; **25:** 530-543.
3. Rittes P G. The use of phosphatidylcholine for correction of lower lid bulging due to prominent fat pads. *Dermatol.Surg.* 2001; **27:** 391-392.
4. Rittes P G. The use of phosphatidylcholine for correction of localized fat deposits. *Aesthetic Plast.Surg.* 2003; **27:** 315-318.
5. Hexsel D, Serra M, Mazzuco R, Dal'forno T, Zechmeister D. Phosphatidylcholine in the treatment of localized fat. *J.Drugs Dermatol.* 2003; **2:** 511-518.
6. Ablon G, Rotunda A M. Treatment of lower eyelid fat pads using phosphatidylcholine: clinical trial and review. *Dermatol.Surg.* 2004; **30:** 422-427.
7. Rose P T, Morgan M. Histological changes associated with mesotherapy for fat dissolution. *J.Cosmet.Laser Ther.* 2005; **7:** 17-19.
8. Khashimov K, Okur F, Orekhov A N, Kurdanov K, Tertov V. Effect of lipostabil on cholesterol levels in atherosclerotic plaques of the human aorta and the aggregative capacity of thrombocytes (in vitro study). *Biull.Vsesoiuznogo.Kardiol.Nauchn. Tsentra. AMN.SSSR* 1988; **11:** 95-98.
9. Ma X, Zhao J, Lieber C S. Polyenylphosphatidylcholine attenuates non-alcoholic hepatic fibrosis and accelerates its regression. *J.Hepatol.* 1996; **24:** 604-613.
10. Lieber C S. Alcoholic liver injury: pathogenesis and therapy in 2001. *Pathol.Biol.(Paris)* 2001; **49:** 738-752.
11. Pogozheva A V, Bobkova S N, Samsonov M A, Vasil'ev A V. Comparative evaluation of hypolipidemic effects of omega-3 polyunsaturated acids and lipostabil. *Vopr.Pitan.* 1996; 31-33.
12. Bobkova V I, Lokshina L I, Korsunskii V N, Tananova G V. Metabolic effect of lipostabil-forte. *Kardiologiia.* 1989; **29:** 57-60.
13. Kirsten R, Heintz B, Nelson K, Hesse K, Schneider E, Oremek G, Nemeth N. Polyenylphosphatidylcholine improves the lipoprotein profile in diabetic patients. *Int.J.Clin.Pharmacol.Ther.* 1994; **32:** 53-56.
14. Jones M N. Surfactants in membrane solubilisation. *Int.J.Pharm.* 1999; **177:** 137-159.
15. le Maire M, Champeil P, Moller J V. Interaction of membrane proteins and lipids with solubilizing detergents. *Biochim.Biophys.Acta* 2000; **1508:** 86-111.
16. Lichtenberg D, Robson R J, Dennis E A. Solubilization of phospholipids by detergents. Structural and kinetic aspects. *Biochim.Biophys.Acta* 1983; **737:** 285-304.
17. Hammad M A, Muller B W. Increasing drug solubility by means of bile salt-phosphatidylcholine-based mixed micelles. *Eur.J.Pharm.Biopharm.* 1998; **46:** 361-367.
18. Alkan-Onyuksel H, Ramakrishnan S, Chai H B, Pezzuto J M. A mixed micellar formulation suitable for the parenteral administration of taxol. *Pharm.Res.* 1994; **11:** 206-212.
19. Wiedmann T S, Kamel L. Examination of the solubilization of drugs by bile salt micelles. *J.Pharm.Sci.* 2002; **91:** 1743-1764.

20. Hasengschwandtner F, Furtmueller F, Spanbauer M, Silye R, Linz W J. Detailed documentation of one lipolysis treatment: blood values, histology, and ultrasound findings. *Aesthet.Surg.J.* 2007; **27:** 204-211.

21. Young V L. Lipostabil: the effect of phosphatidylcholine on subcutaneous fat. *Aesthet.Surg.J.* 2003; **23:** 413-417.

22. Rotunda A M, Suzuki H, Moy R L, Kolodney M S. Detergent effects of sodium deoxycholate are a major feature of an injectable phosphatidylcholine formulation used for localized fat dissolution. *Dermatol.Surg.* 2004; **30:** 1001-1008.

23. Almgren M. Mixed micelles and other structures in the solubilization of bilayer lipid membranes by surfactants. *Biochim.Biophys.Acta* 2000; **1508:** 146-163.

24. Banerjee P, Joo J B, Buse J T, Dawson G. Differential solubilization of lipids along with membrane proteins by different classes of detergents. *Chem.Phys.Lipids* 1995; **77:** 65-78.

25. Janke J, Engeli S, Gorzelniak K, Luft F C, Jordan J. Compounds used for 'injection lipolysis' destroy adipocytes and other cells found in adipose tissue. *Obes.Facts.* 2009; **2:** 36-39.

26. Rotunda A M, Kolodney M S. Mesotherapy and phosphatidylcholine injections: historical clarification and review. *Dermatol.Surg.* 2006; **32:** 465-480.

27. Bechara F G, Sand M, Hoffmann K, Sand D, Altmeyer P, Stucker M. Fat tissue after lipolysis of lipomas: a histopathological and immunohistochemical study. *J.Cutan.Pathol.* 2007; **34:** 552-557.

28. Bechara F G, Skrygan M, Kreuter A, Altmeyer P, Gambichler T. Cytokine mRNA levels in human fat tissue after injection lipolysis with phosphatidylcholine and deoxycholate. *Arch.Dermatol.Res.* 2008; **300:** 455-459.

29. Bechara F G, Sand M, Sand D, Rotterdam S, Stucker M, Altmeyer P, Hoffmann K. Lipolysis of lipomas in patients with familial multiple lipomatosis: an ultrasonography-controlled trial. *J.Cutan.Med.Surg.* 2006; **10:** 155-159.

30. Fischbach C, Spruss T, Weiser B, Neubauer M, Becker C, Hacker M, Goepferich A, Blunk T. Generation of mature fat pads in vitro and in vivo utilizing 3-D long-term culture of 3T3-L1 preadipocytes. *Experimental Cell Research* 2004; **300:** 54-64.

31. Fischbach C, Seufert J, Staiger H, Hacker M, Neubauer M, Goepferich A, Blunk T. Three-dimensional in vitro model of adipogenesis: Comparison of culture conditions. *Tissue Engineering* 2004; **10:** 215-229.

32. Green H, Meuth M. An established pre-adipose cell line and its differentiation in culture. *Cell* 1974; **3:** 127-133.

33. Zuk P A, Zhu M, Ashjian P, De Ugarte D A, Huang J I, Mizuno H, Alfonso Z C, Fraser J K, Benhaim P, Hedrick M H. Human adipose tissue is a source of multipotent stem cells. *Molecular Biology of the Cell* 2002; **13:** 4279-4295.

34. Zuk P A, Zhu M, Mizuno H, Huang J, Futrell J W, Katz A J, Benhaim P, Lorenz H P, Hedrick M H. Multilineage cells from human adipose tissue: Implications for cell-based therapies. *Tissue Engineering* 2001; **7:** 211-228.

35. Romanov Y A, Darevskaya A N, Merzlikina N V, Buravkova L B. Mesenchymal stem cells from human bone marrow and adipose tissue: isolation, characterization, and differentiation potentialities. *Bull.Exp.Biol.Med.* 2005; **140:** 138-143.

36. Niemela S M, Miettinen S, Konttinen Y, Waris T, Kellomaki M, Ashammakhi N A, Ylikomi T. Fat tissue: views on reconstruction and exploitation. *J.Craniofac.Surg.* 2007; **18:** 325-335.

37. Patrick C W, Jr. Tissue engineering strategies for adipose tissue repair. *Anat.Rec.* 2001; **263:** 361-366.

38. Schling P, Schafer T. Human adipose tissue cells keep tight control on the angiotensin II levels in their vicinity. *Journal of Biological Chemistry* 2002; **277:** 48066-48075.

39. Kim Y J, Sah R L, Doong J Y, Grodzinsky A J. Fluorometric assay of DNA in cartilage explants using Hoechst 33258. *Anal.Biochem.* 1988; **174:** 168-176.

40. Moore A, Donahue C J, Bauer K D, Mather J P. Simultaneous measurement of cell cycle and apoptotic cell death. *Methods Cell Biol.* 1998; **57:** 265-278.

41. Loo D T, Rillema J R. Measurement of cell death. *Methods Cell Biol.* 1998; **57:** 251-264.

42. Tsuboi K, Tazuma S, Nishioka T, Chayama K. Partial characterization of cytoprotective mechanisms of lecithin against bile salt-induced bile duct damage. *J.Gastroenterol.* 2004; **39:** 955-960.

43. Lieber C S, Robins S J, Li J, DeCarli L M, Mak K M, Fasulo J M, Leo M A. Phosphatidylcholine protects against fibrosis and cirrhosis in the baboon. *Gastroenterology* 1994; **106:** 152-159.

44. Treacy P J, Goldberg D J. Use of phosphatidylcholine for the correction of lower lid bulging due to prominent fat pads. *J.Cosmet.Laser Ther.* 2006; **8:** 129-132.

45. Salti G, Ghersetich I, Tantussi F, Bovani B, Lotti T. Phosphatidylcholine and sodium deoxycholate in the treatment of localized fat: a double-blind, randomized study. *Dermatol.Surg.* 2008; **34:** 60-66.

46. Mathur S N, Born E, Murthy S, Field F J. Phosphatidylcholine increases the secretion of triacylglycerol-rich lipoproteins by CaCo-2 cells. *Biochem.J.* 1996; **314 (Pt 2):** 569-575.

47. Rotunda A M, Ablon G, Kolodney M S. Lipomas treated with subcutaneous deoxycholate injections. *J.Am.Acad.Dermatol.* 2005; **53:** 973-978.

48. Singer S J, Nicolson G L. The fluid mosaic model of the structure of cell membranes. *Science* 1972; **175:** 720-731.

49. Lichtenberg D. Characterization of the solubilization of lipid bilayers by surfactants. *Biochim.Biophys.Acta* 1985; **821:** 470-478.

50. Ebihara L, Hall J E, MacDonald R C, McIntosh T J, Simon S A. Effect of benzyl alcohol on lipid bilayers. A comparisons of bilayer systems. *Biophys.J.* 1979; **28:** 185-196.

51. Gordon L M, Sauerheber R D, Esgate J A, Dipple I, Marchmont R J, Houslay M D. The increase in bilayer fluidity of rat liver plasma membranes achieved by the local anesthetic benzyl alcohol affects the activity of intrinsic membrane enzymes. *J.Biol.Chem.* 1980; **255:** 4519-4527.

52. Salles A G, Valler C S, Ferreira M C. Histologic response to injected phosphatidylcholine in fat tissue: experimental study in a new rabbit model. *Aesthetic Plast.Surg.* 2006; **30:** 479-484.

Chapter 5

Effect of a Prolyl Hydroxylase Inhibitor on Adipogenesis in 2-D and 3-D Culture

To be submitted to BBRC Journal

1. Abstract

Adipose tissue is a highly specialized connective tissue that is involved in energy metabolism of the organism by storing excess energy as lipid. Cellular and molecular processes of adipocyte development can be studied sufficiently when the *in vitro* adipocyte microenvironment resembles adipose tissue *in vivo* as closely as possible. Therefore, three-dimensional (3-D) culture systems that mimic *in vivo* tissue environment can be used to further improve the understanding of cellular mechanisms and, respectively, the role of the extracellular matrix during the differentiation of adipocytes. In this study, the utilized 3-D culture system is based on the formation of spheroids. Ethyl-3,4-dihydroxybenzoate (EDHB), a specific inhibitor of collagen prolyl hydroxylase, was used to examine the role of collagens in a tissue-like context during adipogenesis of 3T3-L1 *in vitro*. In contrast to two-dimensional (2-D) culture, EDHB prevented the differentiation of adipocytes in 3-D spheroids as detected by oil red O staining. Accordingly, triglyceride accumulation and glycerol-3-phosphate dehydrogenase activity were significantly inhibited by EDHB in 3-D compared to 2-D cell system. Measurement of the hydroxyproline content during adipogenic differentiation assessed that the activity of the prolyl hydroxylases was reduced by EDHB in 3-D culture, whereas in 2-D culture the enzyme was still active. Further investigations of the gene expression of collagen prolyl-4-hydroxylase alpha 1 during adipogenesis by qRT-PCR analysis revealed an increase of this gene in 2-D culture in contrast to 3-D spheroids. Furthermore, the effect of EDHB on the adipogenesis was investigated in adipose-derived stem cells (ADSCs) in which EDHB prevented the differentiation in both 2-D and 3-D culture. In conclusion, these results demonstrate the importance of a 3-D tissue-like context for *in vitro* studies and furthermore, the importance of collagens for the adipogenesis.

2. Introduction

A better understanding of the mechanism of adipose tissue differentiation is of paramount importance in the development of therapeutic strategies for the treatment and prevention of obesity and type 2 diabetes mellitus. 2-D culture of preadipocytes following differentiation into adipocytes is the most frequently used adipogenic model system to study adipogenesis *in vitro*. Despite of this, the 2-D culture system cannot fully capture the relevant complexity of the *in vivo* adipose tissue. White adipose tissue consists of various cell types such as preadipocytes, mature adipocytes, interstitial cells, and epithelial cells which are embedded in a highly organized extracellular matrix (ECM) composed of multiple types of collagen and other ECM proteins. Accordingly, many important factors such as tissue-specific architecture as well as cell-cell and cell-matrix communication are lost in 2-D [1-3]. Indeed, these tissue-inherent factors are known to govern biological processes including adipocyte development [3-8]. Therefore, to elucidate the role of cell-matrix interactions in adipocyte biology, a 3-D cell system is required. Several approaches have been reported to generate 3-D constructs *in vitro*. Reconstructing the architecture of adipose tissue *in vitro* can be achieved by seeding preadipocytes either on synthetic fibrous scaffolds [3,7,9,10] or into collagen gels [6,11] followed by adipogenic differentiation. However, scaffold or gel-based systems also bear several disadvantages. Most notably, the exogenous materials prevent the formation of a coherent cellular context, at least at early stages of the culture. Accordingly, direct cell-cell and cell-matrix interactions are limited. To dissolve this problem, we used a 3-D model system based on the formation of cellular aggregates utilizing the liquid overlay technique [12,13] which was previously developed by our group [14]. 3T3-L1 preadipocytes are seeded onto non-adherent surfaces and, as a consequence, are forced to attach to each other and form multicellular aggregates. These constructs differentiate to homogeneous adipose tissue-like structures. The spheroid model has the great advantage that it does not require an exogenous scaffold. The preadipocytes aggregate after seeding and subsequently secrete their own ECM resulting in a coherent tissue-like context. This characteristic renders the 3-D spheroids a suitable model system for studying the importance of the matrix for adipocyte development.

The ECM is more than a passive structure that fills space and offers structural support for cells both *in vitro* and *in vivo*. Besides the function as a structure component, the ECM is known to be an important factor for the regulation of different cell functions. Especially differentiation processes into various types of cells are regulated by cell-cell and cell-ECM interactions [15,16]. Previous studies showed that the ECM components play a role in differentiation of preadipocytes into adipocytes [17,18]. This highly controlled process has

been extensively characterized on cellular and molecular levels, however, the extracellular components involved in signaling mechanisms of adipogenesis are only marginally identified [19]. Changes in the composition of the ECM lead to morphological alterations and reorganization of the cytoskeleton in adipocytes, both important processes for the expression of mRNA encoding for lipogenic enzymes in adipose cells [8,20-22].

The most abundant components of the ECM are collagens. During differentiation, the expression of some collagens such as collagen I, III, IV, and VI are known to vary [23]. The modulation of the ECM by remodeling its structure and activity has profound effects on its functionality and consequently on the behavior of cells residing within the matrix. The matrix structure can be disturbed by use of modulating inhibitors such as EDHB that inhibits collagen assembly [8,17,24-27]. EDHB is an inhibitor of collagen prolyl hydroxylases due to its analog structure of ascorbate and α-ketoglutarate which are essential cofactors for enzyme activity. The collagen prolyl-4-hydroxylase is specifically involved in the synthesis of procollagens by converting proline residues to 4(R)-hydroxyproline within the endoplasmic reticulum. This posttranslational modification is essential for the triple-helical assembly of collagens and for subsequent secretion into the extracellular space. Inhibition of the collagen triple helix formation leads to nonfunctional proteins which are rapidly degraded both in the intracellular and extracellular space [25,28].

Previous studies have shown that EDHB affected the adipogenic development of mouse 3T3-L1 and TA1 preadipocytes as well as bovine intramuscular preadipocytes (BIP) in 2-D culture [17,18,29]. However, only a partial reduction of adipogenesis was achieved in all studies. As the well organized matrix structure of 3-D adipose tissue seems to be an important modulator of adipocyte differentiation, we hypothesized that EDHB has even more profound effects on adipogenesis in coherent tissue-like 3-D cultures.

Thus, the aim of this study was to examine the influence of the collagen organization on the adipogenic differentiation of 3T3-L1 cells in 3-D spheroids compared to 2-D culture by using EDHB as an inhibitor of collagen synthesis. For this, 3T3-L1 preadipocytes as well as ADSCs cultured in 2-D and 3-D were differentiated in the presence of EDHB and subsequently, adipogenic development was assessed. Even though it has been reported that EDHB indirectly affected the adipogenic differentiation through inhibition of collagen synthesis, the activity of the collagen prolyl hydroxylase was not yet investigated regarding adipogenesis. Therefore, we directly determined the prolyl hydroxylase activity during adipogenesis by measurement of the hydroxyproline content in 3-D compared to 2-D cell culture. In this context, also the

expression of the collagen-4-prolyl hydroxylase was investigated during adipogenic differentiation of both cell culture systems.

3. Materials and Methods

Materials

Murine 3T3-L1 preadipocytes were obtained from ATCC (Manassas, VA, USA). ADSCs were isolated from human abdomen lipoaspirate obtained from cosmetic surgery as described in detail in chapter 3 (Page 47). Dulbecco's Modified Eagle's Medium (DMEM) was purchased from Biochrom (Berlin, Germany). Preadipocyte Basal Medium-2 (PBM-2) was bought from Lonza (Köln, Germany). Fetal bovine serum (FBS, Lot. No. 40A0044K), phosphate buffered saline (PBS), 0.25% trypsin-EDTA solution, penicillin-streptomycin solution, Superscript II reverse transcriptase, and SYBR Green Supermix were from Invitrogen (Karlsruhe, Germany). Collagenase NB4 and 3-isobutyl-methylxanthine (IBMX) were bought from Serva Electrophoresis (Heidelberg, Germany). Papainase was from Worthington (Lakewood, NJ, USA). Thesit was obtained from Gepepharm GmbH (Siegburg, Germany). Bovine insulin was kindly provided by Sanofi-Aventis (Frankfurt a. M., Germany). Minimum Essential Medium alpha modification (α-MEM), agarose, dexamethasone, corticosterone, indomethacin, transferrin, sodium selenite, bovine serum albumin, cysteine, bovine DNA, 2-mercaptoethanol, Tris base, dihydroxyacetone phosphate (DHAP), EDHB, and oil red O were obtained from Sigma-Aldrich (Taufkirchen, Germany). Hoechst 33258 dye was obtained from Polysciences (Warrington, PA, USA). Nicotinamide adenine dinucleotide (NADH) and random hexamer primers were from Roche (Mannheim, Germany). Osmium tetroxide was purchased from Carl Roth (Karlsruhe, Germany). If not stated otherwise, all other chemicals were from Merck KGaA (Darmstadt, Germany). Deionized water was obtained using a Milli-Q water purification system from Millipore (Schwalbach, Germany). All cell culture plastics were purchased from Corning (Bodenheim, Germany).

Methods

3.1. 2-D cell culture

3.1.1. 3T3-L1

3T3-L1 is a mouse embryonic fibroblast cell line. These cells are derived from the original line 3T3-Swiss albino and are used as an *in vitro* model of adipocytes [30]. 3T3-L1 preadipocytes were expanded in DMEM supplemented with 10% FBS, penicillin (100 U/ml), and streptomycin (100 µg/ml) [7,9]. For 2-D monolayer cultures, preadipocytes were seeded in basal medium (α-MEM, 10% FBS, penicillin (100 U/ml), and streptomycin (100 µg/ml)) into tissue-culture polystyrene well plates at a density of 40,000 cells/cm^2. This high seeding density guaranteed that 2-D cultures grew to confluence within two days after seeding. Hormonal induction was initiated two days after seeding by exchanging half of the medium with induction medium (basal media with 1 µM insulin, 0.1 µM corticosterone, 0.5 mM IBMX, and 60 µM indomethacin (final concentration) [7,9]. The time point of induction was referred to as day 0 throughout all experiments. At day 2, induction medium was replaced with differentiation medium (basal medium, 1 µM insulin). Subsequently, cells were fed with differentiation medium every other day up to day 6 or 9. Feeding was performed by exchanging only half of the medium volume in order to treat cells in the same way as in 3-D culture (see 3.2.). During the adipogenic phase, induction and differentiation media were supplemented with different concentrations of EDHB ranging from 0 – 200 µM. Cells were incubated in a humidified atmosphere at 37°C and 5% CO_2 during the complete culture period.

3.1.2. Human adipose-derived stem cells (ADSCs)

ADSCs were isolated from human subcutaneous adipose tissue obtained during abdominal plastic surgery from healthy women or men aged 17 - 69 years as previously described in chapter 3 (Page 47).

For 2-D monolayer cultures, cells were seeded in basal medium (PBM-2 supplemented with 10% FBS, penicillin (100 U/ml), and streptomycin (100 µg/ml)) at a density of 30,000 cells/cm^2. At confluence, cells were induced to undergo adipogenesis by exchanging half of the medium with basal media supplemented with 1.7 µM insulin, 1 µM dexamethasone, 0.5 mM IBMX, and 200 µM indomethacin (final concentration). Different concentrations of EDHB (0-200 µM) were added to the medium. The time point of induction was referred to as day 0 throughout all experiments. Both inducers and EDHB were present during the entire

adipogenic period. Medium was exchanged every other day up to day 14. Feeding was performed by exchanging only half of the medium volume in order to treat cells in the same way as in 3-D culture (see 3.2.). Cells were incubated in a humidified atmosphere at 37°C and 5% CO_2.

3.2. 3-D cell culture

Spheroids were generated according to the liquid overlay technique (Figure 1) [13,14].

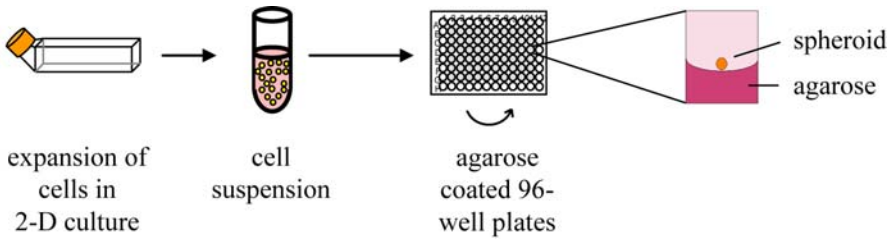

Figure 1: Generation of spheroids utilizing the liquid overlay technique (from Weiser B. [14]). Initially, 3T3-L1 preadipocytes were expanded in conventional 2-D cell culture. Then, cells were seeded into agarose-coated 96-well plates. Cells cannot adhere to the agarose surface, but, supported by the meniscus of the agarose layer and the agitation on an orbital shaker, cells accumulated in the center of the well, attached to each other and formed one multicellular spheroid per well.

Tissue culture polystyrene (TCPS) 96-well plates were coated with 50 µl of 1.5% agarose in α-MEM per well [31]. Spheroid formation was initiated by seeding cells in basal medium (3.1.1 and 3.1.2) into the agarose-coated wells (Figure 1). The outermost rows and columns of the well plate, respectively, were not used for culture due to the increased evaporation of medium from the wells during prolonged culture; they were only filled with PBS supplemented with penicillin (100 U/ml) and streptomycin (100 µg/ml). Two days after seeding, cells were induced to undergo adipogenesis by exchanging half of the medium with induction medium (see 3.1.1 and 3.1.2). Feeding was performed by exchanging only half of the medium volume, otherwise spheroids would be aspirated with complete removal of the medium from the wells. The induction medium was applied either without or with EDHB (50, 100, 200 µM). For 3T3-L1 preadipocytes, adipogenic induction was performed for another two days. Then half of the medium was exchanged with differentiation medium (see 3.1.1). This medium exchange was performed three times to further reduce the concentrations of inducers. Because ADSCs were cultured in the presence of inducers during the entire adipogenic phase, this washing step was not necessary. For either cell type, subsequently, cells were fed by exchanging half of the medium with differentiation medium every other day

(see 3.1.1 and 3.1.2). Spheroid cultures were incubated in a humidified atmosphere at 37°C and 5% CO_2 on an orbital shaker at 60 rpm (Heidolph, Schwabach, Germany).

During the present study, the 3-D spheroids of ADSCs consisted of 3000 cells per aggregate. Notably, the size of the 3-D spheroids of 3T3-L1 was changed. The initial experiments for studying the effect of EDHB on adipogenesis as well as the cytotoxicity caused by EDHB were performed with spheroids consisting of 750 cells per aggregate (Figure 3, 4, 7, and 8, Page 116, 117, 120 and 121). Previous studies showed that this cell aggregate size ensured the generation of homogeneous adipocyte constructs due to a sufficient supply of nutrients, oxygen, and adipogenic inducers. However, this small spheroid size generates disadvantages especially concerning the practical handling. For certain analyses, a higher cell number is necessary for quantification. Hence, in the following experiments (Figure 9, Page 123) larger spheroids were generated by seeding 3000 cells per well. In Figure 2, spheroids consisting of 750 or 3000 cells per construct are compared. Spheroids grew significantly up to day 9 and the relative increase in spheroid size was comparable in both groups (Figure 2 A). Adipogenic maturation of the cells occurred homogeneously throughout both spheroids until day 9 after induction as detected by oil red O staining (Figure 2 B). A gradient in cellular TG accumulation from the outside to the center area of the spheroids was not observed. Small and large spheroids did not differ in the TG content per cell (Figure 2 B). For the spheroids consisting of 750 cells per aggregate, a reducing effect of EDHB on spheroid volume was described (Figure 3 A and C, Page 116). This effect was also observed with the spheroids composed of 3000 cells. In presence of 100 µM EDHB, the increase of the spheroid volume was suppressed (Figure 2 C).

In conclusion, these results revealed that the adipogenic development was independent from spheroid size. Furthermore, the larger spheroids did not alter the effect of EDHB and therefore, the change of the use of spheroids consisting of 3000 cells was uncritical.

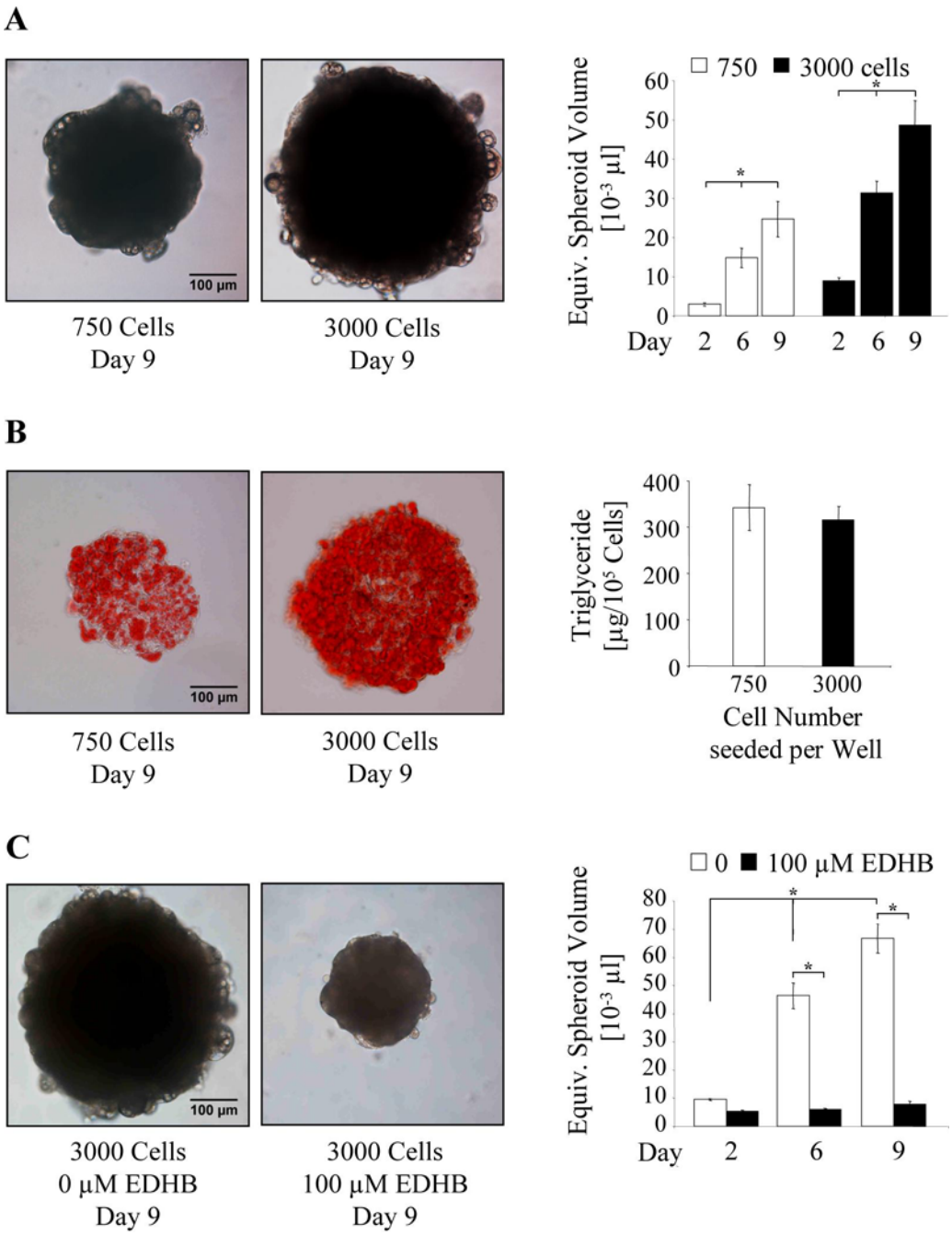

Figure 2: Comparison of different sizes of 3T3-L1 spheroids with regard to morphology, TG accumulation and effect of EDHB at day 9 after induction. 750 and 3000 cells were seeded per 96-well and induced to undergo adipogenesis. **A)** Phase contrast images of 3-D spheroids of differentiated 3T3-L1. On the right, kinetics of spheroid growth are displayed (n=10). **B)** Oil red O staining of intracellular lipid droplets in cryosections of 3-D spheroids. Sections from the center area are displayed. The intracellular TG contents were quantified (n=3) and normalized to cell numbers (on the right). **C)** Phase contrast images of 3-D spheroids treated without or with 100 µM EDHB. Development of spheroid sizes is shown on the right. Equivalent spheroid volumes at different time points of differentiation in absence or presence of EDHB were quantified morphometrically from n=10 randomly selected spheroids. Statistically significant differences are denoted by * ($p<0.05$). Three independent cell culture experiments were performed **(A-C)**; representative photographs from one experiment are shown. Bar=100 µm.

3.3. Microscopical determination of spheroid growth

Microscopical bright field pictures of spheroids were acquired using a CCD camera (DS-5M, Nikon, Düsseldorf, Germany) attached to an inverted microscope (Leica DM IRB, Leica Microsystems, Wetzlar, Germany) at 20x magnification. At specific time points, sizes of spheroids were determined by encircling the circumference of ten randomly selected spheroids and calculation of the equivalent diameter with the software Eclipse Net (Laboratory Imaging, Praha, Czech Republic). Spheroid volumes were calculated thereof.

3.4. Scanning electron microscopy (SEM)

Fixation of spheroids for SEM was performed according to the procedure described previously [14]. Briefly, entire spheroids were washed once with PBS and fixed in 10% PBS-buffered formalin. In order to crosslink intracellular lipids, spheroids were incubated in 1% aqueous osmium tetroxide solution for 30 minutes. After extensive rinsing with double-distilled water, spheroids were put onto aluminum stubs using conductive carbon tape and subjected to lyophilization (Christ Beta 2-16, Martin Christ Gefriertrocknungsanlagen; Osterode am Harz, Germany). Lyophilized spheroids were coated with gold-palladium and micrographs were obtained at 2 kV on a JEOL JSM-840 (Jeol Ltd., Tokyo, Japan).

3.5. Oil red O staining

In order to visualize accumulated cytoplasmic triglyceride droplets, oil red O staining was performed at day 9 or 14 after hormonal induction of adipogenesis. For this purpose, cells or entire spheroids were washed once with PBS, fixed in 10% PBS-buffered formalin overnight and then stained with oil red O (3 mg/ml solution in 60% isopropanol) for 4 hours [7,32]. Excess dye was removed by washing three times with PBS. For histological investigations, the stained spheroids were embedded in Tissue-Tek (Hartenstein Laborbedarf, Würzburg, Germany), snap frozen and finally cut into 12 µm-thick cryosections. After dissolution of Tissue-Tek in water, cryosections were incubated for 30 seconds in 60% isopropanol to remove unspecific oil red O staining, washed in water and mounted in glycerol [33]. Serial sections were prepared from all spheroids and sections from the center region were used for histological evaluation. Microscopical bright field pictures were acquired at 20x magnification using an inverted microscope (Leica DM IRB, Leica Microsystems, Wetzlar, Germany) equipped with a CCD camera (DS-5M, Nikon, Düsseldorf, Germany) and the software Eclipse Net (Laboratory Imaging, Praha, Czech Republic).

3.6. Quantitative analysis of intracellular triglyceride (TG) accumulation

For analysis of the intracellular TG content, 2-D monolayers and 3-D spheroids were washed twice with PBS and harvested in 0.5% aqueous thesit solution. After sonication with a digital sonifier (Branson Ultrasonic Corporation, Danburg, CT, USA), the spectroscopic quantification of TG was performed using the enzymatic serum triglyceride determination kit from Sigma-Aldrich (Taufkirchen, Germany) according to the manufacturer's instructions. All measurements were done in three biological replicates; one replicate was derived from one well for 2-D cultures and from approximately 20 spheroids for 3-D cultures, respectively. The amount of TG per well or per spheroid was calculated and normalized to the DNA content as determined by the DNA assay.

3.7. Determination of the glycerol-3-phosphate dehydrogenase (GPDH) activity

GPDH activity was measured according to a protocol adapted from Pairault and Green [34]. Briefly, after washing with PBS, cells were harvested in lysis buffer (50 mM Tris, 1 mM EDTA, 1 mM 2-mercaptoethanol, pH 7.5), sonicated with a digital sonifier (Branson Ultrasonic Corporation, Danburg, CT, USA) and centrifuged (16,000 g, 5 min). GPDH activity was measured by adding an aliquot of the lysate supernatant to the substrate buffer (0.1 M triethanolamine, 2.5 mM EDTA, 0.5 mM 2-mercaptoethanol, 0.12 mM NADH, 2 mM DHAP) and monitoring the consumption of NADH photometrically at 340 nm for 4.2 minutes. Measurements were done in three biological replicates; one replicate was derived from one well for 2-D cultures and approximately 30 spheroids for 3-D cultures, respectively. GPDH activities were normalized to the DNA content of the samples as determined by the DNA assay.

3.8. Determination of prolyl hydroxylase activity

The activity of prolyl hydroxylases was quantified by measuring the amount of hydroxyproline, an amino acid that is genetically uncoded and exists in significant amounts in collagen, according to Woessner [35] with some modifications as reported previously [36] [37]. Briefly, after washing with PBS, cells together with surrounding matrix components were harvested and digested in lysis buffer (0.1 M Na_2HPO_4, 10 mM Na_2EDTA and 2.5 mM cysteine, pH 6.5) for 16 hours at 60°C. Digested samples were hydrolyzed by incubation with 6 N HCl for 16 hours at 105°C. After hydrolysis, hydrochloric acid was evaporated by heating up to 100°C. The dry samples were dissolved in 500 µl double-distilled water. Standard

dilutions of hydroxyproline were treated under the same hydrolysis conditions. Subsequent reactions were performed in microtiter plates. 100 µl aliquots of the samples/standards were oxidized by addition of 50 µl chloramine T (0.05 M in citrate buffer, pH 6) for 20 minutes. Afterwards, 50 µl of p-dimethylaminobenzaldehyde (15%, 4 M perchloric acid in 70% isopropanol/water) was added and the microtiter plate was incubated for 30 minutes at 60°C. The plate was cooled down to room temperature and the absorbance of the samples was immediately measured at 557 nm on a microplate reader (TitertekPlus-MS2 Microplate Reader, ICN Biomedicals, Huntsville, USA). Measurements were done in three biological replicates; one replicate was derived from one well for 2-D cultures and from approximately 100 spheroids for 3-D cultures, respectively. The amount of hydroxyproline per sample was normalized to the DNA content of the samples as determined by the DNA assay.

3.9. Determination of the DNA content with DNA assay

Aliquots of cell lysates from GPDH activity measurements (see 3.7) or prolyl hydroxylase activity measurements (see 3.8) were digested with papainase (3.2 U/ml in 0.1 M Na_2HPO_4 buffer, pH 6.5 containing 1 mM Na_2EDTA and 2.5 mM cysteine) for 16 hours at 60°C, and the DNA content was determined using the intercalating Hoechst 33258 dye (0.1 µg/ml in 0.1 M NaCl containing 1 mM Na_2EDTA, 10 mM Tris, pH 7.4) [38]. Fluorescence intensities were determined at 365 nm excitation wavelength and 458 nm emission wavelength on a LS 55 Fluorescence Spectrometer (PerkinElmer, Wiesbaden, Germany) and correlated to DNA contents using standard dilutions of double-stranded DNA (from calf thymus). Cell numbers of 3T3-L1 cells were calculated with a conversion factor of 26.1 pg of DNA per cell, which was determined previously [14].

3.10. Determination of membrane integrity with propidium iodide staining

Propidium iodide (PI) intercalates into double-stranded nucleic acids. Under normal condition, PI is excluded by viable cells but it is ingested by dying or dead cells [39,40]. Cells were treated with EDHB during the entire adipogenic phase. One or nine days after induction and, thus, after addition of EDHB, cells were stained with 5 µg/ml PI added to medium for 5 minutes. Then, medium was replaced by fresh medium without PI. Cells treated with 1% Triton-X served as a positive control. PI has an absorption maximum at 535 nm and a fluorescence emission maximum at 617 nm and can be excited with an argon-ion laser. Microscopical fluorescence pictures were acquired at 20x magnification using a Zeiss

Axiovert 200 M microscope equipped with a Zeiss AxioCam HRc camera and the software LSM Image Browser (Carl Zeiss MicroImaging GmbH, Jena, Germany).

3.11. Total RNA extraction

Prior to isolation of total RNA, 2-D monolayers as well as entire spheroids were washed once with PBS. Total RNA was isolated using Qiagen RNeasy Mini Kit (Qiagen, Hilden, Germany), based on affinity columns from either freshly isolated or frozen (-80°C) cells according to the manufacturer's protocol. For one biological replicate a sufficient number of wells and spheroids, respectively, was pooled to yield a minimum of 1 µg total RNA per sample. RNA content and purity were determined spectrophotometrically at 260 nm/280 nm (Nanodrop Analyzer, NanoDrop, Wilmington, DE, USA). The ratio of adsorption values at 260 nm to 280 nm was optimal at about 1.8 to 2.0 and guaranteed pure RNA.

3.12. Quantitative real-time reverse transcription-polymerase chain-reaction (qRT-PCR)

The mRNA expression levels of selected genes (see Table 1) were analyzed with qRT-PCR SYBR Green assays. First strand cDNA was synthesized from 1 µg of total RNA using random hexamer primers and Superscript II reverse transcriptase according to the manufacturer's instructions.

Relative quantitative PCR was performed with SYBR Green Dye I with an ABI 7000 Prism Sequence detection system (Applied Biosystem, Darmstadt, Germany) using the following cycling conditions: 50°C for 2 minutes, 95°C for 10 minutes followed by 40 cycles at 95°C for 15 seconds and 60°C for 1 minute. Each primer was suspended in a concentration of 0.2 µM in SYBR Green Supermix and the reaction was carried out in 96-well plates with 10 µl diluted cDNA in a final volume of 25 µl. Experiments were performed in triplicates for each sample. Primers were designed with the free, open-source PerlPrimer software (www.perlprimer.sourceforge.net [41]) and obtained from Biomers (Ulm, Germany). Except for 18S rRNA, primer pairs were designed to span an intron-exon boundary (Table 1). Specificity of primer pairs and amplification conditions were verified by melting curve analysis and agarose gel electrophoresis. To determine qPCR assay efficiencies, equal amounts of cDNA from all conditions of the experimental setup were pooled and used in serial dilutions as template in qPCR measurements. A calibration curve was calculated by

plotting Ct values against the log of concentrations and efficiencies (E) were calculated from the slope (S) of the calibration curve according to the equation $E = 10^{-1/S}$ (Table 1).

Table 1: Primer sequences, amplicon lengths and PCR efficiencies for SYBR Green PCR assays.

Gene	Forward Primer Sequence (5' ➔ 3')	Reverse Primer Sequence (5' ➔ 3')	Amplicon Length (bp)	PCR Efficiency
18S	taacgaggatccattggaggg	cgctcccaagatccaactac	115	1,98
Prolyl-4-hydroxylase α1	agccaccatttcaaacccag	ggataccacagggtcttcgt	100	2,02

To determine gene expression levels, three biological replicates of each condition were analyzed in the qPCR assays. Ct values were obtained using SDS software (Applied Biosystems). Relative expression levels of target genes were calculated with PCR efficiency correction and normalized to the expression of 18S rRNA according to the equation: expression = $E_{target}^{Ct,target}/E_{18S}^{Ct,18S}$. 18S rRNA expression was evaluated not to be regulated between the different experimental conditions in previous experiments. Expression levels were further normalized to expression levels of the samples from 2-D culture at day 0.

3.13. Statistics

For spheroid growth, DNA assay, GPDH activity, TG and hydroxyproline accumulation, results are presented as mean value ± standard deviation. Significances were determined using GraphPadPrism v.5 (GraphPad Software, La Jolla, CA, USA). Differences between groups were analyzed for significance using unpaired Student's t-test. Differences between different groups at specific time points or between different time points within one group were analyzed for significance using one-way analysis of variances (ANOVA) with subsequent multiple comparisons according to Tukey's post hoc test. A value of $p<0.05$ was regarded as statistically significant.

4. Results

4.1. Differential effect of EDHB on the adipogenesis of 3T3-L1 in 2-D and 3-D culture

3T3-L1 preadipocytes cultured in 2-D monolayer or 3-D spheroids were exposed to increasing concentrations of EDHB (0-200 µM) during the entire adipogenic period. Figure 3 A shows bright field pictures of the differentiated adipocytes in 2-D and 3-D culture on day 9 after adipogenic induction. A clear difference can be recognized between both culture systems. Cells in 2-D culture were able to differentiate into adipocytes also in the presence of EDHB (Figure 3 A, upper row). Contrarily in 3-D culture, EDHB exerted a decreased adipogenesis with increasing concentrations (Figure 3 A, lower row). The EDHB treated spheroids were smaller in size and lipid droplets were only marginally developed. The adipocytes in spheroids which were cultured without EDHB developed large lipid vacuoles which were embedded within the ECM structures (Figure 3 B). With increasing concentration of EDHB the number of adipocytes with large lipid droplets decreased. Under normal conditions, the volume of adipogenically induced spheroids increased during differentiation phase up to 6-fold due to accumulation of TGs (Figure 3 C). This increase was strongly reduced in the presence of 50 µM EDHB and completely suppressed by higher concentrations of the inhibitor (Figure 3 C).

The differential effect of EDHB on the adipogenesis in 2-D and 3-D was confirmed in further experiments. Histological images after oil red O staining of intracellular lipid droplets of differentiated adipocytes are shown in Figure 4 A. Adipocytes cultured in 2-D monolayer accumulated large lipid droplets both in absence or presence of EDHB. The concentration of the inhibitor did not play a crucial role for the differentiation rate. In contrast, cells in 3-D aggregates did not differentiate into adipocytes when they were treated with EDHB. The section of the control group presented strongly stained lipid droplets, whereas the EDHB treated spheroids were marginally stained. Sections of spheroids that were exposed to 200 µM EDHB could not be cut because of the unstable structure. Measurements of the TG content (Figure 4 B) and the GPDH activity (Figure 4 C) confirmed the histological observations. Both accumulation of TGs and increased GPDH activity are characteristics of adipogenesis and describe the progress of the differentiation process. The TG contents and GPDH activities did not vary in 2-D in the presence of EDHB at day 9, whereas in 3-D, an extensive decrease was determined dependent on the EDHB concentrations.

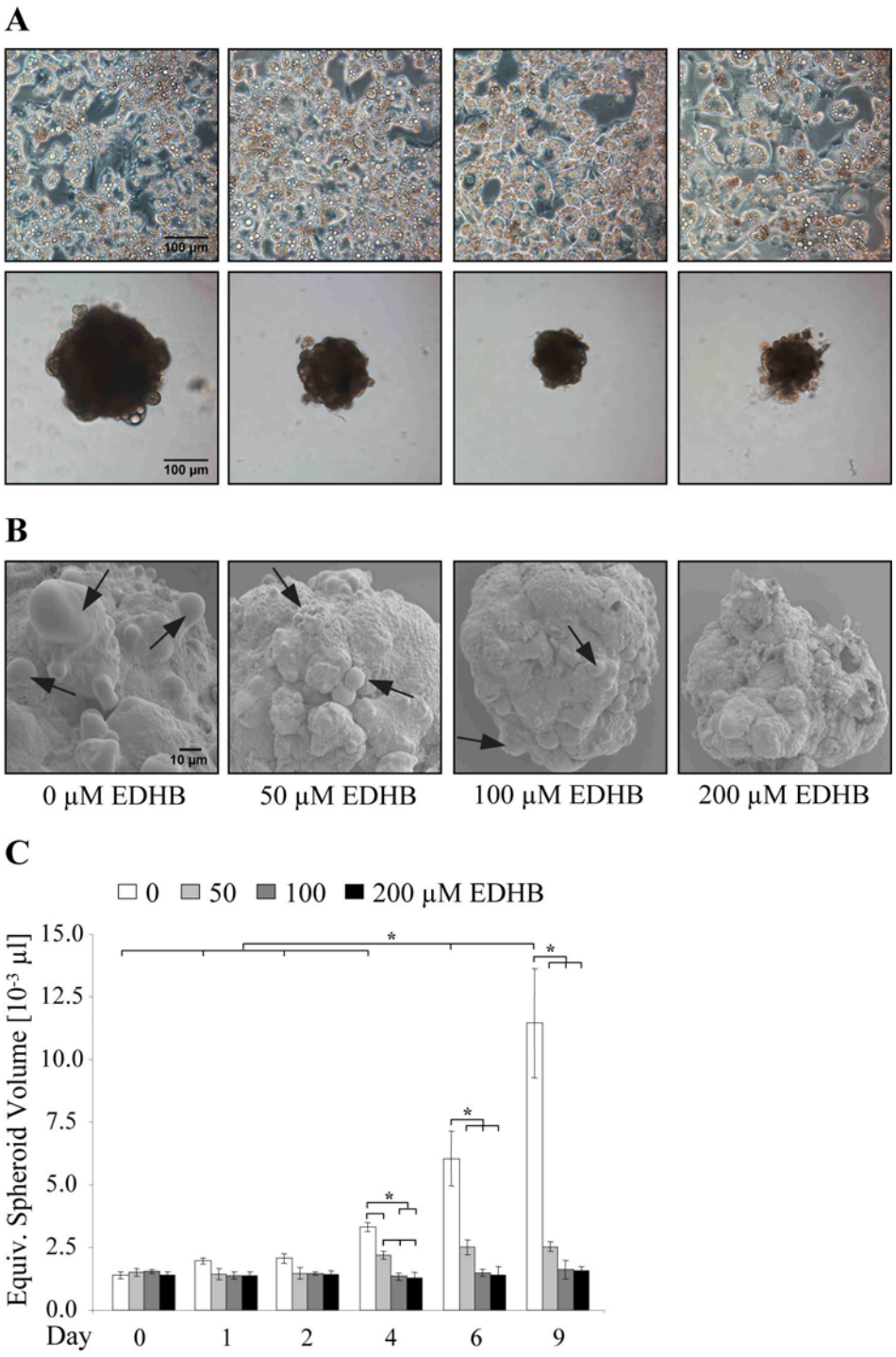

Figure 3: Effect of EDHB on the cell morphology of 3T3-L1 in 3-D spheroids in comparison to 2-D cell cultures. 3T3-L1 preadipocytes were induced to undergo adipogenesis in the absence or presence of EDHB at the indicated concentrations. EDHB was administered during the entire adipogenic period. Cell morphology was assayed at day 9 after induction. **A)** Phase contrast images of 3T3-L1 cultured in 2-D cultures (upper row) and 3-D spheroids (lower row). Bar=100 µm. **B)** SEM photographs of 3T3-L1 spheroids 9 days after induction which display the microscopic morphology of the surface of the spheroids in presence of EDHB. Exemplarily, some lipid droplets are denoted by black arrows. Bar=10 µm. Three independent cell culture experiments were performed **(A, B)**; representative photographs from one experiment are shown. **C)** Development of spheroid sizes. Equivalent spheroid volumes at different time points of differentiation in dependence of various concentrations of EDHB were quantified morphometrically from n=10 randomly selected spheroids. Statistically significant differences are denoted by * ($p<0.05$).

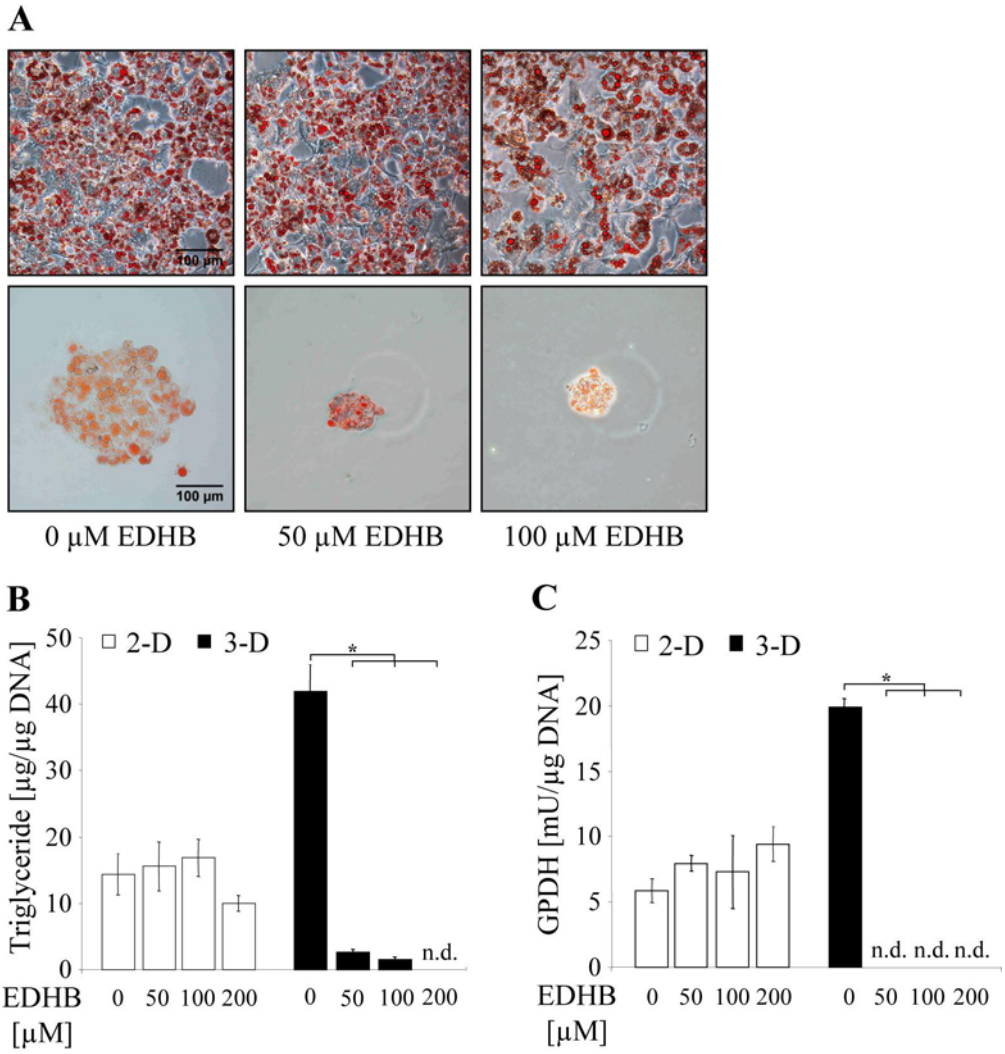

Figure 4: Effect of EDHB on the TG accumulation of 3T3-L1 in 3-D spheroids in comparison to 2-D cell cultures. 3T3-L1 preadipocytes were induced to undergo adipogenesis in the absence or presence of EDHB at the indicated concentrations. EDHB was administered during the entire adipogenic period. TG accumulation was determined at day 9 after induction. **A)** Oil red O staining of intracellular lipid droplets in 2-D cultures (upper row) and cryosections of 3-D spheroids (lower row). Sections from the center area are displayed. Three independent cell culture experiments were performed; representative photographs from one experiment are shown. Bar=100 µm. **B)** Quantification of intracellular TG content (n=3). TG contents were normalized to DNA contents. **C)** Quantification of specific GPDH activity (n=3). Enzyme activity was normalized to DNA contents. Statistically significant differences are denoted by * ($p<0.05$). n.d.=not detectable.

4.2. Inhibitory effect of EDHB on the adipogenesis of ADSCs in 2-D and 3-D culture

Furthermore, the effect of EDHB on adipogenesis was tested in another cell system, i.e., ADSCs. ADSCs can differentiate into adipocytes by supplementing various inducers of adipogenesis into the culture medium. The effect of EDHB on the adipogenesis of these human stem cells was investigated by addition of the inhibitor during the adipogenic phase. EDHB treatment yielded a reduced differentiation rate of adipocytes both in 2-D and 3-D culture (Figure 5). In contrast to 3T3-L1 adipocytes, no differences could be observed

between the monolayer and spheroid culture system. The spheroids were unstable in presence of EDHB so that the volume was reduced over time (Figure 5 B). A reduced cell number was seen in cells treated with high concentrations. This was obvious in 2-D (Figure 5 A, upper row), but also in 3-D, where a decreased cell number was measured by the DNA assay (data not shown).

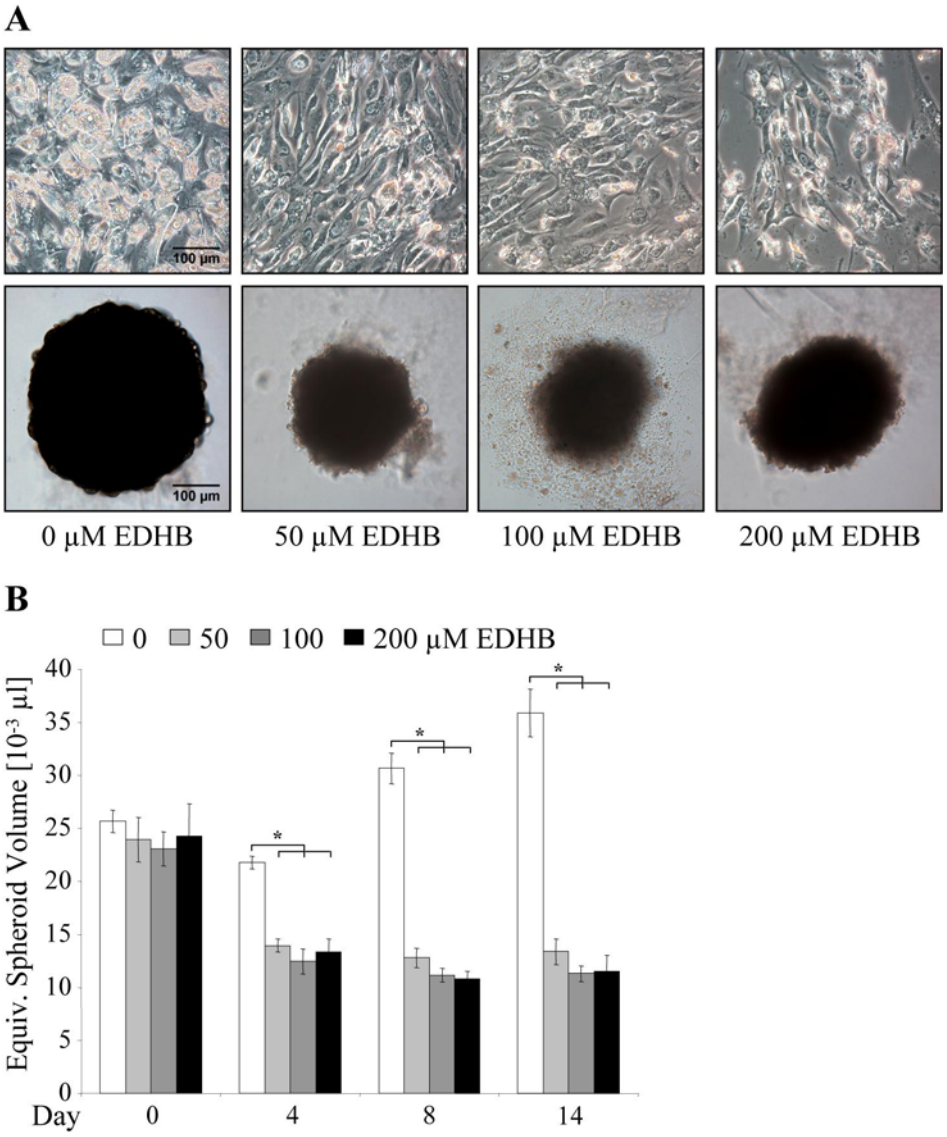

Figure 5: Effect of EDHB on the cell morphology of ADSCs in 3-D spheroids in comparison to 2-D cell cultures. ADSCs were induced to undergo adipogenesis in the absence or presence of EDHB at the indicated concentrations. EDHB was administered during the entire adipogenic period. Cell morphology was assayed at day 14 after induction. **A)** Phase contrast images of ADSCs differentiated in 2-D cultures (upper row) and 3-D spheroids (lower row). Three independent cell culture experiments were performed; representative photographs from one experiment are shown. Bar=100 µm. **B)** Development of spheroid sizes. Equivalent spheroid volumes at different time points of differentiation in dependence of various concentrations of EDHB were quantified morphometrically from n=10 randomly selected spheroids. Statistically significant differences are denoted by * ($p<0.05$).

The differentiation of adipocytes was determined by oil red O staining as well as measurement of TGs and GPDH activity (Figure 6). All methods confirmed the previous observations that EDHB prevented adipogenesis. ADSCs were only marginally able to differentiate into adipocytes when EDHB was added to the culture medium. Only few intracellular lipid droplets were demonstrated by oil red O staining (Figure 6 A). The TG content was significantly decreased by EDHB in 2-D and 3-D culture and the GPDH activity was also reduced at a concentration of 50 µM EDHB and no longer detectable in cells treated with 100 µM or 200 µM EDHB (Figure 6 B and C).

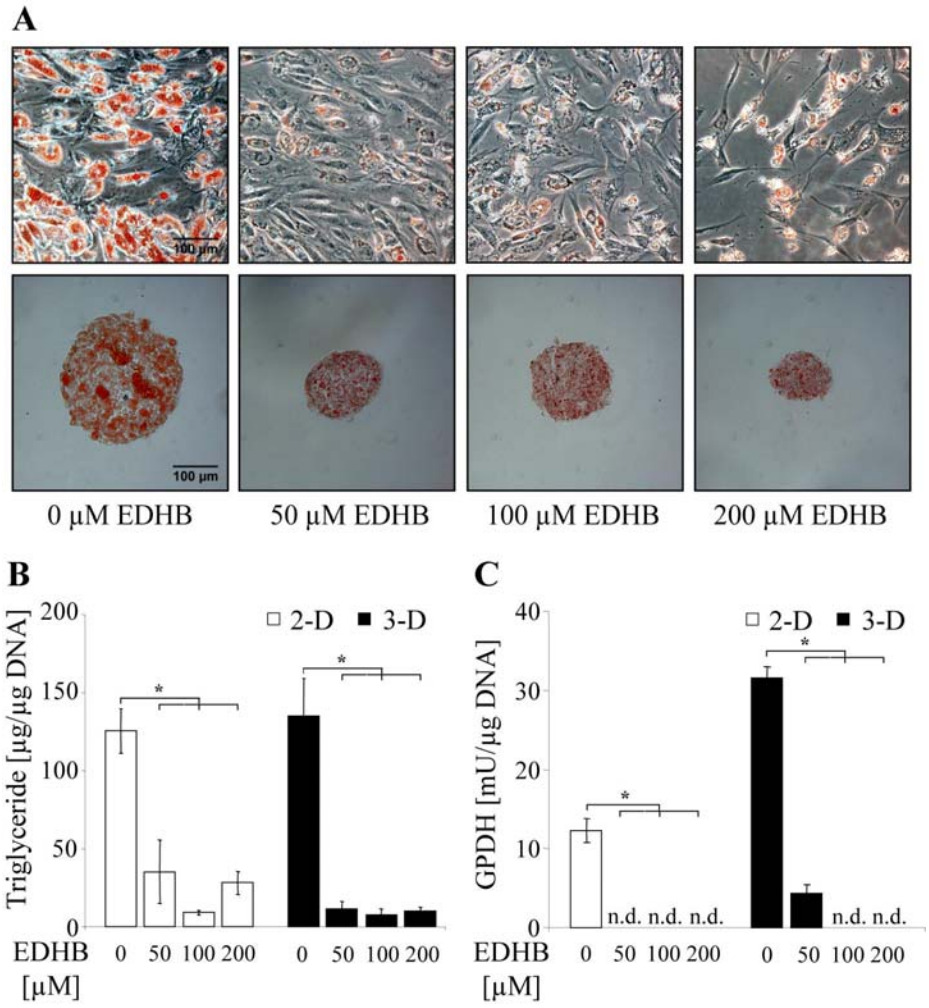

Figure 6: Effect of EDHB on the TG accumulation of ADSCs in 3-D spheroids in comparison to 2-D cell cultures. ADSCs were induced to undergo adipogenesis in the absence or presence of EDHB at the indicated concentrations. EDHB was administered during the entire adipogenic period. TG accumulation was determined at day 14 after induction. **A)** Oil red O staining of intracellular lipid droplets in 2-D cultures (upper row) and cryosections of 3-D spheroids (lower row). Sections from the center area are displayed. Three independent cell culture experiments were performed; representative photographs from one experiment are shown. Bar=100 µm. **B)** Quantification of intracellular TG content (n=3). TG contents were normalized to DNA contents. **C)** Quantification of specific GPDH activity (n=3). Enzyme activity was normalized to DNA contents. Statistically significant differences are denoted by * ($p<0.05$). n.d.=not detectable.

4.3. Reduced cell number in 3-D spheroids caused by EDHB

During the previous experiments, it was noticed that EDHB caused a loss of cell number. This phenomenon was more drastic in 3-D spheroids in which it could be observed even in the presence of the lowest concentration of EDHB (Figure 7).

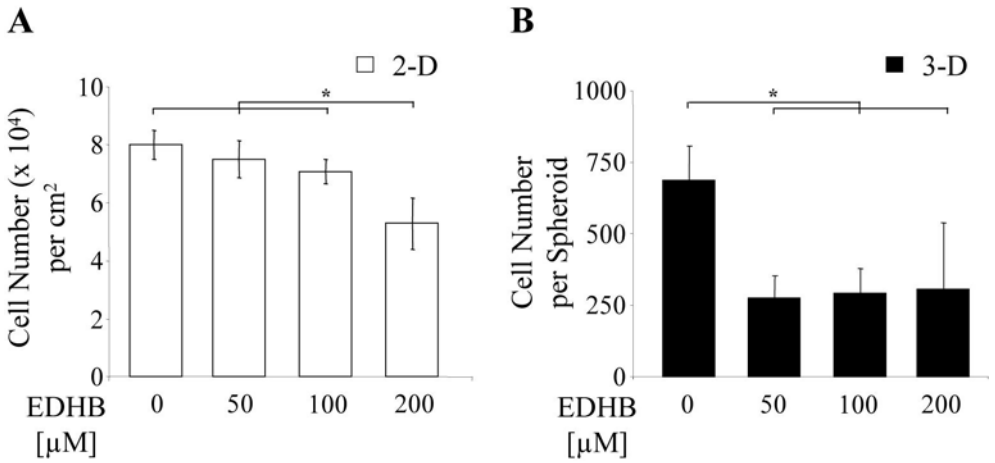

Figure 7: Effect of EDHB on the cell number of 3T3-L1 in 3-D spheroids in comparison to 2-D cell cultures. 3T3-L1 preadipocytes were induced to undergo adipogenesis in the absence or presence of EDHB at the indicated concentrations. EDHB were administered during the entire adipogenic period. Cell number was determined at day 9 after induction. **A)** Quantification of the cell number in 2-D cultures (n=3). **B)** Quantification of the cell number per spheroid (n=3). Cell numbers **(A, B)** were determined in two independent cell culture experiments; representative data are shown. Statistically significant differences are denoted by * ($p<0.05$).

To further investigate the effect of EDHB on the cell number of the 3T3-L1 cells, EDHB was added at day 0, the time point of induction and maintained in the adipogenic media until the adipocytes were harvested at day 9. The cell number was measured at different time points of the adipogenic phase by DNA assay. If the cell number decreases directly after addition of EDHB, a toxic effect is possible.

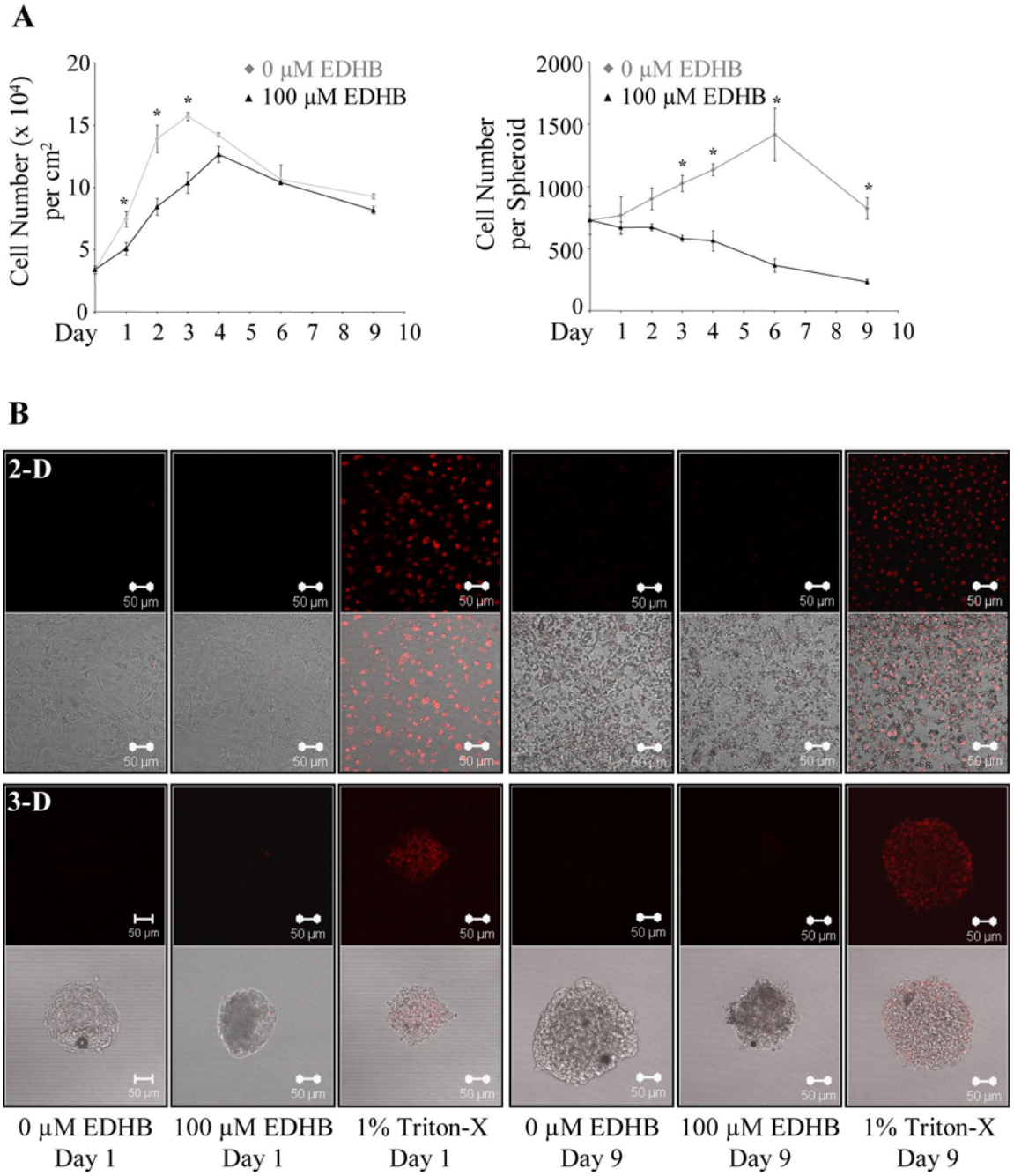

Figure 8: Effect of EDHB on the viability of 3T3-L1 in 2-D cell culture and 3-D spheroids. Cells were adipogenically induced and differentiated in the absence or presence of EDHB. **A)** Evaluation of cell numbers at different time points of adipocyte development in 2-D (left) and 3-D (right) culture (n=3). * indicates statistically significant differences between the tested groups ($p<0.05$). **B)** Fluorescent images of PI-stained cells at indicated times (red fluorescence) and the corresponding bright field images in 2-D monolayer culture (upper row) and in 3-D spheroids (lower row). The positive control was treated with 1% Triton-X four hours prior to staining. Bar=50 µm.

Cells proliferated in 2-D monolayer during the days of induction (Figure 8 A, left). This is consistent with the clonal expansion that is a prerequisite for differentiation of 3T3-L1 preadipocytes into adipocytes. The proliferation rate was reduced and retarded in the presence of 100 µM EDHB in the first days but at day 4, the cell numbers of the control and the EDHB

treated group were almost the same. From day 4 on, the cell number declined in both group. At day 9, only a marginal difference between both groups was detected with regard to the cell number. The capability of the cells to proliferate in the presence of EDHB indicated that the inhibitor did not have a toxic effect in 2-D culture. The cell number of 3-D spheroids was also measured. Cells that were cultured in media without EDHB proliferated until day 6 (Figure 8 A, right). Then, a loss of cells was detected during the next three days. In 3-D culture with 100 µM EDHB, a continuously slight decrease of the cell number was determined during the entire adipogenic phase. At day 9, the cell number of EDHB treated cells was clearly diminished in comparison to the control. Nevertheless, the constantly slow reduction of cells by EDHB over an extended period of time suggests a non-toxic effect of the inhibitor. The loss of cells was rather attributed to the instability of the spheroids resulting from the modified structure of the ECM caused by EDHB.

Additionally, to exclude that the loss of cells was caused by a possible toxic effect of EDHB, cells were stained with PI. PI is an intercalating agent and fluorescence dye that can be used to stain DNA. Because PI cannot penetrate the intact membrane of viable cells, it can be used for identifying dying or dead cells. PI passes the membrane of dead cells, binds to DNA and can be detected using a 562-588 nm band pass filter when excited by a 488 nm argon laser.

To identify dead cells in the EDHB treated population, cells were stained with 5 µg/ml PI for 5 minutes at different time points. As positive control, cells were treated with 1% Triton-X, a lethal detergent that led to an intense red staining after incubation with PI both in 2-D and 3-D culture (Figure 8 B). Untreated cells and cells that were treated with 100 µM EDHB were stained neither at day 1 nor at day 9 of treatment which means that the cells were viable and EDHB did not have a toxic effect.

4.4. The role of prolyl-4-hydroxylase alpha 1 in the adipogenesis of 3T3-L1

To investigate whether EDHB really inhibits the activity of the prolyl-4-hydroxylases in 2-D and 3-D, the content of hydroxyproline that was produced by cells in absence or presence of EDHB up to day 6 was determined (Figure 9 A). This and the following experiment were performed with spheroids consisting of 3000 cells due to practical handling as described in more detail in the methods (see 3.2, Figure 2, Page 109).

In the presence of the inhibitor, the cells should not to be able to hydroxylate prolines due to the lacking activity of the enzyme. In both 2-D and 3-D cell cultures, hydroxyprolines were produced during the development of adipocytes, but cells in a 3-D context hydroxylated more prolines. When the activity of the prolyl hydroxylases was blocked by EDHB, a decreased

amount of hydroxyprolines was measured in 3-D spheroids, whereas in 2-D culture hydroxylation of prolines continued. Here, the activity of the prolyl hydroxylases seemed not to be affected.

In this context, we investigated the gene expression of the collagen prolyl-4-hydroxylase during the development of adipocytes which has not been described yet. qRT-PCR analysis showed that the gene expression pattern of the α1-subunit of the prolyl-4-hydroxylase was different in 2-D cell culture in comparison to 3-D spheroids (Figure 9 B). Whereas the gene expression of the enzyme increased strongly in 2-D up to day 6 after induction, in 3-D spheroids a downregulation of the expression occurred during adipogenic differentiation.

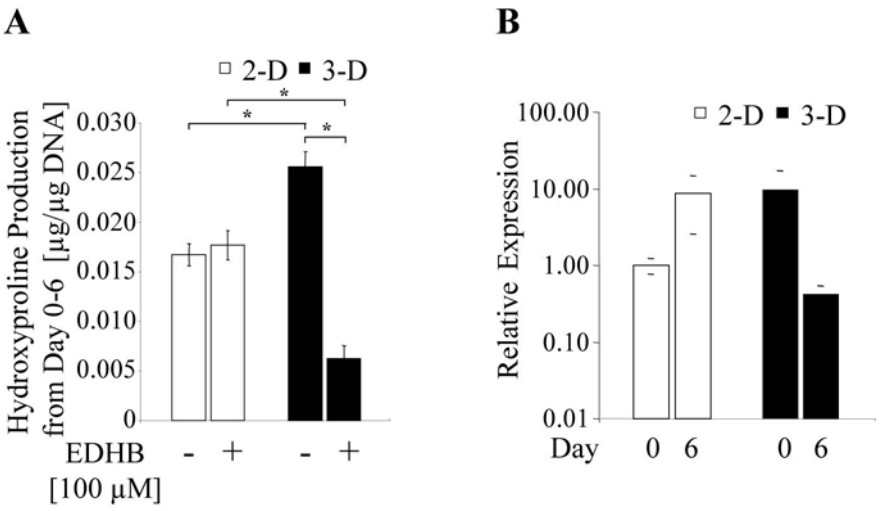

Figure 9: Analysis of the enzyme activity and gene expression of prolyl-4-hydroxylase α1 during adipocyte differentiation of 3T3-L1 in 2-D and 3-D cell culture. **A)** Accumulation of hydroxyproline at day 0 to day 6 after induction (n=3). EDHB was added at the indicated concentration upon induction and were maintained throughout differentiation. Measurements were normalized to DNA content. Statistically significant differences are denoted by * ($p<0.05$). **B)** qRT-PCR measurments of prolyl-4-hydroxylase α1 (n=2). Expression is reported as the ratio of prolyl-4-hydroxylase α1/18S. Dashes represent the individual values of both biological replicates.

5. Discussion

In general, the ECM is important for the mechanical stability of tissues, for cell adhesion as well as for the regulation of growth and differentiation of the residing cells [42-44]. The matrix contributes to the microenvironment specificity through its mechanical features and its molecular composition which enables binding of growth factors, enzymes, and other diffusible molecules [45]. These interactions along with the communication with other cells are of pivotal importance for normal cell differentiating and functioning [3,46]. In adipose tissue, the ECM microenvironment also influences adipocyte development and functionality

(lipolysis, lipogenesis, hormone secretion, and insulin sensitivity), but the underlying mechanisms are unknown [8,20,44,47,48]. It has been described that collagens play an essential role for the terminal differentiation of preadipocytes into adipocytes *in vitro* and that EDHB, an inhibitor of prolyl-4-hydroxylase, partially reduces the differentiation of BIP and adipocytes of the mouse TA1 cell line [17,18]. These results are based on 2-D culture experiments. However, cells behave differently *in vitro* when cultured in a 3-D context [1,2,4,5,49]. 2-D cultures do not recapitulate the unique architecture observed with adipose tissue *in vivo* in contrast to 3-D culture systems with a tissue-like geometry and microenvironment [3,9,46,50]. Therefore, we hypothesized that the remodeling of the collagen structures during adipogenic differentiation is more crucial in a 3-D tissue-like context and accordingly, EDHB has an even more profound impact on the adipocyte development of the spheroids.

In this *in vitro* study, we investigated the influence of EDHB on the adipogenic differentiation of 3T3-L1 in a 3-D tissue-like context. We observed differential effects of EDHB in 2-D monolayer and 3-D spheroid culture systems. 3T3-L1 cells incorporated into spheroids were prevented to undergo adipogenesis in the presence of EDHB, whereas in 2-D culture adipogenesis was not affected after 9 days (Figure 4, Page 117)

It is likely that the presence of EDHB prevented preadipocytes from newly organizing the collagen matrix in the surrounding ECM during the adipogenic development, whereas differentiated adipocytes in spheroids without EDHB were embedded in an organized ECM structure resulting in the accumulation of TGs within large lipid droplets. It is known that the development of adipose tissue is accompanied by alterations of the ECM architecture leading to an increased deposition and synthesis of certain collagens and other ECM proteins [8,51-54]. Moreover, collagen remodeling has been previously reported as a relevant process for differentiation into adipocytes. Studies identified that various collagens such as collagen type I, III, IV, V, and VI are involved in adipogenesis [18,23,54] and especially collagen type V and VI altered their network structure during the adipogenic differentiation of BIP [18].

Furthermore, we have observed that the interrupted ECM organization caused by EDHB led to destabilization of the spheroid structure and subsequent detachment of the cells residing in the outer regions from the aggregate (Figure 3 A, Page 116). Thus, the continuous loss of cells in 3-D determined by measurements of the DNA content apparently arose from the unstable spheroid structure and not from toxic effects caused by EDHB as evidenced with propidium iodide staining (Figure 8, Page 121). This is well in agreement with a study

reported by Sasaki *et al.* in which EDHB did also not affect the viability, proliferative capacity or plating efficacy of cells [25].

In another experiment, we directly determined the inhibitory effect of EDHB on the activity of prolyl hydroxylases in 3-D spheroids compared to 2-D culture. Well in agreement with the results showing the effect of EDHB on adipogenesis (Figure 4, Page 117), different enzyme activities were observed in 2-D and 3-D culture in the presence of EDHB (Figure 9 A, Page 123). The measured hydroxyproline content demonstrated that prolyl hydroxylases were still active in 2-D in presence of EDHB. In 2-D culture treated with EDHB, hydroxyprolines were produced from day 0 to day 6 to the same degree as non-treated adipocytes after induction. In contrast, production of hydroxylated prolines was significantly reduced by EDHB in 3-D spheroids. We hypothesize that the differential activities of prolyl hydroxylases in 2-D and 3-D cell cultures after EDHB treatment resulted from the different gene expression pattern of the collagen prolyl-4-hydroxylase in the two systems (Figure 9 B, Page 123). The gene expression of the α-subunit of collagen prolyl-4-hydroxylase increased during transition from preadipocytes to adipocytes in 2-D, whereas in 3-D a comparable increase was not observed. Thus, despite of the inhibition through EDHB, enough α-subunits might have been available in 2-D which could assemble and form active enzymes. In 3-D spheroids, prolyl-4-hydroxylases were expressed to a lower extent so that EDHB apparently suppressed enzyme activity effectively resulting in inhibition of the collagen synthesis and subsequent adipogenic differentiation. This hypothesis has to be further investigated in future studies.

However, notably, EDHB is not specific for collagen prolyl-4-hydroxylase but it is an inhibitor for the complete family of prolyl hydroxylases. All prolyl hydroxylases belong to the group of 2-oxoglutarate coupled dioxygenases that require Fe^{2+}, 2-oxoglutarate, O_2, and ascorbate for their activity. Distinct members of this family are the prolyl hydroxylase domain-containing enzymes (PHDs); PHDs are responsible for hydroxylation of hypoxia inducible factor 1 alpha (HIF-1α), a regulator of the transcription of hypoxia-regulated genes [8,55]. Floyd *et al.* investigated if the inhibition of adipogenesis in the presence of PHD inhibitors such as EDHB is correlated with HIF-1α indeed, but they were not able to show a connection [29]. In their study, Floyd *et al.* also demonstrated that the expression of PHDs increased during stages of adipogenesis and that it was downregulated by EDHB [29]. However, this downregulation provided no evidence for the correlation between the PHD activity and the formation of adipocytes. It is also possible that another factor relevant for adipogenesis, presumably collagen prolyl-4-hydroxylase, was inhibited by EDHB and the low expression level of PHDs was a consequence of the preadipose state. Unfortunately, Floyd *et*

al. did not discuss any possible role of collagens in the differentiation process of adipocytes. However, we assume that the effect of EDHB on adipogenesis was indeed based on the failed collagen synthesis as collagens are the most abundant proteins in animal tissue with the highest hydroxyproline content [56]. Nevertheless, the role of PHDs and other subtypes of 2-oxoglutarate coupled dioxygenases, e.g., the lysyl hydroxylase, in adipogenesis should be investigated in further experiments.

Regarding the effect of EDHB on adipogenesis in 2-D monolayer culture, our results were differential to studies of Floyd *et al.*, Ibrahimi *et al.*, and Nakajima *et al.* in which treatment with EDHB reduced the adipogenic differentiation of 3T3-L1, BIP, and TA1 preadipose cells [17,18,29]. Regarding Ibrahimi and Nakajima, one could assume that the different cell sources which were used in the respective studies were responsible for this discrepancy. Preadipocytes from different cell source vary in their responsiveness to specific substances [46] as we have also demonstrated in our studies with ADSCs which were not able to differentiate into adipocytes in the presence of EDHB (Figure 6, Page 119).

However, Floyd *et al.* have observed a reducing effect on the adipogenesis of 3T3-L1 cells under the same EDHB concentrations as we used, whereas in our 2-D experiments, EDHB did not affect the formation of adipocytes. In the following, possible reasons for this discrepancy are discussed. First, one reason could be the different medium exchange. The 3-D culture demanded a procedure where only half of the medium was exchanged; otherwise spheroids would be aspirated with complete removal of the medium from the wells. For comparability, 2-D monolayer cultures were equally treated. The correct final concentrations of the inducers were obtained by duplicating their quantities. However, this type of medium exchange did not influence the effect caused by EDHB. Even with complete removal of the medium, EDHB did not inhibit the differentiation of 3T3-L1 adipocytes in 2-D cell culture (data not shown). A second possible reason for the discrepant results is the distinct composition of the induction medium. The induction medium used in our studies was α-MEM supplemented with 1 µM insulin, 0.1 µM corticosterone, 0.5 mM IBMX, and 60 µM indomethacin [7], whereas Floyd's medium consisted of DMEM with 1.7 µM insulin, 1 µM dexamethasone, and 0.5 mM IBMX [29]. After 48 h, the medium was replaced by differentiation medium. In contrast to Floyd, insulin was added during the entire differentiation phase of our experiments. Therefore, we tested the influence of the distinct media compositions on the efficiency of EDHB by inducing adipogenesis with the two different media supplemented with 100 µM EDHB. Under Floyd's differentiation conditions we also observed a decreased number of adipocytes in the presence of 100 µM EDHB as detected by oil red O (Figure 10, Page 127).

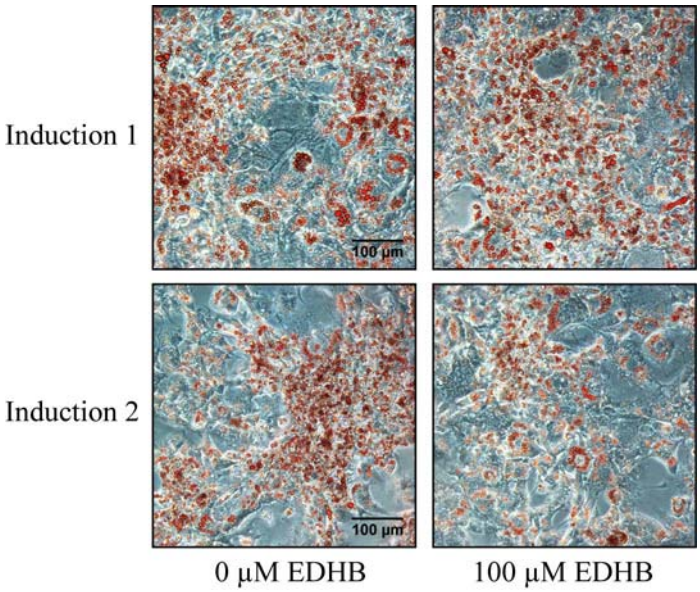

Figure 10: The effect of EDHB on the adipogenesis of 3T3-L1 cells subjected to various differentiation media. 3T3-L1 preadipocytes were adipogenically induced with two different induction cocktails. Induction medium 1 consisted of α-MEM supplemented with 1 µM insulin, 0.1 µM corticosterone, 0.5 mM IBMX, and 60 µM indomethacin [7], whereas the induction medium 2 was composed of DMEM with 1.7 µM insulin, 1 µM dexamethasone, and 0.5 mM IBMX [29]. EDHB was added at the indicated concentration upon induction and were maintained throughout differentiation. Intracellular lipid droplets were stained with oil red O in 2-D culture. Two independent cell culture experiments were performed; representative photographs from one experiment are shown. Bar=100 µm.

In the present study, it seemed that the used inducers stimulated the adipocyte differentiation more potently as those in Floyd's induction cocktail. One difference between the two media compositions was the addition of different glucocorticoids, corticosterone and dexamethasone, respectively, which may have been effective in different ways. Differential effects of corticosterone and dexamethasone have been already described in other cell functions, for example, in hippocampal neurogenesis or in muscle wasting responses in cultured L6 and C2C12 myotubes [57,58]. Furthermore, the presence of indomethacin in our induction cocktail was also different to the cocktail used in Floyd's study. It has been also described that indomethacin stimulated the differentiation of the mouse adipogenic TA1 cell line even more rapidly and completely than dexamethasone [59]. The permanent administration of insulin during the entire adipogenic differentiation phase did not affect the differentiation rate (data not shown). Another important difference of the two media compositions was the basal medium itself which could also have an influence on the differentiation of adipocytes. The cultivation of cells in α-MEM yielded enhanced TG storage as compared to DMEM [60]. Thereby, the most interesting point appears to be that DMEM lacks ascorbic acid which is a cofactor for prolyl hydroxylase activity. It was reported that the

inhibitory effect of EDHB on enzyme activity can be compensated by addition of high concentrations of ascorbic acid [61]. Thus, it is hypothesized that ascorbic acid contained in α-MEM was responsible for EDHB not affecting the adipogenesis in 2-D culture. Further experiments have to be conducted to verify this hypothesis.

In conclusion, the current results suggest a complex relationship between prolyl hydroxylase activity, collagens and adipogenesis which is more essential in a coherent 3-D tissue-like context. The activity of prolyl hydroxylases is important for collagen assembly and accordingly, it is assumed that remodeling of the collagen structures influences adipocyte development. This study underlines the importance of a 3-D cell model for further investigations of cell-matrix interactions to approach *in vivo* adipose architecture as closely as possible.

References

1. Pedersen J A, Swartz M A. Mechanobiology in the third dimension. *Ann.Biomed.Eng* 2005; **33:** 1469-1490.
2. Mazzoleni G, Di Lorenzo D, Steimberg N. Modelling tissues in 3D: the next future of pharmaco-toxicology and food research? *Genes Nutr.* 2009; **4:** 13-22.
3. Kang X, Xie Y, Kniss D A. Adipose tissue model using three-dimensional cultivation of preadipocytes seeded onto fibrous polymer scaffolds. *Tissue Eng* 2005; **11:** 458-468.
4. Bissell M J, Radisky D C, Rizki A, Weaver V M, Petersen O W. The organizing principle: microenvironmental influences in the normal and malignant breast. *Differentiation* 2002; **70:** 537-546.
5. Yamada K M, Cukierman E. Modeling tissue morphogenesis and cancer in 3D. *Cell* 2007; **130:** 601-610.
6. Chun T H, Hotary K B, Sabeh F, Saltiel A R, Allen E D, Weiss S J. A pericellular collagenase directs the 3-dimensional development of white adipose tissue. *Cell* 2006; **125:** 577-591.
7. Fischbach C, Spruss T, Weiser B, Neubauer M, Becker C, Hacker M, Goepferich A, Blunk T. Generation of mature fat pads in vitro and in vivo utilizing 3-D long-term culture of 3T3-L1 preadipocytes. *Experimental Cell Research* 2004; **300:** 54-64.
8. Mariman E C, Wang P. Adipocyte extracellular matrix composition, dynamics and role in obesity. *Cell Mol.Life Sci.* 2010.
9. Fischbach C, Seufert J, Staiger H, Hacker M, Neubauer M, Goepferich A, Blunk T. Three-dimensional in vitro model of adipogenesis: Comparison of culture conditions. *Tissue Engineering* 2004; **10:** 215-229.
10. Patrick C W, Jr., Chauvin P B, Hobley J, Reece G P. Preadipocyte seeded PLGA scaffolds for adipose tissue engineering. *Tissue Eng* 1999; **5:** 139-151.
11. von Heimburg D, Kuberka M, Rendchen R, Hemmrich K, Rau G, Pallua N. Preadipocyte-loaded collagen scaffolds with enlarged pore size for improved soft tissue engineering. *Int.J.Artif.Organs* 2003; **26:** 1064-1076.
12. Kunz-Schughart L A, Freyer J P, Hofstaedter F, Ebner R. The use of 3-D cultures for high-throughput screening: the multicellular spheroid model. *J.Biomol.Screen.* 2004; **9:** 273-285.
13. Santini M T, Rainaldi G. Three-dimensional spheroid model in tumor biology. *Pathobiology* 1999; **67:** 148-157.
14. Weiser B. Adipose Tissue Engineering - Precultivation Strategies towards Clinical Applications & A Novel 3-D Model of Adipogenesis for Basic Research. *Ph.D. thesis* 2008. University of Regensburg, Regensburg, Germany.
15. Suzuki S, Narita Y, Yamawaki A, Murase Y, Satake M, Mutsuga M, Okamoto H, Kagami H, Ueda M, Ueda Y. Effects of Extracellular Matrix on Differentiation of Human Bone Marrow-Derived Mesenchymal Stem Cells into Smooth Muscle Cell Lineage: Utility for Cardiovascular Tissue Engineering. *Cells Tissues.Organs* 2009.
16. Streuli C. Extracellular matrix remodelling and cellular differentiation. *Curr.Opin.Cell Biol.* 1999; **11:** 634-640.
17. Ibrahimi A, Bonino F, Bardon S, Ailhaud G, Dani C. Essential role of collagens for terminal differentiation of preadipocytes. *Biochem.Biophys.Res.Commun.* 1992; **187:** 1314-1322.

18. Nakajima I, Muroya S, Tanabe R, Chikuni K. Extracellular matrix development during differentiation into adipocytes with a unique increase in type V and VI collagen. *Biol.Cell* 2002; **94:** 197-203.

19. Rosen E D, Spiegelman B M. Molecular regulation of adipogenesis. *Annu.Rev.Cell Dev.Biol.* 2000; **16:** 145-171.

20. Spiegelman B M, Ginty C A. Fibronectin modulation of cell shape and lipogenic gene expression in 3T3-adipocytes. *Cell* 1983; **35:** 657-666.

21. Antras J, Hilliou F, Redziniak G, Pairault J. Decreased biosynthesis of actin and cellular fibronectin during adipose conversion of 3T3-F442A cells. Reorganization of the cytoarchitecture and extracellular matrix fibronectin. *Biol.Cell* 1989; **66:** 247-254.

22. Kuri-Harcuch W, Arguello C, Marsch-Moreno M. Extracellular matrix production by mouse 3T3-F442A cells during adipose differentiation in culture. *Differentiation* 1984; **28:** 173-178.

23. Weiner F R, Shah A, Smith P J, Rubin C S, Zern M A. Regulation of collagen gene expression in 3T3-L1 cells. Effects of adipocyte differentiation and tumor necrosis factor alpha. *Biochemistry* 1989; **28:** 4094-4099.

24. Majamaa K, Sasaki T, Uitto J. Inhibition of prolyl hydroxylation during collagen biosynthesis in human skin fibroblast cultures by ethyl 3,4-dihydroxybenzoate. *J.Invest Dermatol.* 1987; **89:** 405-409.

25. Sasaki T, Majamaa K, Uitto J. Reduction of collagen production in keloid fibroblast cultures by ethyl-3,4-dihydroxybenzoate. Inhibition of prolyl hydroxylase activity as a mechanism of action. *J.Biol.Chem.* 1987; **262:** 9397-9403.

26. Nandan D, Clarke E P, Ball E H, Sanwal B D. Ethyl-3,4-dihydroxybenzoate inhibits myoblast differentiation: evidence for an essential role of collagen. *J.Cell Biol.* 1990; **110:** 1673-1679.

27. Rocnik E F, Chan B M, Pickering J G. Evidence for a role of collagen synthesis in arterial smooth muscle cell migration. *J.Clin.Invest* 1998; **101:** 1889-1898.

28. Kivirikko K I, Myllyla R, Pihlajaniemi T. Protein hydroxylation: prolyl 4-hydroxylase, an enzyme with four cosubstrates and a multifunctional subunit. *The FASEB Journal* 1989; **3:** 1609-1617.

29. Floyd Z E, Kilroy G, Wu X, Gimble J M. Effects of prolyl hydroxylase inhibitors on adipogenesis and hypoxia inducible factor 1 alpha levels under normoxic conditions. *J.Cell Biochem.* 2007; **101:** 1545-1557.

30. Green H, Meuth M. An established pre-adipose cell line and its differentiation in culture. *Cell* 1974; **3:** 127-133.

31. Kunz-Schughart L A, Schroeder J A, Wondrak M, Van Rey F, Lehle K, Hofstaedter F, Wheatley D N. Potential of fibroblasts to regulate the formation of three-dimensional vessel-like structures from endothelial cells in vitro. *American Journal of Physiology-Cell Physiology* 2006; **290:** C1385-C1398.

32. Ramirez-Zacarias J L, Castro-Munozledo F, Kuri-Harcuch W. Quantitation of adipose conversion and triglycerides by staining intracytoplasmic lipids with Oil red O. *Histochemistry* 1992; **97:** 493-497.

33. Romeis B. *Mikroskopische Technik*. Urban & Schwarzenberg: Munich, Vienna, Baltimore, 1989.

34. Pairault J, Green H. A study of the adipose conversion of suspended 3T3 cells by using glycerophosphate dehydrogenase as differentiation marker. *Proc.Natl.Acad.Sci.U.S.A* 1979; **76:** 5138-5142.

35. Woessner J F, Jr. The determination of hydroxyproline in tissue and protein samples containing small proportions of this imino acid. *Arch.Biochem.Biophys.* 1961; **93:** 440-447.

36. Sommer F, Kobuch K, Brandl F, Wild B, Framme C, Weiser B, Tessmar J, Gabel V P, Blunk T, Goepferich A. Ascorbic acid modulates proliferation and extracellular matrix accumulation of hyalocytes. *Tissue Eng* 2007; **13:** 1281-1289.

37. Weiser B, Sommer F, Neubauer M, Seitz A, Tessmar J, Goepferich A, Blunk T. Ascorbic acid enhances adipogenesis of bone marrow-derived mesenchymal stromal cells. *Cells Tissues.Organs* 2009; **189:** 373-381.

38. Kim Y J, Sah R L, Doong J Y, Grodzinsky A J. Fluorometric assay of DNA in cartilage explants using Hoechst 33258. *Anal.Biochem.* 1988; **174:** 168-176.

39. Moore A, Donahue C J, Bauer K D, Mather J P. Simultaneous measurement of cell cycle and apoptotic cell death. *Methods Cell Biol.* 1998; **57:** 265-278.

40. Loo D T, Rillema J R. Measurement of cell death. *Methods Cell Biol.* 1998; **57:** 251-264.

41. Marshall O J. PerlPrimer: cross-platform, graphical primer design for standard, bisulphite and real-time PCR. *Bioinformatics.* 2004; **20:** 2471-2472.

42. Hausman G J, Richardson R L. Newly recruited and pre-existing preadipocytes in cultures of porcine stromal-vascular cells: morphology, expression of extracellular matrix components, and lipid accretion. *J.Anim Sci.* 1998; **76:** 48-60.

43. Daley W P, Peters S B, Larsen M. Extracellular matrix dynamics in development and regenerative medicine. *J.Cell Sci.* 2008; **121:** 255-264.

44. Yonemitsu N, Bittenger F, Gerhard T, Sugihara H, Mittenmayer C, Kirkpatrick C J. Influence of Extracellular Matrix on the Lipogenesis of Cultured White Fat Cells. *Acta Histochemica et Cytochemica* 1998; **31:** 9-15.

45. Rozario T, Desimone D W. The extracellular matrix in development and morphogenesis: A dynamic view. *Dev.Biol.* 2009.

46. Gregoire F M, Smas C M, Sul H S. Understanding adipocyte differentiation. *Physiol Rev.* 1998; **78:** 783-809.

47. Rodriguez Fernandez J L, Ben Ze'ev A. Regulation of fibronectin, integrin and cytoskeleton expression in differentiating adipocytes: inhibition by extracellular matrix and polylysine. *Differentiation* 1989; **42:** 65-74.

48. Smas C M, Sul H S. Control of adipocyte differentiation. *Biochem.J.* 1995; **309 (Pt 3):** 697-710.

49. Cukierman E, Pankov R, Stevens D R, Yamada K M. Taking cell-matrix adhesions to the third dimension. *Science* 2001; **294:** 1708-1712.

50. Kang X, Xie Y, Powell H M, James L L, Belury M A, Lannutti J J, Kniss D A. Adipogenesis of murine embryonic stem cells in a three-dimensional culture system using electrospun polymer scaffolds. *Biomaterials* 2007; **28:** 450-458.

51. Nakajima I, Yamaguchi T, Ozutsumi K, Aso H. Adipose tissue extracellular matrix: newly organized by adipocytes during differentiation. *Differentiation* 1998; **63:** 193-200.

52. Kubo Y, Kaidzu S, Nakajima I, Takenouchi K, Nakamura F. Organization of extracellular matrix components during differentiation of adipocytes in long-term culture. *In Vitro Cellular & Developmental Biology-Animal* 2000; **36:** 38-44.

53. Lilla J, Stickens D, Werb Z. Metalloproteases and adipogenesis: a weighty subject. *Am.J.Pathol.* 2002; **160:** 1551-1554.

54. Aratani Y, Kitagawa Y. Enhanced synthesis and secretion of type IV collagen and entactin during adipose conversion of 3T3-L1 cells and production of unorthodox laminin complex. *J.Biol.Chem.* 1988; **263:** 16163-16169.

55. Wright G, Higgin J J, Raines R T, Steenbergen C, Murphy E. Activation of the prolyl hydroxylase oxygen-sensor results in induction of GLUT1, heme oxygenase-1, and nitric-oxide synthase proteins and confers protection from metabolic inhibition to cardiomyocytes. *J.Biol.Chem.* 2003; **278:** 20235-20239.

56. Udenfriend S. Formation of hydroxyproline in collagen. *Science* 1966; **152:** 1335-1340.

57. Yu I T, Lee S H, Lee Y S, Son H. Differential effects of corticosterone and dexamethasone on hippocampal neurogenesis in vitro. *Biochem.Biophys.Res.Commun.* 2004; **317:** 484-490.

58. Menconi M, Gonnella P, Petkova V, Lecker S, Hasselgren P O. Dexamethasone and corticosterone induce similar, but not identical, muscle wasting responses in cultured L6 and C2C12 myotubes. *J.Cell Biochem.* 2008; **105:** 353-364.

59. Knight D M, Chapman A B, Navre M, Drinkwater L, Bruno J J, Ringold G M. Requirements for triggering of adipocyte differentiation by glucocorticoids and indomethacin. *Mol.Endocrinol.* 1987; **1:** 36-43.

60. Fischbach, C. Adipose Tissue engineering - Development of a 3-D Model of Adipogenesis. *Ph.D. thesis* 2003; 35-59. University of Regensburg, Regensburg, Germany.

61. Kivirikko K I, Myllyharju J. Prolyl 4-hydroxylases and their protein disulfide isomerase subunit. *Matrix Biol.* 1998; **16:** 357-368.

Chapter 6

Collagen Type XVI is Regulated during *in vitro* Adipogenesis of 3T3-L1

To be submitted to Matrix Biology

1. Abstract

Adipocytes are surrounded by a unique extracellular matrix (ECM) which provides mechanical support and participates in a variety of signaling events. Collagens are important components of the ECM environment and are regulated during adipose conversion. However, the collagen network and its remodeling during adipocyte development are not well characterized. FACITs (fibril-associated collagens with interrupted triple helices) such as collagen XVI are adapter molecules that arrange the structural integrity of the ECM and, therefore, may be involved in adipose conversion. So far, the expression and the role of collagen XVI in adipogenesis have not been elucidated. In this *in vitro* study, we demonstrated a downregulation of collagen type XVI during hormonally induced adipogenesis in 2-D and 3-D adipocyte culture. When confluent 3T3-L1 preadipocytes or human adipose-derived stem cells from adipose tissue (ADSCs) were stimulated with adipogenic medium, a significant decrease of procollagen XVI(α1) mRNA was found which was associated with a decrease in protein expression of collagen XVI as detected by qRT-PCR and Western blot analyses. In 3-D spheroid culture with 3T3-L1, the decrease of collagen XVI protein expression was additionally visualized by immunostaining. Further studies identified corticosterone as an inducing substance that provoked the downregulation of procollagen XVI(α1) mRNA. A functional role of collagen XVI in adipogenesis can be elucidated by using cellular overexpression of collagen XVI or exogenous addition of recombinant collagen XVI protein. Whereas recombinant collagen XVI did not affect the adipogenic differentiation of 3T3-L1 in 2-D culture, preliminary overexpression experiments showed that collagen XVI overexpressing 3T3-L1 cells failed to differentiate into adipocytes after hormonal induction in contrast to non-transfected cells in 2-D culture suggesting a possible functional role of collagen XVI in *in vitro* adipogenesis of 3T3-L1. For the first time, this study associates collagen XVI expression with adipogenesis and contributes to the emerging picture of the complexity and the role of the ECM in adipose tissue.

2. Introduction

Adipose tissue is a connective tissue composed of adipocytes that functions as a key regulator of systemic energy homeostasis. Adipocytes are responsible for the synthesis, storage, and hydrolysis of nutritional energy in form of triglycerides. Many studies focused on characterizing the development of preadipocytes into mature adipocytes on the cellular and molecular levels [1-4]. This differentiation process involves a coordinated progression of the expression of various proteins and their cognate mRNAs. The changes of the expression pattern directly related to the increase in lipid synthesis are not limited to intracellular mechanisms; alterations also occur in the intercellular space during adipocyte differentiation. An important component of the adipocyte microenvironment is the ECM, a complex of versatile proteins and polysaccharides, secreted and assembled by different surrounding cells. The macromolecules interact with cells and are able to regulate cell behavior indirectly or directly through receptor-mediated interactions. The ECM components are associated with the cytoskeleton via receptors, such as integrins, playing an important role in the morphological changes of the preadipocytes into mature adipocytes [5,6]. These complex cell-cell and cell-ECM interactions which are present within *in vivo* fat tissue can not be captured by conventional 2-D monolayer cultures which are commonly used for investigation of adipogenic differentiation *in vitro* [7-11]. In order to enable studies on adipocyte function and development within an environment more resembling *in vivo* conditions, we recently established a coherent tissue-like 3-D model system utilizing 3T3-L1 and also human ADSCs which is based on the formation of spheroids. The 3-D tissue-like context of the spheroids enables the investigation of interactions among adipose cells and their ECM [12,13].

So far, only few studies focused on the components of the ECM that are associated with the development of the adipocyte phenotype and many discrepancies are found in the literature. The development of adipocytes is accompanied by perpetual changes in the level and type of ECM components [14]. During development, the ECM is continually reorganized by proteolytic degradation and assembly of de novo matrix. Degradation action is mainly modulated by matrix metalloproteinases (MMPs) and their inhibitors (TIMPs) [14-17]. The first ultrastructural changes in the differentiation of adipose cells are marked by the increase of laminins, entactin, and glycosaminoglycans [18-21]. Additionally, a decline in cell-associated fibronectin was detected during differentiation of 3T3-F442A and 3T3-L1 [5,22]. Collagens, the most ubiquitous and best-characterized proteins of the ECM, have also been implicated in the differentiation of adipocytes. Green *et al.* demonstrated that collagens were synthesized at substantial levels in 3T3-L1 preadipocytes [23]. Upon differentiation of 3T3-

L1 preadipocytes into adipocytes, the gene expression of fibrillar collagens such as type I and III declined [21], whereas basement membrane collagen type IV accumulated [19,21]. In addition, Nakajima *et al.* reported that upon differentiation into adipocytes, the mRNA expression of collagen type I, II, III, IV, V, and VI as well as laminin and fibronectin increased three- to sixfold in bovine intramuscular preadipocytes (BIP) [24]. Nevertheless, the organization of the collagen network through interactions of the molecules during adipogenesis is not well characterized. FACITs are important components for connection of the ECM network. Members of the FACIT family (collagen type IX, XII, XIV, XVI, XIX, XX, XXI, XXII) are localized on the surface of major collagen fibrils and act as molecular bridges that arrange the structural integrity of the ECM. So far, FACITs were not investigated during adipocyte development.

Collagen XVI, one member of the FACIT group, is a homotrimeric molecule composed of three 220-kDa α1(XVI) chains [25]. The structure of collagen XVI is characterized by 10 collagenous domains, which are interrupted by 11 non-collagenous domains (Figure 1). The high thermal stability of the homotrimer in the form of disulfide bonds arises from 32 cysteine residues which are almost all located in the non-collagenous domains at the junction with the precedent collagenous regions [26]. The terminal non-collagenous NC11 consists mainly of a 200-residue motif referred to as proline-arginine-rich protein (PARP) in various other collagen types. This motif is responsible for the binding of certain integrins [27].

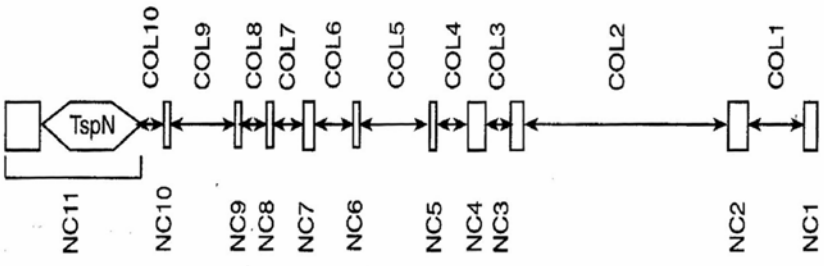

Figure 1: The domain structure of collagen XVI [28].

Collagen XVI is widely distributed in the heart, intestine, kidney, testis, ovary, eye, arterial wall, and smooth muscle cells of adult mice. In human, collagen XVI is predominantly expressed in skin and cartilage, where it is integrated into tissue specific aggregates [29,30], and it has been further detected in the nervous system [31]. Pathophysiologically, a dysregulation of collagen XVI was observed recently. It was demonstrated that collagen XVI is upregulated in glioblastoma as a part of tumor-specific remodelling of the ECM [32]. Furthermore, a role in the remodelling of the matrix in Crohn's disease was described [33].

However, the physiological function of this type of collagen is not well understood so far. Eble *et al.* detected collagen XVI in fat tissue around adipocytes, but neither a regulation nor a role of this collagen type has been described in adipocyte development so far [27].

Therefore, in the current study, we investigated the expression of collagen XVI during the *in vitro* adipogenesis of 3T3-L1 preadipocytes and ADSCs in 2-D and 3-D culture. The adipogenic differentiation was induced by a hormonal cocktail consisting of insulin, a glucocorticoid, IBMX, and indomethacin. We determined the gene and protein expression of collagen XVI at different differentiation stages of 3T3-L1 and ADSCs by qRT-PCR and Western blot analyses. Further studies revealed the influence of the adipogenic inducers on gene expression of collagen XVI. Finally, preliminary experiments were performed to examine a possible functional role of collagen XVI in *in vitro* adipogenesis.

3. Materials and Methods

Materials

Murine 3T3-L1 preadipocytes were obtained from ATCC (Manassas, VA, USA). Human ADSCs were bought from Promocell (Heidelberg, Germany). Dulbecco's Modified Eagle's Medium (DMEM) was purchased from Biochrom (Berlin, Germany). Preadipocyte Basal Medium-2 (PBM-2) was bought from Lonza (Köln, Germany). Fetal bovine serum (FBS, Lot. No. 40A0044K), phosphate buffered saline (PBS), 0.25% trypsin-EDTA solution, penicillin-streptomycin solution, 4',6-diamidino-2-phenylindole (DAPI), Superscript II reverse transcriptase, SYBR Green Supermix, and Lipofectamine 2000 were from Invitrogen (Karlsruhe, Germany). 3-isobutyl-methylxanthine (IBMX), Coomassie Blue G250, bisacrylamide, bromphenol blue, SDS, Tris, and Tween 20 were bought from Serva Electrophoresis (Heidelberg, Germany). Papainase was from Worthington (Lakewood, NJ, USA). Bovine insulin was kindly provided by Sanofi-Aventis (Frankfurt a. M., Germany). Minimum Essential Medium alpha modification (α-MEM), agarose, dexamethasone, corticosterone, indomethacin, bovine serum albumin (BSA), cysteine, bovine DNA, 2-mercaptoethanol, bisphenol A diglycidyl (BADGE), Ponceau S, and oil red O were obtained from Sigma-Aldrich (Taufkirchen, Germany). Thesit was purchased from Gepepharm GmbH (Siegburg, Germany) and collagen I was from Cardiovascular Sciences GmbH (Hamburg, Germany). Hoechst 33258 dye was obtained from Polysciences (Warrington, PA, USA). Complete Mini and random hexamer primers were from Roche (Mannheim, Germany). TEMED and dry milk powder were purchased from Carl Roth (Karlsruhe, Germany). Normal

goat serum and fluorescence mounting medium were bought from Dako (Glostrup, Denmark). Puromycin 2HCl was obtained from Biomol (Hamburg, Germany). If not stated otherwise, all other chemicals were from Merck KGaA (Darmstadt, Germany). Deionized water was obtained using a Milli-Q water purification system from Millipore (Schwalbach, Germany). All cell culture plastics were purchased from Corning (Bodenheim, Germany). Recombinant collagen XVI, the expression vector pCEP-PU-BM40SP-colXVI and all antibodies were kindly provided by the Department of Experimental Orthopedics, University Hospital of Regensburg (Regensburg, Germany) [30].

Methods

3.1. Cell culture methods

3.1.1. 2-D cell culture

3T3-L1

3T3-L1 is a mouse embryonic fibroblast cell line. These cells are derived from the original line 3T3-Swiss albino and are used as an *in vitro* model of adipocytes [23]. 3T3-L1 preadipocytes were expanded in DMEM supplemented with 10% FBS, penicillin (100 U/ml), and streptomycin (100 µg/ml) [34,35]. For 2-D monolayer cultures, preadipocytes were seeded in basal medium (α-MEM, 10% FBS, penicillin (100 U/ml), and streptomycin (100 µg/ml)) into tissue-culture polystyrene well plates at a density of 40,000 cells/cm^2. This high seeding density guaranteed that 2-D cultures grew to confluence within two days after seeding. Hormonal induction was initiated two days after seeding by exchanging half of the medium with induction medium (basal media with 1 µM insulin, 0.1 µM corticosterone, 0.5 mM IBMX, and 60 µM indomethacin (final concentration) [34,35]. The time point of induction was referred to as day 0 throughout all experiments. At day 2, induction medium was replaced with differentiation medium (basal medium, 1 µM insulin). Subsequently, cells were fed with differentiation medium every other day up to day 6. Feeding was performed by exchanging only half of the medium volume in order to treat cells in the same way as in 3-D culture (see 3.1.2.). Cells were incubated in a humidified atmosphere at 37°C and 5% CO_2 during the complete culture period.

Human adipose-derived stem cells (ADSCs)

For 2-D monolayer cultures, cells were seeded in basal medium (PBM-2 supplemented with 10% FCS, penicillin (100 U/ml), and streptomycin (100 µg/ml)) at a density of 30,000

cells/cm^2. At confluence, cells were induced to undergo adipogenesis by exchanging half of the medium with basal medium supplemented with 1.7 µM insulin, 1 µM dexamethasone, 0.5 mM IBMX, and 200 µM indomethacin (final concentration). The time point of induction was referred to as day 0 throughout all experiments. The inducers were present during the entire adipogenic period. Medium was exchanged every other day up to day 10. Feeding was performed by exchanging only half of the medium volume in order to treat cells in the same way as in 3-D culture (see 3.1.2.). Cells were incubated in a humidified atmosphere at 37°C and 5% CO_2.

3.1.2. 3-D cell culture

Spheroids were generated according to the liquid overlay technique as already described in Chapter 5 (Page 101) [36,37]. Briefly, tissue culture polystyrene (TCPS) 96-well plates were coated with 50 µl of 1.5% agarose in α-MEM per well [38]. Spheroid formation was initiated by seeding 3,000 cells per well in basal medium (see 3.1.1) into the agarose-coated well. The outermost rows and columns of the well plate, respectively, were not used for culture due to the increased evaporation of medium from the wells during prolonged culture; they were only filled with PBS supplemented with penicillin (100 U/ml) and streptomycin (100 µg/ml). Two days after seeding, cells were induced to undergo adipogenesis by exchanging half of the medium with induction medium (see 3.1.1). Feeding was performed by exchanging only half of the medium volume, otherwise spheroids would be aspirated with complete removal of the medium from the wells. For 3T3-L1 preadipocytes, adipogenic induction was performed for another two days. Then half of the medium was exchanged with differentiation medium (see 3.1.1). This medium exchange was performed three times to further reduce the concentrations of inducers. Because ADSCs were cultured in the presence of inducers during the entire adipogenic phase, this washing step was not necessary. For either cell type, subsequently, cells were fed by exchanging half of the medium with differentiation medium every other day. Spheroid cultures were incubated in a humidified atmosphere at 37°C and 5% CO_2 on an orbital shaker at 60 rpm (Heidolph, Schwabach, Germany).

3.1.3. Stable transfection with Lipofectamine 2000

The expression vector pCEP-PU-BM40SP-colXVI for stable transfection of 3T3-L1 with collagen XVI was kindly provided by the Department of Experimental Orthopedics, University Hospital of Regensburg (Regensburg, Germany) (Figure 2).

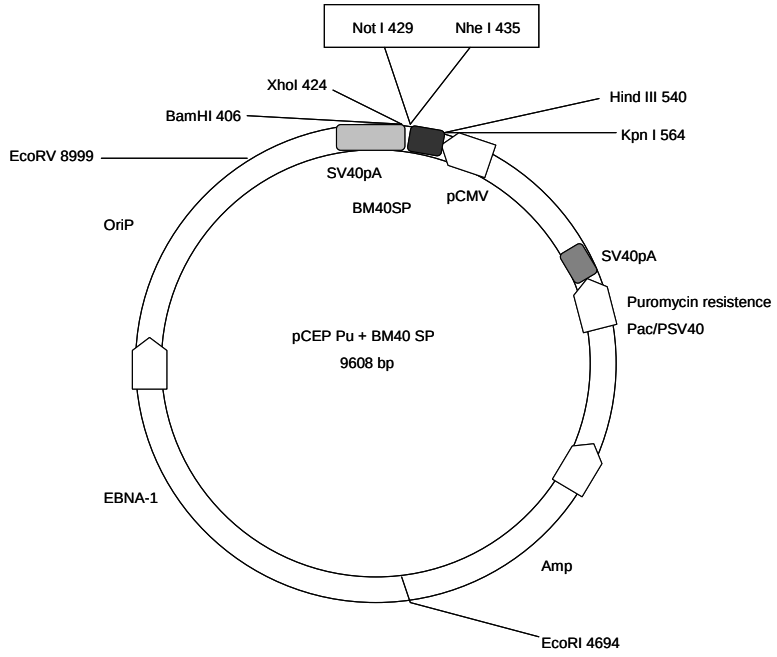

Figure 2: Expression vector pCEP-PU-BM40SP
This vector is based on a previous commercially available expression vector pCEP-Pu from Invitrogen (Karlsruhe, Germany). The vector has been modified by insertion of a BM40 signal peptide and several tag sequences [39-41] and recombinant expression of collagen XVI with this vector has been established previously [26]. The restriction sites Not I and Nhe I within the multiple cloning site are framed. The black area refers to the coding sequence of the BM40 signal peptide (BM40SP). The vector contains an ampicillin resistance for selection in prokaryotes and a puromycin resistance for selection in mammalian cells.

Plasmid DNA was isolated by using a silica membrane system commercially available from Peqlab (Erlangen, Germany). According to the manufacturer's protocol for Spin Miniprep kits 5 ml of bacteria suspension were initially applied. Higher volumes up to 50 ml were purified with Qiagen Midiprep kit (Hilden, Germany) yielding up to 500 µg plasmid DNA.

Transfection was carried out using Lipofectamine 2000, a lipid-based transfection reagent. Cells were seeded at a density of 20,000 cells/cm^2 in a 12-well plate. Firstly, 2 µl Lipofectamine 2000 and 48 µl culture medium without FBS were mixed and incubated for 5 minutes. DNA (2 µg/reaction) was separately prepared with FBS-free medium up to a volume of 50 µl. Lipofectamine and DNA solutions were gently mixed and incubated for 20 minutes at room temperature. Afterwards, the reaction volume was added to the cells together with usually applied culture medium and the cells were incubated for 8 hours at 37°C and 5% CO_2. After this time, medium was replaced by serum-containing medium. Selection medium containing puromycin in a final concentration of 15 µg/ml as previously determined in a kill curve for non-transfected cells (see 3.1.4) was applied 48 hours after transfection procedure. By the time all non-transfected cells were eliminated upon antibiotic application,

resistant clones were transferred to larger flasks and further cultivated. Finally, cells were harvested by trypsin digestion and used for analyses.

3.1.4. Titration of antibiotic stocks (kill curve)

Prior to application of puromycin in order to establish stable cell lines, selection agent stocks had to be titrated to determine the optimal concentration for selection with the chosen cell line. 20,000 non-transfected cells per cm^2 were plated in 12-well plates containing the culture medium plus increasing amounts of puromycin (0, 2.5, 5.0, 7.5, 10.0, 15.0, and 25.0 µg/ml). The cells were incubated for 10 days to 14 days and the selection medium was replaced every three days. For selecting stable transfectants, the lowest concentration that induces massive cell death in about 5 days and kills all the cells within two weeks was used.

3.1.5. Coating of well plates with proteins

48-well plates were coated with collagen I (10 µg/ml) and recombinant collagen XVI (10 µg/ml) overnight at 4°C [26]. Unspecific binding sites were blocked with 1% (w/v) BSA solution for 2 hours at room temperature. The plates were washed two times with PBS and stored at 4 °C until usage. Collagen IV-coated well plates were purchased from BD Biosciences (Heidelberg, Germany).

3.2. Analysis of triglyceride (TG) accumulation

3.2.1. Oil red O staining

In order to visualize accumulated cytoplasmic TG droplets, oil red O staining was performed at day 6 after hormonal induction of adipogenesis. For this purpose, cells or entire spheroids were washed once with PBS, fixed in 10% PBS-buffered formalin overnight and then stained with oil red O (3 mg/ml solution in 60% isopropanol) for 4 hours [34,42]. Excess dye was removed by washing three times with PBS. For histological investigations, the stained spheroids were embedded in Tissue-Tek (Hartenstein Laborbedarf, Würzburg, Germany), snap frozen and finally cut into 12 µm-thick cryosections. After dissolution of Tissue-Tek in water, cryosections were incubated for 30 seconds in 60% isopropanol to remove unspecific oil red O staining, washed in water and mounted in glycerol [43]. Serial sections were prepared from all spheroids and sections from the center region were used for histological evaluation. Microscopical bright field pictures were acquired at 20x magnification using an inverted microscope (Leica DM IRB, Leica Microsystems, Wetzlar, Germany) equipped with

a CCD camera (DS-5M, Nikon, Düsseldorf, Germany) and the software Eclipse Net (Laboratory Imaging, Praha, Czech Republic).

3.2.2. Quantitative analysis of intracellular TG accumulation

For analysis of the intracellular TG content, 2-D monolayers were washed twice with PBS and harvested in 0.5% aqueous thesit solution. After sonication with a digital sonifier (Branson Ultrasonic Corporation, Danburg, CT, USA), the spectroscopic quantification of TG was performed using the enzymatic serum triglyceride determination kit from Sigma-Aldrich (Taufkirchen, Germany) according to the manufacturer's instructions. Measurements were done in three biological replicates; one replicate was derived from one well for 2-D cultures. The amount of TG was calculated and normalized to the cell number per sample as determined by the DNA assay.

3.3. Determination of the DNA content with DNA assay

After washing with PBS, cells were harvested in lysis buffer (50 mM Tris, 1 mM EDTA, 1 mM 2-mercaptoethanol, pH 7.5) and sonicated with a digital sonifier (Branson Ultrasonic Corporation, Danburg, CT, USA). Aliquots of the cell lysates were digested with papainase (3.2 U/ml in 0.1 M Na_2HPO_4 buffer, pH 6.5 containing 1 mM Na_2EDTA and 2.5 mM cysteine) for 16 hours at 60°C, and the DNA content was determined using the intercalating Hoechst 33258 dye (0.1 µg/ml in 0.1 M NaCl containing 1 mM Na_2EDTA, 10 mM Tris, pH 7.4) [44]. Fluorescence intensities were determined at 365 nm excitation wavelength and 458 nm emission wavelength on a LS 55 Fluorescence Spectrometer (PerkinElmer, Wiesbaden, Germany) and correlated to DNA contents using standard dilutions of double-stranded DNA (from calf thymus). Cell numbers of 3T3-L1 cells were calculated with a conversion factor of 26.1 pg of DNA per cell, which was determined previously [37].

3.4. Molecular biology methods

3.4.1. Total RNA extraction

Prior to isolation of total RNA, 2-D monolayers as well as entire spheroids were washed once with PBS. Total RNA was isolated using Qiagen RNeasy Mini Kit (Qiagen, Hilden, Germany), based on affinity columns from either freshly isolated or frozen (-80° C) cells according to the manufacturer's protocol. For one biological replicate a sufficient number of wells and spheroids, respectively, was pooled to yield a minimum of 1 µg total RNA per

sample. RNA content and purity were determined spectrophotometrically at 260 nm/280 nm (Nanodrop Analyzer, NanoDrop, Wilmington, DE, USA). The ratio of adsorption values at 260 nm to 280 nm was optimal at about 1.8 to 2.0 and guaranteed pure RNA.

3.4.2. Microarray Analysis: RNA transcription, hybridization, and data acquisition

For microarray analysis, integrity of total RNA was verified by electrophoresis using an Agilent Bioanalyzer 2100 (Agilent Technologies, Waldbronn, Germany). All following procedures, i.e., RNA transcription, fragmentation, hybridization, scanning, and data processing were performed according to the manufacturer's instructions (Agilent Technologies, One-Color Microarray-Based Gene Expression Analysis Protocol, G4140-90040). 1 µg of total RNA per sample was transcribed into cyanine 3 (Cy3)-labeled cRNA using the Low RNA input Fluorescent Linear Amplification Kit (Agilent Technologies). Labeled cRNAs were purified using RNeasy Mini Kit (Qiagen, Hilden, Germany) and quality parameters (cRNA yield > 1.5 µg and Cy3-incorporation rate > 9 pmol/µg RNA) were assessed spectrophotometrically (NanoDrop Analyzer). Using the Gene Expression Hybridization Kit (Agilent Technologies) 1.5 µg of cRNA was fragmented (60°C, 30 minutes) and hybridized (60°C for 17 hours) to 44K Whole Mouse Genome Oligo Microarrays (G4122F, 4x44K slide format, Agilent Technologies). Each array contains 41,534 60-mer oligonucleotide probes representing approximately 41,000 mouse genes and transcripts. After washing, microarrays were scanned with a DNA Microarray Scanner (Agilent Technologies) and background corrected spot intensities were acquired using Feature Extraction Software (Version 9.1.1.1, FE Extraction Protocol: GE1-v5_91_0806, grid: 014868_D_20060807, Agilent Technologies). RNA transcription, hybridization, and scanning of the microarrays were performed by the Kompetenzzentrum für Fluoreszente Bioanalytik (Regensburg, Germany). Resulting data were imported into GeneSpring GX software (Version 7.3.1, Agilent Technologies) and spot intensities of collagen type XVI alpha 1 (GenBank accession number NM_028266) were normalized to the median of all spot intensities of the respective chip (median normalization). For each experimental condition two biological replicates were analyzed.

3.4.3. Quantitative real-time reverse transcription-polymerase chain-reaction (qRT-PCR)

To validate results from microarray analysis and for further experiments, mRNA expression levels of collagen XVI(α1) (see Table 1) was analyzed with qRT-PCR SYBR Green assays.

First strand cDNA was synthesized from 1 µg of total RNA using random hexamer primers and Superscript II reverse transcriptase according to the manufacturer's instructions.

Relative quantitative PCR was performed with SYBR Green Dye I with an ABI 7000 Prism Sequence detection system (Applied Biosystem, Darmstadt, Germany) using the following cycling conditions: 50°C for 2 minutes, 95°C for 10 minutes followed by 40 cycles at 95°C for 15 seconds and 60°C for 1 minute. Each primer was suspended in a final concentration of 0.2 µM in SYBR Green Supermix and the reaction was carried out in 96-well plates with 10 µl diluted cDNA in a final volume of 25 µl. Experiments were performed in triplicates for each sample. Primers were designed with the free, open-source PerlPrimer software (www.perlprimer.sourceforge.net [45]) and obtained from Biomers (Ulm, Germany). Specificity of primer pairs and amplification conditions were verified by melting curve analysis and agarose gel electrophoresis.

Table 1: Primer sequences and amplicon lengths for SYBR Green PCR assays.

Gene	Forward Primer Sequence (5' ➔ 3')	Reverse Primer Sequence (5' ➔ 3')	GenBank Accession No.	Amplicon Length (bp)
mouse col XVI(α1)	tacctccaggatgcagttcc	caccttggtaccaggcagt	NM_028266	181
human col XVI(α1)	gcctggtaccaaaggtgaaa	catagcctggaggaccttga	M92642	97

To determine gene expression levels, three biological replicates of each condition were analyzed in the qPCR assays. Ct values were obtained using SDS software (Applied Biosystems). For absolute quantification a standard curve of serially diluted plasmids of known copy number (10 up to $10x10^7$) was plotted and sample Ct values were used to determine the exact copy numbers of the genes of interest.

3.5. Protein biochemical methods

3.5.1. Protein isolation, precipitation, and quantification

For detection of secreted proteins in 2-D culture, the supernatant per well was taken. In 3-D culture, the culture medium of 100-200 spheroids collected in one 96-well was used. In order to concentrate proteins, the solution was incubated on ice for 20 minutes with a final concentration of 0.14% (w/v) Triton X-100 and 15.5% (w/v) trichloric acid (TCA).

Centrifugation with 18,000 x g for 20 minutes at 4°C resulted in a protein pellet that was washed two times with pre-chilled acetone. After air-drying, the pellet was resuspended in an appropriate volume of sample buffer.

For detection of proteins within the cell, cells were washed with PBS, harvested in lysis buffer (3.5 mM SDS, 8.3 mM Tris ad 250 ml, pH 7.4, adding protease inhibitor (complete mini)) and sonicated with a digital sonifier (Branson Ultrasonic Corporation, Danburg, CT, USA). Protein content was determined using the Bradford method [46]. Measurements were done in three biological replicates; one replicate was derived from one well for 2-D cultures and a number of approximately 200 spheroids at day 0 and 3 and of 100 spheroids at day 6 and 10, respectively, for 3-D cultures.

3.5.2. SDS-PAGE according to Laemmli

Table 2: Buffer concentrations for SDS-PAGE according to Laemmli.

Solutions	Concentration of ingredients
Resolving gel buffer	1.5 M Tris/HCl, pH 8.8 0.4% (w/v) SDS
Stacking gel buffer	0.5 M Tris/HCl, pH 6.8 0.4% (w/v) SDS
Acrylamide stock solution	30% (w/v) bisacrylamide
TEMED	100% triethylmethylethylendiamine
APS	10% (w/v) ammonium persulfate in water
Sample loading buffer	0.1 M Tris/HCl, pH 6.8 1% (w/v) SDS 20% (v/v) glycerol 5% (v/v) ß-mercaptoethanol 0.01% (w/v) bromphenol blue

The discontinuous sodium dodecyl sulphate polyacrylamide gel electrophoresis (SDS-PAGE) according to Laemmli [47] was used to discriminate heterogeneous protein samples comprising different protein fractions. After addition of sample loading buffer to the protein samples, they were denatured for 5 minutes at 95°C and added into a 4.5% to 15% gradient

resolving gel with a 4.5% stacking gel. Collagen XVI was detected by Western blot of 20 µg total protein. Concentrations of the ingredients are listed in Table 2. The gel run was performed at a maximum current of 20 mA. A pre-stained protein marker was always co-separated to determine the molecular weight of the sample (Precision Plus™ Protein All Blue Standard, BioRad, München, Germany).

3.5.3. Western blot analysis

Table 3: Buffer concentrations for Western blot analysis.

Solutions	Concentration of ingredients
Blotting buffer	50 mM Tris 380 mM glycine 0.1% (w/v) SDS 10% (v/v) methanol
1x TBST	140 mM NaCl 15 mM Tris/HCl 5 mM EDTA 0.1% (v/v) Tween 20 in TBS
Blocking solution	5% (w/v) dry milk powder in 1xTBST

Proteins were electrotransferred to a nitrocellulose membrane (Protran, Schleicher & Schuell, Germany) with the BioRad Mini Trans Blot Electrophoretic Cell (BioRad, München, Germany) in a sandwich of three layers whatman paper (BioRad, München, Germany), nitrocellulose membrane, polyacrylamide gel and again three layers of whatman paper. Per cm^2 of nitrocellulose membrane 0.8 mA current was applied for 60 to 75 minutes according to the fragment size of the protein. Prior to transfer, whatman paper and nitrocellulose membrane were soaked in blotting buffer (Table 3). After blotting, transfer of proteins was confirmed by a reversible Ponceau red staining of the membrane with a 0.2% (w/v) Ponceau S solution in 3% (v/v) TCA. After removal of the Ponceau red staining with water, unspecific binding sites were blocked with blocking solution (Table 3) for 1.5 hours at room temperature. After a short washing step in Tris-buffered saline Tween 20 (TBST), the membrane was incubated at 4°C overnight with the polyclonal guinea pig-anti-colXVI antibody (1:1,000) in blocking solution. Unspecificly bound antibody was removed in three

washing steps for 20 minutes each in TBST. The secondary goat-anti-guinea pig peroxidase-conjugated antibody was diluted 1:30,000 in blocking solution and the membrane was incubated for 60 minutes at room temperature. Washing steps were repeated as described for the primary antibody. Protein bands were detected by incubating the membrane with Super Signal West Femto Trial ECL reagent (Thermo Scientific, Rockford, IL, USA) for 1 minute. Wrapped in clear foil, the luminescent signal was detected by application of an x-ray film for 10 seconds to 5 minutes (Amersham, UK).

3.5.4. Immunofluorescence

Cells grown on coverslips (Sarstedt, Nümbrecht, Germany) or entire spheroids were washed once with PBS, fixed in 4% (w/v) paraformaldehyde (PFA) in PBS overnight and washed thoroughly in PBS. The spheroids were embedded in Tissue-Tek (Hartenstein Laborbedarf, Würzburg, Germany), snap frozen and finally cut into 12 µm-thick cryosections. Serial sections were prepared from all spheroids and sections from the center region were used for histological evaluation. After dissolution of Tissue-Tek in water, cryosections were fixed in ice-cold acetone for 10 minutes at 4°C. Further procedures were performed with both cells in monolayer and cryosections of spheroids. Unspecific binding sites were blocked with 5% (v/v) normal goat serum, 1% (w/v) BSA and protease inhibitor (complete mini, 1:5) in PBS for 60 minutes at 37°C. Guinea pig-anti-colXVI primary antibody was diluted 1:100 in blocking buffer and incubated at 4°C overnight. After washing with PBS, the goat-anti-guinea pig Alexa Fluor® 555 antibody diluted in PBS at a final concentration of 5 µg/ml was applied and incubated at 37°C for 1 hour. Nuclei were counterstained with 300 nM DAPI for 10 minutes and the slides were washed again with PBS before they were mounted with fluorescence mounting medium. All histological incubation steps were performed in humid chambers. The stained structures were visualized with confocal laser scanning microscopy (C1 confocal microscope, C4 camera and software Nikon, Germany).

3.6. Statistics

For TG accumulation, DNA measurements and qRT-PCR data, results are presented as mean values ± standard deviation. Statistical analyses were determined using GraphPadPrism v.5 (GraphPad Software, La Jolla, CA, USA). Differences between two groups were analyzed for significance using the unpaired Student's t-test. Differences between multiple groups were analyzed for significance using one-way analysis of variances (ANOVA) with subsequent

multiple comparisons according to Tukey's post hoc test. A value of $p<0.05$ was regarded as statistically significant. For microarray analysis, the mean value and the values of both replicates are depicted.

4. Results

4.1. Gene expression of collagen XVI(α1) during adipogenesis of 3T3-L1 in 2-D and 3-D

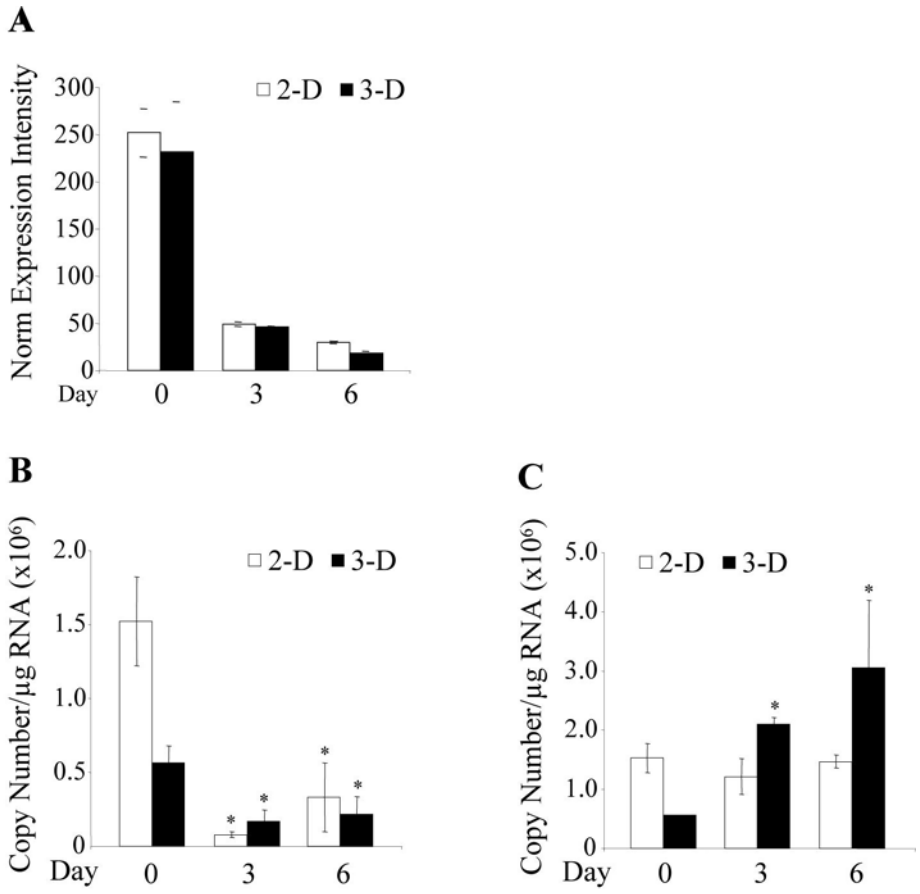

Figure 3: Gene expression of collagen XVI(α1) in 3T3-L1 in 2-D and 3-D cultures.
A) Microarray analysis (n=2) of collagen XVI(α1) after adipogenic induction in 2-D cultures and 3-D spheroids. Bars represent the mean value of the median-normalized spot intensities. Dashes represent the individual values of both biological replicates. **B)** Microarray analysis was verified by qRT-PCR measurements (n=3). Collagen XVI(α1) gene expression during differentiation of 3T3-L1. **C)** qRT-PCR measurements of the collagen XVI(α1) gene expression in uninduced 3T3-L1 (n=3). Expression is reported as exact copy numbers of the collagen XVI(α1) gene per µg RNA **(B, C)**. * indicates statistically significant differences to the corresponding group at day 0 ($p<0.05$).

3T3-L1 preadipocytes were adipogenically induced in 2-D and 3-D cell culture and RNA samples were taken at day 0, 3, and 6. The gene expression of collagen XVI(α1) was firstly identified by microarray analysis (Figure 3 A) and the result was further ascertained by qRT-PCR analyses in independent cell culture experiments (Figure 3 B). In 2-D as well as in 3-D culture**,** collagen XVI gene expression was clearly downregulated after adipogenic induction observed both in microarray analysis and qRT-PCR measurements. In contrast, when preadipocytes were not induced to undergo adipogenesis, the gene expression of collagen XVI(α1) was not decreased until day 6 after induction in 2-D and 3-D culture (Figure 3 C). In fact, in 3-D culture, collagen XVI expression was clearly increased.

4.2. Protein expression of collagen XVI during adipogenesis of 3T3-L1 in 2-D and 3-D

To confirm the qRT-PCR results on the protein level, we examined the expression pattern of collagen XVI during adipogenesis of 3T3-L1 in 2-D cell culture and 3-D spheroids by Western blotting analyses. Cell extracts for analysis of intracellular collagen XVI were prepared and culture medium for detection of secreted collagen XVI at different stages of differentiation was additionally collected. Moreover, the expression of preadipocytes which were not adipogenically induced by a hormonal cocktail was determined. An equal amount of protein was loaded onto each lane and blotted on a nitrocellulose membrane, as confirmed by Ponceau S staining (Figure 4). By Western blotting, we mostly detected proteolytically processed fragments of collagen XVI as already reported for smooth-muscle cells, dermal fibroblasts, and intestinal subepithelial myofibroblasts [25,33]. The shown Western blots demonstrated the presence of five different-sized polypeptides (Figure 4) with about 210 kDa, 180 kDa, 130 kDa, 80 kDa, and 60 kDa. Most of the bands correspond to the recombinant collagen XVI fragments after proteolytic degradation as previously described by Kassner *et al.* [26]. The ~210 kDa band represents the full-length collagen XVI protein (Figure 1), whereas the ~180 kDa fragment shows the collagen XVI molecule lacking almost the entire NC11 domain. The ~130 kDa fragment results from elimination of parts of the C-terminal domains and the ~80 kDa polypeptide corresponds to the C-terminal part of collagen XVI starting at amino acid 941 harboring the non-collagenous domains 1-4 and the collagenous domains 1-3. However, the polypeptide with the molecular mass of 60 kDa was not detected in HEK 293 EBNA cells transfected with recombinant collagen XVI by Kassner *et al.* [26], thus, it seems to be a proteolytic fragment typical for 3T3-L1. Tillet *et al.* have also detected this 60 kDa polypeptide in transfected human embryonic kidney cell clones and they assumed that this fragment corresponds to the largest collagenous domain Col2 (Figure 1) [48].

The results of the Western blot analyses demonstrated that collagen XVI was highly expressed on day 0 in undifferentiated 3T3-L1 and gradually decreased from day 3 to day 6 of differentiation (Figure 4 A). At day 6 after induction, no collagen XVI protein was detectable in both 2-D and 3-D cultures. Notably, collagen XVI was more abundant in 3-D culture at day 0 and the downregulation was more obvious in 3-D culture compared to 2-D culture. The clearly reduced protein expression of collagen XVI was not detected in the preadipocytes cultured for 6 days without the addition of the adipogenic inducers, neither in 2-D nor in 3-D cell culture (Figure 4 B).

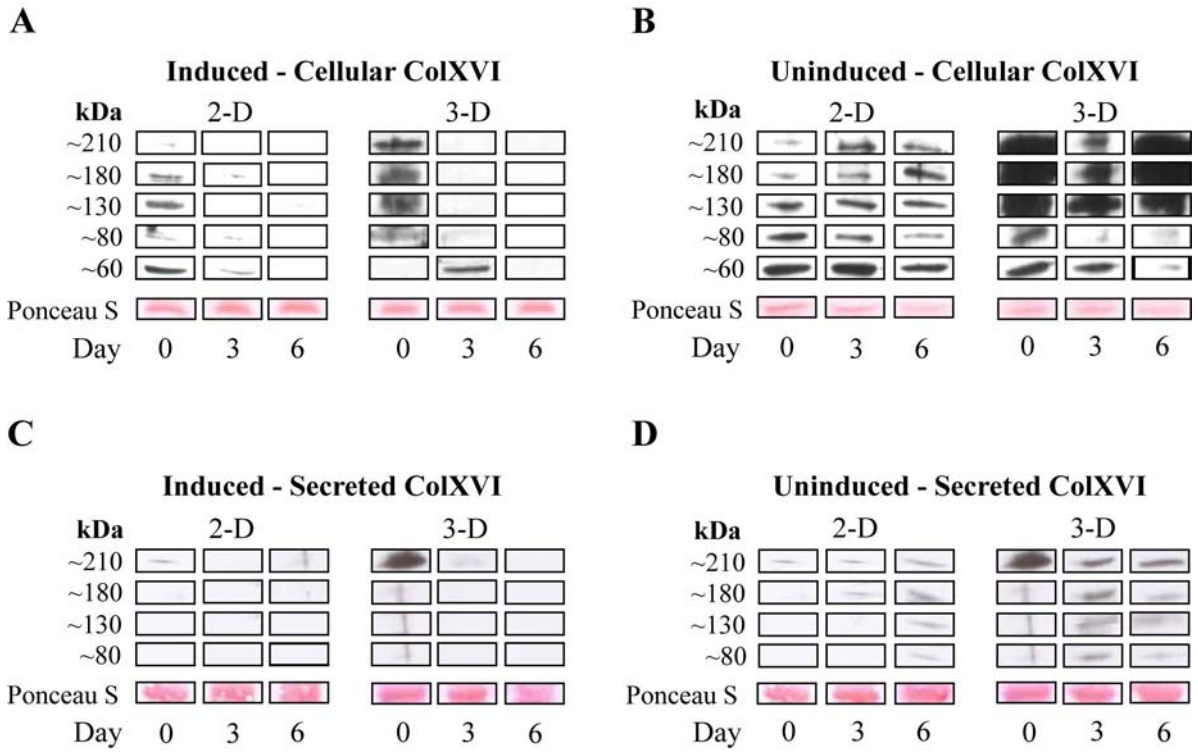

Figure 4: Protein expression of collagen XVI in 3T3-L1 in 2-D and 3-D cultures.
Cell extracts as well as culture medium of induced or uninduced 3T3-L1 were isolated at day 0, 3, and 6. 20 µg total protein per group were separated by SDS-PAGE and transferred to a nitrocellulose membrane. The blots were probed with anti-collagen XVI antibody. **A)** Western blot of cellular collagen XVI after adipogenic induction in 2-D cultures and 3-D spheroids. **B)** Western blot of cellular collagen XVI in 3T3-L1 that were not induced in 2-D and 3-D cultures. **C)** Western blot of secreted collagen XVI after adipogenic induction in 2-D cultures and 3-D spheroids. **D)** Western blot of secreted collagen XVI in 3T3-L1 which were not induced in 2-D and 3-D cultures. Ponceau S staining is shown as control for protein loading. Three independent cell culture experiments were performed; representative data from one experiment is shown (A-D). Abbreviation: ColXVI=collagen XVI.

Additionally, the secretion of collagen XVI into the culture medium was analyzed in 2-D and 3-D (Figure 4 C and D). A small content of secreted protein was detected in 2-D cell culture at day 0 and no secretion was found at later stages of differentiation (Figure 4 C). In contrast,

cells incorporated in spheroids secreted much more collagen XVI at day 0 compared to 2-D culture, but the amount of secreted protein was also diminished during adipose conversion (Figure 4 C). Non-induced preadipocytes also secreted more collagen XVI into the medium in 3-D culture. The secretion gradually decreased up to day 6 of culture in 3-D, whereas in 2-D a slight upregulation was detected (Figure 4 D).

Additionally to the Western blot analyses, the decreased collagen XVI protein expression was confirmed with immunofluorescence staining in 3-D culture. The staining did not work in 2-D due to autofluorescence of the cells in 2-D monolayer culture in contrast to 3-D sections. 3T3-L1 spheroids were induced to differentiate into adipocytes and at day 0, 3, and 6 after induction, cryosections of 3-D spheroids were stained with Alexa Fluor® 555 antibody linked to the anti-collagen XVI antibody. Cryosections of the central region of the spheroid showed a homogeneous distribution of collagen XVI at day 0 which was drastically reduced during differentiation (Figure 5, red fluorescence). Nuclei were counterstained with DAPI (Figure 5, blue fluorescence).

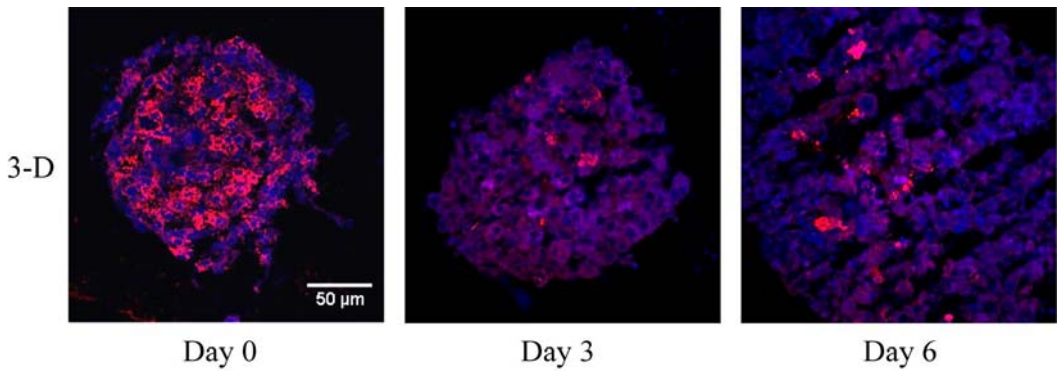

Figure 5: Distribution of collagen XVI in 3-D spheroids during differentiation of adipocytes detected by immunofluorescence. Cryosections from spheroids were stained with anti-collagen XVI antibody (red fluorescence) and additionally counterstained with DAPI (blue fluorescence). Sections from the center area are displayed. Bar=50 µm.

4.3. Gene and protein expression of collagen XVI(α1) during adipogenesis of ADSCs in 2-D and 3-D

In further experiments, we investigated whether the reduced expression of collagen XVI during adipogenic differentiation *in vitro* was specific for 3T3-L1 or was also observed in other adipogenic cell systems such as human ADSCs. Therefore, the gene and protein expression of collagen XVI in adipogenically induced ADSCs were analyzed in 2-D and 3-D cell culture. RNA samples were prepared at day 0, 3, and 10 and the gene expression of collagen XVI(α1) was determined by qRT-PCR analyses (Figure 6 A). A clear

downregulation of collagen XVI(α1) gene expression after adipogenic induction was not detected in 2-D culture of ADSCs in contrast to 3T3-L1, in which this gene was decreased in both 2-D and 3-D (Figure 6 and 3). However, a significantly reduced gene expression of collagen XVI was evident in 3-D spheroids at day 10 after induction compared to day 0 (Figure 6 A). The observation made in 3-D was verified on protein level by Western blot analyses (Figure 6 C). In 2-D, Western blot technique also showed a slight downregulation of collagen XVI at day 10, which was less obvious than in 3-D. Another difference to 3T3-L1 was the finding that collagen XVI proteins were more abundant in 2-D culture compared to 3-D at all time points (Figure 6 C, D). When ADSCs were not induced to undergo adipogenesis the gene as well the protein expression of collagen XVI did not decrease in 2-D culture up to day 10 of cultivation (Figure 6 B, D). The same was observed for protein expression in 3-D culture (Figure 6 D). Only the collagen XVI(α1) gene expression in 3-D was reduced at day 10 (Figure 6 B).

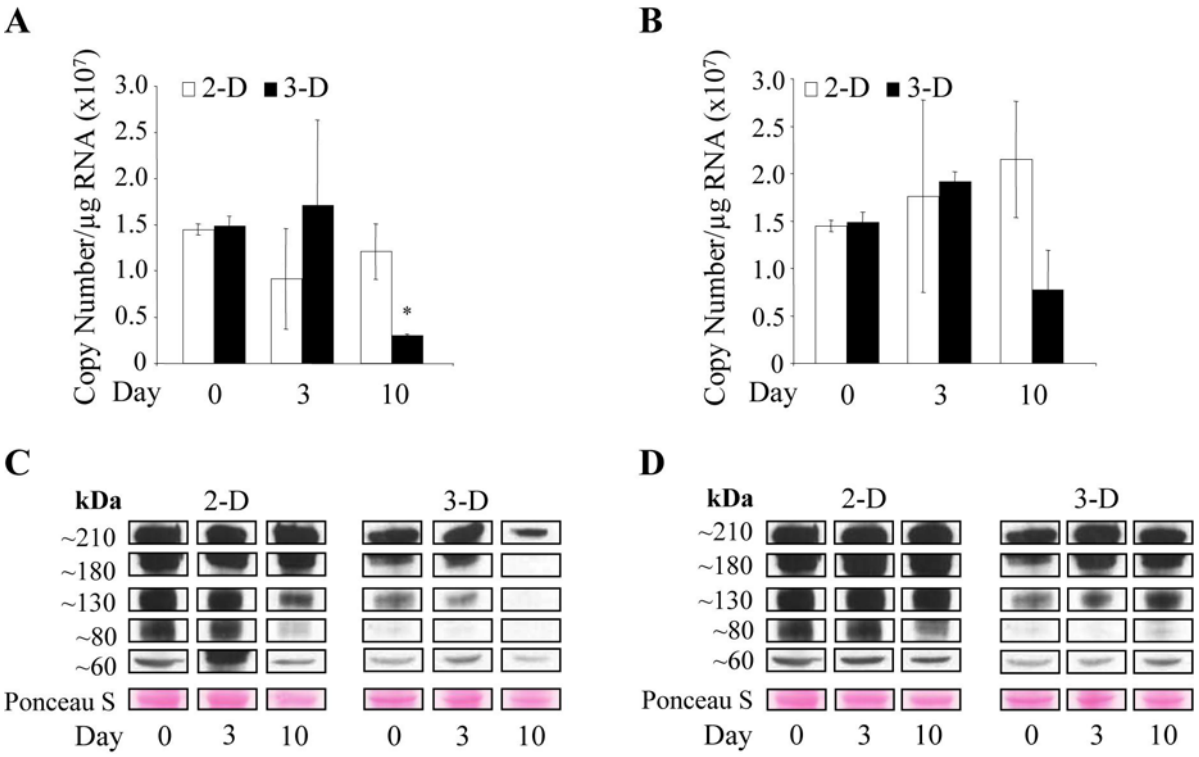

Figure 6: Gene and protein expression of collagen XVI in ADSCs in 2-D and 3-D cultures.
A) qRT-PCR measurements (n=3) of collagen XVI(α1) after adipogenic induction in 2-D cultures and 3-D spheroids. **B)** qRT-PCR measurements of the collagen XVI(α1) gene expression in uninduced ADSCs (n=3). Expression is reported as exact copy numbers of the collagen XVI(α1) gene per µg RNA (A, B). **C)** Western blot of cellular collagen XVI after adipogenic induction in 2-D cultures and 3-D spheroids. **D)** Western blot of cellular collagen XVI in ADSCs that were not induced in 2-D and 3-D cultures. Ponceau S staining is shown as control for protein loading. Three independent cell culture experiments were performed; representative data from one experiment is shown (C, D). * indicates statistically significant differences to the corresponding group at day 0 ($p<0.05$).

4.4. Influence of the adipogenic inducers on gene expression of collagen XVI in 2-D

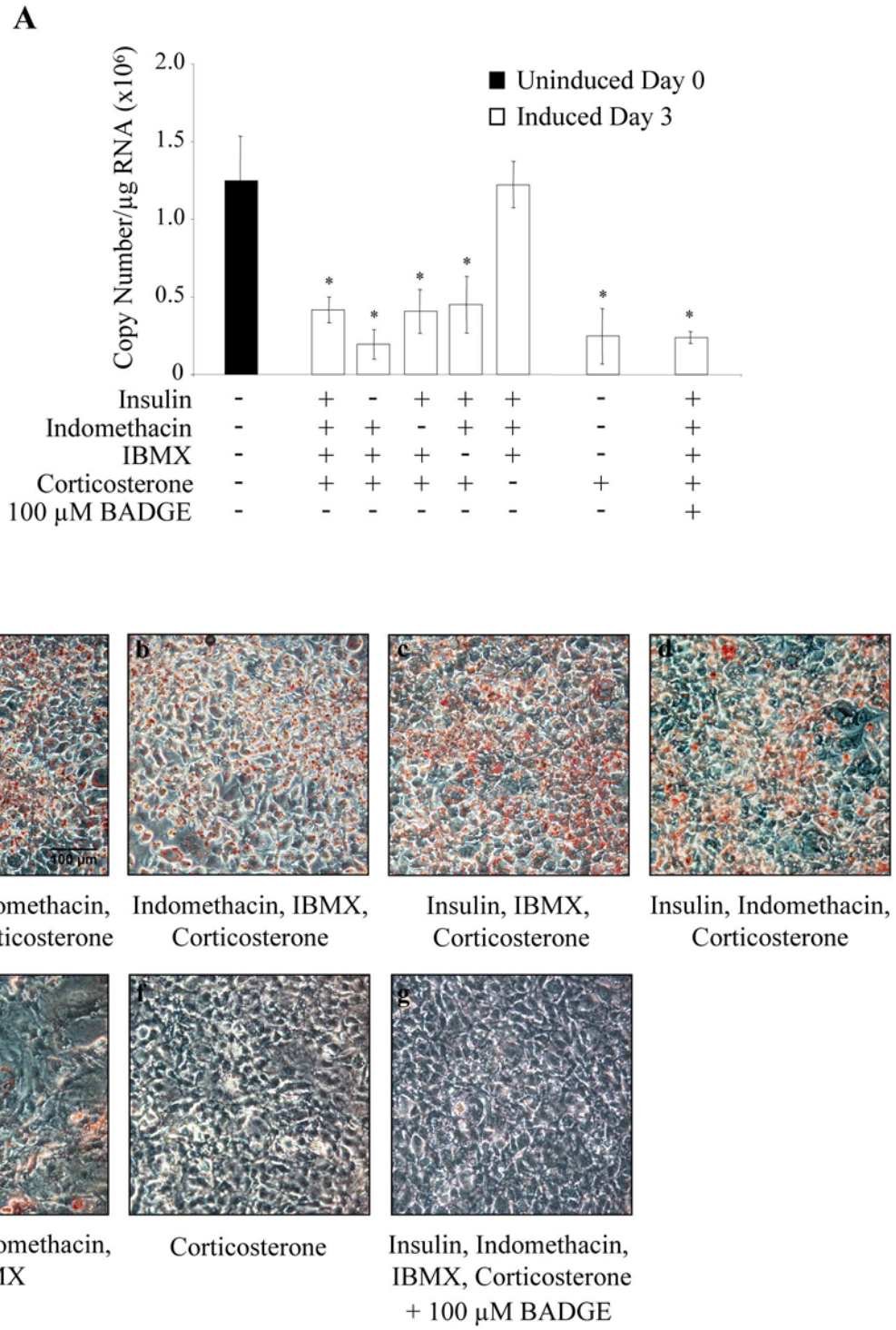

Figure 7: Influence of the adipogenic inducers on gene expression of procollagen XVI(α1). 3T3-L1 preadipocytes were adipogenically induced with differently composed induction cocktails. **A)** qRT-PCR measurements (n=3) of procollagen XVI(α1) at day 3 after induction. * indicates statistically significant differences to the uninduced preadipocytes at day 0 ($p<0.05$). **B)** Oil red O staining of lipid droplets within adipocytes 6 days after adipogenic induction. Bar=100 µm. Three independent cell culture experiments were performed; representative images from one experiment are shown.

To study whether one of the adipogenic inducers has a direct influence on collagen XVI expression, we stimulated the differentiation of 3T3-L1 preadipocytes with different induction media. The control induction medium consisted of the generally used adipogenic cocktail containing insulin, indomethacin, IBMX, and corticosterone. In further experiments, always one of the inducers was eliminated from the medium. At day 3 after induction, qRT-PCR analysis demonstrated that the cocktails containing corticosterone induced a decrease of procollagen XVI(α1) gene expression (Figure 7 A) which was accompanied by adipogenesis as shown by oil red O staining (Figure 7 B, a-d). In contrast, cells induced without corticosterone (i.e., only with insulin, indomethacin, and IBMX) did not downregulate procollagen XVI(α1) mRNA. Adipogenic differentiation was strongly affected in this group (Figure 7 B, e). Therefore, subsequently, preadipocytes were incubated in presence of corticosterone alone. These preadipocytes showed a reduced procollagen XVI(α1) gene expression without differentiating into adipocytes (Figure 7 A and B, f). Finally, bisphenol A diglycidyl ether (BADGE), which is an antagonist of peroxisome proliferator-activated receptor γ (PPARγ), was added to the conventionally used induction medium consisting of the four inducers. BADGE has been experimentally used to inhibit hormone-induced differentiation of 3T3-L1 preadipocytes [49]. Preadipocytes which were incubated with BADGE showed a reduced procollagen XVI(α1) gene expression and did not differentiate into adipocytes (Figure 7 A and B, g).

It can be deduced that downregulation of collagen XVI was not sufficient to result in adipogenic differentiation. Nevertheless, from these results, it is still possible that collagen XVI has a functional role in adipogenesis and has to be downregulated in order that adipocyte development proceeds.

4.5. Differentiation of 3T3-L1 on different collagen substrata

A possible functional role of collagen XVI on *in vitro* adipogenesis was initially investigated by the exogenous addition of recombinant collagen XVI protein. Adipogenic differentiation of 3T3-L1 cells was compared for different collagen substrata, i.e., collagen I, collagen IV, and collagen XVI relative to BSA-coated tissue-culture plastic as control. Collagen I and IV were also used as controls to eliminate unspecific effects of collagens. Collagen IV is the most abundant collagen in adipocytes and is known to be increased during adipogenesis [19,21]. In contrast, collagen I is downregulated during adipogenic differentiation [21]. Our coating experiments revealed that the extent of adipogenesis after induction with the usual hormonal cocktail was independent of the composition of the substrate. In all groups,

differentiation was evident in the accumulation of TG within intracellular lipid droplets as detected by oil red O staining (Figure 8 A) and TG measurements (Figure 8 B).

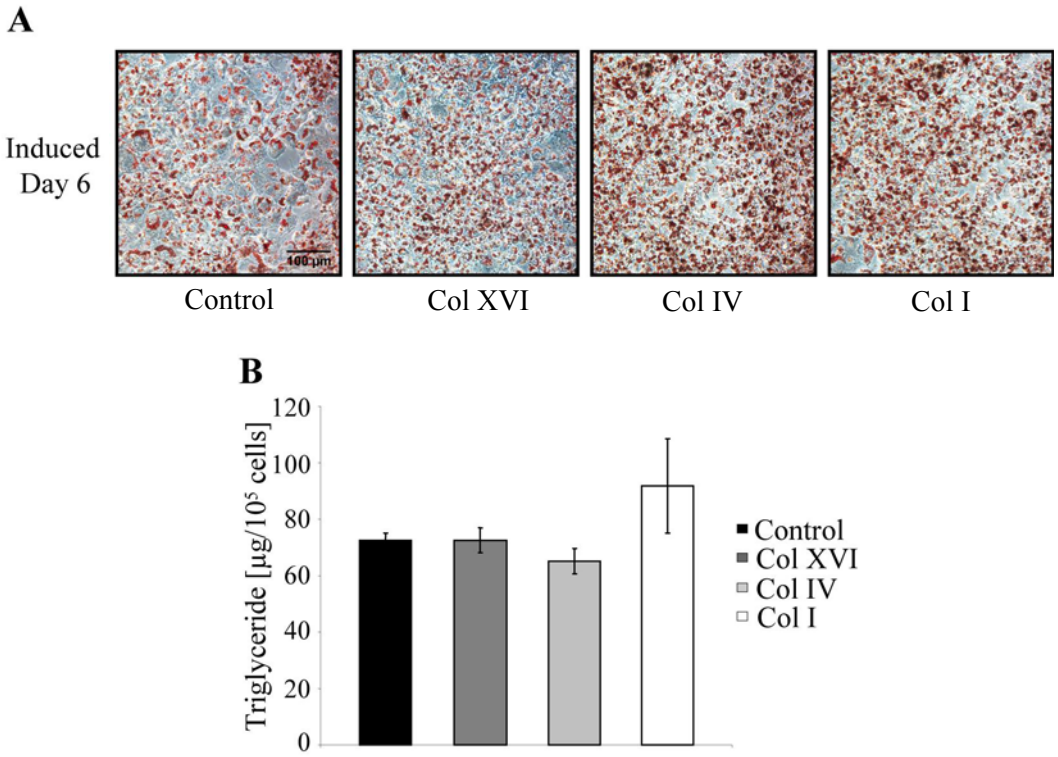

Figure 8: Differentiation of 3T3-L1 on different collagen substrata in 2-D culture. Preadipocytes were seeded on different collagen-coated plates: collagen I, IV, and XVI. BSA-coated plastics served as control. TG accumulation was determined at day 6 after adipogenic induction. **A)** Oil red O staining of lipid droplets within adipocytes 6 days after adipogenic induction. Bar=100 µm. Two independent cell culture experiments were performed; representative images from one experiment are shown. **B)** Quantification of intracellular TG content (n=3). TG contents were normalized to cell numbers.

4.6. Effect of collagen XVI(α1) overexpression on *in vitro* differentiation of 3T3-L1 preadipocytes

To further investigate if collagen XVI has a functional role in the adipogenesis of 3T3-L1 preadipocytes, we generated a stably transfected 3T3-L1 cell line overexpressing human collagen XVI(α1). We hypothesized that the downregulation of collagen XVI is essential for the adipogenic process and, thus, the overexpression of this ECM component would prevent the differentiation into adipocytes. 3T3-L1 preadipocytes were transfected with the vector pCEP-PU-BM40SP modified by insertion of collagen XVI(α1) [26] using the Lipofectamine 2000 reagent and transfectants were selected with puromycin. The success of the transfection procedure was verified by qRT-PCR measurements. In cells overexpressing collagen

XVI(α1), six-fold increased mRNA levels were monitored by qRT-PCR as compared to non-transfected cells referred to as control (Figure 9 A).

In the following, we performed first experiments to investigate a possible effect of the collagen XVI overexpression on the adipocyte differentiation *in vitro*. Non-transfected 3T3-L1 referred to as control and 3T3-L1 stably overexpressing collagen XVI were induced to undergo adipogenesis. Six days after induction, the intracellular lipid content was higher in the control cells as compared to the collagen XVI(α1) overexpressing cells as detected by oil red O staining (Figure 9 B). Quantification of the TG content confirmed the impaired adipogenesis resulted from overexpression of collagen XVI (Figure 9 C).

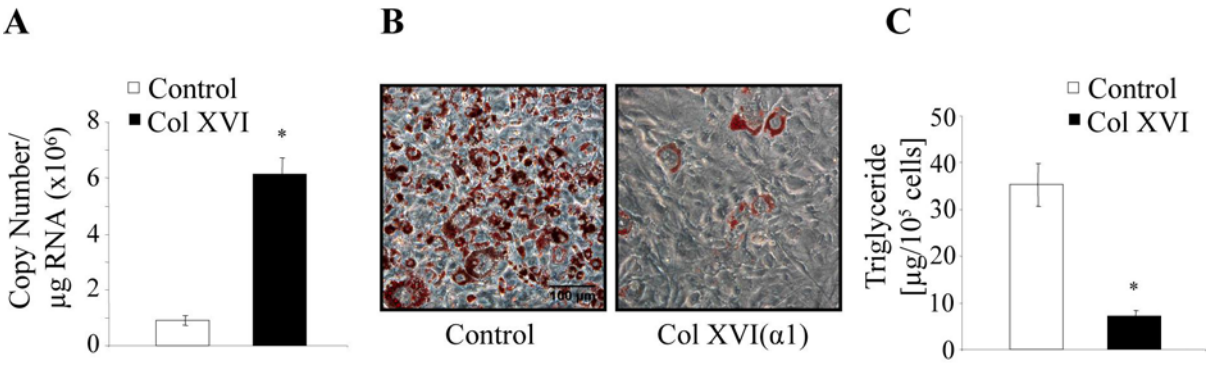

Figure 9: Effect of collagen XVI(α1) overexpression on *in vitro* differentiation of 3T3-L1 preadipocytes. 3T3-L1 preadipocytes were stably transfected with pCEP-PU-BM40SP modified by insertion of human collagen XVI(α1). Non-transfected 3T3-L1 preadipocytes served as control.
A) The overexpression of collagen XVI mRNA was verified by qRT-PCR. **B)** Oil red O staining of lipid droplets within adipocytes is shown for non-transfected preadipocytes (left) and for cells overexpressing collagen XVI(α1) (right) at day 6 after adipogenic induction. Bar=100 µm. Three independent cell culture experiments were performed; representative images from one experiment are shown. **C)** Quantification of intracellular TG content in control cells and in cells overexpressing collagen XVI(α1) at day 6 after adipogenic induction (n=3). TG contents were normalized to the cell number. * indicates statistically significant differences to the control group ($p<0.05$).

5. Discussion

Besides the changes directly related to the intracellular increase in lipid synthesis, alterations also occur in the ECM surrounding the cells during adipocyte differentiation. The ECM, whose main components are collagens, is continuously remodeled during the adipogenic process. Studies on collagen matrix turnover during adipose conversion have been focused on fibrillar collagens, i.e., type I, III, and V as well as collagen IV and VI, whose expressions are regulated in adipogenesis [19,21,24]. However, the association of the major matrix molecules like fibrillar collagens is organized by specific sets of minor components, e.g., FACIT

collagens. Members of this collagen family act as adapter molecules interconnecting macromolecular networks. The presence and distribution of FACIT in skin, cornea, and cartilage have been reported previously [50]. So far, FACITs are not well documented in adipose tissue. Apart from one study in which collagen XVI was observed around adipocytes by immunofluorescence staining of adult mouse skin sections [27], no reports exist connecting type XVI collagen and adipose tissue. Changes in collagen type XVI expression during adipocyte differentiation have not been described previously at all.

In the current study, for the first time, we examined the expression of collagen type XVI mRNA and protein in 3T3-L1 and ADSCs during the development into adipocytes after adipogenic induction *in vitro*. 3T3-L1 preadipocytes constitutively expressed procollagen XVI(α1) mRNA and upon differentiation into adipocytes, the expression level distinctly decreased as detected by qRT-PCR analyses (Figure 3 B, Page 148). In addition, the reduction of procollagen XVI mRNAs was associated with parallel decrease in protein expression of collagen XVI shown by Western blot analyses and immunofluorescence staining (Figure 4 A and 5, Page 150 and 151). Cells which were not adipogenically induced did not exhibit a downregulation of collagen XVI (Figure 4 B, Page 150). ADSCs also showed a downregulation of collagen XVI during *in vitro* adipogenesis (Figure 6, Page 152). Interestingly, in ADSCs, in which adipogenesis progresses slower than in 3T3-L1, the collagen XVI downregulation was also observed at a later time point as compared to 3T3-L1.

Comparing the 2-D and 3-D culture systems, differences in the expression pattern of collagen XVI were detected in 3T3-L1. In 3-D spheroids, collagen XVI gene expression was strongly diminished in preadipocytes at day 0 compared to 2-D culture (Figure 3 B, Page 148). Interestingly, contrary results were determined on protein level. Here, collagen XVI was more expressed in preadipocytes cultured in 3-D spheroids and, subsequently, the downregulation was more obvious in 3-D culture compared to 2-D culture (Figure 4 A, Page 150). In contrast to 3-D spheroids, in which the cells were in close contact from the beginning of spheroid formation occurring few hours after seeding, in 2-D monolayer, the cells were not confluent shortly after seeding, but grew to confluence within two days up to the time of induction (referred to as day 0). During this time, the cells proliferated more rapidly in 2-D compared to 3-D culture (data not shown). Presumably, these different conditions influence the collagen XVI gene expression. Furthermore, cells in 2-D culture do not generate the complex ECM organization presented in a 3-D tissue-like context. Consequently, it is assumed that cells in 2-D monolayer synthesize and secrete a limited number of matrix proteins including collagen XVI as detected by Western blot analyses (Figure 4 A, Page 150). The differential results in

2-D and 3-D point out the presence of differences between the two culture systems and the importance of a 3-D tissue-like model system which likely resembles *in vivo* conditions more closely for studying cell-matrix interactions. 3-D systems offer a better representation of the complexity of the *in vivo* microenvironment which influences various essential cell processes including adipocyte differentiation [10,35,51-53]. This microenvironment also involves cell adhesion complexes including several integrins which are of pivotal physiological relevance since they connect cells with specialized fibrils and, thus, contribute to the matrix organization [27]. Few studies implicated integrins in adipogenesis [54-56]. Furthermore, it was reported that collagen XVI interacts with integrin α1β1 and α2 β1 [27,33]. Thus, in future studies, it would be interesting to investigate possible molecular interactions of collagen XVI with integrins with regard to adipogenic differentiation, especially in a 3-D coherent tissue-like context.

Further experiments in this study revealed that corticosterone, one of the adipogenic inducers, had a reducing effect on procollagen XVI(α1) expression and apparently was responsible for the downregulation of this type of procollagen (Figure 7, Page 153). Pantoja *et al.* have revealed that dexamethasone, a synthetic glucocorticoid, modulated the expression of genes that participate in ECM processes and the transforming growth factor ß (TGF-ß), WNT (wingless/Int), and MAP kinase pathways [57]. Furthermore, it was reported that glucocorticoids inhibited the TGF-β-induced expression of ECM proteins such as fibronectin [58] and collagen [59,60]. It was shown that the glucocorticoid receptor repressed TGF-β signaling by directly targeting smad 3 and 4 proteins [61]. Smad proteins are signaling effectors of TGF-β and regulate the transcription by binding to DNA and interaction with other transcription factors. Furthermore, it was reported that collagen XVI expression was increased by exogenous addition of TGF-β [62]. In our study, it may be that after induction of 3T3-Ll preadipocytes with a glucocorticoid the corresponding receptor inhibited the TGF-β signaling pathway by interacting with smads. In turn, it is supposed that the inhibition of the TGF-β signaling by glucocorticoids repressed the collagen XVI transcription. This hypothesis has to be further investigated in future studies.

To date, we have not clarified the consequence of collagen XVI downregulation on adipogenesis. From the experiments with differently composed induction media (Figure 7, Page 153), it can be deduced that downregulation of collagen XVI was not sufficient to result in adipocyte differentiation. It is possible that the collagen XVI downregulation introduced by adipogenic signals is a side effect of induction which does not influence the adipogenic

process. Thus, it would be interesting to examine whether collagen XVI is downregulated during adipocyte differentiation which is induced independently of any glucocorticoids.

Nevertheless, it is very well still possible that collagen XVI plays a functional role in adipogenesis and has to be downregulated for adipocyte maturation. A possible functional role of the downregulation of collagen XVI in adipogenesis was investigated by overexpression studies as well as exogenous addition of collagen XVI. The exogenous addition of collagen XVI by coating the bottom of culture plates did not influence the morphology and development of adipocytes (Figure 8, Page 155). Qualitative and quantitative assessment using oil red O staining and measurements of the TG content showed that preadipocytes grown on collagen XVI coated or on uncoated plates differentiated into adipocytes at the same rate. Collagen I and IV substrates served as controls, but again, no significant changes in the differentiation rate were detectable. The effect was not amplified by an increase in coating density (50 µg/ml) of the single collagen types (data not shown). It is assumed that the used hormonal induction cocktail was sufficient to induce adipocyte differentiation so that the differentiation of 3T3-L1 adipocytes always proceeded to maximal level. Thereby, responses of cells to altered conditions such as different coating substrates were potentially impaired. For this reason, we also investigated adipogenic self-induction of the preadipocytes which occurs spontaneously, i.e., without adding any inducing substances when confluent cells are further cultured. However, also under these conditions, exogenous collagen XVI did not influence adipocyte differentiation (data not shown). Thus, the abundant presence of collagen XVI in the surrounding of the cells did not influence adipocyte differentiation. Presumably, the matrix protein has to be correctly inserted into the ECM network in order to cause significant effects.

In overexpression studies, 3T3-L1 preadipocytes were stably transfected with collagen XVI(α1). Collagen XVI(α1) overexpression in 3T3-L1 preadipocytes had a considerable effect on their differentiation into mature adipocytes. It was shown that only a minor fraction of the cells were able to differentiate into adipocytes compared to non-transfected cells (Figure 9 B, Page 156). In further experiments it has to be investigated whether the reduced adipocyte differentiation was caused by the overexpression of collagen XVI(α1) or if it was a phenomenon of the transfection procedure or the vector itself. In this study, we used non-transfected cells as control, however, the transfection using an empty vector as control is inevitable to exclude that the effect resulted from the transfection procedure, even if we do not expect it to affect the results. Many published overexpression studies have shown that various vectors did not impact the differentiation of 3T3-L1 preadipocytes into adipocytes

including the activation of key transcription factors [63-66]. If in experiments with an empty vector control it can be verified that expression of collagen XVI prevents adipocyte development, in further experiments the nature of the functional role of collagen XVI in adipogenesis, i.e., in intracellular or extracellular events, may be investigated.

In summary, this study showed for the first time that collagen XVI was regulated in hormonally induced adipogenesis. Thereby, corticosterone induced a downregulation of procollagen XVI(α1). Preliminary overexpression experiments suggest a possible functional role of collagen XVI in *in vitro* adipogenesis of 3T3-L1. Further analyses will be required for a better understanding of the underlying mechanism of regulation and its biological significance to clarify the role of this FACIT collagen member in adipogenesis.

References

1. Rosen E D, Spiegelman B M. Molecular regulation of adipogenesis. *Annu.Rev.Cell Dev.Biol.* 2000; **16:** 145-171.
2. Rosen E D, Walkey C J, Puigserver P, Spiegelman B M. Transcriptional regulation of adipogenesis. *Genes Dev.* 2000; **14:** 1293-1307.
3. Gregoire F M, Smas C M, Sul H S. Understanding adipocyte differentiation. *Physiol Rev.* 1998; **78:** 783-809.
4. Feve B. Adipogenesis: cellular and molecular aspects. *Best.Pract.Res.Clin.Endocrinol. Metab* 2005; **19:** 483-499.
5. Rodriguez Fernandez J L, Ben Ze'ev A. Regulation of fibronectin, integrin and cytoskeleton expression in differentiating adipocytes: inhibition by extracellular matrix and polylysine. *Differentiation* 1989; **42:** 65-74.
6. Smas C M, Sul H S. Control of adipocyte differentiation. *Biochem.J.* 1995; **309 (Pt 3):** 697-710.
7. Abbott A. Cell culture: biology's new dimension. *Nature* 2003; **424:** 870-872.
8. Cukierman E, Pankov R, Stevens D R, Yamada K M. Taking cell-matrix adhesions to the third dimension. *Science* 2001; **294:** 1708-1712.
9. Chun T H, Hotary K B, Sabeh F, Saltiel A R, Allen E D, Weiss S J. A pericellular collagenase directs the 3-dimensional development of white adipose tissue. *Cell* 2006; **125:** 577-591.
10. Green J A, Yamada K M. Three-dimensional microenvironments modulate fibroblast signaling responses. *Adv.Drug Deliv.Rev.* 2007; **59:** 1293-1298.
11. Pedersen J A, Swartz M A. Mechanobiology in the third dimension. *Ann.Biomed.Eng* 2005; **33:** 1469-1490.
12. Rosen E D, MacDougald O A. Adipocyte differentiation from the inside out. *Nat.Rev.Mol.Cell Biol.* 2006; **7:** 885-896.
13. Wu Z, Puigserver P, Spiegelman B M. Transcriptional activation of adipogenesis. *Curr.Opin.Cell Biol.* 1999; **11:** 689-694.
14. Mariman E C, Wang P. Adipocyte extracellular matrix composition, dynamics and role in obesity. *Cell Mol.Life Sci.* 2010.
15. Lijnen H R, Maquoi E, Hansen L B, Van Hoef B, Frederix L, Collen D. Matrix metalloproteinase inhibition impairs adipose tissue development in mice. *Arterioscler.Thromb.Vasc.Biol.* 2002; **22:** 374-379.
16. Chavey C, Mari B, Monthouel M N, Bonnafous S, Anglard P, Van Obberghen E, Tartare-Deckert S. Matrix metalloproteinases are differentially expressed in adipose tissue during obesity and modulate adipocyte differentiation. *J.Biol.Chem.* 2003; **278:** 11888-11896.
17. Maquoi E, Munaut C, Colige A, Collen D, Lijnen H R. Modulation of adipose tissue expression of murine matrix metalloproteinases and their tissue inhibitors with obesity. *Diabetes* 2002; **51:** 1093-1101.
18. Kuri-Harcuch W, Arguello C, Marsch-Moreno M. Extracellular matrix production by mouse 3T3-F442A cells during adipose differentiation in culture. *Differentiation* 1984; **28:** 173-178.
19. Aratani Y, Kitagawa Y. Enhanced synthesis and secretion of type IV collagen and entactin during adipose conversion of 3T3-L1 cells and production of unorthodox

laminin complex. *J.Biol.Chem.* 1988; **263:** 16163-16169.

20. Ono M, Aratani Y, Kitagawa I, Kitagawa Y. Ascorbic-Acid Phosphate Stimulates Type-Iv Collagen-Synthesis and Accelerates Adipose Conversion of 3T3-L1 Cells. *Experimental Cell Research* 1990; **187:** 309-314.
21. Weiner F R, Shah A, Smith P J, Rubin C S, Zern M A. Regulation of collagen gene expression in 3T3-L1 cells. Effects of adipocyte differentiation and tumor necrosis factor alpha. *Biochemistry* 1989; **28:** 4094-4099.
22. Antras J, Hilliou F, Redziniak G, Pairault J. Decreased biosynthesis of actin and cellular fibronectin during adipose conversion of 3T3-F442A cells. Reorganization of the cytoarchitecture and extracellular matrix fibronectin. *Biol.Cell* 1989; **66:** 247-254.
23. Green H, Meuth M. An established pre-adipose cell line and its differentiation in culture. *Cell* 1974; **3:** 127-133.
24. Nakajima I, Muroya S, Tanabe R, Chikuni K. Extracellular matrix development during differentiation into adipocytes with a unique increase in type V and VI collagen. *Biol.Cell* 2002; **94:** 197-203.
25. Grassel S, Timpl R, Tan E M, Chu M L. Biosynthesis and processing of type XVI collagen in human fibroblasts and smooth muscle cells. *Eur.J.Biochem.* 1996; **242:** 576-584.
26. Kassner A, Tiedemann K, Notbohm H, Ludwig T, Morgelin M, Reinhardt D P, Chu M L, Bruckner P, Grassel S. Molecular structure and interaction of recombinant human type XVI collagen. *J.Mol.Biol.* 2004; **339:** 835-853.
27. Eble J A, Kassner A, Niland S, Morgelin M, Grifka J, Grassel S. Collagen XVI harbors an integrin alpha1 beta1 recognition site in its C-terminal domains. *J.Biol.Chem.* 2006; **281:** 25745-25756.
28. Pan T C, Zhang R Z, Mattei M G, Timpl R, Chu M L. Cloning and Chromosomal Location of Human Alpha-1(Xvi) Collagen. *Proceedings of the National Academy of Sciences of the United States of America* 1992; **89:** 6565-6569.
29. Grassel S, Unsold C, Schacke H, Bruckner-Tuderman L, Bruckner P. Collagen XVI is expressed by human dermal fibroblasts and keratinocytes and is associated with the microfibrillar apparatus in the upper papillary dermis. *Matrix Biol.* 1999; **18:** 309-317.
30. Kassner A, Hansen U, Miosge N, Reinhardt D P, Aigner T, Bruckner-Tuderman L, Bruckner P, Grassel S. Discrete integration of collagen XVI into tissue-specific collagen fibrils or beaded microfibrils. *Matrix Biol.* 2003; **22:** 131-143.
31. Hubert T, Grimal S, Ratzinger S, Mechaly I, Grassel S, Fichard-Carroll A. Collagen XVI is a neural component of the developing and regenerating dorsal root ganglia extracellular matrix. *Matrix Biol.* 2007; **26:** 206-210.
32. Senner V, Ratzinger S, Mertsch S, Grassel S, Paulus W. Collagen XVI expression is upregulated in glioblastomas and promotes tumor cell adhesion. *FEBS Lett.* 2008; **582:** 3293-3300.
33. Ratzinger S, Eble J A, Pasoldt A, Opolka A, Rogler G, Grifka J, Grassel S. Collagen XVI induces formation of focal contacts on intestinal myofibroblasts isolated from the normal and inflamed intestinal tract. *Matrix Biol.* 2009.
34. Fischbach C, Spruss T, Weiser B, Neubauer M, Becker C, Hacker M, Goepferich A, Blunk T. Generation of mature fat pads in vitro and in vivo utilizing 3-D long-term culture of 3T3-L1 preadipocytes. *Experimental Cell Research* 2004; **300:** 54-64.
35. Fischbach C, Seufert J, Staiger H, Hacker M, Neubauer M, Goepferich A, Blunk T. Three-dimensional in vitro model of adipogenesis: Comparison of culture conditions.

Tissue Engineering 2004; **10:** 215-229.

36. Santini M T, Rainaldi G. Three-dimensional spheroid model in tumor biology. *Pathobiology* 1999; **67:** 148-157.
37. Weiser, B. Adipose Tissue Engineering - Precultivation Strategies towards Clinical Applications & A Novel 3-D Model of Adipogenesis for Basic Research. *Ph.D. thesis* 2008. University of Regensburg, Regensburg, Germany.
38. Kunz-Schughart L A, Schroeder J A, Wondrak M, Van Rey F, Lehle K, Hofstaedter F, Wheatley D N. Potential of fibroblasts to regulate the formation of three-dimensional vessel-like structures from endothelial cells in vitro. *American Journal of Physiology-Cell Physiology* 2006; **290:** C1385-C1398.
39. Kohfeldt E, Gohring W, Mayer U, Zweckstetter M, Holak T A, Chu M L, Timpl R. Conversion of the Kunitz-type module of collagen VI into a highly active trypsin inhibitor by site-directed mutagenesis. *Eur.J.Biochem.* 1996; **238:** 333-340.
40. Kohfeldt E, Maurer P, Vannahme C, Timpl R. Properties of the extracellular calcium binding module of the proteoglycan testican. *FEBS Lett.* 1997; **414:** 557-561.
41. Smyth N, Odenthal U, Merkl B, Paulsson M. Eukaryotic expression and purification of recombinant extracellular matrix proteins carrying the Strep II tag. *Methods Mol.Biol.* 2000; **139:** 49-57.
42. Ramirez-Zacarias J L, Castro-Munozledo F, Kuri-Harcuch W. Quantitation of adipose conversion and triglycerides by staining intracytoplasmic lipids with Oil red O. *Histochemistry* 1992; **97:** 493-497.
43. Romeis B. *Mikroskopische Technik*. Urban & Schwarzenberg: Munich, Vienna, Baltimore, 1989.
44. Kim Y J, Sah R L, Doong J Y, Grodzinsky A J. Fluorometric assay of DNA in cartilage explants using Hoechst 33258. *Anal.Biochem.* 1988; **174:** 168-176.
45. Marshall O J. PerlPrimer: cross-platform, graphical primer design for standard, bisulphite and real-time PCR. *Bioinformatics.* 2004; **20:** 2471-2472.
46. Bradford M M. A rapid and sensitive method for the quantitation of microgram quantities of protein utilizing the principle of protein-dye binding. *Anal.Biochem.* 1976; **72:** 248-254.
47. Laemmli U K. Cleavage of structural proteins during the assembly of the head of bacteriophage T4. *Nature* 1970; **227:** 680-685.
48. Tillet E, Mann K, Nischt R, Pan T C, Chu M L, Timpl R. Recombinant Analysis of Human Alpha-1(Xvi) Collagen - Evidence for Processing of the N-Terminal Globular Domain. *European Journal of Biochemistry* 1995; **228:** 160-168.
49. Wright H M, Clish C B, Mikami T, Hauser S, Yanagi K, Hiramatsu R, Serhan C N, Spiegelman B M. A synthetic antagonist for the peroxisome proliferator-activated receptor gamma inhibits adipocyte differentiation. *J.Biol.Chem.* 2000; **275:** 1873-1877.
50. Gelse K, Poschl E, Aigner T. Collagens--structure, function, and biosynthesis. *Adv.Drug Deliv.Rev.* 2003; **55:** 1531-1546.
51. Mazzoleni G, Di Lorenzo D, Steimberg N. Modelling tissues in 3D: the next future of pharmaco-toxicology and food research? *Genes Nutr.* 2009; **4:** 13-22.
52. Kang X, Xie Y, Kniss D A. Adipose tissue model using three-dimensional cultivation of preadipocytes seeded onto fibrous polymer scaffolds. *Tissue Eng* 2005; **11:** 458-468.

53. Kang X, Xie Y, Powell H M, James L L, Belury M A, Lannutti J J, Kniss D A. Adipogenesis of murine embryonic stem cells in a three-dimensional culture system using electrospun polymer scaffolds. *Biomaterials* 2007; **28:** 450-458.

54. Kawaguchi N, Sundberg C, Kveiborg M, Moghadaszadeh B, Asmar M, Dietrich N, Thodeti C K, Nielsen F C, Moller P, Mercurio A M, Albrechtsen R, Wewer U M. ADAM12 induces actin cytoskeleton and extracellular matrix reorganization during early adipocyte differentiation by regulating beta1 integrin function. *J.Cell Sci.* 2003; **116:** 3893-3904.

55. Liu J, DeYoung S M, Zhang M, Zhang M, Cheng A, Saltiel A R. Changes in integrin expression during adipocyte differentiation. *Cell Metabolism* 2005; **2:** 165-177.

56. Farnier C, Krief S, Blache M, Diot-Dupuy F, Mory G, Ferre P, Bazin R. Adipocyte functions are modulated by cell size change: potential involvement of an integrin/ERK signalling pathway. *Int.J.Obes.Relat Metab Disord.* 2003; **27:** 1178-1186.

57. Pantoja C, Huff J T, Yamamoto K R. Glucocorticoid Signaling Defines a Novel Commitment State during Adipogenesis In Vitro. *Molecular Biology of the Cell* 2008; **19:** 4032-4041.

58. Guller S, Wozniak R, Kong L, Lockwood C J. Opposing Actions of Transforming Growth-Factor-Beta and Glucocorticoids in the Regulation of Fibronectin Expression in the Human Placenta. *Journal of Clinical Endocrinology & Metabolism* 1995; **80:** 3273-3278.

59. Slavin J, Unemori E, Hunt T K, Amento E. Transforming Growth-Factor-Beta (Tgf-Beta) and Dexamethasone Have Direct Opposing Effects on Collagen-Metabolism in Low Passage Human Dermal Fibroblasts In-Vitro. *Growth Factors* 1994; **11:** 205-213.

60. Meisler N, Keefer K A, Ehrlich H P, Yager D R, MyersParrelli J, Cutroneo K R. Dexamethasone abrogates the fibrogenic effect of transforming growth factor-beta in rat granuloma and granulation tissue fibroblasts. *Journal of Investigative Dermatology* 1997; **108:** 285-289.

61. Song C Z, Tian X, Gelehrter T D. Glucocorticoid receptor inhibits transforming growth factor-beta signaling by directly targeting the transcriptional activation function of Smad3. *Proceedings of the National Academy of Sciences of the United States of America* 1999; **96:** 11776-11781.

62. Grassel S, Tan E M L, Timpl R, Chu M L. Collagen type XVI expression is modulated by basic fibroblast growth factor and transforming growth factor-beta. *Febs Letters* 1998; **436:** 197-201.

63. Mandrup S, Sorensen R V, Helledie T, Nohr J, Baldursson T, Gram C, Knudsen J, Kristiansen K. Inhibition of 3T3-L1 adipocyte differentiation by expression of acyl-CoA-binding protein antisense RNA. *Journal of Biological Chemistry* 1998; **273:** 23897-23903.

64. Lin F T, Lane M D. Antisense Ccaat Enhancer-Binding Protein Rna Suppresses Coordinate Gene-Expression and Triglyceride Accumulation During Differentiation of 3T3-L1 Preadipocytes. *Genes & Development* 1992; **6:** 533-544.

65. Wolfrum C, Shih D Q, Kuwajima S, Norris A W, Kahn C R, Stoffel M. Role of Foxa-2 in adipocyte metabolism and differentiation. *Journal of Clinical Investigation* 2003; **112:** 345-356.

66. Pierantoni G M, Battista S, Pentimalli F, Fedele M, Visone R, Federico A, Santoro M, Viglietto G, Fusco A. A truncated HMGA1 gene induces proliferation of the 3T3-L1 pre-adipocytic cells: a model of human lipomas. *Carcinogenesis* 2003; **24:** 1861-1869.

Chapter 7

Poly(ethylene glycol)-based Hydrogels for Adipose Tissue Engineering

Published in parts in: Biomaterials, 31(14), 3957-66, 2010.

1. Abstract

Adipose tissue engineering is a promising strategy to augment soft tissue defects in many reconstructive, corrective, and cosmetic indications. Successful engineering of adipose tissue requires suitable biomaterials that guarantee adipocyte function and differentiation. For these purposes, our group recently developed *in situ* forming, poly(ethylene glycol) (PEG)-based hydrogels that can be easily functionalized with degradation sites and various other factors, such as adhesion peptides or growth factors.

In the present study, the suitability of the developed hydrogels for adipose tissue engineering was investigated by seeding them with 3T3-L1 preadipocytes. By determining the intracellular triglyceride (TG) content, we investigated the influence of substrate stiffness, adhesiveness, and degradability on the differentiation of adipocytes. Compared to conventional two-dimensional (2-D) cell culture, the adipocytes encapsulated in hydrogels accumulated higher TG amounts. Further increasing the gel strength resulted in reduced TG accumulation; gel functionalization with the laminin-derived adhesion peptide Cys-Asp-Pro-Gly-Tyr-Ile-Gly-Ser-Arg (YIGSR) enhanced the lipid synthesis of encapsulated adipocytes. Long-term *in vitro* studies revealed that enzymatically degradable hydrogels promoted the formation of coherent adipose tissue-like structures characterized by many mature unilocular adipocytes.

In conclusion, the developed biomimetic PEG hydrogels provide an appropriate environment for 3T3-L1 cells to differentiate into adipocytes and are, therefore, suggested as a promising new biomaterial for adipose tissue engineering.

2. Introduction

Adipose tissue engineering aims at the reconstruction of adipose tissue by generating suitable grafts, which must be equivalent to native adipose tissue regarding its composition and biological function. Engineered adipose tissue equivalents are increasingly acknowledged as a possible alternative in plastic and reconstructive surgery to augment soft tissue defects after tumor resection, deep burns, severe trauma or congenital defects. However, despite the increasing clinical demand for suitable tissue substitutes, none of the current approaches has proven to be ideal for adipose tissue reconstruction. Low graft survival and necrosis due to insufficient vascularization accompanied with fibrous tissue invasion and formation of fatty cysts are widely observed problems [1-3]. To overcome these limitations and guarantee a successful adipose tissue development, the scaffold is an essential factor and has to be optimized. An appropriate scaffolding material must be biocompatible, support the formation of functional tissue, and demonstrate considerable mechanical stability to allow for successful integration of the newly formed tissue into the surrounding host tissue [4]. Thereby, the mechanical properties of the scaffold should resemble *in vivo* adipose tissue as closely as possible. Thus, very rigid scaffolds are not suitable materials to augment soft tissues. However, PEG-based hydrogels are proposed to be an appropriate alternative for adipose tissue engineering [5-11]. These hydrophilic polymer networks absorb large amounts of water enabling the unrestricted diffusion of low molecular weight nutrients and metabolites [12]. Furthermore, the biocompatible hydrogels provide tissue-forming adipocytes with an environment mimicking the native extracellular matrix (ECM) [8,13-16]. Another important characteristic of scaffolding materials are their degradability. Current tissue engineering strategies are based on biodegradable cell carriers which provide transient mechanical support until cells have produced their own ECM and developed new tissue structures that are ideally integrated into the host tissue. Thus, the degradation rate has to be adapted to the progression of tissue formation [14,17]. Since the most synthetic hydrogels are biologically inert, the incorporation of certain peptide sequences, such as collagenase-sensitive peptides, is required to render the resulting hydrogels susceptible to proteolytic breakdown. Lutolf and coworkers prepared such biomimetic PEG hydrogels by cross-linking vinylsulfone terminated PEG macromers with cysteine-containing matrix metalloproteinase (MMP)-sensitive peptides [18,19]. These *in situ* forming gels were degraded by cell-secreted and cell-activated proteases and proved to be suitable for the repair of bone and cartilage defects [20,21]. In another approach, amine-reactive PEG monoacrylates were reacted with collagenase-sensitive peptides (Gly-Gly-Leu↓Gly-Pro-Ala-Gly-Gly-Lys) and integrin-binding domains (Tyr-Ile-

Gly-Ser-Arg) resulting in triblock copolymers terminated by acrylate groups. These copolymers were photopolymerized to form hydrogels that promoted viability, adhesion, and proliferation of preadipocytes [9].

But despite these promising results, direct transfer into clinical practice could be a challenge. The radical cross-linking scheme often results in cytotoxic byproducts, such as unreacted monomers or degradation products of the polymers, which have to be removed prior to their implantation [22]. To cope with the problems associated with radical cross-linking, our group developed injectable, biomimetic hydrogels that are prepared without the use of free-radical initiators (Figure 1) [12,23]. For the preparation of enzymatically degradable hydrogels, branched PEG-amines were modified with collagenase-sensitive peptides and cross-linked with branched PEG-succinimidyl propionates. Alanin-modified PEG-amines were used for non-degradable hydrogels.

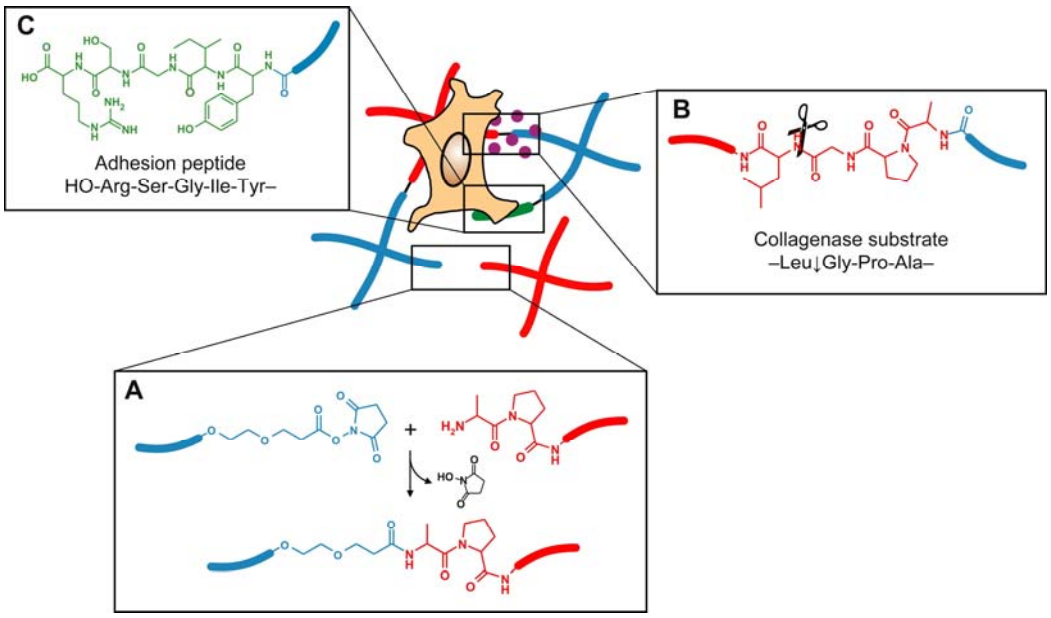

Figure 1: Principle of injectable, biomimetic hydrogels for adipose tissue engineering. **A)** For gel preparation, branched PEG-succinimidyl propionates are cross-linked with branched, amino acid-modified PEG-amines. **B)** The collagenase-sensitive peptide sequence Ala-Pro-Gly↓Leu allows for enzymatic gel degradation. **C)** The integrin-binding motif Tyr-Ile-Gly-Ser-Arg is reacted with branched PEG-succinimidyl propionates and mediates cell adhesion. Reprinted with permission from Brandl *et al.* [23]. ©2010 Elsevier B.V.

The use of these hydrogels as injectables directly applied into the soft tissue defect and cross-linked *in vivo* may facilitate the treatment in a minimally invasive and less painful way [24].

Additionally, the developed hydrogels can be further optimized by functionalization with adhesion molecules or growth factors to promote cell adhesion, migration, proliferation, and

differentiation [14,17,24]. Thus, the newly developed hydrogels were functionalized with the synthetic nonapeptide YIGSR, which has been identified as the major cell binding site in the B1 chain of laminin and mediates cell adhesion [9,25-27].

The present *in vitro* studies investigate the efficiency of the newly developed PEG-based hydrogels as scaffold material for adipose tissue engineering. 3T3-L1 preadipocytes, a commonly used model system for studying adipocyte biology, were encapsulated into the hydrogels and subsequently differentiated into mature adipocytes. We tested the effects of substrate stiffness, adhesiveness, and degradability on adipocyte development by quantifying the intracellular TG accumulation and compared the adipogenic differentiation capacity with the outcome of 2-D cell culture. Finally, we investigated the influence of biodegradability on the formation of adipose tissue-like structures in an *in vitro* long-term study.

3. Materials and Methods

Materials

Murine 3T3-L1 preadipocytes were obtained from ATCC (Manassas, VA). Dulbecco's Modified Eagle's Medium (DMEM) was purchased from Biochrom (Berlin, Germany). Fetal bovine serum (FBS, Lot. No. 40A0044K), 0.25% trypsin-EDTA solution, penicillin-streptomycin solution, and phosphate buffered saline (PBS) were from Invitrogen GmbH (Karlsruhe, Germany). Hoechst 33258 dye was obtained from Polysciences (Warrington, PA) and bovine insulin was kindly provided by Sanofi-Aventis (Frankfurt am Main, Germany). 3-isobutyl-methylxanthine (IBMX) was bought from Serva Electrophoresis (Heidelberg, Germany). Corticosterone, cysteine, DNA from calf thymus, indomethacin, the laminin fragment YIGSR, Minimum Essential Medium alpha modification (α-MEM), oil red O, and Sigmacote® were purchased from Sigma-Aldrich (Taufkirchen, Germany). Papainase was bought from Worthington (Lakewood, NJ). Thesit was obtained from Gepepharm GmbH (Siegburg, Germany). All other chemicals were of analytical grade and obtained from Merck KGaA (Darmstadt, Germany). Deionized water was obtained using a Milli-Q water purification system from Millipore (Schwalbach, Germany). All cell culture plastics were purchased from Corning (Bodenheim, Germany).

Amine-reactive polymers (4armPEG10k-SPA), collagenase-sensitive polymers (4arm-PEG10k-LGPA), and non-degradable polymers (4arm-PEG10k-Ala) were kindly provided by Ferdinand Brandl, Department of Pharmaceutical Technology, University of Regensburg

(Regensburg, Germany). The synthesis of these polymers is described in detail by Brandl *et al*. [23].

Methods

3.1. Cell seeding and cell culture

3T3-L1 preadipocytes were plated in T150 culture flasks and expanded in DMEM supplemented with 10% FBS, penicillin (100 U/ml), and streptomycin (100 µg/ml). At confluence, the 3T3-L1 cells were harvested using trypsin-EDTA, centrifuged to a pellet (1200 rpm, 5 minutes) and washed with PBS.

For the preparation of hydrogels, accurately weighed amounts of 4armPEG10k-LGPA (degradable gels) or 4armPEG10k-Ala (non-degradable gels) were dissolved in phosphate buffer (50 mM, pH 7.4) at 125 mg/ml. A solution of YIGSR (c = 10 µmol/ml) or phosphate buffer was added, so that the final polymer concentrations were 100 mg/ml. In a similar manner, accurately weighed amounts of 4armPEG10k-SPA were dissolved in water at 100 mg/ml. All polymer solutions were kept on ice until use. For cell seeding, the prepared 3T3-L1 preadipocytes were suspended in the amino component (4armPEG10k-LGPA or 4armPEG10k-Ala). Subsequently, an equal volume of 4armPEG10k-SPA was added. After vortexing, 50 µl of the polymer-cell solution were cast into cylindrical glass molds (5 mm inner diameter) that had been treated with Sigmacote®. The final polymer concentration was 10% (w/v) and the cell number 100,000 cells per hydrogel construct. For long-term cell culture 5,000,000 cells were used. After 30 minutes of gelation at 37°C, the glass rings were removed. Each gel sample was transferred into one well of 24-well plates and covered with 2 ml of basal medium (α-MEM supplemented with 10% FBS, 100 U/ml penicillin, and 100 µg/ml streptomycin). For standard 2-D cell culture, 100,000 3T3-L1 cells were seeded in 24-well plates and covered with 2 ml of basal medium. Two days after cell seeding, adipogenesis was induced by applying induction medium (basal medium supplemented with 1 µM insulin, 0.1 µM corticosterone, 0.5 mM IBMX, and 60 µM indomethacin). The time point of induction was referred to as day 0. At day 2, the induction medium was replaced by differentiation medium (basal medium supplemented with 1 µM insulin). The hydrogel constructs were dynamically cultured on an orbital shaker at 60 rpm (Heidolph Instruments, Schwabach, Germany) in a humidified atmosphere at 37°C and 5% CO_2. The culture medium was exchanged every two days.

3.2. Oil red O staining

In order to visualize cytoplasmic lipid droplets, the hydrogel constructs were washed with PBS, fixed in formalin (10% in PBS) overnight, and stained with oil red O (3 mg/ml in 60% isopropanol) for 12 hours [28]. Excessive dye was removed by washing three times with PBS. Microscopical phase contrast images were acquired at 20× magnification using a Zeiss Axiovert 200 M microscope equipped with a Zeiss AxioCam HRc camera and the software ZEN 2008 (Carl Zeiss MicroImaging GmbH, Jena, Germany).

3.3. Quantitative analysis of intracellular TG accumulation

Nine days after induction, the intracellular TG content was quantified using a serum triglyceride determination kit (Sigma-Aldrich, Taufkirchen, Germany). After washing with PBS, the hydrogel constructs were harvested in 0.5% thesit solution, disintegrated using a micropistill (Hartenstein Laborbedarf, Würzburg, Germany) and sonicated (Branson Ultrasonic Corporation, Danbury, CT). The spectroscopic quantification of TGs was performed according to the manufacturer's instructions. All measurements were done in three biological replicates. The amount of TGs per hydrogel construct was calculated and normalized to the cell number of the respective sample as determined by the DNA assay.

3.4. Determination of the cell number with DNA assay

Aliquots of disintegrated and sonicated hydrogel constructs were completely digested with papainase (3.2 U/ml in 0.1 M Na_2HPO_4 buffer, pH 6.5 containing 1 mM Na_2EDTA and 2.5 mM cysteine) for 16 hours at 60°C, and the DNA content was determined using the intercalating Hoechst 33258 dye (0.1 µg/ml in 0.1 M NaCl containing 1 mM Na_2EDTA and 10 mM Tris, pH 7.4) [29]. Fluorescence intensities were determined at 365 nm excitation wavelength and 458 nm emission wavelength on a LS 55 Fluorescence spectrometer (PerkinElmer, Wiesbaden, Germany) and correlated to DNA contents using standard dilutions of double-stranded DNA (from calf thymus). Cell numbers were calculated with a conversion factor of 26.1 pg of DNA per cell, which was determined previously [30].

3.5. Statistics

All quantitative results are presented as mean values ± standard deviation. Statistical analyses were determined using GraphPadPrism v.5 (GraphPad Software, La Jolla, CA, USA). Differences between two groups were analyzed for significance using the unpaired Student's

t-test. Differences between multiple groups were analyzed for significance using one-way analysis of variances (ANOVA) with subsequent multiple comparisons according to Tukey's post hoc test. A value of $p<0.05$ was regarded as statistically significant.

4. Results

4.1. Effect of hydrogel strength on 3T3-L1 adipocytes *in vitro*

The strength of the PEG-based hydrogels increased with rising polymer concentrations [23]. To find an optimal gel strength supporting adipocyte proliferation and adipogenesis *in vitro*, biodegradable hydrogels with polymer contents ranging from 5% - 20% were seeded with 3T3-L1 preadipocytes at a cell density of 100,000 cells per hydrogel. Two days after seeding, the cell-polymer constructs were adipogenically induced with a hormonal cocktail composed of insulin, corticosterone, indomethacin, and IBMX. Nine days after induction, the cell number per gel and the intracellular TG content per cell were determined. Microscopic inspection of the differentiated cell-hydrogel constructs revealed a homogeneous cell distribution within the hydrogel regardless of the initial polymer concentrations (Figure 2 A). Differentiated lipid-loaded adipocytes appeared as dark dots in the microscopic photographs (Figure 2 A). In hydrogels prepared from 5% or 10% polymer, many differentiated adipocytes were visible. However, the number of cells generally decreased with increasing polymer concentrations. This observation was also confirmed by quantifying the cell number per hydrogel construct (Figure 2 B). The determined cell number was generally lower than the seeded cell number of 100,000 cells. Apparently the cells did not proliferate within the hydrogels. Regarding adipogenesis, the intracellular TG accumulation was comparable for adipocytes encapsulated in hydrogels prepared from 5%, 10% and 15% polymer. In contrast to that, significant lower values were observed for cells cultured in gels prepared from 20% polymer (Figure 2 C). The microscopic picture confirmed the reduced number of adipocytes in the 20% hydrogel. Almost no lipid-filled adipocytes were detectable (Figure 2 A).

Altogether, the PEG-based hydrogels seemed to provide an appropriate environment for 3T3-L1 preadipocytes to differentiate into adipocytes. In particular, the hydrogels containing 10% polymer showed the most promising results with regard to cell number and adipogenic differentiation capacity and we, therefore, used these hydrogels for all further experiments.

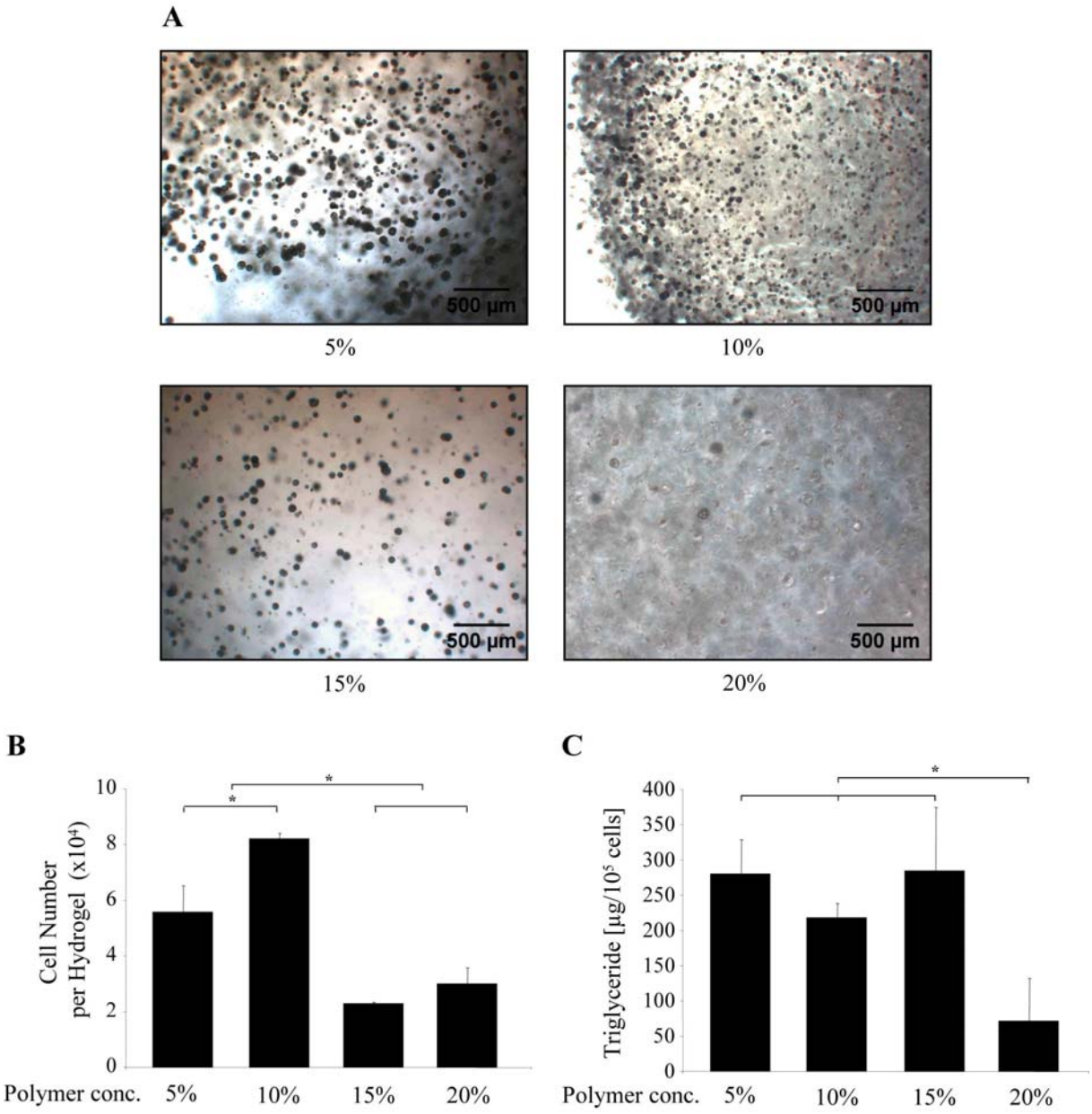

Figure 2: Effect of hydrogel strength on cell number and adipogenic differentiation of 3T3-L1 preadipocytes encapsulated within degradable gels prepared from different polymer concentrations. The 3T3-L1 preadipocytes were seeded at a density of 100,000 cells per hydrogel; two days after seeding, the obtained three-dimensional (3-D) cell constructs were adipogenically induced with a hormonal cocktail. At day 9 after induction, the differentiated cell-hydrogel constructs were analyzed. **A)** Phase contrast images of differentiated cell-hydrogel constructs. Three independent cell culture experiments were performed; representative photographs from one experiment are shown. Bar=500 µm. **B)** Quantification of the cell number per hydrogel (n=3). **C)** Quantification of intracellular TG accumulation (n=3). TG contents were normalized to cell numbers. Statistically significant differences are denoted by * ($p<0.05$).

4.2. Adipogenic differentiation of 3T3-L1 cells cultured within hydrogels and under standard 2-D cell conditions

In this experiment, we compared the cell number and adipogenic differentiation of 3T3-L1 preadipocytes cultured either in conventional monolayer cell culture (2-D cell culture) or within hydrogels (degradable and non-degradable cells, 3-D cell culture) at day 9 after induction (Figure 3).

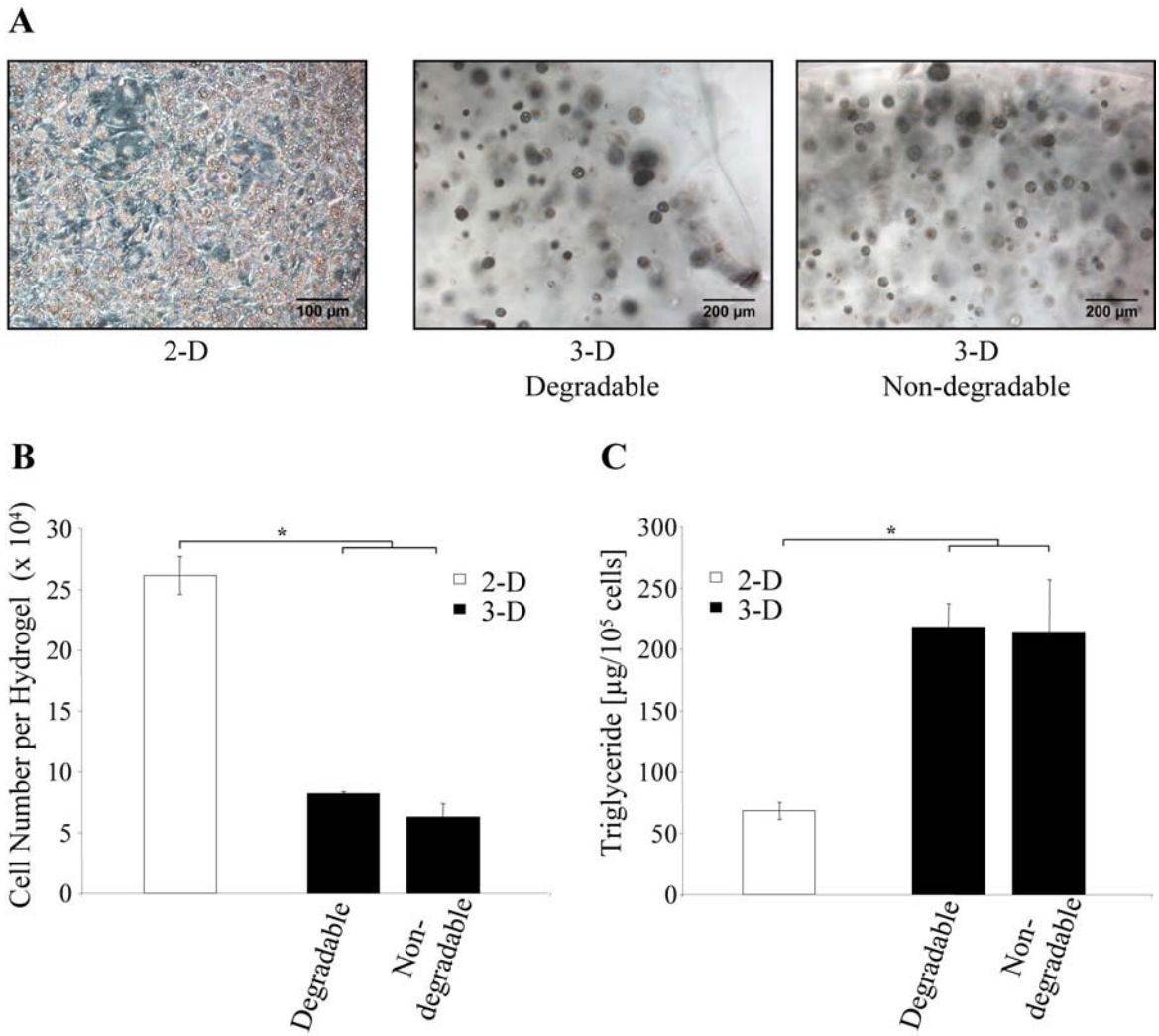

Figure 3: Comparison of 2-D and 3-D cell culture. In 2-D culture, 3T3-L1 preadipocytes were seeded at a density of 100,000 cells in a 24-well plate, whereas in 3-D culture, the same number of preadipocytes was encapsulated into degradable or non-degradable hydrogels (50 µl). Two days after seeding, the cells were adipogenically induced with a hormonal cocktail. At day 9 after induction, the adipocytes were analyzed. **A)** Phase contrast images of differentiated adipocytes cultured under 2-D (left) and 3-D conditions (right). Three independent cell culture experiments were performed; representative photographs from one experiment are shown. Bar=100 µm and 200 µm, respectively. **B)** Quantification of the cell number per hydrogel (n=3). **C)** Quantification of intracellular TG accumulation (n=3). TG contents were normalized to cell numbers. Statistically significant differences are denoted by * ($p<0.05$).

In 2-D culture, the seeded 3T3-L1 cells proliferated during the initial culture period; at day 9 after induction, approximately 260,000 cells per well were detected by DNA assay (Figure 3 B). Compared to this data, the number of cells found within hydrogels was clearly reduced after the same culture period. The determined cell number of about 80,000 cells per degradable hydrogel corresponded to the initial cell number quantified immediately after gel preparation in separate experiments (Figure 4). This indicates that the proliferation of 3T3-L1 cells was suppressed when cultured within hydrogels.

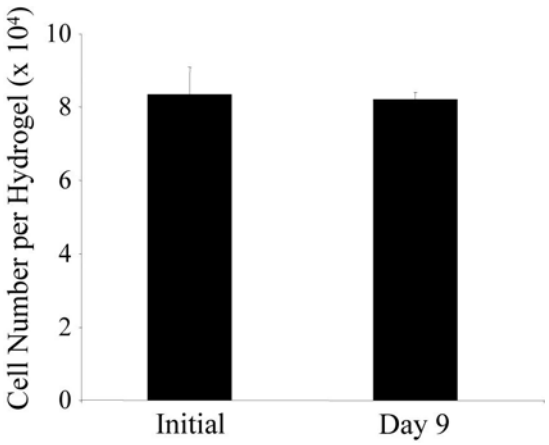

Figure 4: Determination of the cell number within degradable gels immediately after gel preparation and at day 9 after induction (n=3).

Regarding adipogenesis, 3T3-L1 preadipocytes were able to differentiate after adipogenic induction in 2-D as well as in 3-D culture systems resulting in lipid-filled adipocytes (Figure 3 A). Under 2-D culture conditions, the differentiated 3T3-L1 cells had a well spread morphology and contained a large number of small lipid droplets. Within 3-D hydrogels, however, the adipocytes had a rounded shape probably resulting from the large lipid vacuoles (Figure 3 A). Quantification of the intracellular TG content verified the increased TG accumulation in adipocytes encapsulated within hydrogels (Figure 3 C). The degradability of the gel did not influence the adipogenic differentiation of the cells compared to the non-degradable system.

4.3. Influence of YIGSR functionalization on proliferation and adipogenesis of 3T3-L1 cells

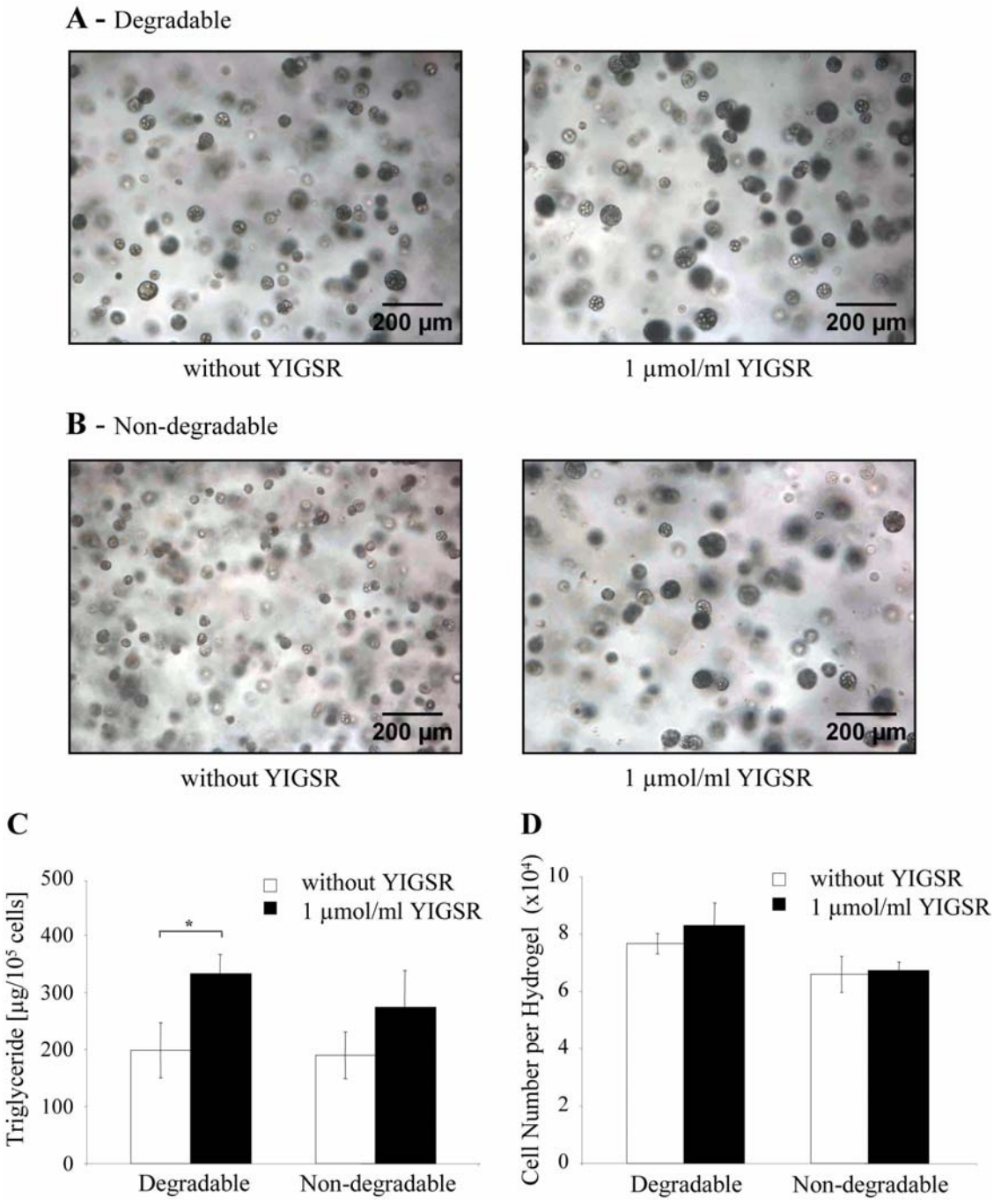

Figure 5: Effect of YIGSR on the proliferation and adipogenic differentiation of 3T3-L1 cells which were encapsulated within degradable and non-degradable hydrogels. 3T3-L1 preadipocytes were seeded at a density of 100,000 cells into the different hydrogels. Two days after seeding, the cells were adipogenically induced with a hormonal cocktail. At day 9 after induction, the adipocytes were analyzed. **A)** Phase contrast images of differentiated adipocytes cultured in degradable hydrogels without YIGSR (right) and with 1 µmol/ml YIGSR (left). Bar=200 µm. **B)** Phase contrast images of differentiated adipocytes cultured in non-degradable hydrogels without YIGSR (right) and with 1 µmol/ml YIGSR (left). Bar=200 µm. Three independent cell culture experiments were performed; representative photographs from one experiment are shown **(A, B)**. **C)** Quantification of the cell number per hydrogel (n=3). **D)** Quantification of intracellular TG accumulation (n=3). TG contents were normalized to cell numbers. Statistically significant differences are denoted by * ($p<0.05$).

To enable cell adhesion, which is critical for cell viability and function, the virtually non-adhesive PEG gels have been modified by incorporation of various adhesion ligands [9,31]. In the present study, we tested the effect of the laminin-derived peptide YIGSR on the proliferation and adipogenic differentiation of 3T3-L1 cells. For this purpose, degradable and non-degradable cell-hydrogel constructs were prepared either without YIGSR or with 1 µmol/ml YIGSR. Two days after seeding, the gel samples were hormonally induced to undergo adipogenesis. At day 9 after induction, the cell-laden hydrogels were analyzed for their cell number and their intracellular TG content (Figure 5).

Isolated adipocytes were homogeneously distributed throughout the hydrogels (Figure 5 A and B). In comparison to gels containing no YIGSR, adipocytes cultured in hydrogels with 1 µmol/ml YIGSR seemed to accumulate more lipids resulting in larger droplets (Figure 5 A and B). This observation was verified by quantifying the intracellular TG content (Figure 5 C). In degradable hydrogels containing YIGSR, the TG amount was significantly increased in comparison to gels without YIGSR. A similar trend was observed in non-degradable constructs. Regarding the cell number, no differences were detected between gel samples containing YIGSR and those without (Figure 5 D). Again, degradable and non-degradable systems did not influence the proliferative behavior of 3T3-L1 cells (see section 4.2 for comparison).

4.4. Effect of the substrate degradability on adipose tissue development *in vitro*

To investigate the effect of substrate degradability on adipose tissue development *in vitro*, degradable and non-degradable hydrogels were seeded with 5,000,000 preadipocytes per construct and cultured over a period of 6 weeks. At day 42 after adipogenic induction, the two groups were analyzed microscopically (Figure 6).

The capability of non-degradable and degradable hydrogels to support the development of adipose tissue-like structures varied dramatically. 3T3-L1 preadipocytes encapsulated within non-degradable hydrogels differentiated into adipocytes with multiple intracellular lipid droplets (Figure 6 A and B, left). However, the isolated adipocytes were not able to form coherent, tissue-like structures within these gels. In contrast, preadipocytes cultured within degradable hydrogels matured to unilocular adipocytes with a single large lipid droplet that occupied most of the cytoplasm (Figure 6 A and B, right). Under these conditions, the differentiated adipocytes were able to form adipose tissue-like structures; single cells could no longer be detected.

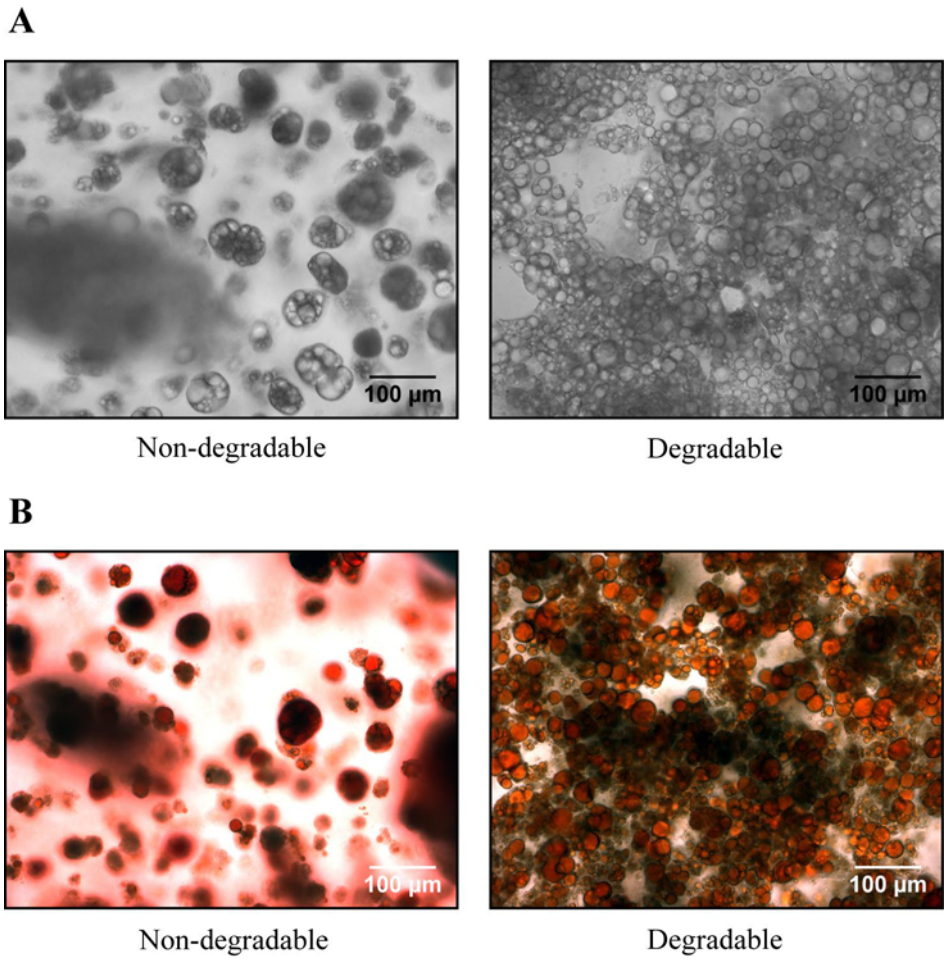

Figure 6: Effect of the substrate degradability on adipose tissue development *in vitro*. 3T3-L1 preadipocytes were seeded at a density of 5,000,000 cells into degradable and non-degradable hydrogels. Two days after seeding, the cells were adipogenically induced with a hormonal cocktail. At day 42 after induction, the adipocytes were microscopically analyzed. **A)** Phase contrast images of differentiated adipocytes cultured in non-degradable (left) and degradable (right) hydrogels. Bar=100 µm. **B)** Oil red O staining of intracellular lipid droplets within differentiated adipocytes cultured in non-degradable (left) and degradable (right) hydrogels. Bar=100 µm.

5. Discussion

Current tissue engineering approaches include the use of various natural, synthetic, and hybrid scaffolding materials to correct soft tissue deficits. However, rigid materials such as poly(lactic-co-glycolic) acid (PLGA) are not appropriate for adipose tissue engineering. In contrast, *in situ* forming PEG-based hydrogels have been proposed as suitable scaffold systems for this application because of their mechanical and elastic properties. Furthermore, these hydrogels can be modified by incorporation of cell-specific degradation sites and adhesion ligands resulting in a suitable environment that supports adipose tissue development [9]. However, the previously reported PEG hydrogels were prepared by photopolymerization which often leads to cytotoxic byproducts. Therefore, our group developed an alternative,

non-radical cross-linking approach that allows for the preparation of injectable, biomimetic hydrogels.

In this study, we analyzed the utility of these biomimetic PEG-based hydrogels for adipose tissue engineering. 3T3-L1 preadipocytes were encapsulated within degradable and non-degradable PEG-based hydrogels and, subsequently, differentiated into adipocytes within this 3-D environment. The developed gel systems appeared to provide a suitable environment for preadipocyte differentiation *in vitro*. However, the gel strength, which can be influenced by the polymer concentrations [23], affected the adipogenic differentiation of 3T3-L1 preadipocytes (Figure 2 A and C, Page 173). Up to a polymer concentration of 15%, the gels supported the adipogenic differentiation of seeded preadipocytes; in gels containing 20% polymer, adipogenic differentiation was obviously suppressed. Possibly, the high mechanical strength of these hydrogels prevented entrapped adipocytes from expanding, which is a prerequisite for the accumulation of lipid droplets. Similar findings have also been reported in literature. Khan *et al.* found that with increasing rigidity of the surrounding ECM the expansion of adipocytes was more and more restricted due to the massive pressure on their cell membrane [32]. Additionally, we detected decreased cell numbers in gels with polymer concentrations of 15% and 20% (Figure 2 B, Page 173). Although the polymers were shown to be non-toxic on cells [33], high concentrations may affect the cell viability due to osmotic effects or the detergent character of the polymers. It has to be further investigated whether this cell loss is really caused by cell death or by detachment of cells from the gel. In general, the detected cell numbers were decreased compared to the initially seeded cell numbers. It is assumed that this phenomenon is associated with the preparation of the samples for DNA measurements and resulted from insufficient digestion of the adipocytes within the gels.

After evaluation of the optimal polymer concentrations (10% initial polymer concentration), we compared the proliferation and differentiation capacity of the adipocytes within the 3-D gel construct with conventional 2-D monolayer culture. In 2-D culture, the 3T3-L1 preadipocytes proliferated during the initial period of two days, until induction forced the preadipocytes to undergo growth arrest. In contrast, cells within the hydrogels were not able to expand during this time (Figure 3 B, Page 174). It is supposed that the growth phase of two days was not sufficient for significant cell proliferation within the stiff gel structure. The hydrogels do not provide the additional space required for the morphological changes during cell proliferation and prevents, therefore, the spreading and expansion of the cells [9]. Furthermore, it is possible that the PEG polymers elicited an anti-proliferative effect on the preadipocytes.

With regard to the adipocyte differentiation, the opposite trend was observed (Figure 3 A and C, Page 174). Here, more intracellular TGs were found in cell-containing hydrogels than in 2-D cell culture. In 3-D cell constructs, the preadipocytes differentiated into mature adipocytes with multiple large lipid droplets in their intracellular space resulting in a spherical cell shape. In 2-D culture, the lipid vacuoles were smaller and the cells were well spread. It is known from the literature that the morphology of differentiating adipocytes shifts from a fibroblast-like phenotype to a more rounded shape due to the accumulation of lipids [34,35]. It has been furthermore shown that adipogenesis of preadipocytes was inhibited when cells were attached on strongly adhesive, fibronectin coated substrates preventing morphological changes of the cells [36,37]. Keeping the cells in a rounded configuration, e.g., by disrupting the cytoskeleton, reversed the inhibitory effect of fibronectin on adipogenic differentiation [36,37]. The differences between 2-D and 3-D culture detected in our study are probably caused by similar effects. In 2-D culture, the preadipocytes strongly adhered on the polystyrene substrate which presumably prevented morphological changes. In contrast, PEG-based hydrogels are completely inert so that the embedded preadipocytes did only loosely interact with the gel network. Together with the elasticity of the hydrogel scaffold, these loose interactions are thought to enable morphological changes that finally support adipogenic differentiation [34]. This illustrates the complex interplay of substrate mechanics and adipocyte function. Therefore, suitable scaffolds for adipose tissue engineering have to meet demands on differentiation, cell attachment, and cell spreading [37].

In a further experiment, we investigated the influence of the substrate adhesiveness on adipogenic differentiation by functionalizing the PEG-based hydrogels with the laminin-derived cell adhesion motif YIGSR (Figure 5, Page 176). Patel *et al.* have reported that incorporation of YIGSR into photopolymerizable hydrogels promoted adhesion of preadipocytes to the virtually non-adhesive PEG gels [9]. We showed that addition of YIGSR resulted in an increased intracellular TG accumulation accompanied by the development of adipocytes with enlarged lipid vacuoles (Figure 5 A and B, Page 176). Obviously, the increased adhesiveness significantly enhanced the differentiation of preadipocytes *in vitro*. Regarding the cell proliferation, we could not detect any effects of YIGSR on the growth of 3T3-L1 preadipocytes (Figure 5 C, Page 176). Patel *et al.* found enhanced proliferation of preadipocytes within degradable PEG hydrogels in the presence of YIGSR [9]. However, the detected differences were significant only on day 6 after cell seeding. In the present study, the seeded preadipocytes were forced to undergo growth arrest at the time point of induction

(day 2 after seeding). During these two days, no significant cell proliferation had occurred, which is in accordance to Patel *et al.* [9].

A key feature of the prepared hydrogels is their degradability by cell-secreted enzymes, such as MMPs. The cell carrier is expected to provide initial mechanical support for the developing adipose tissue. Simultaneously, the hydrogel scaffold is degraded over time. In our *in vitro* studies, degradable and non-degradable systems were compared with respect to the adipocyte development. We hypothesized that the degradability presumably promote the generation of a coherent adipose tissue-like context. The biodegradable mechanics of the gels enables adipocyte enlargement as well as cell-cell and cell-matrix interactions which are important for adipocyte function [38-40]. However, no significant differences between degradable and non-degradable hydrogels were observed in our short-term cell culture experiments (Figure 3 and 5, Page 174 and 176). During this culture period, it seems that the cells did not secrete a sufficient amount of enzymes which are responsible for degradation of the hydrogels. Accordingly, the differentiating adipocytes were not able to generate adipose tissue-like structures (Figure 2, 3 and 5, Page 173, 174 and 176) and only isolated cells were found. Additionally, it has to be noted that the seeded cell number of 100,000 cells per hydrogel obviously was not sufficient for the development of coherent tissue. Therefore, higher numbers of 3T3-L1 cells were encapsulated into the hydrogels and their ability for adipose tissue development was investigated in an *in vitro* long-term study over 6 weeks (Figure 6, Page 178). In this experiment, the degradability of the gels clearly influenced the formation of adipose tissue-like structures. Within non-degradable hydrogels, the cells were not able to generate a coherent tissue-like context and only single, multilocular adipocytes were found. In contrast to that, coherent adipose tissue-like structures with many unilocular fat cells were observed in enzymatically degradable gels after 6 weeks of culture. The polymer network of these gels was obviously broken down by adipocyte-derived enzymes, which presumably facilitated the development of coherent adipose tissue-like structures.

In summary, we successfully developed a 3-D *in vitro* model for adipose tissue engineering based on 3T3-L1 preadipocytes embedded in a new type of PEG-based hydrogels which are non-radically cross-linked. The developed hydrogels represented mechanical properties resembling adipose tissue and additional functionalization of the gels with adhesion peptides or degradation sites provided a suitable 3-D environment for adipocyte differentiation and the development of coherent tissue-like structures. Future experiments may include the use of different cell densities, extended culture periods, and the incorporation of various angiogenic and adipogenic growth factors as well as hormones in PEG-based hydrogels to optimize

adipocyte development. Ultimately, *in vivo* testing is essential to prove the suitability of the developed scaffold for clinical applications.

References

1. Smahel J. Adipose tissue in plastic surgery. *Ann.Plast.Surg.* 1986; **16:** 444-453.
2. Beahm E K, Walton R L, Patrick C W, Jr. Progress in adipose tissue construct development. *Clin.Plast.Surg.* 2003; **30:** 547-58.
3. Abberton K M, Bortolotto S K, Woods A A, Findlay M, Morrison W A, Thompson E W, Messina A. Myogel, a novel, basement membrane-rich, extracellular matrix derived from skeletal muscle, is highly adipogenic in vivo and in vitro. *Cells Tissues.Organs* 2008; **188:** 347-358.
4. Rahaman M N, Mao J J. Stem cell-based composite tissue constructs for regenerative medicine. *Biotechnol.Bioeng.* 2005; **91:** 261-284.
5. Patrick C W, Jr. Tissue engineering strategies for adipose tissue repair. *Anat.Rec.* 2001; **263:** 361-366.
6. Weiser B, Neubauer M, Goepferich A, Blunk T. Tissue Engineering, Fat. In: *Encyclopedia of Biomaterials and Biomedical Engineering* 1 edition 2005.
7. Hemmrich K, von Heimburg D. Biomaterials for adipose tissue engineering. *Expert.Rev.Med.Devices* 2006; **3:** 635-645.
8. Alhadlaq A, Tang M, Mao J J. Engineered adipose tissue from human mesenchymal stem cells maintains predefined shape and dimension: implications in soft tissue augmentation and reconstruction. *Tissue Eng* 2005; **11:** 556-566.
9. Patel P N, Gobin A S, West J L, Patrick C W, Jr. Poly(ethylene glycol) hydrogel system supports preadipocyte viability, adhesion, and proliferation. *Tissue Eng* 2005; **11:** 1498-1505.
10. Patel P N, Smith C K, Patrick C W, Jr. Rheological and recovery properties of poly(ethylene glycol) diacrylate hydrogels and human adipose tissue. *J.Biomed.Mater.Res.A* 2005; **73:** 313-319.
11. Vashi A V, Keramidaris E, Abberton K M, Morrison W A, Wilson J L, O'Connor A J, Cooper-White J J, Thompson E W. Adipose differentiation of bone marrow-derived mesenchymal stem cells using Pluronic F-127 hydrogel in vitro. *Biomaterials* 2008; **29:** 573-579.
12. Brandl F, Kastner F, Gschwind R M, Blunk T, Tessmar J, Goepferich A. Hydrogel-based drug delivery systems: comparison of drug diffusivity and release kinetics. *J.Control Release* 2010; **142:** 221-228.
13. Lee K Y, Mooney D J. Hydrogels for tissue engineering. *Chem.Rev.* 2001; **101:** 1869-1879.
14. Drury J L, Mooney D J. Hydrogels for tissue engineering: scaffold design variables and applications. *Biomaterials* 2003; **24:** 4337-4351.
15. Nguyen K T, West J L. Photopolymerizable hydrogels for tissue engineering applications. *Biomaterials* 2002; **23:** 4307-4314.
16. Burdick J A, Anseth K S. Photoencapsulation of osteoblasts in injectable RGD-modified PEG hydrogels for bone tissue engineering. *Biomaterials* 2002; **23:** 4315-4323.
17. Lutolf M P, Hubbell J A. Synthetic biomaterials as instructive extracellular microenvironments for morphogenesis in tissue engineering. *Nat.Biotechnol.* 2005; **23:** 47-55.

18. Lutolf M P, Hubbell J A. Synthesis and physicochemical characterization of end-linked poly(ethylene glycol)-co-peptide hydrogels formed by Michael-type addition. *Biomacromolecules.* 2003; **4:** 713-722.

19. Lutolf M P, Lauer-Fields J L, Schmoekel H G, Metters A T, Weber F E, Fields G B, Hubbell J A. Synthetic matrix metalloproteinase-sensitive hydrogels for the conduction of tissue regeneration: engineering cell-invasion characteristics. *Proc.Natl.Acad.Sci.U.S.A* 2003; **100:** 5413-5418.

20. Lutolf M P, Weber F E, Schmoekel H G, Schense J C, Kohler T, Muller R, Hubbell J A. Repair of bone defects using synthetic mimetics of collagenous extracellular matrices. *Nat.Biotechnol.* 2003; **21:** 513-518.

21. Park Y, Lutolf M P, Hubbell J A, Hunziker E B, Wong M. Bovine primary chondrocyte culture in synthetic matrix metalloproteinase-sensitive poly(ethylene glycol)-based hydrogels as a scaffold for cartilage repair. *Tissue Eng* 2004; **10:** 515-522.

22. Timmer M D, Shin H, Horch R A, Ambrose C G, Mikos A G. In vitro cytotoxicity of injectable and biodegradable poly(propylene fumarate)-based networks: unreacted macromers, cross-linked networks, and degradation products. *Biomacromolecules.* 2003; **4:** 1026-1033.

23. Brandl F P, Seitz A K, Tessmar J K, Blunk T, Goepferich A M. Enzymatically degradable poly(ethylene glycol) based hydrogels for adipose tissue engineering. *Biomaterials* 2010; **31:** 3957-3966.

24. Shin H, Jo S, Mikos A G. Biomimetic materials for tissue engineering. *Biomaterials* 2003; **24:** 4353-4364.

25. Patrick C W, Jr., Wu X. Integrin-mediated preadipocyte adhesion and migration on laminin-1. *Ann.Biomed.Eng* 2003; **31:** 505-514.

26. Ranieri J P, Bellamkonda R, Bekos E J, Vargo T G, Gardella J A, Jr., Aebischer P. Neuronal cell attachment to fluorinated ethylene propylene films with covalently immobilized laminin oligopeptides YIGSR and IKVAV. II. *J.Biomed.Mater.Res.* 1995; **29:** 779-785.

27. Bellamkonda R, Ranieri J P, Aebischer P. Laminin oligopeptide derivatized agarose gels allow three-dimensional neurite extension in vitro. *J.Neurosci.Res.* 1995; **41:** 501-509.

28. Ramirez-Zacarias J L, Castro-Munozledo F, Kuri-Harcuch W. Quantitation of adipose conversion and triglycerides by staining intracytoplasmic lipids with Oil red O. *Histochemistry* 1992; **97:** 493-497.

29. Kim Y J, Sah R L, Doong J Y, Grodzinsky A J. Fluorometric assay of DNA in cartilage explants using Hoechst 33258. *Anal.Biochem.* 1988; **174:** 168-176.

30. Weiser B, Adipose Tissue Engineering - Precultivation Strategies towards Clinical Applications & A Novel 3-D Model of Adipogenesis for Basic Research. *Ph.D. thesis* 2008. University of Regensburg, Regensburg, Germany.

31. Boateng S Y, Lateef S S, Mosley W, Hartman T J, Hanley L, Russell B. RGD and YIGSR synthetic peptides facilitate cellular adhesion identical to that of laminin and fibronectin but alter the physiology of neonatal cardiac myocytes. *Am.J.Physiol Cell Physiol* 2005; **288:** C30-C38.

32. Khan T, Muise E S, Iyengar P, Wang Z V, Chandalia M, Abate N, Zhang B B, Bonaldo P, Chua S, Scherer P E. Metabolic dysregulation and adipose tissue fibrosis: role of collagen VI. *Mol.Cell Biol.* 2009; **29:** 1575-1591.

33. Teramura Y, Kaneda Y, Totani T, Iwata H. Behavior of synthetic polymers immobilized on a cell membrane. *Biomaterials* 2008; **29:** 1345-1355.

34. Smas C M, Sul H S. Control of adipocyte differentiation. *Biochem.J.* 1995; **309 (Pt 3):** 697-710.

35. Gregoire F M, Smas C M, Sul H S. Understanding adipocyte differentiation. *Physiol Rev.* 1998; **78:** 783-809.

36. Spiegelman B M, Ginty C A. Fibronectin modulation of cell shape and lipogenic gene expression in 3T3-adipocytes. *Cell* 1983; **35:** 657-666.

37. O'Connor K C, Song H, Rosenzweig N, Jansen D A. Extracellular matrix substrata alter adipocyte yield and lipogenesis in primary cultures of stromal-vascular cells from human adipose. *Biotechnology Letters* 2003; **25:** 1967-1972.

38. Fischbach C, Spruss T, Weiser B, Neubauer M, Becker C, Hacker M, Goepferich A, Blunk T. Generation of mature fat pads in vitro and in vivo utilizing 3-D long-term culture of 3T3-L1 preadipocytes. *Experimental Cell Research* 2004; **300:** 54-64.

39. Kang X, Xie Y, Kniss D A. Adipose tissue model using three-dimensional cultivation of preadipocytes seeded onto fibrous polymer scaffolds. *Tissue Eng* 2005; **11:** 458-468.

40. Mariman E C, Wang P. Adipocyte extracellular matrix composition, dynamics and role in obesity. *Cell Mol.Life Sci.* 2010.

Chapter 8

Summary

and

Conclusions

1. Summary

For both basic cell biology research and the development of new therapeutic strategies related to adipose tissue, *in vitro* adipocyte culture is helpful to understand adipocyte and adipose tissue development. Commonly, two-dimensional (2-D) monolayer cultures are used to study adipocyte biology on the cellular and molecular level. The first part of this thesis focused on conventional 2-D adipocyte culture to investigate the efficacy of therapeutic substances used for injection lipolysis (**Chapter 3 and 4**).

To study the influence of the surrounding tissue architecture on adipocyte function, three-dimensional (3-D) culture systems are required mimicking an *in vivo*-like adipose tissue context. Recently, a novel 3-D adipocyte culture system based on the formation of spheroids was developed by our group [1]. This spheroid model is characterized by a coherent tissue-like context and represents a suitable model system to investigate tissue-inherent factors such as cell-cell and cell-matrix interactions. In the second part of this work, the influence of collagens, the most abundant components of the extracellular matrix (ECM), on adipocyte development was investigated *in vitro* (**Chapter 5 and 6**).

Besides the benefit of 3-D adipocyte culture models in basic research, the generation of 3-D adipose substitutes appears desirable in tissue engineering strategies for plastic and reconstructive surgery to augment soft tissue defects, e.g., after deep burns or tumor resections [2]. The third part of this work investigated the suitability of a newly developed poly(ethylene glycol) (PEG)-based hydrogel for the use in adipose engineering (**Chapter 7**).

1.1. 2-D culture

1.1.1. Investigation of therapeutic substances used for injection lipolysis

The injection of Lipostabil®, referred to as injection lipolysis, is a non-invasive aesthetic procedure to reduce localized fat depositions [3-5]. So far, the underlying mechanisms have not been fully understood. In cooperation with "Network Lipolysis", the effect of Lipostabil® as well as its single substances sodium deoxycholate (DC) and phosphatidylcholine (PC) on mature adipocytes were investigated by using *in vitro* 2-D culture systems with the 3T3-L1 cell line and human adipose-derived stem cells (ADSCs) (**Chapter 4**). ADSCs are a previously identified cell source isolated from adipose tissue and were used in this study to reflect a more native situation. We evaluated the isolation and culture conditions in order to optimize the adipogenic differentiation rate of the ADSCs (**Chapter 3**). The introduction of additional filtrations steps during the isolation procedure led to a more purified cell

population with higher differentiation capacity. Additionally, the supplementation of the culture medium with basic fibroblast growth factor (bFGF) enhanced the adipogenic differentiation of ADSCs. Finally, a 2-D adipogenic culture system with ADSCs was successfully developed and was used in further experiments to investigate the underlying mechanisms of injection lipolysis.

The treatment of the differentiated cells, both 3T3-L1 and ADSCs, with DC and Lipostabil® clearly affected the cell membrane integrity as detected microscopically and confirmed by propidium iodide staining (**Chapter 4**). In contrast to that, PC did not have any toxic effects on the adipocytes. PC was identified as a partially protective substance against the cell-lysing effect of DC. Lipolytic activities, e.g., via adrenergic receptors, were not observed for the Lipostabil® formula and its single components. Therefore, it is concluded that the reduction of fat tissue volumes after injection of Lipostabil® is caused by disruption of the cell membrane integrity and not by lipolytic mechanisms. DC as a detergent substance could be identified to be the effective substance in the Lipostabil® compound applied for injection lipolysis.

1.2. 3-D culture

1.2.1. Investigation of collagens in adipogenesis in vitro

Collagens are important components of the ECM network and are regulated during adipogenesis [6-9]. The collagen network and its remodeling during adipocyte development are not well characterized. Since the adipose tissue architecture is better reflected in a 3-D context, the role of collagens during adipose conversion was investigated in 3-D spheroids in comparison to 2-D monolayer culture (**Chapter 5 and 6**). Ethyl-3,4-dihydroxybenzoate (EDHB), an inhibitor of collagen prolyl hydroxylase and, thus, collagen synthesis was used to examine the influence of the collagen organization in a tissue-like context on the adipogenesis of 3T3-L1 *in vitro* (**Chapter 5**). In contrast to 2-D culture, EDHB prevented the differentiation of adipocytes in 3-D spheroids as detected by reduced oil red O staining, triglyceride (TG) content and glycerol-3-phosphate dehydrogenase activity. Measurement of the hydroxyproline content during adipogenic differentiation showed a reduced activity of prolyl hydroxylases in 3-D culture, whereas in 2-D culture the enzyme was still active. Further investigations of the gene expression of collagen prolyl-4-hydroxylase alpha 1 during adipogenesis by qRT-PCR analysis revealed an increase of this gene in 2-D culture in comparison to 3-D spheroids. These results suggest a complex relationship between prolyl hydroxylase activity, collagens and adipogenesis.

The complex organization of the collagen network is partially arranged by a specified family of collagens, the FACIT (fibril-associated collagens with interrupted triple helices). Members of this family are localized on the surface of major collagen fibrils and contribute to the connection of the ECM network itself. Collagen XVI is one member of the FACIT sub-family and it was reported to mediate anchoring processes and remodeling of the ECM [10,11]. Since the matrix is remodeled during adipocyte differentiation, we hypothesized that this type of collagen is involved in this process. In our study, collagen XVI was identified to be highly expressed in 3T3-L1 preadipocytes and undifferentiated ADSCs. Upon hormonally induced adipogenesis, however, its gene and protein expression was strongly downregulated in 2-D and 3-D adipocyte culture (**Chapter 6**). Further studies identified corticosterone, one component of the adipogenic induction cocktail, as a substance inducing downregulation of procollagen XVI(α1) mRNA. A functional role of collagen XVI in the adipogenesis could not be clarified so far. However, preliminary experiments showed that 3T3-L1 cells overexpressing collagen XVI failed to differentiate into adipocytes after hormonal induction in contrast to non-transfected cells. For the first time, collagen XVI expression was associated with adipogenesis contributing to the emerging picture of the complexity and the role of the ECM in adipose tissue. To clarify the role of this FACIT in adipogenesis, further analyses are required to understand the underlying mechanisms.

1.2.2. Novel hydrogels for adipose tissue engineering

Recently, our group developed *in situ* forming PEG-based hydrogels that can be easily functionalized with degradation sites and various other factors such as adhesion peptides, growth factors or hormones. In the last part of this thesis (**Chapter 7**), the suitability of the developed hydrogels for fat tissue engineering was investigated by encapsulating 3T3-L1 preadipocytes within the hydrogels. Thereby, the influence of different parameters such as substrate stiffness, adhesiveness, and degradability on the adipogenic differentiation was assessed. Compared to conventional 2-D cell culture, the entrapped adipocytes in the hydrogels accumulated higher intracellular TG amounts. Increasing gel strength resulted in a reduced TG accumulation. However, gel functionalization with the laminin-derived adhesion peptide YIGSR enhanced the lipid synthesis of encapsulated adipocytes. Long-term *in vitro* studies revealed that only enzymatically degradable hydrogels promoted the formation of coherent adipose tissue-like structures characterized by many mature unilocular adipocytes. In summary, the developed biomimetic PEG hydrogels provided an appropriate environment for 3T3-L1 cells to differentiate into adipocytes and are, therefore, suggested as a promising new

biomaterial for adipose tissue engineering. Future *in vivo* testing is essential to prove the suitability of the developed scaffold for clinical applications.

2. Conclusion

This thesis presents the variability of *in vitro* adipocyte culture for different applications in basic research and developments towards clinical application. Conventional 2-D monolayer culture is useful for the investigation of mechanism on the cellular and molecular level. Thereby, the choice of the cell source is essential. The 3T3-L1 preadipocyte cell line is a well established culture system, but its use is limited, particularly in clinical applications. ADSCs are an alternative cell culture model to further approach human conditions. In this thesis, a standardized isolation and culture procedure of ADSCs was established leading to a highly differentiated adipocyte culture. By utilizing the established culture systems with 3T3-L1 and ADSCs, it was clarified that the fat reducing effect after injection of Lipostabil® are caused by cell-lysing and not receptor-mediated lipolytic actions.

Adipocyte cell culture is particularly used in basic research. In the last decades, many 2-D *in vitro* studies contributed to the understanding of molecular mechanisms of adipogenesis. However, the influence of the surrounding tissue architecture on adipocyte development is not well characterized. In this thesis, a complex interplay of collagens and adipogenesis was shown. Particularly collagen XVI was downregulated during *in vitro* adipogenesis and it is supposed to play a functional role in this process. Moreover, this thesis showed the importance of a 3-D adipocyte culture system when investigating the surrounding architecture. The appropriate collagen organization appeared to be more relevant in a 3-D tissue-like context for adipocyte development.

3-D adipocyte culture systems are not only essential for basic research purposes, but also for clinical approaches. The improvement of adipose tissue engineering for use in reconstructive surgery requires suitable scaffold biomaterials. A new PEG-based hydrogel developed by our group was suggested to be an appropriate scaffold for adipose engineering. The gel provided a suitable environment that directed adipocyte differentiation. Furthermore, functionalization of the gel with degradation sites promoted the development of coherent adipose tissue-like structures. Once placed at the application site, it is assumed that the gel is degraded by cell-secreted proteases. Thereby, the degradation rate is spatially and temporarily synchronized with the deposition of ECM. Although future *in vivo* experiments have to be carried out, the developed gel system is proposed as a promising scaffold for a variety of applications in regenerative medicine.

In conclusion, adipocyte cell culture is an adequate tool for basic research and the development of clinical applications. Whereas 2-D culture is an easily accessible and widely used model system, 3-D cell systems open up new possibilities for future research, especially when a tissue-like context is of importance.

References

1. Weiser, B. Adipose Tissue Engineering - Precultivation Strategies towards Clinical Applications & A Novel 3-D Model of Adipogenesis for Basic Research. *Ph.D. thesis* 2008. University of Regensburg, Regensburg, Germany.
2. Patrick C W, Jr. Tissue engineering strategies for adipose tissue repair. *Anat.Rec.* 2001; **263:** 361-366.
3. Hasengschwandtner F. Phosphatidylcholine treatment to induce lipolysis. *J.Cosmet.Dermatol.* 2005; **4:** 308-313.
4. Duncan D I, Hasengschwandtner F. Lipodissolve for subcutaneous fat reduction and skin retraction. *Aesthet.Surg.J.* 2005; **25:** 530-543.
5. Rittes P G. The use of phosphatidylcholine for correction of lower lid bulging due to prominent fat pads. *Dermatol.Surg.* 2001; **27:** 391-392.
6. Aratani Y, Kitagawa Y. Enhanced synthesis and secretion of type IV collagen and entactin during adipose conversion of 3T3-L1 cells and production of unorthodox laminin complex. *J.Biol.Chem.* 1988; **263:** 16163-16169.
7. Weiner F R, Shah A, Smith P J, Rubin C S, Zern M A. Regulation of collagen gene expression in 3T3-L1 cells. Effects of adipocyte differentiation and tumor necrosis factor alpha. *Biochemistry* 1989; **28:** 4094-4099.
8. Green H, Meuth M. An established pre-adipose cell line and its differentiation in culture. *Cell* 1974; **3:** 127-133.
9. Nakajima I, Muroya S, Tanabe R, Chikuni K. Extracellular matrix development during differentiation into adipocytes with a unique increase in type V and VI collagen. *Biol.Cell* 2002; **94:** 197-203.
10. Senner V, Ratzinger S, Mertsch S, Grassel S, Paulus W. Collagen XVI expression is upregulated in glioblastomas and promotes tumor cell adhesion. *FEBS Lett.* 2008; **582:** 3293-3300.
11. Eble J A, Kassner A, Niland S, Morgelin M, Grifka J, Grassel S. Collagen XVI harbors an integrin alpha1 beta1 recognition site in its C-terminal domains. *J.Biol.Chem.* 2006; **281:** 25745-25756.

Appendices

List of Abbreviations

18S	18S ribosomal RNA
2-D	two-dimensional
3-D	three-dimensional
α-MEM	minimum essential medium (alpha-modification)
AA	ascorbic acid
ADD-1	adipocyte differentiation and determination factor 1
ADSC	adipose-derived stem cell
Ala	alanine
ANOVA	analysis of variances
APS	ammonium persulfate
Arg	arginine
Asp	asparagine
ATCC	American Type Culture Collection
ATGL	adipose triglyceride lipase
BADGE	bisphenol A diglycidyl
BAT	brown adipose tissue
bFGF	basic fibroblast growth factor
BIP	bovine intramuscular preadipocytes
BMSC	bone marrow-derived stem cell
BSA	bovine serum albumin
bp	base pair
cAMP	cyclic adenosine 3',5"-monophosphate
cDNA	complementary deoxyribonucleic acid
C/EBPα	CCAAT/enhancer binding protein alpha
CEBPβ	CCAAT/enhancer binding protein beta
cGMP	cyclic guanosine 3',5"-monophosphate
colXVI	collagen type XVI
CREB	cAMP-responsive element binding protein
Ct	cycle threshold
Cy 3	cyanine 3
Cys	cysteine
Da	dalton

DAPI	4',6-diamidino-2-phenylindole
DC	sodium deoxycholate
DG	diglyceride
DHAP	dihydroxyacetone phosphate
DMEM	Dulbecco's Modified Eagle's Medium
DMSO	dimethylsulfoxide
DNA	deoxyribonucleic acid
DTT	dithiothreitol
E	efficiency
ECM	extracellular matrix
EDHB	ethyl-3,4-dihydroxybenzoate
EDTA	ethylenediamine tetraacetic acid
e.g.	exempli gratia
EGF	epidermal growth factor
ERK	extracellular-signal-regulated kinase
EST	expressed sequence tag
et al.	et alii
FACIT	fibril-associated collagens with interrupted triple helices
FACS	fluorescence-activated cell sorting
FBS	fetal bovine serum
FCS	fetal calf serum
FDA	Food and Drug Administration
FFA	free fatty acid
GAG	glycosaminoglycan
Gly	glycine
GPDH	glycerol 3-phosphate dehydrogenase
h	hours
HA	hyaluronic acid
HEPES	2-(4-(2-Hydroxyethyl)-1-piperazinyl)-ethansulfonsäure
HIF-1α	hypoxia inducible factor 1 alpha
HSL	hormone-sensitive lipase
IBMX	3-isobutyl-1-methylxanthine
i.e.	id est
IFATS	International Fat Applied Technology Society

IGF	insulin-like growth factor
Ile	isoleucine
INF-γ	interferon gamma
IRF	interferon-regulatory factor
IRS-1	insulin receptor substrate 1
kV	kilo Volt
Leu	leucine
Lys	lysine
mA	milliampere
MAP	mitogen-activated protein
MCP-1	monocyte chemoattractant protein-1
MG	monoglyceride
MMP	matrix metalloproteinase
mRNA	messenger ribonucleic acid
MSC	mesenchymal stem cell
MTT	dimethyl thiazolyl diphenyl tetrazolium
NADH	nicotinamide adenine dinucleotide
OrO	oil red O
PAGE	polyacrylamide gel electrophoresis
PAI	plasminogen activator inhibitor protein
PARP	proline-arginine-rich protein
PBM-2	preadipocyte basal medium-2
PBS	phosphate-buffered saline
PC	phosphatidylcholine
PCR	polymerase chain reaction
PDGF	platelet-derived growth factor
PEG	polyethylene glycol
PFA	paraformaldehyde
PGA	polyglycolic acid
PHD	prolyl hydroxylase domain-containing enzymes
PI	propidium iodide
PLA	polylactic acid
PLGA	poly(lactic-co-glycolic) acid
PPARγ	peroxisome proliferator-activated receptor gamma

Pref-1	preadipocyte factor 1
Pro	proline
qRT-PCR	quantitative reverse transcription-polymerase chain reaction
RNA	ribonucleic acid
rpm	rounds per minute
rRNA	ribosomal ribonucleic acid
S	slope
SDS	sodium dodecyl sulfate
SEM	scanning electron microscopy
Ser	serine
SREBP-1	sterol regulatory element binding protein 1
SVF	stromal vascular fraction
TBST	Tris-buffered saline Tween 20
TCA	trichloric acid
TCF/LEF	T cell-specific transcription factor/lymphoid enhancer-binding factor
TCPS	tissue culture polystyrene
TEMED	triethylmethylethylendiamine
TG	triglyceride
TGF-β	transforming growth factor beta
TIMP	tissue inhibitor of metalloproteinase
TNF-α	tumor necrosis factor alpha
Tris	tris(hydroxymethyl)aminomethane
Tyr	tyrosine
U	units
VLDL	very low density lipoproteins
WAT	white adipose tissue
WNT	wingless/int
w/v	weight/volume
YIGSR	tyrosine-isoleucine-glycine-serine-arginine

Curriculum Vitae

Personal Information

Name:	Anna Katharina Seitz
Date of Birth:	03/04/1980
Place of Birth:	Neumarkt i.d.Opf.
Nationality:	German

Professional Experience and Internships

Since 05/2010	Post Doc at the HNO-Department, University Hospital of Regensburg
03/2006 – 05/2010	PhD program at the Department of Pharmaceutical Technology, University of Regensburg
03/2006 – 07/2009	Assistance of pharmaceutical course, University of Regensburg
06/2005 – 10/2005	Scientific assistant at DKFZ, Heidelberg
08/2004 – 06/2005	Diploma thesis at the Department of Cell and Developmental Biology, University of Würzburg
08/2002	Internship in marine biology, University of Wales, Bangor
09/2001-03/2002	Study abroad at the IBPS, Toulouse, Frankreich

Education

06/2005	Diploma in biology
11/1999 – 06/2005	Study of biology at the University of Würzburg
06/1999	Allgemeine Hochschulreife
09/1990 – 06/1999	Ostendorfer Gymnasium, Neumarkt i.d.Opf.
09/1986 – 07/1990	Primary School Woffenbach, Neumarkt i.d.Opf.

List of Publications

Publications:

1. **Seitz A.K.**, Muhr C., Ratzinger S., Bauer-Kreisel P., Goepferich A., Blunk T. Effect of a prolyl hydroxylase inhibitor on adipogenesis in 2-D and 3-D culture. *To be submitted to BBRC Journal.*

2. **Seitz A.K.**, Ratzinger S., Muhr C., Bauer-Kreisel P., Grässel S., Goepferich A., Blunk T. Collagen XVI is downregulated during adipogenesis *in vitro*. *To be submitted to Matrix Biology.*

3. Brandl F., **Seitz A.K.**, Teßmar J., Blunk T., Goepferich A. Enzymatically degradable poly(ethylene glycol)-based hydrogels for adipose tissue engineering. *Biomaterials, 31(14), 3957-66, 2010.*

4. Weiser, B., **Seitz, A.K.**, Kunz-Schughart, L., Tessmar, J., Goepferich, A., Blunk, T. A novel 3-D spheroid model of adipogenesis exhibits differential adipokine expression in comparison to 2-D culture. *To be submitted to FASEB Journal.*

5. Weiser, B., Sommer, F., Neubauer, M., **Seitz, A**., Tessmar, J., Goepferich, A., Blunk, T. Ascorbic acid enhances adipogenesis of bone marrow-derived mesenchymal stromal cells. *Cells, Tissues, Organs, 189(6), 373-381, 2009.*

6. Weiser, B., Prantl, L., Schubert, T., Zellner, J., Fischbach-Teschl, C., Spruss, T., **Seitz, A**., Tessmar, J., Goepferich, A., Blunk, T. (2008) *In vivo* development and long-term survival of engineered adipose tissue depend on *in vitro* precultivation strategy. *Tissue engineering, Part A, 14(2), 275-284, 2008.*

Conference Contributions:

1. **Seitz, A.**, Weiser, B., Kunz-Schughart, L., Bauer-Kreisel, P., Schüssele, A., Tessmar, J., Goepferich, A., Blunk, T. (2008) A novel 3-D spheroid model of adipogenesis exhibits differential adipokine expression in comparison to 2-D culture. *Keystone symposium "Molecular Control of Adipogenesis and Obesity",* Banff, Canada.

2. **Seitz, A.**, Ratzinger, S., Muhr, C., Weiser, B., Goepferich, A., Bauer-Kreisel, P., Grässel, S., Blunk, T. (2010) Collagen XVI expression is downregulated during adipogenesis in 2-D and 3-D culture. *Keystone symposium "Molecular Control of Adipogenesis and Obesity",* Keystone, Colorado, USA.

Eidesstattliche Erklärung

(1) Ich erkläre hiermit an Eides statt, dass ich die vorliegende Arbeit ohne unzulässige Hilfe Dritter und ohne Benutzung anderer als der angegebenen Hilfsmittel angefertigt habe; die aus anderen Quellen direkt oder indirekt übernommenen Daten und Konzepte sind unter Angabe des Literaturzitats gekennzeichnet.

(2) Bei der Auswahl und Auswertung folgenden Materials haben mir die nachstehend aufgeführten Personen in der jeweils beschriebenen Weise entgeltlich/unentgeltlich geholfen:
1. .....
2. .....
3. .....

(3) Weitere Personen waren an der inhaltlich-materiellen Herstellung der vorliegenden Arbeit nicht beteiligt. Insbesondere habe ich hierfür nicht die entgeltliche Hilfe eines Promotionsberaters oder anderer Personen in Anspruch genommen. Niemand hat von mir weder unmittelbar noch mittelbar geldwerte Leistungen für Arbeiten erhalten, die im Zusammenhang mit dem Inhalt der vorgelegten Dissertation stehen.

(4) Die Arbeit wurde bisher weder im In- noch im Ausland in gleicher oder ähnlicher Form einer anderen Prüfungsbehörde vorgelegt.

Anna Katharina Seitz

Acknowledgments

Am Schluss möchte ich mich noch herzlich bei all denjenigen bedanken, die zum Gelingen dieser Arbeit beigetragen haben.

Mein ganz besonderer Dank gilt Herrn Prof. Dr. Achim Göpferich für die Möglichkeit, an seinem Lehrstuhl promoviert haben zu können, und für die Unterstützung bei der Bearbeitung dieses Themas. Er hatte immer ein offenes Ohr und seine Anregungen waren immer sehr hilfreich für mich. Außerdem möchte ich mich ausdrücklich für die Gelegenheit bedanken, meine Ergebnisse auf internationalen Kongressen präsentiert haben zu dürfen.

Herrn Prof. Dr. Torsten Blunk danke ich herzlichst für die sehr intensive und motivierte Betreuung dieser Arbeit. Von seiner Zuverlässigkeit, Gewissenhaftigkeit, Kompetenz und Begeisterung profitierte ich die ganzen Jahre meiner Promotion. Die freundschaftliche Zusammenarbeit verbunden mit vielen fruchtbaren Diskussionen bereitete mir viel Freude und trug wesentlich zum Gelingen dieser Arbeit bei. Ich danke ihm für sein Vertrauen und dass ich immer auf seine Unterstützung zählen konnte.

Mein Dank gilt auch dem Netzwerk-Lipolyse für die finanzielle Unterstützung des Injektions-Lipolyse Projektes sowie für die gute Zusammenarbeit.

Weiterhin möchte ich mich bei allen ehemaligen Kollegen des Lehrstuhls Pharmazeutische Technologie für das nette Arbeitsklima sowie zahlreiche Aktivitäten, die von der Arbeit ablenkten, bedanken. Ohne Euch wäre es um einiges härter gewesen.

Insbesondere gilt mein Dank:

- Dr. Sabine Ratzinger für die wissenschaftliche, materielle und seelische Unterstützung. Ohne sie wäre vieles in dieser Arbeit nicht machbar gewesen.
- Dr. Jörg Teßmar für viele wissenschaftliche Diskussionen und konstruktive Ratschläge in allen Lebenslagen.
- Dr. Ferdinand Brandl für die gute und motivierte Zusammenarbeit, ohne die das Hydrogel-Kapitel nicht zustande gekommen wäre. Außerdem danke ich ihm, dass er immer an Ort und Stelle war, wenn mein Computer mich mal wieder in den Wahnsinn getrieben hat.
- Dr. Silvan Klein für die gute freundschaftliche Zusammenarbeit im Lipolyse Projekt.

- Lisa Ellmann und Alexandra Frimberger für die Unterstützung im Labor.
- Dr. Petra Bauer-Kreisel, Dr. Barbara Weiser und Christian Muhr für die Unterstützung bei allem, was mit Fett zu tun hatte.
- Andrea Blaimer für die Organisation des Zelllabors.
- Renate Liebl, Angelika Berié, Edith Schindler, Lydia Frommer, Liane Öttl, Stefan Kolb und Dominika Mögele für allerlei technische und organisatorische Hilfe sowie die netten Gespräche beim morgendlichen Kaffeetrinken.
- dem gesamten Bits&Bytes Team für die Hilfe rund um den PC.
- Constantin Hozsa für viele hilfreiche Kleinigkeiten, die mir des Öfteren das Leben erleichtert haben.
- Klaus Pollinger für die sportliche Ablenkung und viele Gespräche rund um den Berg.
- Der Hühnerfarm, Cornelia Rose und Anna Hezinger, für eine schöne gemeinsame Laborzeit und dass sie mich durch alle Höhen und Tiefen begleitet haben.
- Dr. Bianca Kohl und Dr. Maja Klug für die Korrekturen dieser Arbeit. Außerdem möchte ich Ihnen für Ihre langjährige Freundschaft danken und dass ich immer auf sie zählen kann.
- meinen restlichen Freunden, insbesondere Kaddl und Rossl, für die konstruktive Ablenkung, wenn mal wieder gar nichts ging.
- Jörg Nisslbeck, dass er mich in allem unterstützt und immer an mich glaubt. Danke, dass Du immer für mich da bist!

Mein ganz besonderer Dank gilt meinen Eltern, die mir diesen Weg ermöglicht haben und immer hinter mir stehen.